Integrated biorefinery approach towards production of sustainable chemicals and fuel from passion fruit rind

Thesis submitted

in partial fulfillment of requirements

for the award of

Doctor of Philosophy

by

Kakali Borah

(196151004)

School of Energy Science and Engineering

Indian Institute of Technology Guwahati

Guwahati–781039

Assam, India

November 2025

School of Energy Science and Engineering
Indian Institute of Technology Guwahati

Statement

I, hereby declare that the information contained in this thesis, **"Integrated biorefinery approach towards production of sustainable chemicals and fuel from passion fruit rind,"** is the outcome of research I conducted at the School of Energy Science and Engineering, Indian Institute of Technology Guwahati, Guwahati, India, under the supervision of Prof. Vaibhav V. Goud. Wherever the study presented is based on the results of other researchers, appropriate acknowledgments have been provided following the standard procedure for publishing scientific observations.

Date 26.11.2025

Kakali Borah

Kakali Borah
(196151004)

School of Energy Science and Engineering
Indian Institute of Technology Guwahati

Certificate

This is to certify that the work done for the doctor of philosophy thesis by Ms. Kakali Borah (Roll No. 196151004), entitled "**Integrated biorefinery approach towards production of sustainable chemicals and fuel from passion fruit rind**," was completed under the supervision of Prof. Vaibhav V. Goud and has not been submitted elsewhere for a degree.

Date 28.11.2025

Prof. Vaibhav V. Goud
Professor
Department of Chemical Engineering
Indian Institute of Technology Guwahati
Guwahati - 781039, Assam, India.

School of Energy Science and Engineering
Indian Institute of Technology Guwahati

Acknowledgement

I am extremely thankful to all who contributed to the successful culmination of my doctoral journey. I express my profound gratitude to my supervisor, Prof. Vaibhav V. Goud, for granting me the opportunity to join his research group. I am eternally appreciative of his constant support, encouragement, perceptive direction, and unwavering patience during my Ph.D. journey. His guidance has been important in determining my academic and research career.

I express deep appreciation to my doctoral committee members: Prof. Debasish Das, Prof. Chandan Das, and Dr. Selvaraju Narayanasamy, for their positive input and invaluable ideas during my progress seminars, which have led to the successful completion of my Ph.D. thesis. Additionally, I am thankful to my PMRF nodal committee members for their valuable suggestions and guidance during my annual reviews, which greatly enhanced the quality of my thesis.

I like to express my profound gratitude to Dr. Kaustubha Mohanty and Dr. V. S. Moholkar, previous Heads of the School of Energy Science and Engineering at IIT Guwahati, for their assistance and for providing the requisite facilities and resources.

My heartfelt thanks to the faculty members and current/former staff of the School of Energy Science and Engineering, including Dr. Pankaj Kalita, Dr. Lepakshi Barbora, Mr. Dhiren Huzuri, Mr. Debarshi Baruah, Mr. Nabajit Rajbongshi, Mr. Nayan, Mr. Pranjal, Mr. Siba Prakash, Mr. Dipankar, Mr. Wasim, and Ms. Rashmi, for their assistance and cooperation throughout my Ph.D. tenure.

I am profoundly thankful to my M.Sc. thesis supervisor, Prof. Surajit Das (National Institute of Technology Rourkela), for his continuous inspiration and motivation that laid the foundation for my research career.

I would like to express my genuine gratitude to the Department of Chemical Engineering, Central Instrument Facility, Department of Bio-Science and Bio-Engineering, Department of Chemistry, Centre for Environment, Centre for Sustainable Polymers, IIT Guwahati, and NIPER- Guwahati for granting me access to the laboratory facilities. Special thanks to the Assam Science and Technology University, Department of Chemical Engineering, Assam Engineering College, North-Guwahati, for their support in successfully fulfilling my teaching assistantship during my PMRF tenure. I extend my sincere gratitude to Dr. Sidananda Sarma, Mr. Madhurjya Borah, and Mr. Kishore Talukdar for their indispensable support in operating the FESEM and CHNS analyzer at the Central Instrument Facility.

I extend my warmest thanks to my seniors, juniors, interns, and labmates—Dr. Atanu Kumar Paul, Mr. Chitta Ranjan Barik, Dr. Dipsikha Kalita, Dr. Chandan Mukherjee, Dr. Dipesh Kumar, Dr. Debeni Devi, Dr. Sutapa Das, Dr. Sukumar Purohit, Dr. Abebe Moges, Mr. Pravin G. Suryawanshi, Dr. N. N. Deshavath, Mr. Yash Raghav, Ms. Sabari Nandi, Ms. Priyanka P., Ms. Rebika Salam, Mr. Ravichandra C. Patil, Mr. Omkar, Mr. Shubham, Mr. Rupesh, Ms. Sumee, Ms. Angana, Mr. Dalvir, Mr. Mangal, Mr. Abhishek, Mr. Shekhar Chauhan, Ms. Khusbu, Mr. Debarshi, Mr. Sumit, Mr. Gurudatt, Mr. Bhargav, Mr. Suraj, Mr. Vikas, Mr. Karthik, and Mr. Sagar—for fostering a supportive and friendly research environment. Your collaboration, feedback, and camaraderie have made this journey not only productive but also enjoyable.

Some of the most cherished moments of my life have been spent at IIT Guwahati, and I am grateful to my dear friends who made this time special: Ms. Kashmiri Sarma, Ms. Puja Hazarika, Dr. Sarmistha Baruah, Mr. Anurag Handique, Dr. Kaustubh Khaire, Dr. Angana Bhattacharjee, Dr. Maibam Premeshwarii, Mr. Gopinath, Mr. Jyotishman, Mr. Saptshwa, Mr. Anirban Basumatry, Mr. Hirakjyoti Basumatry, Ms. Chayanika Das, Mr. Khanindram Baruah, Mr. Sahil, Mr. Nilotpal, Dr. Nipu Kumar, Ms. Lipika Sha, Ms. Pratyasha Mishra, Dr. Sasanka, Dr. Samik Mishra, Dr. Tripti Paul, Mr. Nilavjyoti Sarmah, Dr. Nilkamal Mahanta, Dr. Ritam Sarma, Ms. Niharika Keot, and Mr. Geetartha Das. Thank you for filling my Ph.D. life with laughter, support, and unforgettable memories.

I gratefully acknowledge the financial support provided by the Prime Minister's Research Fellowship (PMRF) and Ministry of Human Resource Development under the Ministry of Education, Government of India, which made this research possible.

Special thanks to my extended family at IITG to 'IITG-Assamese Group', who provided a homely environment, full of warmth and belonging.

Words cannot express the depth of my gratitude to my parents and siblings for their unconditional love, sacrifices, and support throughout this journey. Your belief in me gave me the strength to keep going. I am also thankful to my paternal and maternal relatives for their constant encouragement and timely help during challenging times.

I fondly remember my late grandparents, whose blessings and faith in my potential continue to inspire me every day. Though they are no longer here, their love has guided me throughout this path.

Finally, I bow in gratitude to the Almighty for bestowing strength, resilience, and grace at every step of this academic pursuit.

Kakali Borah

भारतीय प्रौद्योगिकी संस्थान गुवाहाटी
Indian Institute of Technology Guwahati

Dedicated to my Parents

Table of Contents

Abstract

Agro-industrial waste represents significant potential for the production of biofuels and value-added chemicals, supporting sustainable waste management and resource sustainability. The rising environmental concerns and resource depletion are driving a surge in technologies focused on the conversion of organic waste into economically viable and ecologically beneficial products. Food processing byproducts are particularly abundant in beneficial compounds, including carbohydrates, lipids, proteins, vitamins, polyphenols, and various bioactive substances. Passion fruit (*Passiflora edulis*), a tropical fruit predominantly grown for nutritive juice production, produces over 60% of its weight as byproducts, comprising peel, seeds, and bagasse. This underutilised waste is rich in bioactive compounds, including polyphenols, anthocyanins, vitamins, lipids, carbohydrates, and alkaloids, which possess therapeutic properties such as anti-inflammatory, antitumor, antihypertensive, antioxidant, and anticancer effects. Natural antioxidants extracted from passion fruit waste can serve as efficient stabilisers for edible oils, improving oxidative stability and prolonging shelf life. Simultaneously, the carbohydrate component can be utilised for the production of second-generation biofuels. Northeast India, endowed with two global biodiversity hotspots, cultivates passion fruit on a small scale, with the associated waste being disposed of without valorisation. This study focuses on investigating the antioxidant properties of yellow passion fruit rind from Northeast India and its prospective application in nutraceuticals, food, and biofuels, thereby promoting the sustainable use of agro-industrial waste.

The introductory part of the thesis highlights the importance of passion fruit and its by-products, which are abundant in various bioactive compounds with potential uses in the food and beverage industry, pharmaceutical, and nutraceutical sectors. A comprehensive literature analysis has been presented, outlining diverse extraction methods utilised for the recovery of these beneficial components. Green extraction methods, including ultrasound-assisted extraction and supercritical fluid extraction, have gained significant attention for their efficiency and reduced environmental impact relative to conventional procedures. The following chapters discuss the prospective uses of the extracted antioxidants and fermentable sugars in sustainable biofuel production.

Phenolic and flavonoid compounds from yellow passion fruit rind (YPFR) sourced from Assam, India, were extracted utilising green methods, specifically ultrasound-assisted extraction (UAE) and supercritical fluid extraction (SFE). Ethanol-water was used as the solvent for UAE, instead of SFE, which utilised CO_2 with 10% ethanol as a co-solvent (SC-ET). Each extraction technique was assessed under different operational parameters—temperature, sonication duration, solid-to-liquid ratio, and solvent concentration for UAE; and pressure, temperature, and solvent flow rate for SFE. The optimisation of these parameters was conducted by Central Composite Design (CCD)-based Response Surface Methodology (RSM). The statistical analysis ($p < 0.05$) validated substantial correlations between the process variables and extraction efficiency, facilitating the determination of optimal operating conditions for maximising total phenolic and flavonoid yields.

A comparative study of extracts obtained under optimised conditions from SC-ET and UAE demonstrated significant concentrations of phenolics, flavonoids, and carotenoids, which contributed to their enhanced antioxidant activity. SC-ET extracts showed higher flavonoids and carotenoids, whereas UE extracts exhibited higher total phenolic content. Gas chromatography-mass spectroscopy identified 75 components in the UE extracts and 47 in SC-ET extracts, signifying a broader extraction range for UAE. High-performance liquid chromatography profiling revealed increased specific quantities of phenolics and flavonoids in SC-ET, indicating its enhanced selectivity. Both extracts demonstrated significant antibacterial activity. Thus, it highlights the potential of YPFR as a sustainable source of bioactive compounds for food, medicinal, and cosmetic uses.

YPFR extracts exhibited significant antioxidant activity, supporting their viability as natural substitutes for synthetic antioxidants to improve the oxidative stability of edible oils. Carotenoids were extracted from YPFR utilising sunflower seed oil (SFO) and soybean oil (SBO) as eco-friendly solvents through UAE, with parameters optimised via RSM. The carotenoid-enriched oils exhibited markedly increased phenolic and flavonoid levels, thereby enhancing antioxidant activity. The extract-enriched oils demonstrated increased resistance to lipid oxidation (29.53 - 46.44%) with an enhancement in induction time at 140 °C. Infusion of extracts into oils subsequently improved thermal stability; however, the structural integrity of the oils was preserved. These findings endorse the utilisation of natural antioxidants from YPFR to enhance the shelf life and stability of edible oils.

Following UAE extraction of bioactives from YPFR utilising edible oils, the remaining spent passion fruit rind (SPFR) exhibited a significant carbohydrate content (41.3%), suggesting its potential for bioethanol production. This research optimised the dilute sulphuric acid pretreatment of SPFR by RSM to enhance xylose release and reduce fermentation inhibitors. Under optimal conditions (110 °C, 10 min, 0.2 M H_2SO_4), 121.8 mg/g db of xylose and 2.3 mg/g db of furfural were obtained from dry biomass. Subsequent detoxification through the overliming process of the hydrolysate reduced inhibitors by 10–30%, thus improving fermentability. The fermentation of the detoxified hydrolysate using *Pichia (Scheffersomyces) stipitis* yielded 9.7 g/L of ethanol, demonstrating efficient application of SPFR hemicellulose in the synthesis of second-generation bioethanol.

The residual biomass obtained following dilute acid pretreatment (PUH-PFR) further contained 40.53% cellulose and 28.46% lignin. To improve cellulose accessibility for enzymatic hydrolysis, NaOH treatment facilitates delignification by cleaving ester linkages between lignin and hemicellulose, thus improving cellulose hydrolysis. 2% NaOH treatment in PUH-PFR removed 92.35% lignin with negligible cellulose loss (7.33%). On further enzymatic saccharification of the cellulosic fraction utilising commercial cellulase, 67.19 g/L of glucose was released, achieving a saccharification efficiency of 87.42%. The subsequent fermentation utilising *Saccharomyces cerevisiae* yielded 30.12 g/L of ethanol. This approach illustrates the possibilities of utilising passion fruit rind waste for sustainable bioethanol production and environmental sustainability.

Abbreviations

ABTS: 2,2′-azino-bis-(3-ethylbenzothiazoline-6-sulfonic) acid

AC: Ash content

$Al(NO_3)_3$: Aluminium nitrate

ANOVA: Analysis of Variance

AnV: Anisidine value

AOCS: American oil chemists' society

AV: Acid value

BET: Brunauer-Emmett-Teller

BHA: butylated hydroxyanisole

BHT: butylated hydroxytolune

BS: *Bacillus subtilis*

C: Carbon

$CaSO_4$: Calcium sulfate

$Ca(OH)_2$: Calcium hydroxide

CBP: Consolidated bioprocessing

CCD: Central Composite Design

C_2H_6O: Ethanol

CH_3CO_2K: Potassium acetate

CHNS: Carbon hydrogen nitrogen sulfur

CI: crystallinity index

C/N ratio: carbon to nitrogen ratio

CO_2: carbon dioxide

CV: Coefficient of Variation

DMSO: Dimethyl sulfoxide

DPPH: 2,2-Diphenyl-1-picrylhydrazyl

DSC: Differential scanning calorimetry

DTG: derivative thermogravimetry

EA: *Enterobacter aerogenes*

EC: *Escherichia coli*

EP: Ethanol productivity

ERS: Economic Research Service

EY: Ethanol yield

F-test: Fisher's Satirical test

FAME: Fatty Acid Methyl Ester

FAO: Food and Agricultural Organisation

FC: Fixed carbon

Fe_3O_4: Iron(II,III) oxide or ferrosoferric oxide

FESEM: Field Emission Scanning Electron Microscopy

FTIR: Fourier Transform Infrared Spectroscopy

FTIR-ATR: Fourier Transform Infrared Spectroscopy - Attenuated Total Reflectance

GAE: gallic acid equivalent

GAS: global score of antioxidants

GCMS: Gas chromatography-mass spectrometry

GHG: Greenhouse gas

GRAS: generally recognised safe

H: Hydrogen

HMF: Hydroxymethylfurfural

5-HMF: 5-hydroxymethylfurfural

HPLC: High-performance liquid chromatography

H_2SO_4: Sulfuric acid

$I_{amorphous}$: amorphous peak intensity at $2\theta = 15.6°$

$I_{crystalline}$: peak intensity of cellulose at $2\theta = 22.4°$UV-Vis: Ultraviolet-Visible

IC_{50}: Half-maximal inhibitory concentration

IP: Induction period

KP: *Klebsiella pneumoniae*

LCB: Lignocellulosic biomass

L/S ratio: Liquid to solid ratio

MC: Moisture content

ME: methanolic extract

MIC: minimum inhibitory concentration

MGYP: Malt extract, glucose, yeast extract, peptone

ML: *Micrococcus luteus*

MTCC: Microbial Type Culture Collection and Gene Bank

MUFA: monounsaturated fatty acids

N: Nitrogen

NaCl: Sodium chloride

NaOH: Sodium hydroxide

Na_2CO_3: Sodium carbonate

NCIM: National Collection of Industrial Microorganisms

NLCs: Lipid carriers

NREL: National Renewable Energy Laboratory

O: Oxygen

OD: Optical density

OD600: Optical density at 600 nm

OSI: Oil stability index

P. stipitis: *Pichia* (*Scheffersomyces*) *stipitis* p-value: probability value

PA: *Pseudomonas aeruginosa*

PFGA: Passion Fruit Growers Association

PG: Propyl gallate

PH-RPFR: raw passion fruit rind residue after H_2SO_4 hydrolysis

PUFA: polyunsaturated fatty acids

PUH-PFR: passion fruit rind residue obtained from post-ultrasound-assisted extraction and sulphuric acid treatment.

PV: Peroxide value

QE: Quercetin Equivalent

r^2 value: coefficient of regression

RDI: Recommended Daily Intake

RPFR: Raw passion fruit rind

RSM: Response Surface Methodology

RUE: Rutin Equivalent

S: Sulfur

SA: *Staphylococcus aureus*

S. cerevisiae: Saccharomyces cerevisiae

SBO: soybean oil

SBOE: Soybean oil with YPFR extract

SC: supercritical carbon dioxide extract

SC-ET: supercritical carbon dioxide with 10 percent ethanol extract

SCO_2: Supercritical Carbon dioxide

SE: *Staphylococcus epidermidis*

SFA: saturated fatty acid

SFE: Supercritical fluid extraction

SFO: sunflower seed oil

SFOE: Sunflower oil with YPFR extract

SHF: Separate hydrolysis and fermentation

S/L ratio: solid-to-liquid ratio

SO_2: Sulfur dioxide

SPFR: spent passion fruit rind

SSCF: Simultaneous Saccharification and Co-Fermentation

SSF: Simultaneous saccharification and fermentation

SSFF: Simultaneous Saccharification, Filtration, and Fermentation

TBHQ: tert-butyl hydroquinone

TCC: Total carotenoid content

TFC: Total flavonoid content

TGA: Thermogravimetric analysis

TG curve: Thermogravimetric curve

t_{ON}: onset temperature

TPC: Total phenolic content

UAE: Ultrasound-assisted extraction

VM: Volatile matter

$w_{after\text{-}treatment}$: Residual amount of polymer present in the alkali-treated residue.

$w_{before\text{-}treatment}$: Mass of the cellulose/xylan/lignin present in the pretreated residue

XRD: X-ray diffraction

YP: Yeast extract and peptone

YPD: Yeast extract, peptone, dextrose

YPDX: Yeast extract, peptone, dextrose, xylose

YPFR: Yellow Passion Fruit Rind

ZOI: Zone of Inhibition

Symbols and Units

% - Percentage

Å - Angstrom

°C - Degree Centigrade

°C/min - Degree Centigrade per Minute

CFU/mL - Colony-Forming Units Per Milliliter

cm^{-1} – Per Centimeter

db - Dry Biomass

dw - Dry Weight

eV - Electron Volt

g – Gram

g_P/g_S – Gram of Ethanol Produced Per Gram of Sugar Consumed

g/g - Gram Per Gram

g/kg - Gram Per Kilogram

g/L – Gram Per Litre

g/min - Gram Per Minute

g/L/h - Gram Per Litre Per Hour

h – Hour

kJ/mol – Kilo Joule Per Mole

kg – Kilogram

kg/m3 – Kilogram Per Cubic Meter

L – Litre

M - Molar

MJ/kg – Mega Joule Per Kilogram

MASL - Meters Above Sea Level

m3 – Cubic Meter

mm – Millimeter

mg β-carotene equivalent/kg – Milligram Beta-Carotene Equivalent Per Kilogram

mg GAE/g - Milligram Gallic Acid Equivalent Per Gram

mg/g - Milligram Per Gram

mg/mL - Milligram Per Millilitre

mg QE/g - Milligram Quercetin Equivalent Per Gram

mg RE/g - Milligram Rutin Equivalent Per Gram

mL - Millilitre

mL/g – Millilitre Per Gram

mM – MilliMolar

min – Minute

mg KOH/g – Milligrams of KOH Per Gram

meq O_2/kg - Milliequivalents of Oxygen Per Kilogram

µm - Micrometer

µg β-carotene/g – Microgram Beta-Carotene Per Gram

µg/g - Microgram Per Gram

µg/mL - - Microgram Per Millilitre

µL – Microlitre

nm - Nanometer

ppm – Part Per Million

rpm – Rotation Per Minute

Wh/kg – Watt-Hours Per Kilogram

W/kg - Watt Per Kilogram

wt% – Weight Percentage

w/w – Weight by Weight

w/v – Weight by Volume

vol% – Volume Percentage

List of Tables

CHAPTER 6

CHAPTER 7

List of Figures

CHAPTER 1

CHAPTER 2

CHAPTER 3

CHAPTER 6

CHAPTER 7

1. CHAPTER 1

Introduction and Literature Review

Background
Current status
Objectives
Thesis Organisation

Part of this work has been published as Kakali Borah, Vaibhav V Goud, 2024. Sustainable Waste to Energy Technologies: Fermentation. In: Dr. Arbind Prasad and Dr. Atanu Kumar Paul (Eds). Biodegradable Waste Processing for Sustainable Developments, CRCPress 150-172. DOI: 10.1201/9781003502012-7

Another part has been communicated as Sukumar Purohit, Kakali Borah, Vaibhav V Goud, Unlocking the Potential of Passion Fruit Waste By-Products through Biorefinery and Bioresource Innovation, Bioresource Technology Reports. (Authors contributed equally)

Introduction and Literature Review

This chapter explores the present scenario of agro-industrial waste valorisation and its role in the bio-based economy. This study investigates passion fruit rind as a viable feedstock for the extraction of natural antioxidants and their applications in several industries, such as food, cosmetics, pharmaceuticals, and biofuel production. The rationale behind the study has been discussed and offers an outline of significant concerns related to energy security and the current situation of food waste management. Besides, a thorough analysis of the literature is presented.

Introduction

Background

The rising concern over environmental degradation and the depletion of fossil resources has accelerated the shift towards a bio-based economy. Through the integration of innovation, conservation, and economic growth across agriculture, forestry, and biotechnology, the bio-economy has emerged as a possible solution to address global concerns such as resource shortages, environmental degradation, and climate change [1]. Agro-industrial waste offers tremendous potential for creating valuable chemicals and biofuels, supporting sustainable waste management. The agriculture industry, which includes the production, processing, and marketing of forestry and agricultural goods, substantially contributes to the world economy. According to the World Bank 2020, industry and agriculture together contribute roughly 28% and 4% of the global GDP, respectively [2]. Nevertheless, these operations need a lot of energy, water, and soil, and produce a lot of liquid, solid, and gaseous waste. This is especially true in the food industry, where there is a lot of organic waste and environmental pollutants produced daily. Sharma et al. [3] reported that every year, India burns 92 million tons of agricultural waste (18.4%), which emits greenhouse gases, pollutes the ecosystem, and poses health hazards. The development of modern technologies that support agro-industrial waste valorisation, converting wastes into useful goods, and promoting sustainable waste management solutions, has resulted from the growing concern over these problems.

The agro-industrial waste includes items produced by agricultural operations and associated industries, such as residual crops, animal by-products, and fruit and vegetable waste. Agro-industries, particularly the food sector, generate significant amounts of organic waste from processing, treatment, and disposal activities. These food-processing wastes are usually rich in carbohydrates, lipids, oils, proteins, vitamins, polyphenols and other bioactive compounds [4]. *Passiflora edulis* (Passion fruit) is a typical example of such a crop, which is primarily cultivated for juice processing. Belonging to the *Passifloraceae* family, passion fruit is a tropical and subtropical vine that yields nutritious fruits. The *Passiflora* genus contains more than 600 species, though the main edible varieties are granadilla (*Passiflora quadrangularis* L.), purple passion fruit (*Passiflora edulis* Sims), yellow passion fruit (*Passiflora edulis* f. *flavicarpa* Deg.), and sweet granadilla (*Passiflora ligularis*) [5]. Brazil leads the world in both production and consumption of passion fruit, followed by several other countries such as Colombia, Indonesia, Portugal, Malaysia, Australia, China, and India [5–10]. A survey conducted by Stafne et al. [11] on the passion fruit industry in the United States revealed that the crop is primarily cultivated for commercial purposes (Figure. 1.1). Its demand continues to grow because of its high-quality fruits, favorable yield, and consumers' demand in both domestic and international markets. It is extensively utilised in producing various food items such as cakes, ice cream, sauces, drinks, jams, and jellies [12]. Apart from its economic importance, passion fruit is highly valued for its nutrient profile and therapeutic benefits; it has long been utilised as an anti-inflammatory, antitumor, antihypertensive, antioxidant, and anticancer agent [5]. Bioactive components, such as carbohydrates, polyphenols, vitamins, lipids, and antioxidants, are present in passion fruit leaves and by-products (such as peel, seed, and bagasse), which enhances their potential for medicinal use [13]. However, the fruit peel, which makes up 62% of the fruit overall, has a lot of potential for value-added uses and industrial development [14]. Different parts of passion fruit are mentioned in Figure 1.2. The need for food has surged due to the exponential growth in the world's population, which has fuelled the flourishing of the food processing industry. However, the manufacturing of food items like juice, jam, and wine produces a lot of by-products (such as peel, pulp, and seed), which contribute to environmental pollution and financial strain because they pile up excessively. Passion fruit juice processing industries face similar challenges with by-product accumulation. Significant efforts are being made to repurpose waste materials such as peel, pomace, and seeds for the development of

value-added products, aiming to improve the nutritional and functional properties of new food products, medicinal formulations, cosmetics, and bioenergy products. The valorisation of such waste through sustainable extraction and bioconversion processes helps minimise waste generation and adds economic value.

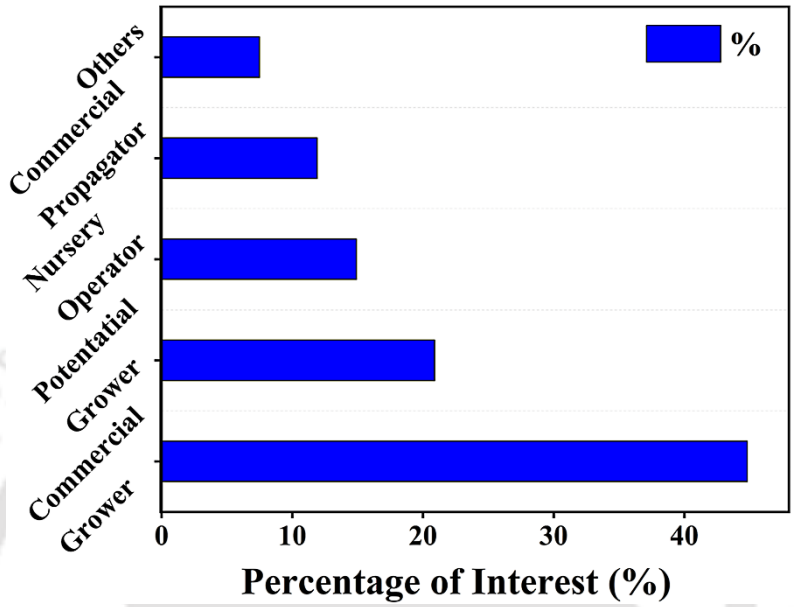

Figure 1.1. Distribution of interest in growing passion fruit throughout tropical and subtropical regions of the United States [11]

Although wastes are a significant secondary carbon resource, it is mostly disposed of by incineration or landfilling in a linear economy, which results in a loss of carbon resources and contributes to social, environmental, and climate problems [15]. The recycling of organic waste as a potential natural resource is in the exploratory stage. Processing passion fruit juice results in a large quantity of waste; more than 60% of the fruit's weight is discarded, accounting for over 1.05 million tons per year [5]. Therefore, the valorisation of passion fruit rind through the extraction of bioactive compounds and biofuel production provides a dual advantage, it minimises generated waste and produces valuable products, while further contributing to tackling the present fossil fuel crisis issues. This study supports international efforts to achieve sustainable development by producing functional food supplements along with renewable energy while managing waste sustainably. By substituting fossil fuels with organic waste as a secondary feedstock, a circular carbon economy seeks to improve environmental protection, conserve resources, and lessen reliance on imported fossil fuels.

Figure 1.2. Overview of different parts of passion fruit. (a) Passion Fruit Vine, (b) Passion Fruit Leave, (c) Passion Fruit Flower, (d) Passion Fruit, (b) Passion Fruit Juice, (b) Passion Fruit Seeds

Passion fruit in North-East India

The species of *the Passifloraceae* family was first discovered in the 16th century as wild in Latin American rain forests, and currently serves as a key component of the world's economy and agriculture in many countries such as Brazil, Colombia, China, and India [16]. Among its 500–600 species found in tropical and subtropical areas, a few species are commonly cultivated, such as the *P. edulis* Sims, *P. edulis* var. *flavicarpa*, *P. ligularis* Juss., *P. alata* Dryander, *P. mixta* L., *P. cumbalensis* (Karst.) Harms, *P. maliformis* L., *P. pinnatistipula* (Cav.) DC., *P. quadranugularis* L., *P. antioquensis* Karst., *P. tripartite* (Juss.) Poir, and *P. serrulata* Jacq., *P. popenovii* Killip [17]. These fruits require particular temperatures, amounts of rainfall, and altitudes for optimal growth in a variety of agroclimatic situations. It favors moderate sandy loamy or sandy clay-loam soils containing a pH of 6.5 to 7.5, and they survive in environments with 60–80% humidity and 1000–2500 mm of yearly rainfall. The ideal circumstances for growth for each species are as follows: *P. ligularis* Juss. prefers 15–23°C and 1,800–2,600 MASL (meter above sea level); *P. alata* Curtis develops at 25–26°C and 100–700 MASL; *P. edulis* sims. f. *edulis* grows at 12–22°C and 1,600–2,800 MASL; *P. mollisima* Kunth needs 13–16°C and 1,800–3,200 MASL; and *P. edulis* Sims. *edulis*

needs 15–22°C during the day and 12–14°C at night. These plants require at least 7 to 8 h of sunlight per day to grow and bloom, as cloudy conditions impede development [18,19].

In the 1800s, passion fruit spread to Europe and Asia, and through Sri Lanka, it reached India in the early 20th century [20,21]. In India, the Northeastern provinces i.e. Manipur, Mizoram, Nagaland, and Sikkim, as well as portions of southern India like Kerala, Tamil Nadu (Kodaikanal and Nilgiri Hills), and Karnataka (Coorg), are the main locations for passion fruit production. It covers 19.01 thousand hectares, and the annual production is 123.94 thousand tons, with Manipur and Nagaland accounting for 93% of that total, as shown in the figure. 1.3 [22].

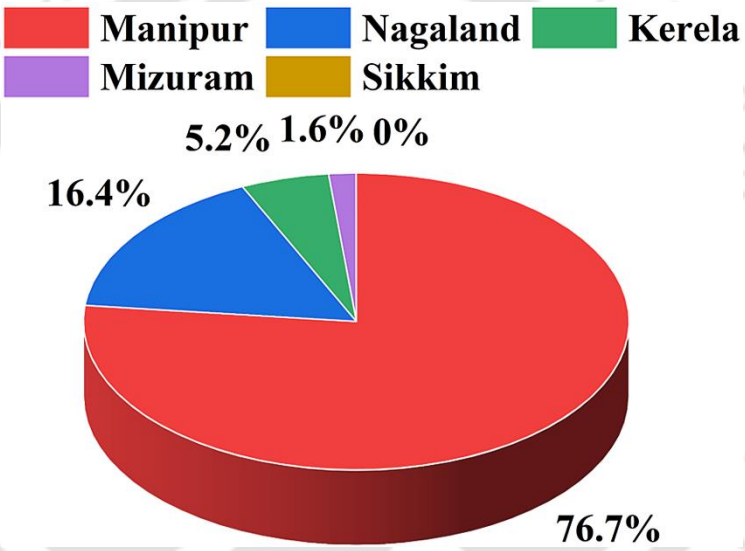

Figure 1.3. Production of PF in India in 2014-15 according to National Horticulture Board [22]

Passion fruit in India is mainly cultivated for its nutritious juice, and it is also used to make other food products such as squash, jams, and jellies. However, compared to fruits like oranges, pineapples, and mangos, its market attractiveness is still limited, even if it is a high-value crop. A few processing facilities have emerged, primarily in the Northeastern states. There are two passion fruit processing plants (Exotic Juices and a new facility) located in Manipur, whilst Nagaland has three: a now-closed site in Lungnak, a privatised plant in Dimapur, and a new one in Mokokchung. Additionally, Mizoram has a new processing facility. One notable product is the juice drink "Pasip," produced by Exotic Juices Ltd. in Manipur, with an annual capacity of 1.5 million litres. It is sold by EcoVerse in major Indian cities and is destined for export [22]. Nevertheless, despite these developments, the passion fruit business faces obstacles to

growth, including poor post-harvest techniques, logistical difficulties, and restricted market accessibility as compared to other fruits.

In India, passion fruit comes in two main edible varieties: purple (*Passiflora edulis* Sims), indigenous to tropical America; and yellow (*Passiflora edulis* f. *flavicarpa* Deg.), a natural cross with another similar species or a variant of the purple form. Additionally, Giant granadilla (*P. quadrangularis* L.) is found in some hot, humid regions on a small scale. Furthermore, the wild species *P. foetida* L. is renowned for its precocity, quick maturity, and tiny fruits. In India, the Northeastern states tend to grow purple and yellow variants, whereas the southern states choose to grow the hybrid variety "Kaveri," which is a cross between purple and yellow developed by the Indian Institute of Horticultural Research and gives high yield [22].

Historically, different portions of passion fruit have been used for many years to treat a variety of illnesses. In Nagaland, dehydrated passion leaves are used to cure hypertension and diarrhoea, while the blossoms are traditionally used to make a tea that relieves pain [23]. Certain types, including *P. incarnata,* have long been used in medicine to treat morphine addiction, hypertension, and pain. Dhawan and his team examined the pharmacological characteristics of the aerial portions of *P. incarnata,* such as leaves, stems, and flowers, in vivo research, and revealed the plant's aphrodisiac effects, bronchospasm-relieving qualities, antitussive potential, and anxiolytic activity [24–29].

The Indian passion fruit industry confronts several obstacles, such as limited market access, poor transportation infrastructure, and ineffective post-harvest practices, despite the fruit's potential for nutrition and medicine. Compared to other fruit sectors, these obstacles restrict its potential for growth. To tackle these problems, the Passion Fruit Growers Association (PFGA) was founded in Manipur in 2004, with the goal of improving the financial status of cultivators and entrepreneurs via passion fruit farming [30]. To encourage grassroots economic growth and improve market participation, the association has incorporated the local rural people into its activities.

Apart from its food production applications, such as making beverages, jams, and jellies, Indian researchers are currently investigating the potential of passion fruit biomass for developing goods with additional value. For possible use in pharmaceutical and dietary applications, this involves extracting dyes, phytochemicals, and antioxidants. The passion fruit sector has the potential to grow sustainably as these

projects move forward, so long as marketing and post-harvest management issues are successfully resolved.

1.1. Literature Review

1.1.1. Assessment of Nutritional and Phytochemical Properties of Passion Fruit

The tropical and subtropical fruit, Passion fruit (*Passiflora edulis*), is recognised for its distinctive aroma and flavour, additionally for its remarkable nutritional and phytochemical composition. It is extensively consumed fresh and employed in commercial processes, such as for the manufacture of juice, jelly, and ice cream [22]. Despite being originally an indigenous fruit, passion fruit cultivation has become more and more popular because of its delicious and nutrient-dense juice. The global yearly production of passion fruit is estimated at 0.85 million tonnes, with Brazil accounting for around 60% of the total output, followed by Indonesia at 10%, India at 9%, and Colombia at 5% (Figure 1.4) [31]. FAOSTAT 2017 reported that the economic worth of Brazil's passion fruit sector exceeds US$340 million, propelled by the cultivation of fresh fruit and juice goods [32].

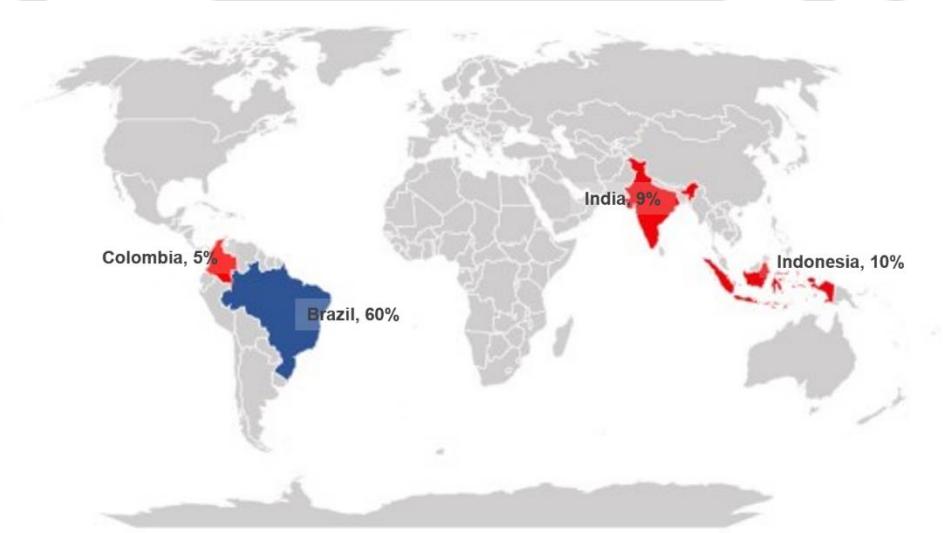

Figure 1.4. Global contribution of leading countries to Passion fruit Production. The map illustrates the distribution of passion fruit cultivation around the world, showing the top-producing countries, based on the information reported by [32].

Industrial processing produces merely 36% juice, with 51% being rind and 11% consisting of seeds, as illustrated in Figure 1.5 [12]. A minor portion of this by-product is utilised as cow feed, while the remainder is disposed of, leading to considerable environmental challenges. The high moisture and organic composition of these wastes result in greenhouse gas emissions, bacterial growth, and environmental deterioration

[33]. The increasing quantity of by-products, propelled by the increasing demand for passion fruit, offers an opportunity to investigate alternative applications across many industries. Employing these by-products provides a sustainable approach to diminishing waste, tackling environmental issues, and augmenting economic value, in accordance with global sustainability and waste reduction agendas.

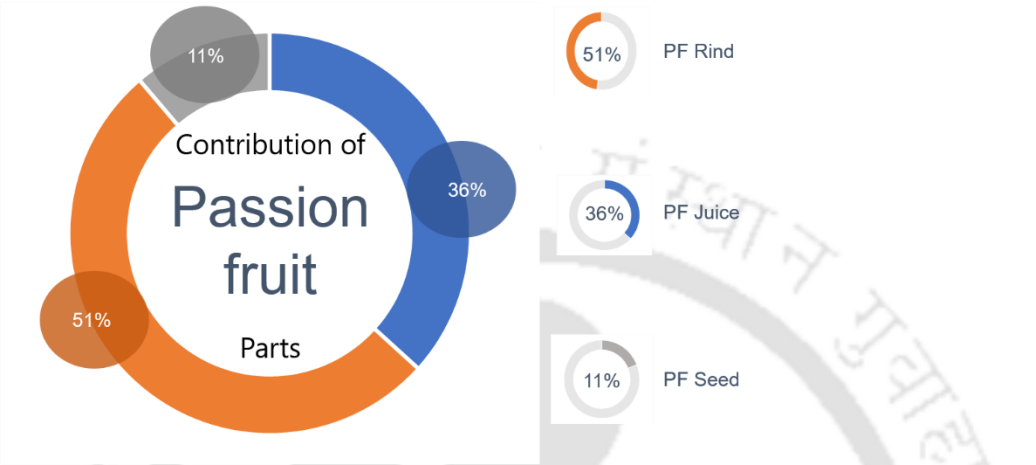

Figure 1.5. Distribution of components of Passion fruit. The graph highlights the quantity of passion fruit parts by showing the proportionate contribution of fruit parts like pulp, peels, and seeds [12].

Numerous studies have found that passion fruit by-products are a significant source of vital nutrients, notably dietary fibre, vitamins, and minerals, as well as phytochemicals, including phenolic acids, flavonoids, and carotenoids. The antioxidant capacities of these bioactive substances help neutralise free radicals, thus mitigating oxidative stress. These molecules have shown promise in diverse applications, ranging from functional food to food preservative development. Historically, passion fruit leaves, juice, and seeds were utilised in herbal remedies for numerous diseases, despite a lack of comprehensive understanding of their composition. Recent studies on phytochemical analysis of passion fruit by-products have shown a variety of beneficial chemicals and investigated many extraction methods along with solvent systems to effectively separate these chemicals from the plant matrix.

1.1.2. Nutritional composition of Passion Fruit

Studies found various essential nutrients, including dietary fibre, vitamins (particularly vitamin C and provitamin A), and minerals such as potassium, magnesium, and iron in passion fruit by-products. Fonseca et al. [34] reported that carbohydrates constitute the majority of passion fruit parts (peel, pulp, and seed), accounting for around 69.9-89.4%

on a dry weight basis, apart from the moisture content (45.9-87.0%). The seeds possess the highest protein content (13.2% DW) and fat content (14.9% DW); however, peels have the greatest fibre content (61.7% DW). The pulp and juice of passion fruit are abundant in vitamin C and could supply up to 40.0% and 93.2% of the Recommended Daily Intake (RDI) per 100 g fresh weight, respectively [35]. The vitamin C content in passion fruit varies by temperature and species, exhibiting notable variances among the types. The leaves of yellow passion fruit contain up to 292.5 mg/100 g of vitamin C, influenced by plant age and agronomic factors [36]. Moreover, according to the Food Composition Database of the US Department of Agriculture, passion fruit is abundant in vitamins A (717–943 IU) and vitamin B [37]. However, the peels and seeds contain substantial amounts of other minerals like potassium, copper, magnesium, zinc, and iron [35]. Minerals are essential for metabolism and are required in minimal amounts in the body. This offers passion fruit to be considered as a significant component of a nutritious diet [36]. Ramaiya et al. [38] revealed that the daily intake of 275 g of it serves micronutrient needs. However, a cup of PF juice fulfils 3–6% of the daily sodium requirement. Apart from that, organic acids are prevalently present in passion fruits. Song et al. [39] reported that *P. foetida* contained citric acid (50.00%) and oxalic acid (29.17%), accounting for 79.17% of the total acids. The high citric acid concentration facilitates its application as a food additive and in cosmetic formulations [36]. Additionally, passion fruit is abundant in amino acids [40], with 17 identified in Passiflora, particularly glutamic acid and arginine [41]. Essential amino acids constitute 26.07% of total amino acids, exceeding human dietary needs [36]. The chemical composition of various passion fruit species is affected by factors like breed, environment, and farming technique, resulting in considerable heterogeneity even among the same species. Additionally, the absence of standardised analytical methodologies and variable units in quantitative studies contributes to variations in outcomes [35].

Hu et al. [42] reported that phytochemicals undergo liberation, absorption, metabolism, and excretion within the human body. Their physiological effects are reliant upon three principal factors: bioaccessibility refers to the portion liberated from the food matrix that is accessible for absorption, bioavailability refers to the proportion that is absorbed into the bloodstream and available to tissues, and bioactivity is the degree to which they enhance advantageous impacts on health at specific locations. The parameters are

affected by the food matrix, processing techniques, and the chemical characteristics of the phytochemical. Lipids frequently improve solubility and absorption, but dietary fibres may obstruct or occasionally facilitate release. Processing can deteriorate compounds (e.g., heat treatment) or enhance accessibility (e.g., ultrasound, microwave, or nonthermal techniques such as freeze-drying, high pressure, pulsed electric field).

1.1.3. Phytochemical Properties of Passion Fruit

In addition to its nutritional content, passion fruit by-products are abundant in phytochemicals such as phenolic acids, flavonoids, and carotenoids. These secondary metabolites are mostly recognised for their bioactivity and utilised in conventional healthcare, the pharmaceutical sector, and nutritional supplementation for humans [35]. A bibliometric analysis of 161 references detailing the bioactive components in passion fruit by-products was performed using VOS viewer. The software depicted co-occurrence networks of keywords that appeared a minimum of 10 times, with the size of circles and labels representing keyword frequency, while closeness indicated co-occurrence. Figure 1.6 illustrates that commonly recurrent phrases encompass “flavonoids,” “anthocyanins,” “phenolics,” and “antioxidants,” emphasising PF by-products as abundant sources of secondary metabolites with significant antioxidant properties.

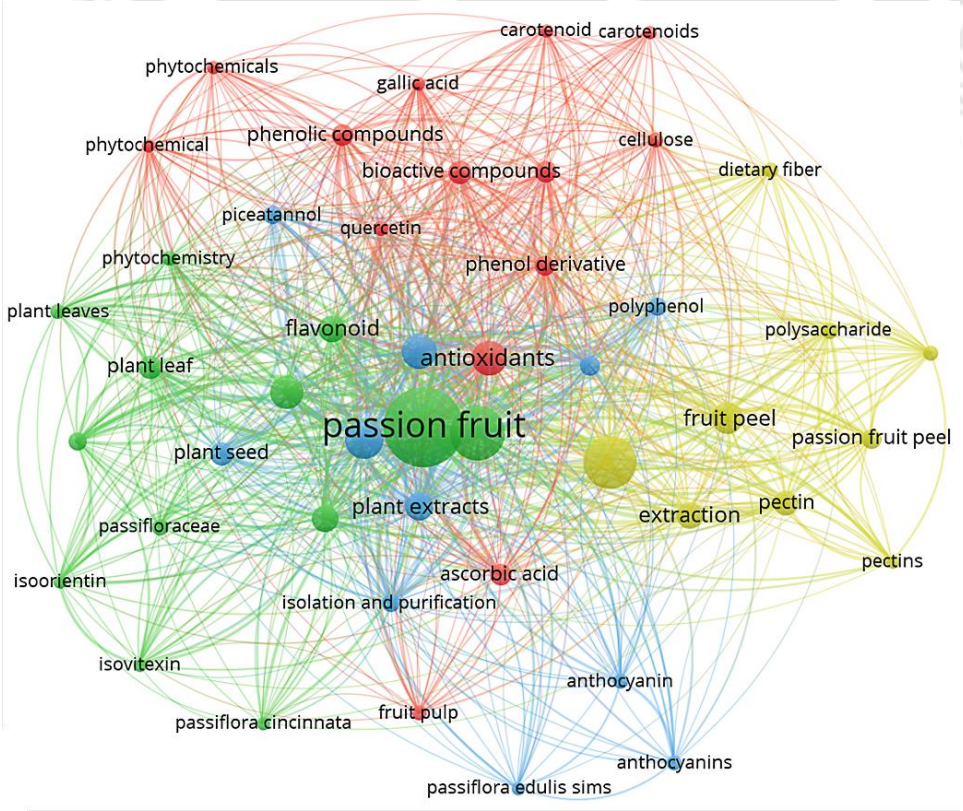

Figure 1.6. A co-occurrence assessment of keywords that appear a minimum of 10 times in research articles addressing the composition of passion fruit from the year 2020 to 2025, performed using VOSviewer (version 1.6.20), with data obtained from Scopus.

Passion fruit species are abundant in polyphenols, comprising phenolic acids, flavonoids, and stilbenes, with total phenolic content varying from 0.36 to 305.8 mg GAE/g [16,43–51]. Principal phenolic acids comprise coumaryl quinic acid derivatives, chlorogenic acid, rosmarinic acid, and syringic acid [16,41]. Shanmugam et al. [52] extracted 24 polyphenolic compounds from *P. leschenaultia*, including caffeic acid, cinnamic acid, and vanillic acid. Flavonoids, such as isoorientin (30.11-75.14 mg/kg), quercetin (20.00 mg/g), and rutin, recognised for their antioxidant and antibacterial characteristics, are prevalently found in PF by products [43,53]. Anthocyanins, including cyanidin-3-O-glucoside (639.36 mg/g), cyanidin-3-O-rutinoside (40.49 mg/g), and peonidin-3-O-rutinoside (30.55 mg/g), have been identified in *P. edulis* epicarp ethanolic extracts [54].

Stilbenes, such as *scirpusin* B and piceatannol, were extracted from purple passion fruit seeds utilising chromatography and liquid extraction methods [55]. Purohit et al. [56] isolate 1.97 mg/g of scirpusin B from yellow passion fruit seed. A triterpene, Squalene (0.91 mg/g), and carotenoid, β-carotene (38.64 mg/kg) were recovered from the by-products of *P. edulis Sims* [57]. dos Reis et al. [58] found the orange peel PF exhibiting the highest carotenoid concentration (25.52 mg/100 g) compared to purple and yellow. PF seed oil, obtained using supercritical fluid extraction, comprises 1.68% α-tocopherol [59]. Other discovered substances comprise flavones (chrysoeriol derivatives), flavanones (pinocembrin), terpenes (limonene, β-caryophyllene), and stilbenes (trans- and cis-resveratrol), underscoring the bioactive potential of passion fruit by-products for nutraceutical and industrial uses [16,48,52].

1.1.4. Extraction Techniques for Bioactive Compounds from Passion Fruit

The extraction of bioactive compounds from passion fruit and its by-products, including the rind, seeds, and pulp residues, has gained significant research attention due to their abundance of antioxidants, phenolics, flavonoids, alkaloids, and other bioactive substances with nutritional benefits and commercial uses. Various techniques have been used to isolate these phytochemicals (Table 1.1), each possessing distinct processes, efficiencies, and environmental impacts. The efficiency and efficacy of extraction techniques are essential for optimising yield and maintaining the biological

activity of these substances. Although, conventional techniques, like maceration, Soxhlet extraction, and hydrodistillation are widely used; however, they have constraints regarding poor process efficiency, high energy, and time requirements, the use of hazardous solvents, the thermal destruction of compounds, a detrimental effect on the environment, and the production of extracts of subpar quality [60]. As a result, a variety of approaches to the sustainable extraction of phytochemicals from biowaste have been developed in order to satisfy the needs of a concerned society. The increasing concentration of targeted molecules and the development of bioassays with high selectivity and sensitivity make the advanced methods more popular [61]. These methods include ultrasound, microwave, supercritical fluid, pressurised liquid extraction, and others. A summary of the application of different extraction methods to extract polyphenols from passion fruit by-products has been listed in Table 1.2. In recent years, extensive research has been done on ultrasound-assisted extraction (UAE) of valuable chemicals from plant waste. UAE is based on the use of ultrasonic energy (sound waves with frequencies more than 20 kHz), which makes it easier for a solvent to extract analytes from a solid sample. The formation, growth, and collapse of microbubbles inside a liquid phase cause the rupture of cell walls. This improves the contact of the solvent with the available extractable cellular material and speeds up diffusion, thus increasing the extraction efficiency [62]. UAE has benefits over the traditional approach, including selectivity, low energy consumption, a shorter extraction time, less solvent use, and less consumption of dangerous chemicals [63]. The application of environment-friendly solvents, such as supercritical fluid, made room for the food industry as a potential area of application. The properties of these fluids are intermediate between gases and liquids under supercritical conditions, which makes compound extraction easier. With high diffusivities and low viscosities, SFE has a number of benefits for extracting natural substances, including essential oils, lipids, tocopherols, and carotenoids from plants and biomass. To increase the rate of extraction and yield, these qualities can be changed by altering the temperature and pressure [64]. A supercritical fluid, carbon dioxide (CO_2), due to its stability and safety, is frequently used in the food business and is also tasteless, odourless, and non-toxic [65]. In this process, the mixture of solvent (supercritical carbon dioxide) and extracted compounds is transferred and separated by depressurising the system, leaving the pure form of the extracted compounds. The lipophilic nature of the CO_2, which normally helps to recover non-polar and moderately polar molecules, is the basic restriction on SFE.

Addition of co-solvents/ modifiers/ entrainers alters the polarity of the solvent system, increasing the capacity of solvating and boosting its affinity for polar molecules [66]. Ethanol is frequently used to entrain or modify supercritical CO_2. Ethanol is categorised as a generally recognised as safe (GRAS) solvent in accordance with the Sustainable Development Goals for good health and well-being established by the United Nations [65]. Table 1.1. demonstrated the advantage of UAE and SFE over conventional methods. Thus, the UAE and SFE are advanced extraction methods that improve efficiency, quality, and sustainability in the extraction of bioactives from passion fruit by-products. The UAE provides high yield, uses minimal solvent, and has a scope of scale-up, making it ideal for phenolics and flavonoids. Supercritical fluid extraction (SFE), devoid of hazardous solvents, demonstrates superior purity, selectivity, and efficacy in extracting lipophilic chemicals such as carotenoids, yielding high-quality extracts for medicinal, nutraceutical, and cosmetic applications. Both approaches maintain bioactivity under mild processing settings, conforming to sustainability objectives and providing diverse applications in harnessing the nutraceutical and functional potential of passion fruit. The schematic of the UAE and SFE setup has been depicted in Figure 1.7.

Table 1.1. Comparison of UAE and SFE with other conventional extraction methods

	Conventional methods	UAE	SFE
Selectivity	Moderate	High	Low
Solvent usage	High	Less	less
Process duration	Long	short	moderate
Temperature sensitivity	Suitable for thermolabile compounds	Suitable for thermolabile compounds	Poor
Environmental impact	Eco-friendly	Eco-friendly	High solvent wastage
Cost	Moderate	High (equipment cost)	Low

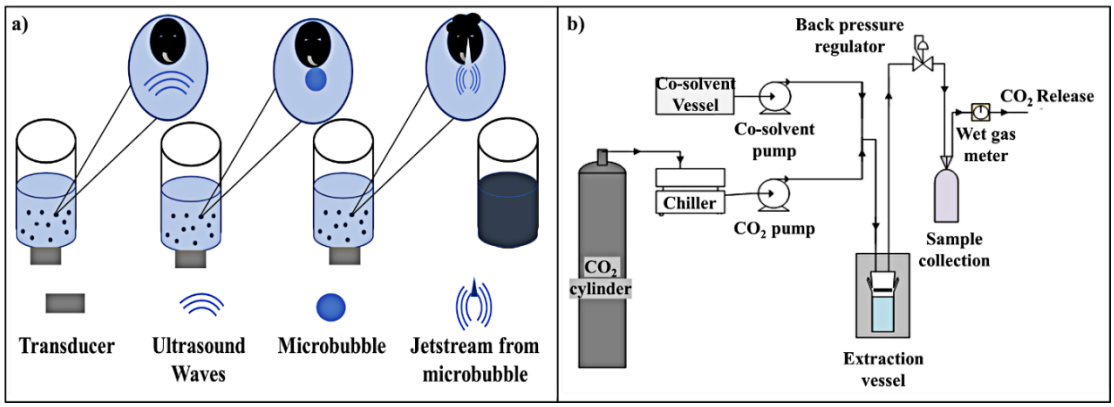

Figure 1.7. The experimental setup for a) UAE and b) SFE

Table 1.2. A summary of the application of different extraction methods to extract polyphenols from passion fruit by-products

Species used	Extraction method	Solvent used	Extracted phenolic compounds	References
Passion fruit peels	Ultrasonic and microwave extraction	Ethanol:water:acetone	TPC = 17.47-38.52 mg GAE/g, TFC =8.72-26.08 mg RE/g	[67]
P. edulis Leaf	Pressurised liquid extraction	70% ethanol	TPC = 30.0-43.2 mg GAE/g, TFC = 30.0-58.8 mg QE/g	[68]
P. edulis Sims peel	Water bath	DES	TPC = 9.68 mg GAE/g	[69]
P. ligularis Juss peel	Pressurised liquid extraction and CO_2-expanded ethanol	ethanol and CO_2	TPC = 1.5-3.0 mg GAE/g	[70]
Passion fruit rinds	Ultrasound-Assisted Pressurised Liquid Extraction	70% ethanol	TPC = 2.07 mg GAE/g	[71]
P. edulis	Maceration	70% ethanol and 70% methanol	TPC = 5.29-9.25mg GAE/g	[72]

seed				
P. edulis Sims by-products	Supercritical fluid extraction	CO_2	TCC = 22.30-38.64 mg β-carotene equivalent/kg, TT = 698.51-1019.12 mg/kg, Squalene = 485.62-913 mg/kg	[57]
P. cincinnata Mast., *P. edulis* Sims	liquid-liquid extraction	ethyl acetate	TPC = 365-476.1 mg/kg, TCC = 0.9-18.7 mg/kg equivalent to β-carotene, Vitamin C = 176.1-264.2 mg/kg	[16]
Yellow and purple passion fruit	Soxhlet	ethyl acetate, acetone, methanol and water	TPC = 26.67-66.53 mg GAE/g, TFC = 29.25-73.39 mg QUE/g	[73]
P. foedita	Maceration	ethyl acetate, methanol, methanol-water (80%), and water	TPC = 39.61-21.30 mg GAE/g, TFC = 50.11-3.22 mg RE/g	[74]
Leaves, flowers, stems and roots of *P. caerulea* L.	Maceration	Water, MeOH:water containing NaF, methanol, ethanol and acetone	10.83-19.77 mg eq GA/g	[75]

TPC = total phenolic content, TFC = total flavonoid content, TCC = total corenoid content, TT = Total Tocols (mg/kg extract)

1.1.5. Application of passion fruit by-products

The by-products of passion fruit, such as its peel, seeds, and pulp leftovers, have attracted notable attention due to multiple uses in the food, pharmaceutical, nutraceutical, and cosmetic sectors. These by-products, frequently seen as waste, are

abundant in vital minerals, phytochemicals, and bioactive substances that present significant opportunities for valorisation. Recycling them not only decreases environmental damage but also conforms to sustainable waste management standards, fostering a circular bio-economy.

1.1.5.1.Food Industry:

Passion fruit has 36% edible content (Figure 1.5). However, its peel and seeds constitute nearly two-thirds of the fruit's waste, presenting opportunities for nutritional and commercial uses in the food sector [76]. Passion fruit-based functional beverages, like kefir, provide improved microbial viability, consistent acidity, and low ethanol levels, positioning them as innovative contributions to the beverage industry [77]. The lactic acid bacteria fermented milk containing 1% (w/v) passion fruit pulp was able to suppress the proliferation of Staphylococcus spp. and Listeria monocytogenes, promote probiotic viability, and extended shelf life and safety [78]. The yoghurt enriched with passion fruit peel, seed, and pericarp flour showed enhanced nutritional, sensory, and rheological characteristics, as well as being rich in fibre and pectin, regulates lactic acid levels and enhances probiotic viability [79–81]. The peel, utilised as a fermentable carbohydrate source, markedly increases folate production in soy-based fermented products [82]. Passion fruit peel has been utilised to produce fiber-rich candies that enhance health and mitigate environmental pollution [83]. A combination of *P. edulis* epicarp and green banana biomass improved the flexibility and moisture content of chicken hamburgers [84]. *P. edulis* flour functions as a stabilising, emulsifying, and thickening agent in goods like nectar, mayonnaise, and ice cream syrups, offering superior stabilisation relative to guar gum and improved viscosity in syrups [85]. However, passion fruit extracts have been employed as preservatives to improve food's nutritional value and technological characteristics. Costa et al. [86] revealed that semi-purified *P. cincinnata* Mast. extracts inhibited *Listeria, S. aureus*, and multidrug-resistant *S. aureus* in traditional Brazilian cheese (coalho), emphasising its antibacterial efficacy. Aqueous and ethanolic extracts enhanced oxidative stability and delayed the decolourization of beef patties by as much as nine days [87]. Although PF by-products have nutritional, dietary, and technological advantages, additional research on their safety and toxicity is essential to fully comprehend their potential.

1.1.5.2.Pharmacology Industry:

The bioactive components in passion fruit by-products make them particularly valuable for pharmaceutical and nutraceutical compositions. Various parts of passion fruit have been utilised as traditional medicine for an extended period without a comprehensive knowledge of their chemical composition [88]. Recent investigations highlighted the pharmacological potential of passion fruit extracts, demonstrating diverse applications. The sub-acute toxicity test of *Passiflora edulis* Sims f. *edulis* (Gulupa) leaves aqueous extract performed by Rodriguez-Usaquen et al. [89] revealed that the extracts (1000 mg/kg/day) were well-tolerated in Wistar rats, though minor histopathological alterations in the liver and kidneys were observed. They observed there was a slight rise in the frequency of focal periportal lymphocytic infiltration in the liver and focal corticomedullary nephrocalcinosis in the kidney due to the extract. Further, *P. tenuifila* extracts, comprising 19 phenolic components, displayed anxiolytic and anticonvulsant effects without acute toxicity in murine models [90]. The Scirpusin B isolated from yellow passion fruit seeds showed strong antioxidant, antidiabetic (inhibited α-amylase and α-glucosidase), antibacterial (against different gram-positive and gram-negative bacteria), and anti-oral cancer (reduced up to 95% SAS oral-cancer cell growth) properties [91]. Ramos et al. [92] revealed that the ethanolic extract of PF leaves dramatically decreased triglycerides (by up to 35% at 24 h) and cholesterol, perhaps suppressing critical enzymes associated with colorectal cancer. Similarly, da Silva et al. [93] found that soluble dietary fibre from yellow passion fruit protected against gastrointestinal mucositis, reversing oxidative stress and inflammation induced by 5-FU chemotherapy. Venkatachalamoorthi et al. [94] reported that 30% *P edulis* extract combined with 17% EDTA demonstrated low erosion and significant efficiency in root canal disinfection. Dewi et al. [95] indicated that 10% seed extract cream significantly reduced acne vulgaris, decreasing lesion counts by more than 70% after eight weeks. Khongrum et al. [96] discovered that daily intake of passion fruit juice markedly benefited lipid profiles in dyslipidemic individuals by decreasing LDL-C and triglycerides, presumably due to improved oxidative stress regulation and decreased inflammation. Although passion fruit exhibits potential therapeutic applications such as antibacterial, anti-inflammatory, anxiolytic, and antidiabetic properties, additional research and clinical trials are necessary to confirm its medicinal efficacy and ensure safety for wider use.

1.1.5.3.Cosmetic Industry:

Protecting skin from adverse external factors, including UV radiation, pigmentation, and photoaging, is a crucial issue. The plant-derived polyphenols help it progressively due to their skin-rejuvenating qualities and, thus, grab interest in the cosmetic industries. *Passiflora edulis* extracts have exhibited considerable dermatological advantages. *P. edulis* f. *edulis* ethanolic seed extract showed significant antiaging potential without toxicity and promoted cell viability [97]. Nazliniwaty et al. [98] similarly documented the anti-aging properties of ethanolic peel extracts (purple, red, yellow), with the purple peel exhibiting enhanced wrinkle repair and melanin reduction. The seed extract exhibited anti-hyaluronidase efficacy with an IC_{50} value of 122.70 ± 6.35 µg/ml, thus suggesting its potential for skin hydration [99]. Additionally, passion fruit extracts are effective against photoaging caused by UV radiation. The sunscreen concealer mousse, incorporated with passion fruit seed extracts, achieved SPF values up to 18.99 without irritation [100]. Maruki-Uchida et al. [101] demonstrated the anti-UVB potential of piceatannol and scirpusin B extracted from passion fruit seeds for keratinocytes, which increased glutathione levels by 77% at 25 µg/ml, reduced ROS by 58% at 22 µg/ml and suppressed MMP1, positioning them as promising anti-UV agents. Furthermore, Jusuf et al. [102] reported the antibacterial activity of passion fruit seed extract (5%), with comparable ZOI to clindamycin, suggesting applications in anti-acne products. Furthermore, nano-emulsions developed using seed oil from *P. setacea, P. cincinnata, P. tenuifila, and P. alata* enhanced HaCaT keratinocyte proliferation, supporting skin tissue rejuvenation due to omega-6 and omega-9 fatty acids [103]. Passion fruit-derived bioactives provide sustainable, multifunctional solutions for the cosmetic industry, aligning with the growing demand for eco-friendly, high-performance beauty products.

1.1.5.4.Renewable energy:

A green approach to waste management that contributes to both the global carbon-neutral goals and the goals for sustainable development is the conversion of *P. edulis* solid waste to bioenergy. Passion fruit residues have been investigated for the production of biogas, bioethanol, biodiesel, and activated carbon (AC) due to their high carbon, cellulose, and nutritional composition.

Biogas production:

Silva et al. [104] documented a 66% methane yield from *P. edulis* peel (3% substrate, 1.243 U/ml cellulase activity) using *Aspergillus japonicus* URM5620 over a 30-day period. The low lignin content (9.5%) of *P. coerulea* waste contributed to higher biomethane output (194.8 mL/g VS in 36 days) than that of litchi, avocado, and cherry residues, attributable to its low lignin content (9.5%) [105]. The considerably high carbon-to-nitrogen ratio (51.6) and cellulose content (25.4%) made passion fruit peel an ideal substrate for anaerobic digestion. dos Santos et al. [106] attained biogas and methane yields of 264 NmL/g VS and 115 NmL CH_4/g VS, respectively, utilising PF peel in conjunction with industrial sludge.

Passion fruit peel with a high value of carbon to nitrogen ratio (C/N= 51.6) and high cellulose content (25.4%) is an ideal substrate for anaerobic digestion. The biogas generation potential of PF peel with industrial sludge was 264 NmL/g VS (volatile solids), and methane was 115 NmL CH_4/g VS [106].

Bioethanol production:

Passiflora peel possesses significant potential for the synthesis of second-generation bioethanol due to its significant carbohydrate content. Megawati et al. [107] generated 8.9% bioethanol from passion fruit peel with a glucose concentration of 66 g/l following enzymatic hydrolysis and fermentation.

Biodiesel production:

The synthesis of biodiesel has demonstrated promise using PF oil (with 85.8% unsaturation). Pantoja et al. [108] generated biodiesel from it, whereas Tippayawong and Chumjai [109] exhibited its commendable engine performance relative to conventional diesel. Jain et al. [110] employed *P. edulis* var. *flavicarpa* seed extract (200 ppm) as a natural antioxidant to enhance the stability of biodiesel to comply with EU and Indian biodiesel regulations.

Activated Carbon for energy storage:

Passion fruit by-products are a suitable raw material for the manufacture of activated carbon for energy applications. The activated carbons synthesised from *P. ligularis* seeds utilising H_3PO_4, achieving a yield of 35-38% [111]. Fu et al. [112] synthesised MnO_2-impregnated activated carbon from passion fruit peel, with a high energy and power density of 42.8 Wh/kg at 499.7 W/kg. A mixture of *P. edulis* shells with

optoelectronic sludge to generate biochar improved combustion efficiency with a calorific value of 17.11 MJ/kg [113].

Passion fruit waste-derived biofuels and materials facilitate clean energy generation, minimise greenhouse gas emissions, and promote efficient waste valorisation, so promoting sustainable and low-carbon progression.

1.1.5.5.Nanotechnology:

Phytochemicals extracted from passion fruit by-products can be utilised to produce nanoparticles, providing a sustainable and cost-effective alternative for tissue engineering, medication delivery, composite materials, and emulsion stabilisation. *Passiflora* sp. peel extracts have been used to produce a variety of nanoparticles, including Ag, Au, and ZnO. These nanoparticles exhibit potent antibacterial effects against *E. coli*, *B. subtilis*, and *S. aureus*, as well as effective dye degradation capabilities, achieving over 90% removal efficiency for methylene blue and rhodamine B dyes [114,115], Santhoshkumar et al. [116] synthesised silver nanoparticles from *P. caerulea* leaves, which decreased hatching rates in zebrafish and suppressed *Trichophyton rubrum*, indicating possible use in the cosmetic industry. Rivas et al. [117] employed spray drying with maltodextrin and inulin to encapsulate carotenoids, phenolics, and vitamin C from mango and passion fruit pulp, obtaining a preserving stability for 90 days. Aerogels infused with piceatannol-enriched bagasse showed significant loading efficiency and potential for bioavailability [118]. However, cellulose nanofibers produced from *P. edulis Sims* stalks immobilised 67% trypsin and maintained 44%, indicating their effectiveness in enzyme immobilisation applications [119]. Lipid carriers (NLCs) formulated with PF seed oil exhibited a high encapsulation effectiveness of 94.91%, enhanced skin penetration (average 68.63 μm), and stability (for over a year at 4°C and 25°C), indicating their potential application in cosmetic formulations [9].

By-products of passion fruit exhibit a great potential in environmental nanotechnology for restoration, drug delivery, enzyme immobilisation, and biomarker applications, and require additional research to understand their full potential.

1.1.5.6.Bioremediation:

Environmental pollution, caused by air, water, and agricultural waste, requires an appropriate solution. *Passiflora* sp. by-products have demonstrated potential as an economical and sustainable resource for bioremediation.

Removal of Dyes and Water Purification:

P. edulis peel has been employed for the removal of dyes and the reduction of water hardness. Gan & Cheok [120] illustrated the effectiveness of both raw and NaOH-treated peel in adsorbing methylene blue and reducing water hardness from 198.75 mg $CaCO_3$/L to acceptable levels at a dosage of 1.8 g. In a similar manner, Nhung et al. [121] decreased 97.9% Rhodamine B dye at a dosage of 1.5 g, showing the efficacy of PF peel as an adsorbent.

Adsorption of Heavy Metals:

The functional groups (-OH, -COOH) in passion fruit peels could efficiently remove heavy metals through ion exchange, adsorption, and micro-precipitation. Chao & Chang [122] documented a cation exchange capacity of 26.9 meq/100 g, facilitating the extraction of Cu, Cd, Ni, and Pb from aqueous solutions at pH 5. Souza et al. [123] discovered that these waste adsorbed Ni^{2+} at a rate of 14.98–46.84 mg/g, which is equivalent to that of commercial activated carbon. Zhao et al. [124] documented the selective removal of Cr(VI) utilising amino-rich passion fruit peel, decreasing 1 mg/L Cr(VI) to 0.05 mg/L after 90 min.

Passion fruit waste functions as an effective, environmentally sustainable adsorbent for the elimination of dyes, heavy metals, and water pollutants. Their application exemplifies a sustainable method for waste valorisation and environmental preservation, presenting opportunities in bioremediation and pollution management.

1.1.6. Effectiveness of Natural Antioxidants in Extending Shelf Life of Edible Oils

Edible oils derived from several plant species, including coconut, palm, soybean, and sunflower, are widely used across several industries, including medicinal products, food items, and beauty products. Yohannes et al. [125] reported that the demand for vegetable oils has consistently increased, with an expected annual growth rate of 5.14% from 2020 to 2025. It constitutes more than 75% of global lipid consumption, is a

critical source of fatty acids, provides energy, regulates body temperature, safeguards tissues, and facilitates the movement of fat-soluble vitamins [126]. These macromolecules, with 9 kcal/g, represent the most concentrated energy source among dietary categories. The Codex Alimentarius suggests that 25 - 30% of energy intake should be derived from oils and fats for a healthy diet [127].

1.1.6.1.Oxidative stability of edible oils

Crude edible oils, mostly consisting of triacylglycerols and several other secondary components such as free fatty acids, phospholipids, phytoconstituents, oxidative by-products, waxes, gums, pesticide residues, and metal ions, are unsuitable for direct consumption due to their undesirable color and odor. Refining is essential to eliminate these undesired elements; however, this process also unintentionally removes advantageous substances (antioxidants) and may produce detrimental by-products such as esters that are carcinogenic, nephrogenic, etc. [127]. Furthermore, lipid oxidation is the main cause of the deterioration of the chemical, sensory, and nutritional qualities of oil during storage and heating, which can lead to health hazards like ageing, harm to the membranes, cardiovascular disease, and cancer [128].

1.1.6.2.Role of antioxidants

Addition of antioxidants, synthetic or natural, is essential to improve oxidative stability and shelf life of edible oil, ensuring their quality and safety. Antioxidants are compounds that prevent oxidation by neutralising free radicals or binding metal ions that promote oxidative processes. They are primarily classified into two categories: synthetic antioxidants and natural antioxidants.

Synthetic antioxidants:

The edible oil industry often utilises artificial antioxidants such as butylated-hydroxyanisole (BHA), tert-butyl hydroquinone (TBHQ), butylated-hydroxytoluene (BHT), and propyl gallate (PG), because of their low cost and antioxidative efficacy; nevertheless, these substances present health risks, including coagulation dysfunction, mutagenesis potential, and carcinogenic risk [129].

Natural antioxidants:

Natural antioxidants are being investigated extensively as a preferable substitute, following customer demands for additives that are naturally sourced and non-toxic.

However, using natural plant-based antioxidants, e.g., green tea, sesame waste, and olive waste [130], especially those made from agro-industrial byproducts, additionally promotes the ideas of waste valorisation and sustainable development.

1.1.6.3.Mechanisms of Action

The oxidative stability of oils can be enhanced with the addition of antioxidants, which hinder oxidation via one or other processes, such as scavenging free radicals, inactivating peroxides, chelating metal ions, quenching secondary oxidation products, and blocking pro-oxidative enzymes [128]. Based on these modes, Mishra et al. [131] classified antioxidants as primary, which neutralise free radicals and disrupt oxidation chain processes, or secondary, which inhibit oxidation promoters such as metal ions and singlet oxygen. Molecules like tocopherols, carotenoids, flavonoids, phenolic acids, polyphenols, and lignans have demonstrated efficacy in improving oil stability. Antioxidant efficiency is influenced by factors such as molecular structure, concentration, temperature, pro-oxidants, and interactions with other antioxidants in edible oils [132]. The factors that affect the edible oil oxidative stability have been described in Figure 1.8.

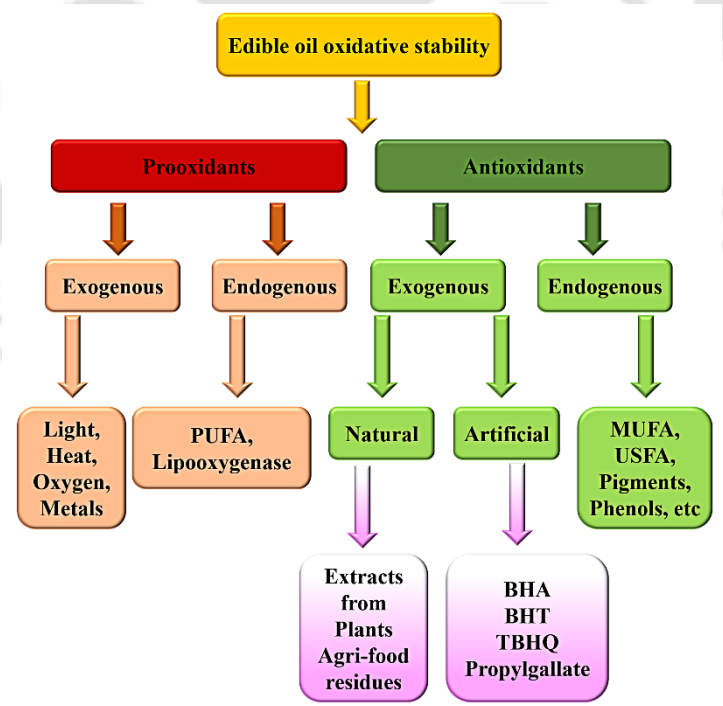

Figure 1.8. Factors involved in the oxidative stability of the edible oil.

1.1.6.4.Applications of natural antioxidants in edible oils

Numerous studies have shown the efficacy of plant-derived antioxidants in improving peroxide value (PV), anisidine value (AnV), and oil stability index (OSI) during storage. Natural antioxidants from olive leaf [133], sea buckthorn [134], and rosemary [135] have been added to edible oils in some studies to increase shelf life.

The addition of 2 g/kg rosemary extract into sunflower, corn, and soybean oils exhibited its stability at frying temperatures, as analysed by thermogravimetric analysis. Oxidative stability studies demonstrated that rosemary extract provided greater protective efficacy than the synthetic antioxidant TBHQ, underscoring its potential as an effective natural antioxidant for edible oils [135]. Refined sunflower oil, cold-pressed sunflower oil, and extra virgin olive oil infused with carotenoids from *Hippophae rhamnoides* by-products exhibited higher oxidative stability, determined by reduced peroxide values, and improved thermal stability. The incorporation of carotenoids lowered oil lightness while enhancing redness and yellowness [134]. To mitigate oxidation and enhance stability, antioxidants are frequently extracted using ethanol and freeze-drying techniques, then incorporated into oils. Environmental variables such as light, heat, pH, and oxygen can deteriorate free-form natural antioxidants, diminishing their antioxidative efficacy, especially at high temperatures [129]. Consequently, the direct integration of natural antioxidants into the oil addresses these constraints. Goula et al. [136] and Chutia et al. [137] had successfully extracted carotenoids from pomegranate peel and passion fruit peel using vegetable oil as a solvent. Thus, edible oil can be utilised as a solvent for the direct extraction of plant-based natural antioxidants, hence improving oil shelf life and satisfying customer demand.

1.1.7. Utilisation of lignocellulosic waste biomass for bioethanol production

The increasing global energy demand and the reduction in crude oil reserves (expected to decline crude oil reserves from 25 billion to 5 billion barrels) pose a significant issue [138]. Moreover, the combustion of fossil fuels substantially contributes to global warming via greenhouse gas (GHG) emissions. Renewable and environmentally sustainable energy options, such as biofuels, have arisen as feasible answers to the energy dilemma. Biofuels, originating from biologically fixed carbon in biomass, function as sustainable alternatives to fossil fuels, simultaneously reducing carbon

dioxide emissions and addressing petroleum resource depletion [139]. Organic waste, comprising significant amount of carbohydrates, proteins, and minerals, poses environmental and health concern due to inadequate management, leading to methane emissions, and leachate-induced pollution of soil and water resources. Waste-to-energy technologies, including microbial fermentation, provide sustainable solutions by transforming organic waste into biofuels, mitigating pollution, and improving resource valorisation [140]. Bioethanol, derived from hexose (C6) and pentose (C5) sugars, serves as a sustainable substitute for transportation fuels, emitting 12–25% less carbon monoxide in E10 blended compared to conventional gasoline [138]. The fuel properties of different types of fuel have been mentioned in Table 1.3. Although food crops such as corn (USA) and sugarcane molasses (Brazil) predominate in bioethanol production, there is an increasing interest in utilising carbohydrate-rich waste as a feedstock to address food security issues [141]. According to the Renewable Fuels Association, in 2021, the USA was the world's major contributor to ethanol, with 55% of total production, followed by Brazil (Figure 1.9).

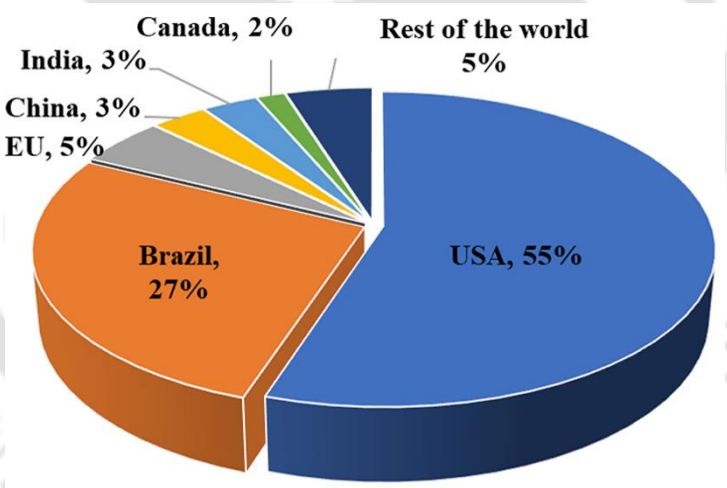

Figure 1.9. Global ethanol production by country in 2021 (Source: Renewable Fuel's Association) 10.07.23 [Renewable Fuel's Association https://ethanolrfa.org/markets-and-statistics/annual-ethanol-production.]

Table 1.3. Comparison of different types of fuel properties

	Gasoline	Ethanol	Butanol	Methane	Hydrogen
Molecular Formula	C_8H_{18}	C_2H_6O	C_4H_8O	CH_4	H_2

Molecular Weight (g/mol)	100.2	46.08	74.121	16.04	2.016
Energy Density (MJ/Kg)	46.4	27	~22	55.6	~120
Viscosity at 25 °C (mPa.s)	0.4–0.8	1.040	2.6	0.01	0.009
Boiling point (°C)	37-205	78.37	117.7	-161.6	-252.9
Autoignition temperature (°C)	247–280	365	314	537	584.85
Flash point (°C)	−43	13	29	−188	Flammable gas
HHV (KJ/g)	46.4	29.7	37.3	55.5	141.8
Octane value	87-94	113	96	120	>130

1.1.7.1.Feedstock for Bioethanol Production

Plant-based resources act as feedstock for bioethanol synthesis, with substrate selection determined by considerations such as crop accessibility (growth problems, geographic locations) and other applications. (including feed or nourishment). Based on the biomass sources, bioethanol can be divided into several categories mentioned in the Figure. 1.10(a). First-generation biomass, such as starch and sugar, predominates in production, with corn comprising 95% of bioethanol in the United States, but food and beverage waste contribute insignificantly. According to the USDA's Economic Research Service (ERS), 38% of cultivated corn was used to manufacture bioethanol in 2016, a threefold increase compared to 2006. Only eight ethanol plants, which use food and alcohol waste as raw biomass, which use food and alcohol waste as raw biomass, produce about 78 million gallons annually, representing roughly 1% of total production [142]. However, reliance on agricultural crops raises concerns about food security. Consequently, second-generation feedstocks derived from lignocellulosic materials—such as agricultural residues and industrial waste—offer a sustainable, non-food alternative that also reduces carbon emissions. Despite challenges in sugar extraction

and production efficiency, lignocellulosic bioethanol provides benefits such as sustainability and reduced competition with food resources.

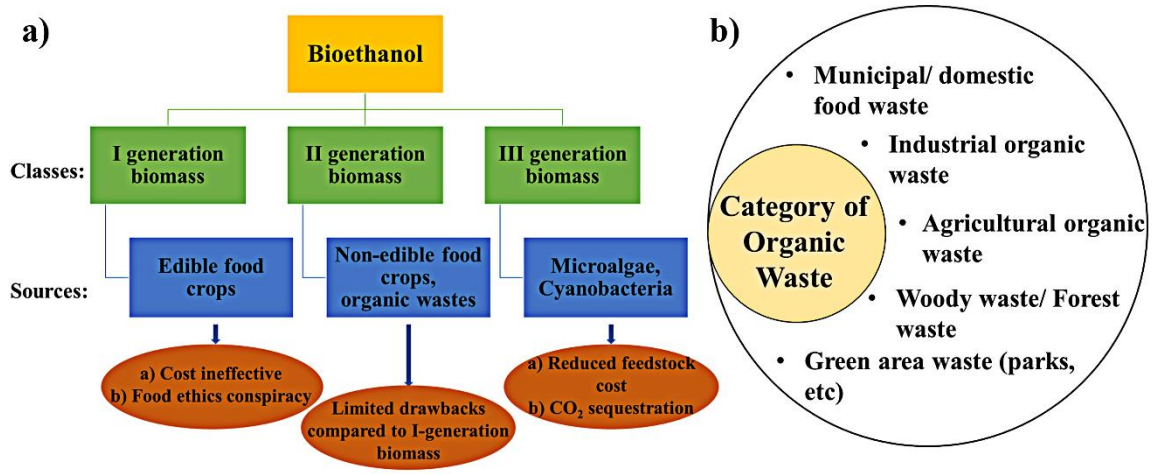

Figure 1.10. a) Classification of bioethanol based on the biomass sources and b) Category of organic waste used as feedstock

1.1.7.2.Effects of Feedstock Composition

Ethanol production from sustainable waste requires an optimal free sugar concentration of 20–30% to avoid fermentation inhibition, along with a balanced carbohydrate-to-protein ratio to maximise yield [143,144]. An optimal C/N ratio of 35.2 was documented by Manikandan and Viruthagiri [145], producing up to 8.85 g/L of ethanol. Lipids such as lecithin and palmitic acid improve yeast ethanol tolerance from 13% to 14% at modest concentrations; moreover, they become inhibitory in excessive amounts [146]. Macronutrients, vitamins, and minerals, particularly Mg^{2+}, Zn^{2+}, and Mn^{2+}, are essential for promoting cellular development, improving ethanol tolerance, and activating crucial enzymes such as pyruvate carboxylase [147].

1.1.7.3.Microbes used for Ethanol Production

Saccharomyces cerevisiae is the primarily used as yeast for ethanol synthesis from glucose, xylose, fructose, and lactose, however other yeasts such as *Kluyveromyces*, *Pichia*, and *Candida oleophila* are employed for other carbon sources (such as lactose source, pentose sugar) and have inhibitor (including furfural, 5-hydroxymethylfurfural (HMF), acetic acid) resistance. *K. marxianus* attained a 14% yield enhancement from lactose-rich waste [148], while *P. guilliermondii* and *C. oleophila* have shown efficacy with xylose [149]. Genetically modified strains such as Rubisco-based *E. coli* transform CO_2 into 100% pure ethanol in 60 h [150]. Thermophilic bacteria, such as *Clostridium*,

Thermoanaerobacter, and *Zymomonas mobilis*, metabolise starch and carbohydrates to produce ethanol [151,152]. Synergistic microbial consortia enhance fermentation efficiency for complicated sugar-rich feedstocks.

1.1.7.4.Mechanism of Ethanol Production

Microorganisms, including yeasts, bacteria, and fungi, effectively convert carbohydrate monomers (hexose and pentose) into ethanol. *Aerobacter*, *Bacillus*, and *Klebsiella* bacteria, along with yeasts such as *Candida shehatae*, *Pichia stipitis*, and fungi like *Fusarium*, *Rhizopus*, ferment xylose through glycolytic and pentose phosphate pathways, whereas gram-negative bacteria, including *Pseudomonas*, and *Z. mobilis* (facultative anaerobe), employ the Entner-Doudoroff pathway [153]. Yeasts synthesise ethanol both anaerobically and aerobically. Under aerobic conditions, yeast metabolises ethanol for growing colony volume and producing CO_2 and acetate. During anaerobic xylose fermentation, the TCA cycle is impaired, transforming glucose into pyruvate, acetaldehyde, and CO_2, yielding merely two ATP molecules per glucose molecule [153]. Further, pyruvate decarboxylase (PDC) transforms pyruvate into acetaldehyde and carbon dioxide, subsequently followed by alcohol dehydrogenase, which reduces acetaldehyde to ethanol. *E. coli* has a gene for pyruvateformatelyase rather than pyruvate [154]. Bioethanol production necessitates the pre-treatment of lignin-dense biomass to liberate fermentable sugars, succeeded by microbial fermentation and ethanol extraction. Several companies engaged in biowaste management have established small-scale ethanol production facilities; however, none operate independent biorefineries. The processes in the commercial manufacture of ethanol encompass raw material preparation, pretreatment, microbial inoculum development, fermentation, and ethanol recovery (Figure 1.11).

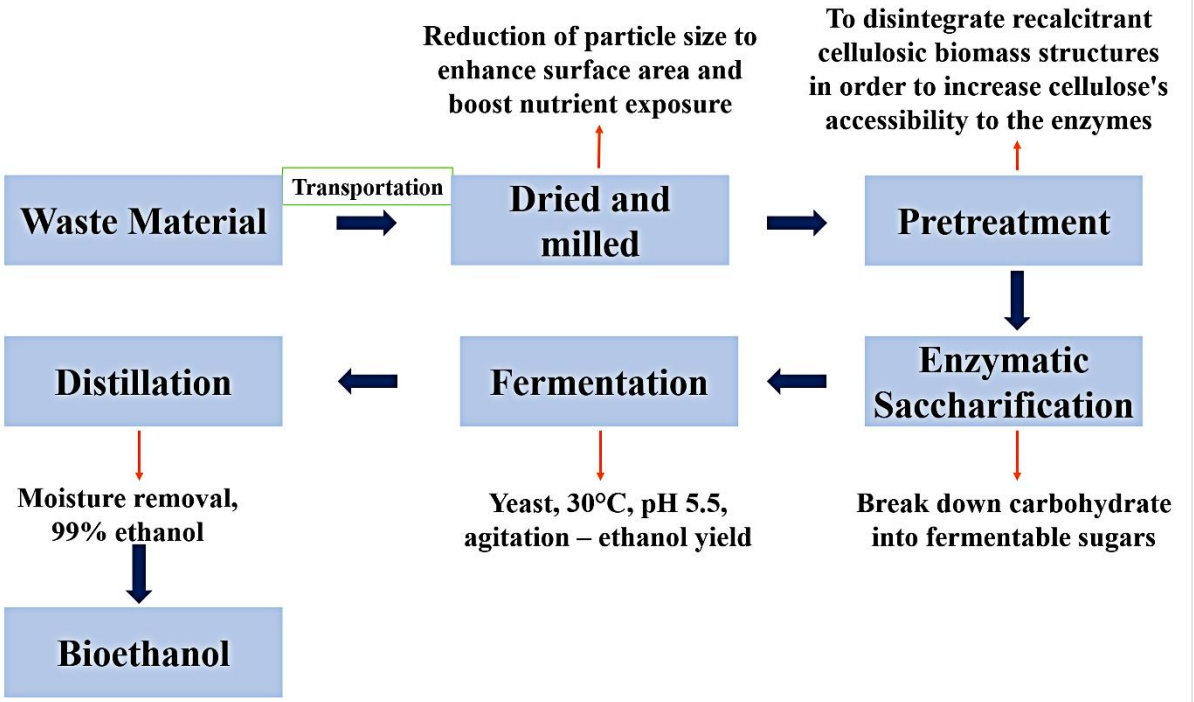

Figure 1.11. Schematic of flow for fermentation process with sustainable waste as feedstock

1.1.7.5.Sample Preparation and Pretreatment

Corn, sugarcane, and sugar beets are the primary substrates for commercial ethanol production, with corn starch acting as the predominant carbon source. Milling lowers particle size to enhance surface area, thus accelerating enzymatic reactions. Organic waste particles must not surpass 2 mm for efficient conversion. Lignocellulosic biomass (LCB) serves as an alternate substrate, consisting of roughly 40% cellulose, 30% hemicellulose, and 15% lignin, with variances determined by species, temperature, and soil conditions [155]. Enzymatic hydrolysis is the most economical and environmentally sustainable process for turning lignocellulosic biomass into bioethanol. Pretreatment processes, such as physical, chemical, physico-chemical, biological, or electrical, improve enzymatic digestibility by decrystallising and depolymerising cellulose, solubilising hemicellulose and lignin, and reducing inhibitory chemicals, while minimising sugar loss and operational expenses [156]. The appropriateness of pretreatment is dependent upon the kind of biomass, the presence of inhibitors, and the use of pentose sugars in bioethanol production.

1.1.7.6.Hydrolysis and fermentation

Lignocellulosic biomass (LCB) serves as a viable substrate for biofuel generation, with ethanol being the most extensively employed type. The U.S. National Petroleum Council estimates that second-generation bioethanol would be a crucial transportation energy source by 2050 [157]. Nonetheless, its economic feasibility relies on effective hydrolysis, fermentation, and ethanol distillation. Enzymatic hydrolysis is favoured over acid hydrolysis because it consumes less energy and has a reduced environmental impact; nonetheless, it encounters obstacles such as enzyme inhibition caused by lignin, pseudo-lignin, and by-products [158]. A major obstacle to large-scale LCB bioethanol production is the scarcity of microorganisms that can efficiently ferment both hexose and pentose carbohydrates. *Saccharomyces cerevisiae*, the most prevalent yeast, demonstrates significant ethanol production and tolerance; yet, it is incapable of fermenting pentose carbohydrates. Genetic engineering represents a viable method to surmount this constraint.

A variety of techniques have been established for the generation of ethanol from lignocellulosic biomass (LCB), including:

Separate hydrolysis and fermentation (SHF): A twofold process in which complex carbohydrates are hydrolysed into monomeric units and subsequently fermented. Excess sugar, however, impedes enzymes, hence diminishing ethanol output.

Simultaneous saccharification and fermentation (SSF): A unified process that integrates hydrolysis and fermentation, resulting in increased ethanol production and reduced wastewater generation. There are risks of contamination [140].

Simultaneous Saccharification and Co-Fermentation (SSCF): An integrated process that ferments hexose and pentose sugars, resulting in reduced capital expenditures and enhanced ethanol yield. Hexose-fermenting bacteria exhibit a more rapid metabolic rate than pentose-fermenting bacteria [152].

Consolidated bioprocessing (CBP): A singular technology employing genetically modified microbes to hydrolyse and ferment lignocellulosic biomass without supplementary enzymes. Notwithstanding its potential, industrial application encounters obstacles including limited productivity, difficulty in gene co-expression, and elevated prices [159].

Simultaneous Saccharification, Filtration, and Fermentation (SSFF): Entails hydrolysis within a reactor integrated with cross-flow filtration to recirculate sugar-laden filtrate

for fermentation. Ishola et al. [160] attained 85% of the predicted ethanol yield utilising this method with a flocculating *S. cerevisiae* strain.

Every approach possesses benefits and drawbacks, with the possibility of future advancements enhancing bioethanol production and sustainability. The efficiency of ethanol production from different biowastes is presented in Table 1.4.

Table 1.4. Reported Studies of Bioethanol Production from Various Wastes

Waste Type	Microbe used	Pretreatment Method	Fermentation Time (h)	Ethanol Output	References
Sugarcane trash	*S. cerevisiae*	Microwave acidic glycerolysis	~180	78.7 g/L	[161]
Corn stover hydrolysate	*Z. mobilis*	-	24	6.99 g/L	[162]
Sugarcane bagasse, rice straw, corncob and sweet sorghum bagasse	*C. tropicalis*	Distilled water or calcium hydroxide solution	24	15.3 g/L	[163]
Sugarcane molasses	*M. caribbica*	Concentrated sulfuric acid	72	56 g/L	[164]
Bamboo	*S. cerevisiae*	Deep eutectic solvent	24	0.128 g/g	[165]
Food waste	*P. kudriavzevii*	Thermochemical/enzymatic pretreatment	72	83.30 g/L	[166]
Corncob	*M. thermophila*	Without any additional cellulases or pretreatment of the substrate	30	39.8 g/L	[167]
Sargassum wightii	*L. phytofermentans*	Alkali pretreatment	96	13.75 g/L	[168]
Fruit waste of banana, apple, pineapple, mango, and melon	*Wickerhamomyces*	Mechanical agitation	9	21.63 g/L	[169]
Rice straw	*S. cerevisiae*	Alkaline pretreatment	12	4.44 g/L	[170]
Waste office paper (OP) and newspaper (NP)	*S. cerevisiae*	Chemical pretreatment	48	OP 11.15 g/L NP 6.65 g/L	[171]
Pineapple fruit peel	*S. cerevisiae*	Alkaline pretreatment	48	5.98 g/L	[172]

Black tea waste	Immobilised *Z. bailii*	Alkaline pretreatment	168	11.5 g/L	[173]
Rice waste	*S. cerevisiae*	Alkali with Acidified sodium chlorite and sodium bicarbonate Pretreatment	48	8.85 g/L	[174]
Waste paper	*P. stipitis*	Dilute acid	24	3.73 g/L	[175]

1.2.Research Gap

Despite growing awareness of sustainable waste management and the transition toward a bio-based economy, significant challenges remain in the efficient utilisation of agro-industrial waste. In processing, large quantities of passion fruit rind are generated, which are often discarded, contributing to environmental pollution. While fruit wastes are known to contain bioactive compounds such as phenolics, flavonoids, and carotenoids, there is limited literature on the systematic extraction of multiple value-added products, such as specialty chemicals, bioethanol, and antioxidants, from a single waste stream, particularly using yellow passion fruit (*Passiflora edulis f. flavicarpa*) waste sourced from Northeast India. The primary challenges of the sustainable utilisation of the yellow passion fruit by-products are outlined below:

1. Limited research on optimising integrated extraction processes using modern, green technologies such as ultrasound-assisted extraction (UAE) and supercritical fluid extraction (SFE) from passion fruit waste collected from Northeast India.
2. Inadequate information on comparative analysis between UAE and SFE for extracting bioactive compounds from passion fruit rind and their impact on phytocomponents, antioxidant activity, and antibacterial properties.
3. No studies have reported the utilisation of natural antioxidants derived from the rind of yellow passion fruit for improving the quality of vegetable oil.
4. The potential of discarded passion fruit biomass from these processes for biofuel production has been largely overlooked, resulting in the underutilisation of valuable cellulose and hemicellulose fractions.

1.3.Objectives

Based on the literature review and research gap, the following primary objectives have been established for this Ph.D. thesis with the title “Integrated biorefinery approach towards production of sustainable chemicals and fuel from passion fruit rind”**.**

1. Optimisation of the extraction of phytochemicals from the Yellow Passion fruit Rind using Ultrasound-assisted and Supercritical fluid extraction.
2. Comparative analysis of ultrasound-assisted and supercritical fluid extraction of bioactive compounds from Passion fruit rinds: phytochemical, functional, and analytical insights.

3. Application of natural antioxidants from yellow passion fruit rind on vegetable oil to improve the quality.
4. Valorisation of hemicellulosic residue from spent passion fruit rind: process optimisation and fermentation using *Pichia stipites.*
5. Delignification and enzymatic hydrolysis of cellulose fraction from Passion fruit rind residue.

1.4.Organisation of thesis

The content of the doctoral thesis is divided into eight chapters.

Chapter 1: This chapter explores the present scenario of agro-industrial waste valorisation and its role in the bio-based economy. This study investigates passion fruit rind as a viable feedstock for the extraction of natural antioxidants and their applications in several industries, such as food, cosmetics, pharmaceuticals, and biofuel production. The rationale behind the study has been discussed and offers an outline of significant concerns related to energy security and the current situation of food waste management. Besides, a thorough analysis of the literature is presented. This chapter offers extensive insights into the conceptualisation of this Ph.D. research.

Chapter 2: This chapter provides a detailed summary of the materials and procedures utilised in this investigation. The document outlines the experimental design and technique employed to optimise extraction conditions for bioactive compounds and sugar recovery to increase desired products. The research framework is fundamentally based on a comprehensive literature review. Standardisation, process optimisation, statistical analysis, and confirmatory evaluations were performed in compliance with experimental specifications.

Chapter 3: This chapter systematically optimises the extraction of phenolic and flavonoid contents from yellow passion fruit rind sourced from Assam, India, employing ultrasound-assisted extraction (UAE) and supercritical fluid extraction (SFE). Ethanol-water was used as the solvent for UAE, while SFE utilised CO_2 with 10% ethanol as a co-solvent (SC-ET). This study illustrates the impact of different independent parameters on the extraction yield. Statistical validation by ANOVA and regression analysis supports the determination of the model's significance. The Design-Expert software was used to predict the optimal conditions for maximal phenolic and

flavonoid yield. This chapter revealed the efficacy of Ultrasound-assisted Extraction (UAE) and Supercritical Fluid Extraction (SFE) as environmentally friendly methods for the recovery of polyphenolics from YPFR.

Chapter 4: This study covers the systematic analysis of extracted bioactive compounds from the yellow passion fruit rind (YPFR) in Chapter 3, with therapeutic properties like antibacterial and antioxidant activity. The extracts obtained at optimised conditions from supercritical fluid extraction with CO_2 and 10% ethanol as co-solvent (SC-ET), and ultrasound extraction (UAE) with 65% ethanol were compared for extraction yield, phytocomponents, antioxidant, and antibacterial activity. The Global Antioxidant Score (GAS) was computed to rank the antioxidant ability of the extracts when correlating the outcomes of antioxidant activity tests with their phytochemical concentration. GC-MS and HPLC profiling of the extracts were performed to identify compounds present in the extracts. In addition to that, antibacterial study findings revealed the potential of using passion fruit peel extract for the food, pharmaceutical, and cosmetic industries, promoting sustainable waste management and resource recovery.

Chapter 5: This chapter addresses the efficacy of passion fruit extracts as sustainable substitutes for synthetic antioxidants in preventing/ delaying the oxidative degradation of edible oils. Carotenoid extraction from passion fruit rind was optimised by ultrasound-assisted extraction, utilising sunflower seed oil and soybean oil as eco-friendly solvents. The carotenoid-enriched oils were assessed for alterations in peroxide and acid values. Additionally, the phenolic and flavonoid concentrations, as well as the antioxidant capacity of the extract-enriched oils, were compared with those of the pure oils. The oxidative and thermal stability of the oil samples was assessed using PetroOxy, differential scanning calorimetry, and thermogravimetric analysis. The structural integrity of the oils after the addition of extracts was evaluated. Further, the research findings highlight the efficacy of natural antioxidants in improving the stability and shelf life of edible oils.

Chapter 6: This study investigates the potential of the underutilised hemicellulose in spent passion fruit rind (SPFR) residue, generated after bioactive component extraction, for bioethanol production. The study included compositional analysis of the SPFR and dilute sulfuric acid pretreatment of SPFR to hydrolyse the hemicellulose component. The pretreatment procedure was statistically optimised with RSM to reduce furfural

and increase hemicellulose contents. Furthermore, the resulting prehydrolysate was detoxified using $Ca(OH)_2$ to enable fermentation with *Pichia stipitis* for bioethanol production.

Chapter 7: This study investigates the complete valorisation of passion fruit rind, using a two-step process of delignification and fermentation to produce bioethanol. Post-ultrasound-assisted extraction, the passion fruit rind was subjected to delignification using NaOH to enhance cellulose accessibility. The characterisation of delignified passion fruit rind via morphology and crystallinity analysis to determine the lignin removal. The delignified cellulose was subsequently hydrolysed using commercial cellulase, followed by fermentation. The lignin was effectively removed by the improved procedure, thereby increasing the amount of cellulose available for enzymatic hydrolysis. The potential of agro-industrial waste valorisation in the manufacture of sustainable bioethanol is highlighted by this work.

Chapter 8: In this chapter, the overall conclusions and scope for future work are summarised.

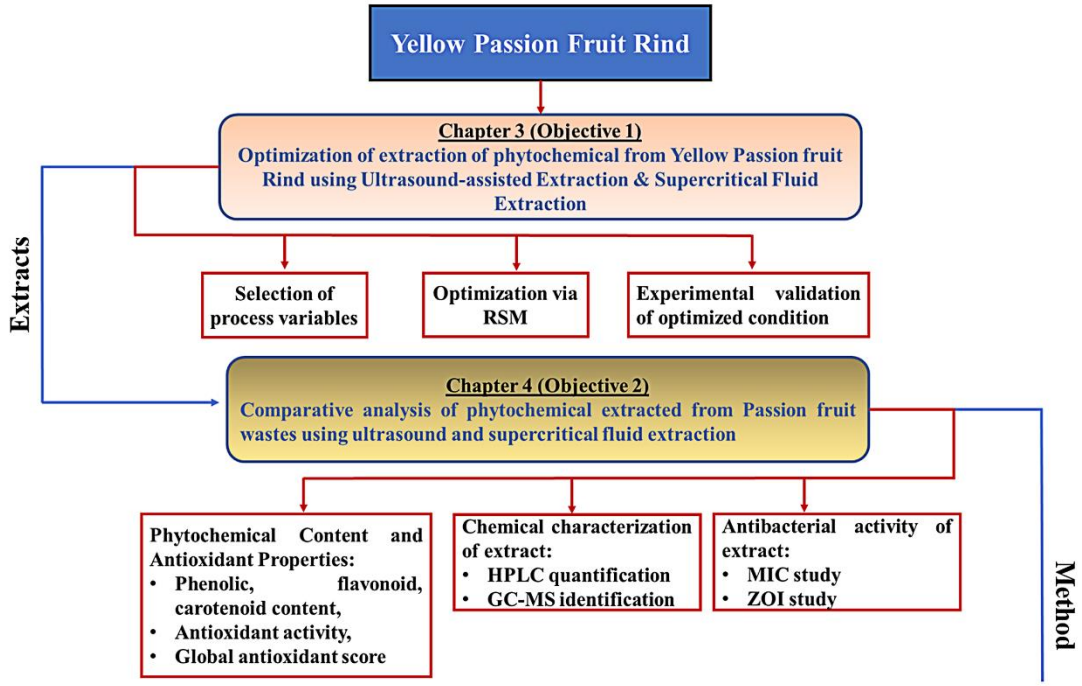

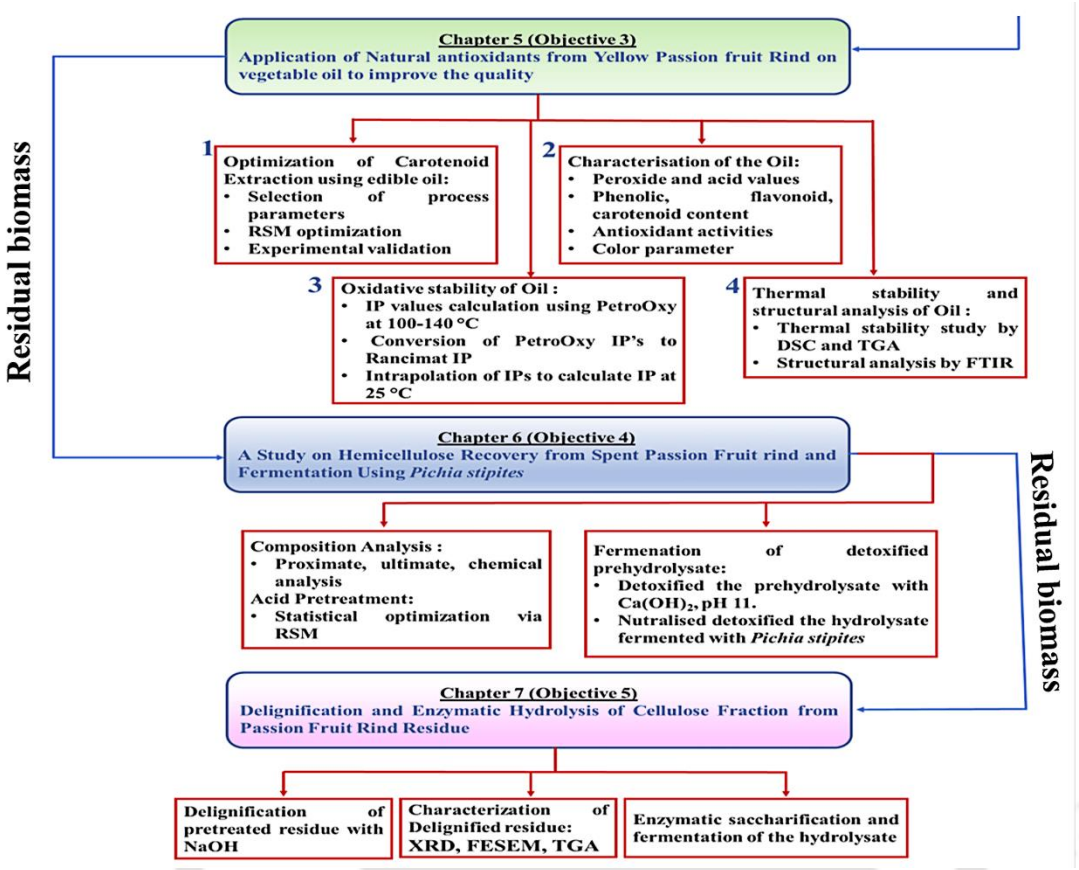

Figure 1.12. Flow chart of PhD thesis

2. CHAPTER 2

Materials and Methods

Materials
Methods
Procedures

CHAPTER 2

Materials and Methods

This chapter presents a comprehensive overview of the materials and methods used in the investigation. It describes the experimental design and techniques employed to optimise extraction conditions for bioactive compounds and sugar recovery, aiming to maximise the yield of desired products. The research framework is grounded in an extensive literature review, with standardisation, process optimisation, statistical analysis, and confirmatory evaluations conducted in accordance with experimental protocols.

2.1. Materials

2.1.1. Raw materials and chemicals

Raw material: The raw materials contain fully ripened fresh fruit samples of *Passiflora edulis* Var. *flavicarpa* (yellow passion fruit) was obtained from the local market of Karbi Anglong, India, in September 2021. The healthy cleaned fruits were diced into separate parts, such as rind and seed, and dried at 40 ± 5 °C in an oven for 3-5 days. The dried rinds were powdered (sieved through BSS 72 mesh) and kept in a firmly sealed Borosil glass bottle.

Chemicals used: All chemicals and reagents employed in this investigation were of analytical grade and utilised in their pure form for their respective applications.

Chemicals used in the extraction of bioactive compounds and bioactivity study, such as BF3-methanol, Supelco 37, BHA, BHT, absolute ethanol, folin-Ciocalteu, methanol, n-hexane, glacial acetic acid, acetonitrile, phosphoric acid, and DMSO, were purchased from Merck India Pvt. Ltd.; and gallic acid, quercetin, β-carotene, p-coumaric, caffeic acid, ferulic acid, myricetin, kaempferol, aluminum nitrate, sodium carbonate, potassium persulfate, and potassium acetate from Himedia; and DPPH, ABTS procured from Sigma Aldrich.

While, chemicals used in the fermentation of biomass to produce bioethanol, such as, absolute ethanol, formic acid, acetic acid, and urea were procured from Merck India Pvt. Ltd. Xylose, glucose, xylobiose, cellobiose, furfural, 5HMF, gallic acid, citric acid,

calcium hydroxide, sodium hydroxide, yeast extract, peptone, agar, and yeast nitrogen base, were purchased from Himedia. Sulfuric acid and malt extract were purchased from Finar and Loba Chemie, respectively. Celluclast 1.5L® was purchased from Sigma-Aldrich.

2.1.2. Microbial cultures used for various studies

The extract's antibacterial activity was tested against eight gram-positive and gram-negative bacterial strains, which were acquired from the Institute of Microbial Technology in Chandigarh, India. The details of the bacterial strains are listed in Table 2.1. The strains were reactivated and cultured using suitable broth and/or agar substrate. Glycerol stocks were created to preserve bacterial cultures and ensure their integrity for future use. For fermentation of biomass, *Pichia stipitis* NCIM 3497 and *Saccharomyces cerevisiae* NCIM 3090 strains as active slant was procured from the National Collection of Industrial Microorganisms (NCIM), Pune, India.

Table 2.1. The gram-positive and gram-negative bacterial strains used in antibacterial activity studies

Gram Postive bacterial strains	Gram Negative bacterial strains
Bacillus subtilis (MTCC 1133)	*Escherichia coli* (MTCC 1687)
Micrococcus luteus (MTCC 2848)	*Enterobacter aerogenes* (MTCC 8558)
Staphylococcus epidermidis (MTCC 9040)	*Pseudomonas aeruginosa* (MTCC 8727)
Staphylococcus aureus (MTCC 9886)	*Klebsiella pneumoniae* (MTCC 4030)

Gram-positive and Gram-negative bacteria basically vary in their cell wall structure, which additionally impacts their staining characteristics, physiological properties, and antibiotic susceptibility. Gram-positive bacteria possess a substantial peptidoglycan layer containing teichoic acids, retain crystal violet after Gram staining, and do not have an outer membrane. Gram-negative bacteria feature a slender peptidoglycan layer, an outer membrane containing lipopolysaccharides (LPS), and exhibit a pink/red colouration from safranin absorption, alongside a periplasm abundant in enzymes and transport proteins.

2.1.3. Microbial cultures preparation

2.1.3.1. Bacterial culture preparation: A single colony of each bacterial strain was aseptically introduced into 5 mL of broth and cultured. Subsequently, 100 µL of this culture was inoculated into 10 mL of new broth and cultured under ambient conditions until the optical density at 600 nm (OD600) attained 0.5. Upon reaching an OD600 of 0.5, repeated dilutions (up to 10^{-5}) were conducted for each strain.

2.1.3.2. Pichia stipitis culture preparation: Pichia (*Scheffersomyces*) *stipitis* NCIM 3497 strain as an active slant was procured from the National Collection of Industrial Microorganisms (NCIM), Pune, India. This strain has the ability to produce ethanol from D-Xylose. *P. stipitis* was maintained in the medium containing (g/L): 3 Malt extract, 3 yeast extract, 5 peptone; 10 glucose, and 20 agar; pH adjusted to 6.4–6.8. For suspension culture of yeast, sterilised YPDX (yeast extract, peptone, dextrose, xylose) media was prepared, including (g/L): 10 yeast extract, 20 peptone, 5 glucose, 15 xylose, 20 agar, and incubated for 48 h at 30 °C. A single colony from the plate was transferred to a 100 mL YPDX liquid growth medium (autoclave sterilised), which was incubated for 18 h at 30 °C and shaken at 150 rpm. The YPDX medium was kept at a pH of 6.

2.1.3.3. Saccharomyces cerevisiae culture preparation: For the fermentation of biomass, *Pichia stipitis* NCIM 3497 and *Saccharomyces cerevisiae* NCIM 3090 strains as active slant was procured from the National Collection of Industrial Microorganisms (NCIM), Pune, India. *Pichia stipitis* NCIM 3497 strain has the ability to produce ethanol from D-Xylose. *P. stipitis* was maintained on the medium containing (g/L): 3 Malt extract, 3 yeast extract, 5 peptone; 10 glucose, and 20 agar; pH adjusted to 6.4–6.8. whereas *Saccharomyces cerevisiae* strain was supplied on MGYP agar slants, which contained (g/L): 3, Malt extract; 10, Glucose; 3, Yeast extract; 5, peptone; and 20, agar; and 6.4–6.8 pH. For suspension culture of *Pichia stipitis*, sterilised YPDX (yeast extract, peptone, dextrose, xylose) media was prepared including (g/L): 10 yeast extract, 20 peptone, 5 glucose, 15 xylose, 20 agar; and incubated for 48 h at 30 °C. *S. cerevisiae* was sub-cultured on YPD agar plates which contains (g/L): 10, yeast extract; 20, peptone; 20, glucose and 20, agar. The yeast strain was incubated at 30 °C for 48 h. A colony from the plate was separately inoculated into 100 mL of autoclave-sterilised YPD liquid growth medium and incubated in a shaking incubator with an agitation speed of 140 rpm at 30 °C for 18 h, and the medium pH 6 was maintained. A single

colony from the plates was transferred to a 100 mL YPDX and YPD liquid growth medium, which was incubated at 150 rpm for 18h at 30 °C. Both medium was kept at a pH of 6.

2.2. Extraction of bioactive compounds from yellow passion fruit rind

2.2.1. Ultrasound-assisted extraction using ethanol-water

The extraction of bioactive compounds from YPFR was performed using bath sonicator (Ultrasonic cleaner, Aczet) at an operating frequency (40kHz) and ultrasonic Power (50W). The different ratios of sample and solvent (1:15, 1:25, 1:35) were taken in an Erlenmeyer flask and kept in the bath sonicator. The process factors used during the experimentation were temperature, time, solvent concentration and L/S ratio. After each extraction, the sample was filtered to eliminate any residue with Whatman filter paper and concentrated under vacuum at 40°C using a rotary evaporator. The concentrated samples were stored in firmly capped amber glass bottles in a deep freezer (-20°C) until further use.

2.2.2. Supercritical carbon-dioxide extraction

The extraction was carried out using a Supercritical fluid extraction unit (SFE 500, Supercritical fluid Technology, Waters, USA) which contains a CO_2 pump (Waters, USA), an approximately 500 mL extraction cell (stainless-steel), a solvent pump (Waters, USA), chiller (Accel 500LC, Thermo-Scientific, USA), a separation vessel, and back pressure regulator (Waters, USA). A small quantity of glass beads was added with 20g of samples in each extraction cell to avoid the clogging effects of the system. Ten per cent ethanol (co-solvent) was pumped to combine it at high pressure with supercritical CO_2 and heated the mixture before entering the extraction cell with a heat exchanger (Waters, USA). With the co-solvent making up 10% of the flow of CO_2, the extractions were carried out using CO_2 at a rate of 10-20 g/min. After the experiment, the mixture was depressurised in a separator at ambient pressure. The extract was then taken out of the separator and stored in airtight amber bottles in a freezer (-20 °C) for further analysis. The extraction time was maintained at 120 min for each trial.

2.2.3. Ultrasound-assisted extraction using edible oil

Bioactive compounds from YPFR using UAE have been extracted following the method described by [136] with a few modifications. The powdered YPFR and solvents

(SFO and SBO) were taken at different ratios (1:10 - 3:10) and kept in an Erlenmeyer flask inside an ultrasonic bath (Aczet, CUB 5). The experiments were conducted with varied process variables: temperature (30-60 °C), treatment time (20-50 min), and S/L ratio (10-30 g/100 mL). Following subsequent extraction, the oil-rich phytochemicals undergo filtering to remove any leftover material using Whatman filter paper, and then it was stored at -20 °C until further analysis. Additionally, the synthetic antioxidants BHA and BHT were added at the maximum approved concentration of 200 mg/L, as specified by the Food Safety and Standards Authority India, 2011 [129].

2.2.3. Experimental designs for extraction process optimisation

2.2.3.1. Ultrasound extraction: The phytochemicals from the passion rind were extracted using a bath sonicator (Aczet Ultrasonic Cleaner) with an ultrasonic power of 50W and an operating frequency of 40kHz, following the protocol described by dos Santos et al. [44]. The schematic of the ultrasonic extraction set-up is shown in Figure 2.1. An Erlenmeyer flask containing the various sample and solvent ratios was placed in the bath sonicator. A central composite design (CCD) based response surface methodology (RSM) was used to optimise the extraction parameters, such as temperature (°C), time (min), solvent concentration (%), and L/S ratio (mL/g). Table 2.2 displays the independent variables together with their corresponding levels. To examine the impact of these independent factors on the yields of flavonoids and phenolic compounds. Regression analysis was used to examine the experimental results using Design-Expert® software 13 (Stat-Ease, Inc., USA). The solvents were then removed by rotary evaporator after each extraction, and the concentrated samples were stored at -20°C.

Table 2.2. The values of independent factors for the ultrasound extraction process

Variables used	Levels		
	-1	0	1
Temperature (°C)	35	52.50	70
Ethanol: Water Concentration (%)	50	65	80
Extraction Time (min)	15	27.50	40
Feed Ratio (mL/g)	15	25	35

The system that expresses the outcome as a function of independent factors is the second-order polynomial model (equation 2.1).

$$Y = \beta_0 + \sum_{a=1}^{n} \beta_a X_a + \sum_{a=1}^{n} \beta_{aa} X_a^{\,2} + \sum_{a=1,a<b}^{n} \sum_{a=1,a\leq b}^{n} \beta_{ab} X_a X_b + € \qquad 2.1$$

The experimental error is represented by the symbol €, where Y is the predicted response factor and X_a and X_b are the uncoded independent variables of the experiment. β_0 is the constant, the coefficients of the linear term are denoted by β_a, the quadratic term by β_{aa}, and the interaction term by β_{ab}. There are three integer variables: a, b, and n. β_{ab} denotes the interaction effects between the variables X_a and X_b when a<b. Fisher's Satirical test (F-test) and an ANOVA test with a probability value ($p<0.05$) were used to determine the statistical significance of the model. The degree to which the model fits the experimental data is shown by the regression coefficient or r^2 value.

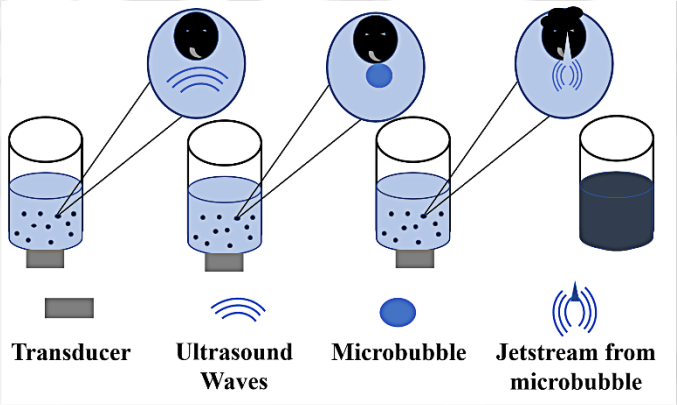

Figure 2.1. Schematic of the ultrasound assisted extraction setup

2.2.1.2. Supercritical carbon-dioxide extraction: Variable levels were determined using the preliminary experimental results obtained by altering one variable at a time while keeping the others constant. On the basis of published literature, a range of three potential parameters has been selected for the optimisation of Supercritical Carbon dioxide (SCO_2) extraction. Response Surface Methodology (RSM) based on Central Composite Design (CCD) was applied to analyse the effects of the selected independent variables: temperature, pressure, and flow rate on the phenolic yield. Table 2.3 shows the experimental parameter range for SCO_2 extraction. Design-Expert® software version 13.0 (Stat-Ease, Inc., Minneapolis, USA) was used to analyse the experimental outcomes using regression analysis. The supercritical fluid extraction schematic diagram is illustrated in Figure 2.2.

Table 2.3. Real and Coded values for the independent parameters for the SCO_2 extraction

Variables	Coded level		
	-1	0	1
Pressure (bar)	180	265	350
Temperature (°C)	45	55	65
Flow rate (g/min)	10	15	20

Each experimental run was carried out in triplicate to assess reproducibility. The second-order polynomial model expresses (equation 2.2) the system that depicts the response as a function of the independent variables.

$$Y = \beta_0 + \sum_{i=1}^{n} \beta_i X_i + \sum_{i=1}^{n} \beta_{ii} X_i^2 + \sum_{i=1,i<j}^{n} \sum_{j=1,i\leq j}^{n} \beta_{ij} X_i X_j + € \qquad 2.2$$

Where Y - the predicted response parameter, β_0 - the constant intercept, β_i- coefficient of the linear term, β_{ii}- coefficient of the quadratic term, β_{ij}- coefficient of the interaction term, X_i and X_j- uncoded independent variable of the experiment, the symbol € stands for the experimental error. Integer variables i, j, and n are used. When i<j is used, β_{ij} refers to the interaction effects between X_i and X_j variables. Fisher's Satirical test (F-test) and ANOVA test with probability value ($p<0.05$) were performed to determine the model's statistical significance. The r^2 value (regression coefficient) indicates that the model fits well with the experimental data.

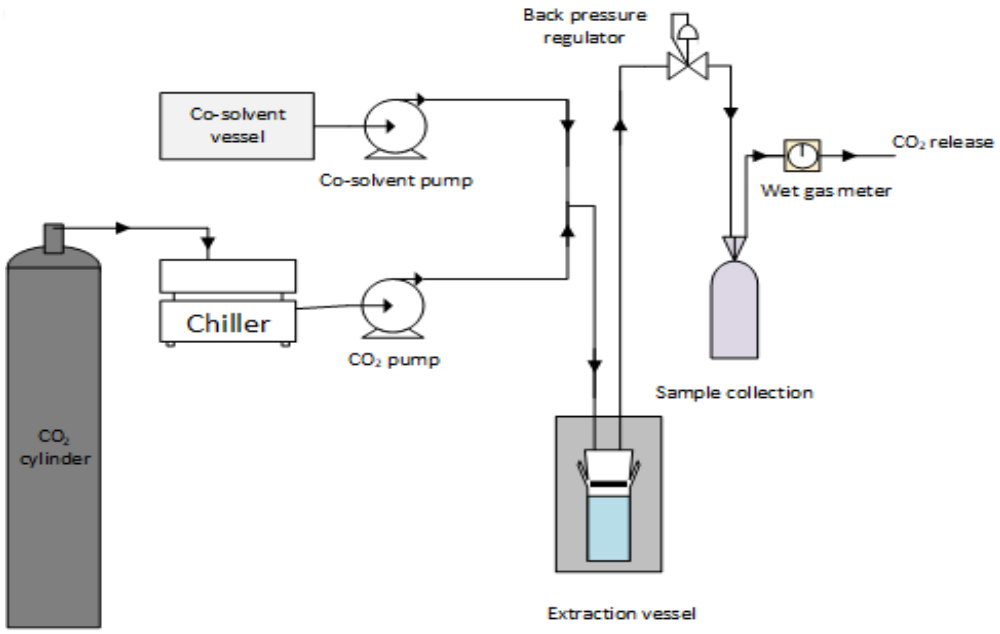

Figure 2.2. Supercritical fluid extraction schematic diagram

2.2.2.3. Ultrasound-assisted extraction using edible oil: The parameter range was established from initial experimental findings (Figure A1) acquired by changing a single factor at a time while holding the remaining at a fixed value. The variables were selected following a careful review of the literature. The impacts of the chosen parameters, including temperature, treatment time, and S/L ratio, on the yield of carotenoids were examined using a CCD-based RSM design at (−1, 0, +1) levels. The experiment results were analysed graphically and via regression using Design-Expert® software trial version 13 (Stat-Ease, USA). A second-order model (equation 2.3) represents the expression of independent variables.

$$Y = \beta_0 + \sum_{i=1}^{n} \beta_i X_i + \sum_{i=1}^{n} \beta_{ii} {X_i}^2 + \sum_{i=1, i<j}^{n} \sum_{j=1, i \leq j}^{n} \beta_{ij} X_i X_j + € \qquad 2.3$$

Where, Y - the predicted response parameter, β_0 - the constant intercept, β_i- coefficient of the linear term, β_{ii}- coefficient of the quadratic term, β_{ij}- coefficient of the interaction term, X_i and X_j- uncoded independent variable of the experiment, € represents the experimental error. The variables i, j, and n are integers. When i<j, β_{ij} represents the interaction effects of the variables X_i and X_j. The ANOVA test with probability value ($p<0.05$ and Fisher's Satirical test (F-test) was performed to determine the statistical significance of the model. The r^2 value (coefficient of regression) signifies the degree of correlation between the expected and experimental responses match together.

2.3. Analytical methods

2.3.1. Phytochemical analysis and antioxidant activity of the extracts

2.3.1.1. Total phenolic content (TPC): The total phenolic content of the extracts was ascertained using the modified Folin-Ciocalteu (FC) method [176]. In each test tube, an aliquot of 500 µl of YPEP extract was mixed with 2.5 ml of 10% FC reagent. After 5 min, 2 mL of 2% Na_2CO_3 was mixed with the sample and incubated under dark conditions. As a blank, the reagent mixture was prepared without any sample. The absorbance was recorded at 765 nm using a UV-spectrophotometer (Orion Aquamate 8000, Thermo Scientific, India). The TPC was calculated using a gallic acid calibration curve as mg GAE/g.

2.3.1.2. Total flavonoid content (TFC): Flavonoid content was determined using the spectrophotometric method explained by Sen et al. [177]. An aliquot of 250 µl of YPEP

extract in methanol was mixed with 50 µl of 10% aluminium nitrate, 50 µl of potassium acetate (1 M), and 2.15 ml of 80% ethanol. The mixer was incubated for 45 min, and UV-spectrophotometric optical density was measured at 415 nm. The reagent mixture without a sample was used as a blank. The TFC was calculated as mg QE/g using a quercetin calibration curve.

2.3.1.3. Total carotenoid content (TCC): Carotenoid content was calculated using the spectrophotometric method described by Jiao et al. [178]. The extract (1 g) was added to 1 mL of n-hexane and vortexed for 30 s, and the absorbance was measured at 460 nm. The hexane was used as a reference for the analysis. A calibration curve was plotted with β-carotene in hexane; thus, the carotenoids were expressed as β-carotene equivalents.

2.3.1.3. Antioxidant activity: The extracts' antioxidant activity was determined by DPPH [179] and ABTS assays [180]. The proportion of scavenged extracts was used to calculate their antioxidant activity using equation 2.4. The percentage IC_{50} value of the sample was determined using the graph showing the percentage of scavenged vs extract concentration. The values were calculated using the control, the mixture of reagents (DPPH or ABTS) with methanol. Methanol was used as a blank in both the tests. The volume of the extract needed to scavenge 50% of radicals in vitro is known as IC_{50} per cent. Pure ascorbic acid was used to compare the IC_{50} per cent values for both DPPH and ABTS assays. A brief description of the DPPH and ABTS analysis is performed using the equation (2.4).

$$\text{Percentage scavanged (\%)} = \left(1 - \frac{A_{Sample}}{A_{Control}}\right) * 100 \qquad 2.4$$

Where, A_{sample} is the absorbance of the sample (at 517 nm for DPPH, 734 nm for ABTS), and $A_{control}$ is the absorbance of the control.

DPPH assay: The DPPH assay was carry out using the technique described by Patial et al. [179]. Different quantities of the extract solution (3 mL) was properly mixed with 1 mL of the DPPH reagent (0.1 mM) and incubated in dark for 30 min. The absorbance was recorded at 517 nm.

ABTS assay: The ABTS assay was conducted following the method described by Moges et al. [180]. ABTS (7 mM) and 2.45 mM potassium persulfate solutions were

mixed in a 1:1 ratio to produce the ABTS free radical. The ABTS solution was diluted after 12 to 16 h of dark incubation so that the absorbance at 734 nm was approximately 0.7 ± 0.05. The absorbance of a 2.5 mL mixture of ABTS solution and varied concentrations of 0.5 mL sample was measured after 20 min of incubation.

2.3.1.4. Global antioxidant score: The GAS value was calculated using the T-score method [181]. T-score is computed using equation 2.5

$$\mathrm{T-score} = \frac{\mathrm{X} - \mathrm{X_{min}}}{\mathrm{X_{max}} - \mathrm{X_{min}}} \qquad 2.5$$

where X_{min} and X_{max} indicate the minimum and maximum values of X within the analysed sample, the GAS value was calculated using total phenolics, carotenoids, flavonoids, and IC_{50} of extracts (DPPH and ABTS).

2.3.2. Quantification of phenolic and flavonoid compounds in the extracts

The HPLC analysis (Shimadzu Corporation, Kyoto, Japan) of all extracts was carried out using a C18 column (250 9 4.6 ID) and a PDA detector. For the measurements of phenolic acids and flavonoids, the mobile phases employed were, respectively, 63 water: 37 acetonitrile with 1% phosphoric acid at a flow of 1 mL/min and 45 water: 40 methanol: 15 acetonitrile with 1% glacial acetic acid at a flow of 0.5 mL/min. Quercetin, rutin, kaempferol, and myricetin were detected at 368 nm. In contrast, P-coumaric acid was measured at 310 nm, ferulic acid and caffeic acid at 296 nm, and gallic acid was detected at 280 nm. The diluted standards were filtered through a 0.2 µm filter (AXIVA). Twenty microlitres of standards were injected at various doses (20–100 µg/mL) to obtain a standard curve. Each extract was injected at a concentration of 1 mg/mL for analysis after filtration through a 0.2 µm filter (AXIVA) with a run time of 60 min. The polyphenol concentrations in the calibration plot were quantified by analysing the retention time of individual peaks.

2.3.3. Phytochemical screening of the extracts using GCMS

The SC-ET and UAE extracts dissolved in n-Hexane were used for GC-MS (GC 9000 and MS 5977B, Agilent Technologies, USA) using a DB-5MS capillary column (30 m X 250 µm i.d. X 0.25 µm film thickness) in split-less mode for phytochemicals screening. The injector temperature was maintained at 300 °C and the oven temperature was initially held at 40 °C for 2 min, then increased to 120 °C at a rate of 10 ºC/min,

held for 10 min, then the second ramp was increased at the rate of 10 °C/min up to 180 °C and was held for 10 min. The third ramp was raised by 10 °C increments until it reached 250 °C, and then it was raised by 10 °C/min increments to 280 °C and was maintained for 5 min. The carrier gas and helium gas flow rates were maintained at 1 mL/min for a run time of 60 min. The data was acquired with the electron ionisation mode at 70 eV. In the mass range of m/z 50–1050, full scan mass spectra were collected with an initial solvent delay of 6 min. Using Agilent Mass Hunter Workstation Qualitative Analysis Software, version 10.0, the peaks obtained by GC-MS were identified based on their NIST Mass Spectral library mass spectra.

2.3.4. Antibacterial activities of the extracts

2.3.4.1. Minimum inhibitory concentration (MIC): The MIC against eight bacterial strains was calculated using the method explained by Sarker et al. [182]. The MIC study was conducted on a few foodborne infectious gram-positive and gram-negative bacterial strains: *B. subtilis, E. aerogenes, M. luteus,* and *P. aeruginosa; E. coli, K. pneumonia, S. aureus* and *S. epidermidis*. The bacterial strains were collected from the Institute of Microbial Technology (Chandigarh, India) to enable the assessment of antibacterial properties of the extracts. Before the experiment, the bacterial strains were inoculated in the appropriate growth media and revived at room temperature. The YFPR extracts were dissolved in 10% DMSO to perform the activity test and further diluted serially from 1000 mg/mL to 0.98 mg/mL. The samples were sterilised using a 0.22 µm Millipore filter. Then, in an aseptic environment, the sample, 3.3X broth media, and the bacteria were mixed in a ratio of 5:3:1 into the 96-well plate. The bacterial suspension, media, and 10% DMSO were used as the positive control, while 10% DMSO and media were used as the negative control. Resazurin indicator (0.01 mL, concentration 1 mg/mL) was added to each well after incubating for 12–14 h at the ambient temperature (30 °C and 37 °C) for bacterial growth. The final bacterial concentration in each well was 5×10^{-5} CFU/mL. In the wells, a pink-red colouration indicated bacterial growth; however, the MIC value was determined by measuring the lowest extract concentration in the absence of this colouration.

2.3.4.2. Zone of inhibition (ZoI): The ZoI was carried out using the agar well diffusion method described by Moges et al. [180]. This study used the gram-positive and gram-negative bacterial strains mentioned in section 4.5.1. On the surface of the solidified

agar, 100 µL of bacterial culture (0.1 mL of 10^3 CFU/mL) was swabbed. Three holes of 0.5 mm were punctured into the agar's surface after the culture had been absorbed. The holes were filled with 50 µL (1 mg/mL) of sterilised extracts. To ensure that the solution was evenly distributed throughout the solidified agar, the plate was left in the laminar flow for 45 min. After 12–14 h of incubation, a clear inhibition zone was observed, and the diameter was determined using a geometric ruler.

2.3.5. Oil composition analysis

The fatty acid composition of the sunflower seed and soybean oil (pure and with extract) was analysed by converting the fatty acids into fatty acid methyl esters (FAMEs) and then using gas chromatography (GC) [183]. BF_3-methanol solution (1 mL) was added to 14–16 mg of the sample and heated to 90 °C for 30 min. To recover the FAME, the solution was mixed with 2 mL of hexane and water, and the upper phase was separated. The esters were evaporated under a nitrogen stream, and the volume was made up of chromatography-grade hexane. PerkinElmer Clarus 590 GC-FID was used to analyse the FAME compositions. A BPX-70 (0.25 mm × 50 m × 0.22 mm) was installed in the GC-FID, and hydrogen (at 2 mL/min) was utilised as the carrier gas in split mode. At the beginning, the column temperature increased progressively from 100 °C to 240 °C at a rate of 3 °C/min for 10 min. The FID and injector temperatures were both set to 250 °C. The Supelco 37 component FAME mixture was used as the FAME standard to quantify the Fatty acid composition of the oil samples.

2.3.6. Phytochemical analysis of the oil samples

2.3.6.1. Total phenolic content (TPC): Following certain modifications, the phenolic content of the sample was measured using the Folin-Ciocalteu method [180]. An aliquot of methanolic oil solution (0.5 mL) was combined with 2.5 mL of diluted Folin-Ciocalteu reagent in every test tube after adding 2 mL of Na_2CO_3 (2%). The solution was then incubated for 30 min in the dark conditions. The UV-spectrophotometer (Thermo Scientific, Orion Aquamate 8000) measured the absorbance at 765 nm, and a calibration curve for gallic acid was used to quantify total phenols.

2.3.6.2. Total flavonoid content (TFC): Using the aluminium nitrate and method described by Zarate et al. [184], the flavonoid content (TFC) was estimated. A mixture of 0.25 L of hydro-methanolic oil solution, 0.05 L of $Al(NO_3)_3$ (10%), 0.05 L of

CH_3CO_2K (1 M), and 0.002 L of C_2H_6O (80%) was incubated for 45 min. The optical density was measured at 415 nm, and TFC was determined using a quercetin calibration curve.

2.3.6.3. Total carotenoid content (TCC): The spectrophotometric approach described by Xu et al. [185] was used to determine the carotenoid concentration with few modifications. After adding 1 g of oil sample to 500 µL of 5% NaCl, the mixture was vortexed for 30 s. The mixture was centrifuged (Eltek, TC 4100 F) at 4500 rpm for 10 min. Then, the supernatant was diluted with hexane, and the absorbance was measured at 460 nm. The carotenoids were expressed as β-carotene equivalents, comparing the absorbance with a β-carotene standard curve.

2.3.6.4. Antioxidant activity: Passion fruits possess different bioactive molecules that enhance their antioxidant capabilities, complicating the assessment of the antioxidant properties of each molecule individually. Various methodologies have been established to evaluate the antioxidant efficacy of plant extracts. In this study, the evaluation of the antioxidant activity of treated and pure oils was performed using DPPH and ABTS assays. These methods are widely recognised for their sensitivity, repeatability, and suitability for both lipophilic and hydrophilic antioxidants. They effectively measure free radical scavenging capacity and strongly correlate with total phenolic, flavonoid, and carotenoid content [186,187]. Alternative assays such as ORAC, FRAP, and metal chelation were excluded due to their specific requirements and non-specific reactions. Further, they could be considered in future studies for a more comprehensive antioxidant assessment [188].

This study assessed quantitatively the antioxidant capacity of the extracts using their IC_{50} values in DPPH and ABTS assays. The IC_{50} percentage denotes the quantity of extract necessary to neutralise 50% of radicals in vitro. The DPPH assay measures the percentage of DPPH radicals scavenged by a oil sample [189]. The oil-methanol mixture (3 mL) at different concentrations was mixed with 1 mL of 0.1 mM DPPH reagent, vortexed, and incubated for 30 min in the dark. The absorbance was measured at 517 nm. Whereas the ABTS assay was performed by following the procedure described by Sarkis et al. [190]. Mixing 7 mM ABTS with 2.45 mM potassium persulfate (1:1), the stock solution was generated and stored in the dark for 12 h. The mixture was subsequently diluted to an absorbance of roughly 0.7 at 734 nm. The

diluted ABTS solution was combined with 10-50 mg of oil per mL of methanol; absorbance was measured after 20 min. Ascorbic acid was used as a reference for both DPPH and ABTS assays. In both DPPH and ABTS assays, the percentage scavenged was analysed using equation 2. The plot percentage scavenged vs. extract concentration was further used to determine each oil sample's percentage of IC_{50} value.

2.3.7. Characterisation of oil

The characterisation of both sunflower and soybean oil samples (with and without extracts) was carried out using the standard methods. Acid values (Te 1a-64) and peroxide values (Cd 8b-90) were measured following AOCS (American Oil Chemists' Society) methods [191].

2.3.7.1. Colour parameter: Colour is essential for consumer acceptability of food products. The colour of both pure and extract-enriched oils was assessed utilising a colourimeter (Datacolor 550, USA) following the procedure described by Goswami et al. [192]. The parameters: L* (0–100, black to white), a* (negative-green, positive-red), and b* (negative-blue, positive-yellow) values were quantified to evaluate treatment-induced changes in the oil samples.

2.3.8. Oxidative stability study

The oil samples' induction period (IP) was determined using an oxidation stability tester (PetroOxy, Anton Paar, P/N 184396). The samples used for analysis were pure oil, oil enriched with extract, and oil with synthetic antioxidants (BHA and BHT), and the standard ASTM D7545 test procedure was followed [110,193]. The oil with synthetic antioxidants was prepared by mixing the oil with synthetic antioxidants at a 200 mg/1000 mL concentration. For the analysis, 5 mL of the sample was added to the cell and charged with oxygen. The samples were examined at temperatures ranging from 100-140 °C.

2.3.9. Thermal degradation analysis of oil

2.3.9.1. Differential scanning calorimetry (DSC): Using a DSC analyser (NETZSCH, DSC 3500 Sirius), the thermal stability of oils with and without antioxidants was determined. A reference crucible and a 10 mg test oil sample were stored in a crucible inside the DSC apparatus. With certain adjustments, the offset point was established following the procedure described by Borugadda and Goud [194]. The temperature was

initially increased to 50 °C at a rate of 2 °C/min and held for 5 min. It was then lowered to 30 °C at the same rate, followed by a return to 50 °C for another 5 min. Next, the temperature was decreased to 30 °C at 2 °C/min and held for 5 min. Subsequently, it was raised to 30 °C at 2 °C/min, then reduced from 30 °C to −30 °C, and finally cycled once more from 30 °C to −30 °C. The onset point was determined by extrapolating the DSC curves.

2.3.9.2. Thermo-gravimetric analysis (TGA): The heat stability and deterioration characteristics of the test samples were determined using a TGA analyser (Perkin Elmer, TGA 4000) [195]. The experiment was conducted in a non-isothermal condition in the N_2 atmosphere with increasing heating rates at 10 °C/min up to 600 °C. Plotting the TG curves and their corresponding derivative curves (DTG) allowed for determining the samples' mass loss percentage and onset temperature. The onset temperature was determined by taking a horizontal line from the TG curve and joining its intercept with the tangent representing the onset temperature.

2.3.10. Structural analysis of oil

FTIR analysis was performed for all test oil samples, both with and without antioxidants, in the range of 4000 cm^{-1} to 400 cm^{-1} using an FTIR spectrometer (Parkin Elmer, L1600300 Spectrum TWO LiTa) as it involves the most relevant modes of vibration for the identification and analysis of organic compounds, including oils and bioactive constituents [196]. A resolution of 2 cm^{-1} was used, with 30 scans recorded per spectrum, following the previously established method [197]. For the analysis, an oil sample of approximately 3–5 mL was introduced into the apparatus.

2.3.11. Composition analysis of the passion fruit rind

The passion fruit rind biomass was analysed for its chemical composition following the National Renewable Energy Laboratory (NREL) analytical modified procedure [198]. For the removal of extractives such as impurities, nitrates, proteins, chlorophyll, and waxes, the raw passion fruit rind (RPFR) was subjected to Soxhlet extraction using water followed by ethanol for 24 h [199]. In order to quantify the extractives, both the water and ethanolic extracts were separated by a rotary evaporator (Buchi, R-210, Switzerland) and then dried at 45°C in a vacuum oven. Following the NREL technique (NREL/TP-510-42618), the structural carbohydrates and lignin contents of the

extractive-free RPFR and SPFR were examined. The biomass (0.3 g) was initially mixed with 0.3 L of 72% (v/v) sulfuric acid and incubated at 30 °C for 1 h. The mixture was then diluted to a final acid concentration of 4% using distilled water and subjected to hydrolysis in an autoclave at 121 °C for 1 h. Following hydrolysis, the mixture was neutralised with calcium carbonate and filtered through a 0.2 µm Axiva nylon syringe filter and analysed using HPLC.

2.3.11.1. Proximate analysis: This approach is frequently employed to analyse solid and liquid fuels by measuring moisture (MC), ash content (AC), volatile matter (VM), and fixed carbon content (FC). Crucibles were dried at specific temperatures: 105 ± 1°C for MC (24 h), 575 ± 5°C for AC (4 h), and 910 ± 5°C for VM (10 min), and subsequently kept in a desiccator prior to measuring the weights.

2.3.11.2. Ultimate analysis: The elemental composition (C, H, N, S, and O) of the lignocellulosic biomasses (raw and spent passion fruit) was analysed using a CHNS analyser (Vario Macro Cube, Germany). Approximately 50 mg of the material was combusted in pure oxygen, and the resultant gases (CO_2, H_2O, N_2, SO_2) were analysed. The oxygen content was determined by the equation 2.6.

$$O = 100 - (C + H + N + S)$$

(2.2.6)

2.3.11.3. Calorific value analysis: Calorific value of biomass was determined using a Toshniwal bomb calorimeter (IS 1350-1, India) [200]. One-gram biomass pellets were burned using a platinum wire and cotton thread in an oxygen environment at 20 bar pressure. The bomb was situated in 1 L of Millipore water, with the calorimeter jacket regulated at 25 °C. The ignition energy was determined using voltage variations across a 1256 or 2900 µF capacitor during discharge.

2.3.12. Acid pretreatment

The The fully-grown fresh fruit samples of *P. edulis* f. *flavicarpa* were obtained from near the vicinity of Guwahati, Assam, India (North-East part of India). The fruits were carefully cleaned and air-dried in the sunlight. The dried rinds were crushed into a fine powder and subjected to ultrasound-assisted extraction (UAE) using vegetable oil as the solvent to extract the bioactive compounds (section 2.2.3). The resulting mixture was subsequently filtered using Whatman No. 1 filter paper to separate the solid residue

and oil. For further analysis, the solid residue was cleaned with hexane to remove any oil traces. After drying at 45°C, the residue was termed as spent passion fruit rind (SPFR). This spent biomass is subjected to bioethanol production in this study. The biomass samples were pretreated with diluted sulfuric acid in a domestic microwave oven (Samsung, CE2877 N, Korea) following the method described by Binod et al. [201]. As microwave treatment accelerates processes over conventional techniques, it is commonly used for heating biomass [202]. Based on the preliminary test, range of temperature, reaction duration, and acid concentration were investigated for the optimum sugar yield. Dilute sulfuric acid pretreatment was conducted in a reagent bottle with a solid loading of 8% (w/v) with different concentrations (0.1-0.4 M) of sulfuric acid. Each mixture was hydrolysed for 1-30 min at distinct temperatures ranging from 80-160 °C (due to instrumental constraints, the reaction at 160 °C was conducted in open reagent bottles). Once the desired time was achieved, the reaction was stopped to enable it to cool to ambient temperature. Then, 100 µL of the reaction mixture was removed, and sugars and fermentation inhibitors were measured using high-performance liquid chromatography (HPLC, Shimadzu Corporation, Kyoto, Japan). The liquid and solid fractions after pretreatment conditions were filtered through a nylon membrane filter with a pore size of 0.2 µm. Then, the solid fraction was neutralised with distilled water and dried for 48 h at 45 ± 3 °C. However, the liquid fraction was stored in an air-tight glass container at -20 °C until further analysis.

Table 2.4. The values of independent factors for the acid pretreatment process

Variables used	Levels		
	-1	0	1
Experimental Temperature (°C)	80	120	160
Reaction Time (min)	1	15.50	30
Sulfuric Acid Concentration (M)	0.1	0.25	0.4

2.3.12.1. Experimental design for optimisation of pretreatment process: Employing Design-Expert software (version 13; State-Ease, Minneapolis, USA), a statistical model was designed with CCD-based RSM for the process optimisation and experimental design of the acid pretreatment. Twenty distinct experiments were conducted, including 6 centre points, considering three variables: temperature, reaction time, and sulfuric acid concentration. A thorough analysis of the available literature and preliminary testing was used to identify the limits for these variables. Table 2.4 illustrates the

labelling of the selected variables, which were temperature: 80 and 160 °C, reaction time: 1 and 30 min, and acid concentration: 0.1-0.4 M. A second-order polynomial model was obtained, based on how these variables affect the expected reactions to xylose and furfural; represented by the equation 2.7.

$$Y = \alpha_0 + \sum_{b=1}^{n} \alpha_b P_b + \sum_{b=1}^{n} \alpha_{bb} P_b^{\,2} + \sum_{b=1,b<c}^{n} \sum_{b=1,b\leq c}^{n} \alpha_{bc} P_b P_c + € \qquad 2.7$$

In the model, the response is represented by Y. The intercept, linear, quadratic, and interaction effects are represented by the regression coefficients α_0, α_b, α_{bb}, and α_{bc}, respectively. P_b and P_c are the codes for the independent variables. A multiple regression analysis was used to determine the coefficients utilising the experimental data, and the F-test of an ANOVA analysis was used to assess the statistical significance of the model. € represents experimental error.

2.3.13. Detoxification of the prehydrolysate via overliming

The prehydrolysate was treated and detoxified by overliming to achieve a pH of 6 and 11, following the method described by Kordala et al. [203] with a few modifications. The procedure included increasing the temperature of the prehydrolysate to 50 °C for fifteen min, followed by gradually adding $Ca(OH)_2$ while agitating for about thirty min. After that, the resulting overlimed hydrolysates were centrifuged to remove the calcium sulfate ($CaSO_4$) sludge, and 10N sulfuric acid was used to reduce the pH of the supernatant to 6. This was termed conditioned hydrolysates. This conditioned hydrolysate was subsequently filter-sterilised for the synthesis of bioethanol.

2.3.14. Delignification of passion fruit rind

Although dilute H_2SO_4 hydrolysis slightly reduces the lignin content (section 2.3.12), additional treatment is necessary to enhance cellulose accessibility for enzymatic hydrolysis. The NaOH treatment of lignocellulosic biomass induces delignification by cleaving ester linkages between lignin and hemicellulose, thus improving biomass permeability [204]. This study utilised different doses of NaOH as delignifying agents, demonstrating a synergistic effect on the delignification of pretreated biomass. The residual biomass obtained from the acid pretreatment was subjected to an additional treatment using a NaOH solution at 120°C with experiments at 10% solid loads for 20 min, varying NaOH concentrations from 1–5%. The samples were filtered, thoroughly

washed until reaching neutral pH, and then oven-dried at 45°C for 24 h. Following filtration, the solid fractions were used for enzymatic hydrolysis. The percentages of lignin, xylan, and cellulose loss computed using equation 2.8.

$$\text{Percentage Loss (\%)} = \frac{W_{\text{after treatment}} - W_{\text{before treatment}}}{W_{\text{before treatment}}} \times 100 \qquad 2.8$$

Where, $W_{\text{before-treatment}}$ is the mass of the cellulose/xylan/lignin present in the pretreated residue and $W_{\text{after-treatment}}$ stands for the residual amount of polymer present in the alkali-treated residue.

2.3.15. Enzymatic Saccharification

Following the delignification procedure, the remaining solid fraction was hydrolysed using cellulase (Celluclast 1.5L®) at a concentration of 30 mg/g of cellulose [205]. The cellulase hydrolysis was conducted at 50 ºC for 72 h at 140 rpm using 0.5 mM citrate buffer, with 10% solid loading to assess the hydrolysis efficiency. An aliquot of 1 mL was taken from the reaction mixture, properly diluted, and then heated for 10 min to deactivate the enzyme. To find the glucose yield, further samples were examined using HPLC. Following the hydrolysis process, the resulting liquid and solid portions were separated using a vacuum filter with a 0.2 µm nylon membrane. After drying, the weight of the solid portion was recorded for mass. Following drying, the amount of the solid portion was measured for mass balance analysis.

2.3.16. Characterisation of Delignified Passion Fruit Rind

2.3.16.1. XRD X-Ray Diffractometer (XRD) Analysis: The crystalline structure of untreated and treated passion fruit rind was analysed using a powder X-ray diffractometer (Smart Lab, Rigaku, Japan) [206]. Scanning was conducted using a CuK_{α} filter with X-ray source wavelength 0.154 nm. The study was conducted in continuous mode in a 2θ range of 10°–30°, with a scanning speed of 2.0 °/min and a step size of 0.05°. The crystallinity index was determined by using equation 2.9.

$$\text{Crystallinity Index (\%)} = \frac{I_{\text{crystalline}} - I_{\text{amorphous}}}{I_{\text{crystalline}}} \times 100 \qquad 2.9$$

Where, $I_{\text{crystalline}}$ is the peak intensity of cellulose at 2θ = 22.4°, and $I_{\text{amorphous}}$ is the amorphous peak intensity at 2θ = 15.6°.

2.3.16.2. Field-emission scanning electron microscopy analysis: The surface morphology of biomass (SPFR, PUH-PFR, RPFR, PH-PFR) was analysed using Field-emission scanning electron microscopy (FE-SEM, Carl Zeiss, Model-Gemini 300) [207]. The samples were prepared on carbon tape and placed over the stub surface. A double gold coating of the sample was performed on a prepared stub and kept in the vacuum chamber before imaging by FE-SEM.

2.3.16.3. Fourier transform infrared spectroscopic analysis: FTIR-ATR analysis was performed on all NaOH-treated and raw biomasses in the range of 4000 cm^{-1} to 400 cm^{-1} using an FTIR spectrometer (Parkin Elmer, L1600300 Spectrum TWO LiTa). The resolution was taken 2 cm^{-1} and 30 scans per spectra, following the prior technique [197]. For each analysis, a sample of about 0.100 mg was introduced to the apparatus.

2.3.16.4. Thermal degradation of Delignified biomass: The changes in physical properties of raw and spent passion fruit rind and delignified PUH-PFR and PH-RPFR were measured by observing the change in temperature, by the thermogravimetric analysis (TGA) [208]. TGA and differential thermogravimetric analysis (DTG) of Delignified biomass were performed by using a TGA analyser (Perkin Elmer, TGA 4000). For the analysis, 10 mg of powdered samples was taken in an alumina crucible and heated from ambient temperature to 900 °C at a rate of 10 °C min^{-1}, and the nitrogen gas was purged at a flow rate of 60 mL/min.

2.3.17. Microbial fermentation process

2.3.17.1. Fermentation acid prehydrolysate using P. stipitis: The hydrolysates were concentrated under reduced pressure to double their sugar concentration. Further, they were filter-sterilised for subsequent fermentation. A 50 mL Erlenmeyer flask with 20 mL of fermentation media was used to accomplish the xylose fermentation [209]. The fermentation media comprised 0.4 mL of a 50X concentrated nutritional solution (consisting of 1.7 g yeast nitrogen base, 1 g urea, and 6.56 g peptone in 20 mL water) was maintained at pH 6. This was followed by the addition of 1 mL of inoculum with a cell concentration of 1.5 g/L (dry cell weight). Later, an adequate quantity of hydrolysate was added to attain the required volume, then the flask was agitated at 200 rpm and incubated at 30 °C. At predetermined time intervals, samples were collected and analysed by HPLC.

2.3.17.2. Fermentation enzymatic hydrolysate using S. cerevisiae: Fermentation experiments were carried out in 250 mL Erlenmeyer flasks [205], containing 100 mL of fermentation medium (cellulosic hydrolysates), 4 mL of 25X YP (10 g of yeast extract and 20 g of peptone in 40 mL of distilled water) nutrient solution, and 6 mL of *S. cerevisiae* (which gives initial concentration of 2.1 g/L on cell dry weight basis). The initial pH of the fermentation broth was maintained at 5.5 and incubated at 30 °C, 150 rpm, and 30 h. All fermentation samples were taken periodically for HPLC analysis.

2.3.17.3. Analytical methods: The optical density results at 600 nm measured using a UV-Vis spectrophotometer (Thermo Scientific, Orion Aquamate 8000) were used to quantify the biomass concentration in the reactor. Further, the OD was correlated with the dry cell weight. The high-performance liquid chromatography (HPLC, Shimadzu Corporation, Japan) unit equipped with a refractive index detector maintained at 50 °C was used to quantify sugars, ethanol, and fermentative inhibitors. The separation was carried out using a Bio-Rad Aminex HPX-87H column (300 x 7.8 mm). The mobile phase, 5 mM sulfuric acid, was added at a flow rate of 0.5 mL/min, while the column oven maintained its temperature at 60 °C. Folin-Ciocalteu technique was employed with gallic acid as the standard to determine the phenolic acid content in the samples [210].

2.3.17.3. Kinetic parameters calculation for fermentation process: The sugar/inhibitor concentration, bioethanol yield, and fermentation efficiency were calculated using equations. (2.10-2.13), respectively, as follows:

$$\text{Sugar/inhibitor concentration (mg/g)} = \frac{\text{Sugar/inhibitor concentration (by HPLC)} \times \text{Dilution factor} \times \text{Total volume of hydrolysate}}{\text{Initial weight of biomass}} \quad 2.10$$

$$\text{Sugar or inhibitor concentration } \left(\frac{\text{g}}{\text{L}}\right) = \text{Sugar or inhibitor concentration (by HPLC)} \times \text{Dilution factor} \quad 2.11$$

$$\text{Bioethanol Yield (g/g)} = \frac{\text{Experimental Bioethanol Produced (g/L)}}{\text{Sugar Consumed (g/L)}} \quad 2.12$$

$$Fermentation\ Efficiency\ (\%) = \frac{Experimental\ Bioethanol\ Yield\ (g/L)}{Theoritical\ Bioethanol\ Yield\ (g/L)} \quad 2.13$$

3. CHAPTER 3

Optimisation of the extraction of phytochemicals from yellow passion fruit rind using ultrasound extraction and supercritical fluid extraction

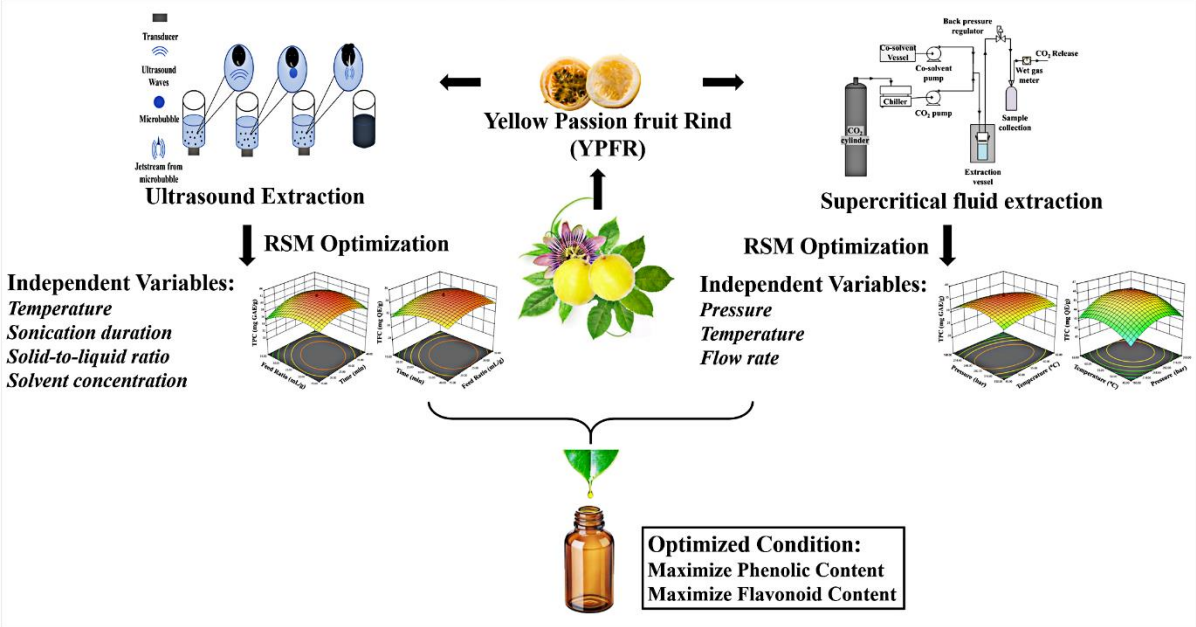

A part of this work has been published as Kakali Borah, Rupesh Kumar, Vaibhav V Goud, 2023. Extraction of Phenolics from Yellow Passion Fruit Rind Using Supercritical Carbon Dioxide Extraction. Agro and Food Processing Technologies: Proceedings of NERC 2022. Springer Nature Singapore 141-156. DOI: 10.1007/978-981-19-9704-48.

Another part of this work has been accepted as Kakali Borah, Rupesh Kumar, Vaibhav V Goud, 2025. A Sustainable Approach to Passion Fruit Waste Utilisation: Statistical Optimization of Ultrasonic Extraction of Polyphenols. Proceedings of RIC 2024. Springer Nature Singapore.

CHAPTER 3

Optimisation of the extraction of phytochemicals from yellow passion fruit rind using ultrasound extraction and supercritical fluid extraction

This study systematically optimises the extraction of phenolic and flavonoid contents from yellow passion fruit rind (YPFR) sourced from Assam, India, employing ultrasound-assisted extraction (UAE) and supercritical fluid extraction (SFE) techniques. Ethanol-water was used as the solvent for UAE, instead SFE utilised CO_2 with 10% ethanol as a co-solvent (SC-ET). Response Surface Methodology (RSM) utilising a Central Composite Design (CCD) optimised independent parameters: temperature, sonication duration, solid-to-liquid ratio, and solvent concentration for Ultrasound-assisted Extraction (UAE); and pressure, temperature, and flow rate for Supercritical Fluid Extraction (SFE). Statistical validation by ANOVA ($p<0.05$) and regression analysis (R^2) supports the model's significance. Interaction effects were analysed by 3D response plots, and Design-Expert software predicted optimal conditions for maximal phenolic and flavonoid yield. The findings highlight the efficacy of Ultrasound-assisted Extraction (UAE) and Supercritical Fluid Extraction (SFE) as environmentally friendly methods for the recovery of polyphenolics from YPFR. The systematic analysis of the extracts obtained at the optimised condition can be envisaged in a future study.

3.1. Selection of process variables

The selection of process variables for ultrasound-assisted extraction (UAE) and supercritical fluid extraction (SFE) was determined by their established impact on extraction efficiency, solubility of bioactive chemicals, and mass transfer rates. Literature research and pre-optimisation testing facilitated the identification of the key factors to enhance the recovery of phenolic and flavonoid compounds from yellow passion fruit rind. Some process factors exhibit substantial effects, whereas others may not significantly influence the extraction efficiency. This study optimised Ultrasound-Assisted Extraction (UAE) by varying four critical variables: extraction temperature

(°C), ethanol-water concentration (% v/v), extraction duration (min), and solid-to-solvent ratio (g/mL). The parameters were chosen for their substantial impact on the solubility, diffusion, and stability of polyphenolic compounds, as well as their appropriateness for optimisation through Response Surface Methodology (RSM). Temperature influences solute transport and cavitation efficacy, whereas ethanol content impacts solvent polarity and the solubility of phytochemicals. The duration of extraction affects ultrasonic exposure and the possible destruction of thermolabile chemicals, while the solid-to-solvent ratio determines the concentration gradient and extraction efficacy. In Supercritical Fluid Extraction (SFE), temperature (°C), pressure (bar), and solvent flow rate (mL/min) were identified as critical factors because of their influence on the density, solvating capacity, and mass transfer dynamics of supercritical CO_2. The incorporation of 10% ethanol as a cosolvent increased the extraction of polar chemicals, including phenolics and flavonoids, which exhibit limited solubility in nonpolar CO_2, thus enhancing extraction yield and efficiency.

3.2. RSM optimisation of process variables

3.2.1. ANOVA and model validation

ANOVA and model validation were conducted to evaluate the statistical significance and reliability of the extraction models for ultrasound-assisted extraction (UAE) and supercritical fluid extraction (SFE) of polyphenolic compounds from the rind of *Passiflora edulis* f. *flavicarpa*. A second-order quadratic model based on response surface methodology (RSM) with a central composite design (CCD) was employed to investigate the interaction, linear, and quadratic impacts of the chosen independent variables. The model's fitness was assessed by the coefficient of determination (R^2) and the lack-of-fit test. In the UAE, ANOVA analysis (Table 3.2) validated the model's validity ($p < 0.0001$), indicating that the feed ratio exhibited the most significant effect on phenolic yield ($F = 48.46$, $p < 0.0001$), whereas extraction duration affected flavonoid yield ($F = 55.11$, $p < 0.0001$). All quadratic terms were statistically significant ($p < 0.0001$), and the high lack-of-fit p-value (> 0.05) validated the model's appropriateness. The adjusted R^2 values (0.97 for phenolics and 0.96 for flavonoids) and regression coefficients ($R^2 = 0.99$ for phenolics, 0.98 for flavonoids) demonstrated significant model correlation, accompanied by a low coefficient of variation (CV = 1.55% and 1.08%, respectively), ensuring precision (Table 3.1) and dependability.

Similarly, ANOVA (Table 3.4) indicated model significance for SC-ET ($p < 0.0001$), with flow rate showing the most influence on phenolic yield ($F = 224.49$, $p < 0.0001$), followed by pressure and temperature ($F = 74.65$ and 9.36, respectively). Pressure demonstrated the highest impact on flavonoid extraction ($F = 39.03$, $p < 0.0001$). All quadratic variables were statistically significant ($p < 0.001$), however, the interaction effects of pressure and temperature ($p = 0.0008$), pressure and flow rate ($p = 0.0011$) were significant for phenolics and flavonoids, respectively. The lack-of-fit test ($p > 0.05$) confirmed the model's reliability. The adjusted R^2 values were near the regression coefficients (R^2 approaching 1), and the predicted R^2 values (> 0.90) confirmed the model's predictive efficacy. The low coefficient of variation (1.41% for phenolics and 0.76% for flavonoids) confirmed experimental accuracy (Table 3.3). Consequently, both the UAE and SC-ET models demonstrated substantial statistical significance, dependability, and appropriateness for enhancing the extraction of phenolics and flavonoids. The quadratic polynomial equations fitted with all the experimental data provided an explanation for the impact of parameters on the response. Equations 3.1 and 3.2 indicate coded factors for total phenolic content and flavonoid content extracted using UAE, while equations 3.3 and 3.4 correspond to those extracted using SC-ET.

$$Y_1 = 42.10 + 0.31a + 0.54b + 0.46c - 0.80d + 0.41ab - 0.37ac - 0.35ad + 0.27bc - 0.97bd + 0.76cd - 0.94a^2 - 1.97b^2 - 2.18c^2 - 2.06d^2 \quad 3.1$$

$$Y_2 = 34.74 + 0.19a - 0.46b + 0.52c + 0.34d - 0.11ab - 0.15ac - 0.023ad + 0.53bc + 0.57bd - 0.27cd - 0.90a^2 - 0.89b^2 - 1.01c^2 - 0.89d^2 \quad 3.2$$

$$Y_1 = 36.16 + 1.05u - 0.37v + 1.82x + 0.76uv + 0.26ux - 0.15vx - 3.58u^2 - 1.50v^2 - 1.42x^2 \quad 3.3$$

$$Y_2 = 45.67 + 0.56u + 0.48v + 0.12x + 0.11uv + 0.53ux - 0.40vx - 1.23u^2 - 0.97v^2 - 0.90x^2 \quad 3.4$$

In coded terms, Y_1 - Total phenolic content, Y_2 - Total flavonoid content, a - temperature (°C), b – ethanol-water concentration (%), c – extraction time (min), and d - feed ratio (mL/g) were parameters used for ultrasound extraction. While u-pressure (bar), v-temperature (°C), and x-flow rate (g/min) were independent variables used for SC-ET.

Table 3.1. CCD analysis and results obtained for phenolic and flavonoid content using UAE

Sl. No.	Temperature (°C)	Ethanol: water Concentration (%)	Extraction Time (min)	Feed Ratio (mL/g)	Total Phenolic content (mg GAE/g)	Total Flavonoid content (mg QE/g)
1	35	5	15	15	34.26 ± 0.80	31.23 ± 0.72
2	70	50	15	15	35.41 ± 0.75	31.62 ± 0.29
3	35	80	15	15	36.22 ± 0.27	28.05 ± 1.02
4	70	80	15	15	38.09 ± 0.88	28.86 ± 1.34
5	35	50	40	15	33.38 ± 0.75	31.62 ± 0.62
6	70	50	40	15	33.65 ± 1.03	32.69 ± 1.14
7	35	80	40	15	36.58 ± 0.52	31.07 ± 0.29
8	70	80	40	15	37.98 ± 0.55	31.03 ± 0.33
9	35	50	15	35	33.35 ± 0.60	30.93 ± 0.70
10	70	50	15	35	33.10 ± 0.92	32.05 ± 0.32
11	35	80	15	35	30.97 ± 1.52	30.08 ± 1.2
12	70	8	15	3	33.43 ± 0.37	31.04 ± 0.75
13	35	5	40	35	36.58 ± 0.29	30.73 ± 0.45
14	70	50	40	35	34.05 ± 0.71	31.06 ± 0.78
15	35	8	40	35	33.95 ± 0.88	32.57 ± 0.66
16	7	80	40	35	34.76 ± 1.09	32.04 ± 0.85
17	17.5	65	27.5	25	37.94 ± 1.00	31.09 ± 0.77
18	87.5	65	27.5	25	39.46 ± 0.60	31.28 ± 0.15
19	52.5	35	27.5	25	33.71 ± 0.66	32.20 ± 0.87
20	52.5	9	27.5	25	35.41 ± 1.46	30.22 ± 0.36
21	52.5	65	2.5	25	32.64 ± 0.85	29.83 ± 0.33
22	52.5	65	52.5	25	34.82 ± 1.80	31.63 ± 0.75
23	52.5	65	27.5	5	35.50 ± 0.44	30.22 ± 0.22
24	52.5	65	27.5	45	32.92 ± 1.01	32.18 ± 0.25
25	52.5	65	27.5	25	42.38 ± 0.87	35.14 ± 1.13
26	52.5	65	27.5	25	42.53 ± 1.65	34.96 ± 1.71

27	52.5	65	27.5	25	41.86 ± 1.04	34.58 ± 0.16
28	52.5	65	27.5	25	42.26 ± 1.16	34.97 ± 0.92
29	52.5	65	27.5	25	42.01 ± 1.01	34.45 ± 0.51
30	52.5	65	27.5	25	41.55 ± 0.56	34.36 ± 1.54

Table 3.2. Experimental data obtained from CCD analysis for phenolic and flavonoid extraction using UAE

Source	Phenolics Sum of Squares	Df	Mean Square	F Value	p-value	Flavonoids Sum of Squares	Df	Mean Square	F Value	p-value
Model	338.71	14	24.19	76.43	$< 1.00 \times 10^{-4}$	92.45	14	6.6	55.53	$< 1.00 \times 10^{-4}$
A-Temperature	2.37	1	2.37	7.49	1.53×10^{-2}	0.8459	1	0.8459	7.11	0.02
B-Ethanol-water concentration	6.99	1	6.99	22.06	$< 3.00 \times 10^{-4}$	5.17	1	5.17	43.5	$< 1.00 \times 10^{-4}$
C-Extraction time	5.16	1	5.16	16.28	$< 1.10 \times 10^{-3}$	6.55	1	6.55	55.11	$< 1.00 \times 10^{-4}$
D- Feed Ratio	15.34	1	15.34	48.46	$< 1.00 \times 10^{-4}$	2.84	1	2.84	23.86	2.00×10^{-4}
AB	2.68	1	2.68	8.46	1.08×10^{-2}	0.1823	1	0.1823	1.53	0.23
AC	2.21	1	2.21	6.97	1.85×10^{-2}	0.3783	1	0.3783	3.18	9.47×10^{-2}
AD	1.91	1	1.91	6.03	2.67×10^{-2}	0.0082	1	0.0082	0.0692	0.80
BC	1.19	1	1.19	3.77	7.12×10^{-2}	4.42	1	4.42	37.19	$< 1.00 \times 10^{-4}$
BD	15.00	1	15.00	47.40	$< 1.00 \times 10^{-4}$	5.19	1	5.19	43.66	$< 1.00 \times 10^{-4}$
CD	9.31	1	9.31	29.42	$< 1.00 \times 10^{-4}$	1.18	1	1.18	9.95	6.60×10^{-3}
A^2	24.05	1	24.05	75.96	$< 1.00 \times 10^{-4}$	22.05	1	22.05	185.43	$< 1.00 \times 10^{-4}$
B^2	106.54	1	106.54	336.53	$< 1.00 \times 10^{-4}$	21.71	1	21.71	182.57	$< 1.00 \times 10^{-4}$
C^2	130.26	1	130.26	411.46	$< 1.00 \times 10^{-4}$	27.98	1	27.98	235.28	$< 1.00 \times 10^{-4}$
D^2	116.23	1	116.23	367.16	$< 1.00 \times 10^{-4}$	21.88	1	21.88	183.98	$< 1.00 \times 10^{-4}$
Residual	4.75	15	0.32			1.78	15	0.1189		
Lack of Fit	4.09	10	0.41	3.12	0.11	1.27	10	0.1266	1.22	0.44
R^2	0.99					0.98				
R_{adj}^2	0.97					0.96				

R_{prep}^2	0.93	0.91
CV%	1.55	1.08

Table 3.3. Experimental data obtained from CCD analysis for phenolic and flavonoid extraction using SC-ET

Sl.No.	Pressure (bar)	Temperature (°C)	Flow rate (g/min)	Total Phenolic content (mg GAE/g)	Total Flavonoid content (mg QE/g)
1	180.00	45.00	10.00	28.19 ± 1.06	41.80 ± 0.95
2	350.00	45.00	10.00	27.94 ± 0.15	41.61 ± 0.54
3	180.00	65.00	10.00	26.09 ± 0.90	43.38 ± 1.28
4	350.00	65.00	10.00	28.95 ± 0.11	43.67 ± 2.04
5	180.00	45.00	20.00	31.7 ± 1.36	41.59 ± 0.53
6	350.00	45.00	20.00	32.6 ± 0.22	43.54 ± 1.33
7	180.00	65.00	20.00	29.07 ± 1.24	41.61 ± 1.46
8	350.00	65.00	20.00	32.91 ± 1.00	43.97 ± 1.05
9	122.05	55.00	15.00	23.93 ± 0.22	41.11 ± 0.64
10	407.95	55.00	15.00	28.08 ± 1.84	43.00 ± 0.96
11	265.00	38.18	15.00	32.37 ± 0.36	42.08 ± 0.46
12	265.00	71.82	15.00	31.39 ± 1.49	43.50 ± 1.49
13	265.00	55.00	6.59	29.22 ± 1.04	42.58 ± 0.97
14	265.00	55.00	23.41	35.00 ± 0.09	43.39 ± 1.57
15	265.00	55.00	15.00	35.42 ± 0.85	46.46 ± 1.38
16	265.00	55.00	15.00	36.15 ± 0.24	45.56 ± 0.44
17	265.00	55.00	15.00	36.35 ± 0.57	45.46 ± 0.54
18	265.00	55.00	15.00	35.86 ± 0.64	45.52 ± 0.78
19	265.00	55.00	15.00	37.08 ± 0.55	45.49 ± 0.50
20	265.00	55.00	15.00	36.12 ± 0.11	45.57 ± 1.09

Table 3.4. Experimental data obtained from CCD analysis for phenolic and flavonoid extraction using SC-ET

Source	Phenolics Sum of Squares	Df	Mean Square	F Value	p-value	Flavonoids Sum of Squares	Df	Mean Square	F Value	p-value
Model	284.80	9	31.64	157.37	$< 1.00 \times 10^{-4}$	50.85	9	5.65	52.25	$< 1.00 \times 10^{-4}$
A-Pressure	15.01	1	15.01	74.65	$< 1.00 \times 10^{-4}$	4.22	1	4.22	39.03	$< 1.00 \times 10^{-4}$
B-Temperature	1.88	1	1.88	9.36	0.01	3.10	1	3.10	28.68	3.00×10^{-4}
C-Flow Rate	45.14	1	45.14	224.49	$< 1.00 \times 10^{-4}$	0.19	1	0.19	1.75	21.50×10^{-2}
AB	4.56	1	4.56	22.69	8.00×10^{-4}	0.10	1	0.10	0.89	36.74×10^{-2}
AC	0.56	1	0.56	2.79	0.13	2.21	1	2.21	20.46	1.10×10^{-3}
BC	0.19	1	0.19	0.93	0.36	1.28	1	1.28	11.86	6.30×10^{-3}
A^2	184.75	1	184.75	918.77	$< 1.00 \times 10^{-4}$	21.91	1	21.91	202.61	$< 1.00 \times 10^{-4}$
B^2	32.50	1	32.50	161.63	$< 1.00 \times 10^{-4}$	13.66	1	13.66	126.27	$< 1.00 \times 10^{-4}$
C^2	29.10	1	29.10	144.70	$< 1.00 \times 10^{-4}$	11.79	1	11.79	109.01	$< 1.00 \times 10^{-4}$
Residual	2.01	10	0.20			1.08	10	0.11		
Lack of Fit	0.50	5	0.10	0.33	0.88	0.33	5	0.07	0.44	0.81
R^2	0.99					0.98				
R_{adj}^2	0.99					0.96				
R_{prep}^2	0.98					0.93				
CV%	1.41					0.76				

3.2.2. Interaction effects of the independent variables on the response

3.2.2.1. Ultrasound-assisted extraction

Three-dimensional response surface plots are used to illustrate the dynamic impacts of parameters on the response. Figure 3.1 showed that all the chosen parameters had significantly impacted TPC and TFC yield. Figure 3.1(a, b, c, g, h, i) reveals that the increasing extraction temperature improves the polyphenols' yield with a p-value <0.05 up to 55°C. The solvent viscosity and surface tension are reduced as the temperature increases, improving the solvent's ability to penetrate the matrix and boosting the effectiveness of the extraction [211]. In this approach, the conditions were created to encourage the release of bound phenolics from plant material and to disrupt the integrity of the cell wall, which intensified solubility and coefficients of diffusion [212]. The adverse effect of temperature, however, indicates that overheating has the opposite effect. The temperature above 55°C might degrade the polyphenols [191].

Under various extraction conditions, utilising 65% ethanol in an aqueous medium as the extractant led to the best performance in terms of total polyphenols, as shown in Figure 3.1(a, d, e, g, j, k). Although the most polar solvent of all is pure water, a higher water percentage did not produce the best results in terms of extract and total phenolic and flavonoid content. This might be explained by the fact that water has a higher viscosity than other solvents, which is a mass transfer issue [213]. Increasing the ethanol concentration lowers the viscosity and has the ability to change the structure of the plant by swelling the matrix, thus increasing the yield of the extract and the polyphenolic content with increasing permeability of the solvent [214]. The water serves as the agent that causes plants to swell, whereas ethanol is thought to cause the connection between the solvents and the plant matrix to break. Thus, the combination of water and ethanol as a solvent agent had the best performance in extracting polyphenols and makes it suitable for use in the food industry. Another possibility is that water has a high dielectric constant, which causes an increase in the polarity indices of aqueous ethanol [213]. Whereas the denaturation of cell membrane proteins caused by greater ethanol concentrations slowed the diffusion rate of polyphenols into the solvent [215]. This might cause a decrease in the yield of the TPC and TFC after increasing the ethanol concentration beyond 65 percent.

From Figure 3.1(b, d, f, h, j, l), it was observed that sonication duration highly influences the yield of phenolics and flavonoids with a p-value <0.001. Initially, in the UE, soluble components on the surfaces of the plant matrix dissolve, and then the solute molecules start to be transferred from the plant matrix into the solvent through osmotic and diffusional processes. However, prolonged sonication led to low extraction yield and breakdown of polyphenolic compounds [216]. As a result, the range of 10 to 20 min was chosen as the ideal extraction period for the RSM study.

The feed ratio had a significant impact (p <0.001) on both phenolics and flavonoids extraction yield by UE. The UE yield increased as the solid-to-liquid ratio increased up to a specific threshold, after which it decreased. From the interaction plot of the feed ratio displayed in Figure 3.1(c, e, f, i, k, l), the yield of both the phenolics and flavonoids increases up to 25 mL/g. When the solvent becomes very viscous at a high feed ratio, cavitation becomes difficult in the rarefaction cycle, as a greater cohesive force in the more viscous solvent must be overcome by the negative pressure. However, at the low feed ratio, the concentration difference increases the diffusivity of the solute and dissolves it more readily in the solvent that penetrates the cell. Additionally, the greater contact area between the solute and solvent contributed to the extraction yield. A very concentrated solute in the solution intensifies the cavitation effect that degrades the targeted molecules [217]. Thus, the extraction yield of phenolics and flavonoids in the UE process is greatly influenced by the feed ratio, with an F value of 48.46.

The perturbation plot (Figure 3.2a, b) assessed the impact of each independent variable on the response, with all other parameters held at their optimal levels within the design space. This figure enables a direct evaluation of the relative impact of each component on the response. A more pronounced curvature in the perturbation curve signifies an increased sensitivity of the reaction to variations in that factor. Figure 3.2 demonstrates that the phenolic yield is most sensitive to the solid-to-solvent feed ratio, while the flavonoid yield is predominantly affected by the extraction period, indicating that both parameters are crucial for optimising their respective outputs.

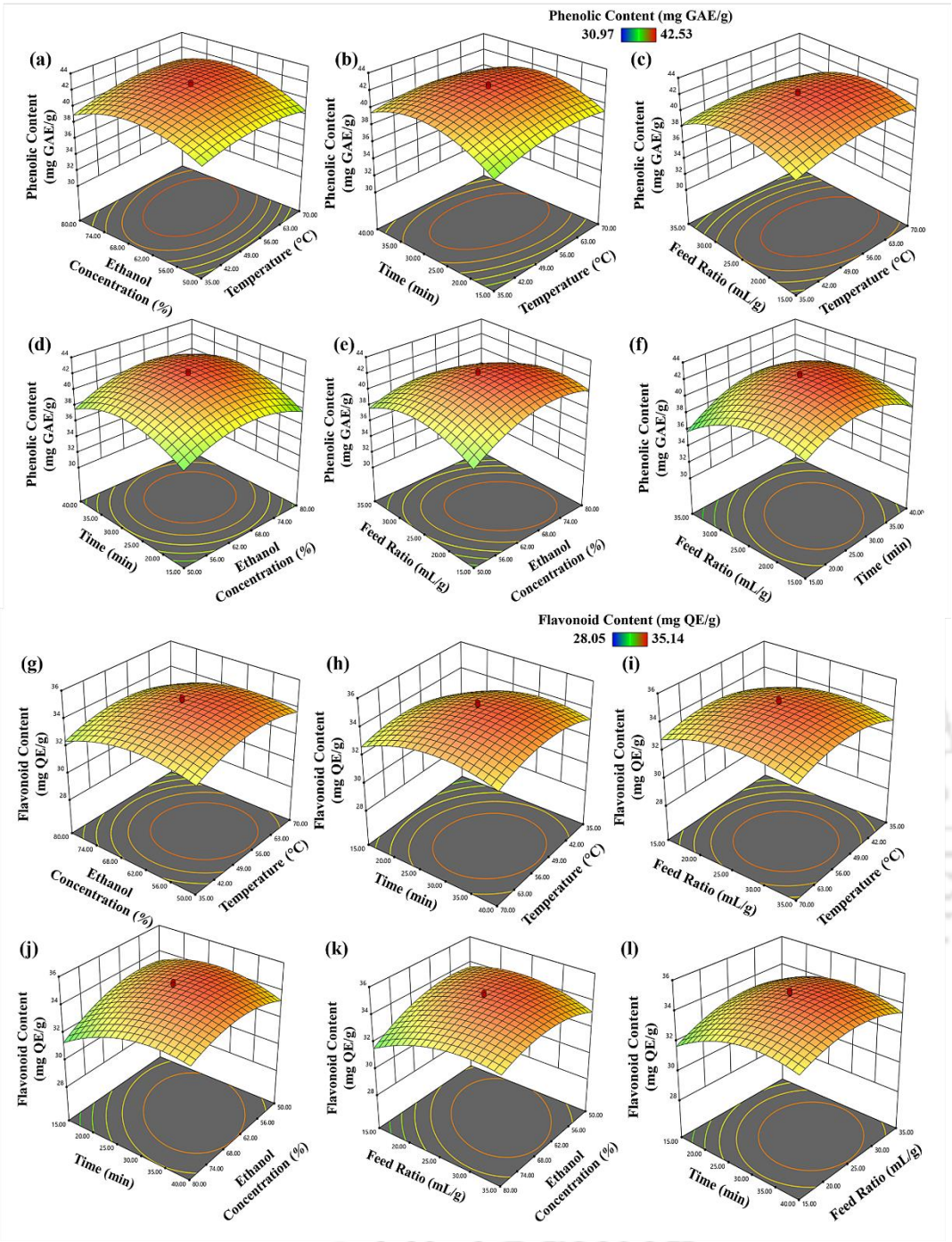

Figure 3.1. 3D Response surface plot of interaction effects of 1.a) Ethanol concentration (%) and Temperature (°C); 1.b) Extraction time (min) and Temperature (°C); 1.c) Temperature (°C) and Feed ratio (mL/g); 1.d) Ethanol concentration (%) and Extraction time (min); 1.e) Ethanol concentration (%) and Feed ratio (mL/g); and 1.f) Extraction time (min) and Feed ratio (mL/g) on total phenolic yield; however, 2.a) Ethanol concentration (%) and Temperature (°C); 2.b) Extraction time (min) and Temperature (°C); 2.c) Temperature (°C) and Feed ratio (mL/g); 2.d) Ethanol concentration (%) and Extraction time (min); 2.e) Ethanol concentration (%) and Feed ratio (mL/g); and 2.f) Extraction time (min) and Feed ratio (mL/g) on total flavonoid yield using UAE.

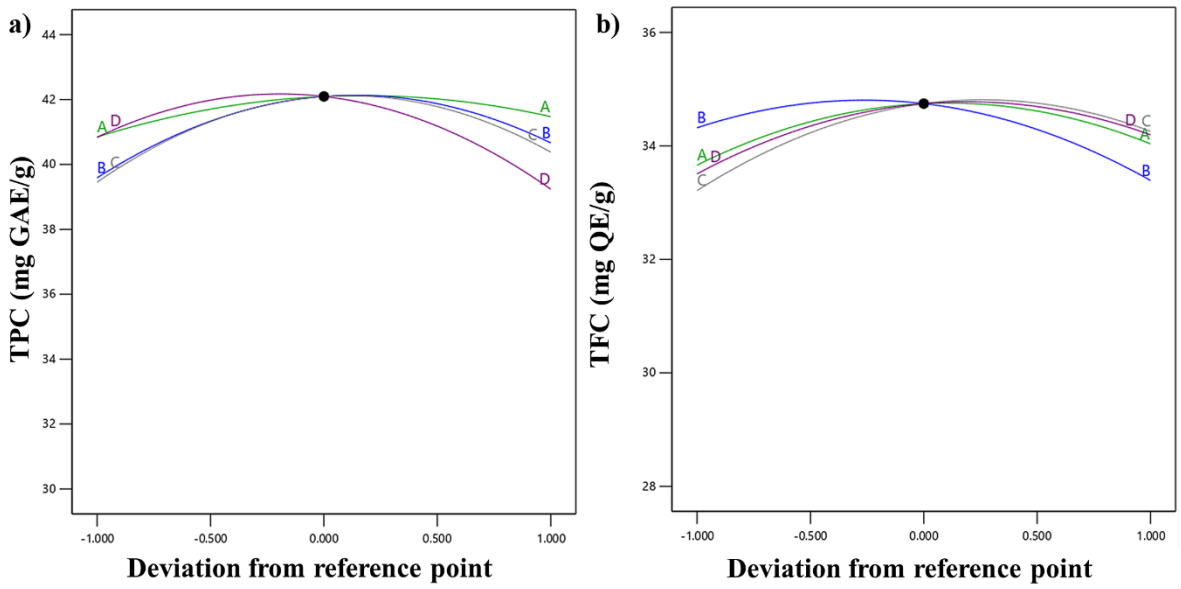

Figure 3.2. Perturbation plot for a) phenolic and b) flavonoid yield using UAE method

3.2.2.2. Supercritical fluid extraction with 10% ethanol

The extraction yield was significantly (With a p-value below 0.05) influenced by the individual factors and their quadratic components chosen in SC-ET extraction. With a probability value <0.001, the interaction between pressure and temperature had a significant impact on the rate of extraction shown in Figure 3.3(a, d). A rapid rise in pressure to 280 bar resulted in a progressive increase in the extraction yield of polyphenolic components. At constant temperature, the viscosity of supercritical carbon dioxide reduces as pressure rises, enhancing the solubility of the substance. By reducing intermolecular distances, reduced viscosity increases the interaction of analytes with carbon dioxide and improves extraction yield [218]. Beyond 280 bar, a pronounced decrease in both phenolic and flavonoid yields was observed. According to Bimakr et al. [219], at elevated pressures within the supercritical fluid medium, a reduction in the rate of solute diffusion was observed, likely due to increased fluid density and reduced mass transfer efficiency. At lower temperatures, increasing the pressure can hinder solute dissolution and solubility by reducing SC-CO_2 diffusivity, initiating solid matrix compaction, decreasing the void fraction, and limiting solvent penetration into the matrix pores.

Figure 3.3(b, e) exhibited the 3D response graphic showing the effect of pressure on flow rate. The yield increased with temperature up to 55 °C, after which further temperature elevation did not result in a statistically significant improvement. On

increasing the rate of flow of carbon dioxide from 10 to 20 g/min, the response output increased up to 15g/min before stabilising. This could be because the high flow rate drives the solvent through the sample, only passing around the matrix of the sample and not diffusing through the pores, preventing carbon dioxide from moving into and out of the sample. Due to intra-particle diffusion resistance, lower flow rates enhance the trapping of analytes and improve extraction efficiency by promoting mass transfer and extending the contact time between the solvent and target solutes. As a result, the fluid's sluggish movement allows for deeper intrusion into the solute matrix while also lowering the linear velocity, resulting in excellent efficiency of extraction [218].

Figure 3.3(c, f) conveyed the combined impact of temperature and flow rate on the response while keeping the pressure constant. In the initial phase, the response yield increased rapidly at a flow rate of 18 g/min, followed by a slight decline. The effect of temperature on the extraction yield had a similar impact to that of pressure. The output increased while increasing the temperature up to 54°C; beyond that, the phenolic yield reduced due to the thermal sensitivity of extracted compounds. Also, at constant pressure, increasing temperature decreases the solvent strength by lowering the density of carbon dioxide. Near the critical pressure, the fluid density depends on the temperature. Therefore, the extraction yield fluctuated over a temperature range of 45-65°C. A moderate increase in temperature can significantly reduce the solvent's solubility by lowering its density. An increasing temperature improves the mass transfer from solute to solvent and increases extraction efficiency [219].

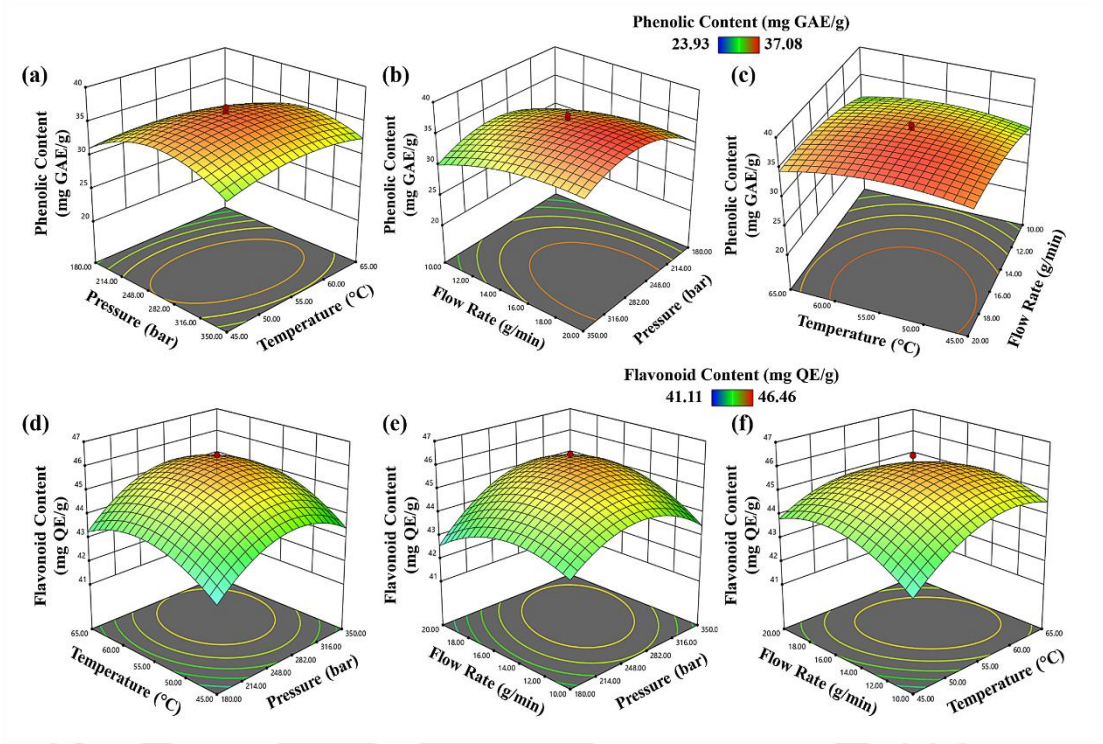

Figure 3.3. 3D Response surface plot of interaction effects of a) Pressure (bar) and Temperature (°C); b) Pressure (bar) and Flow rate (g/ min); c) Temperature (°C) and Flow rate (g/ min); on total phenolic yield; however, d) Pressure (bar) and Temperature (°C); e) Pressure (bar) and Flow rate (g/ min); f) Temperature (°C) and Flow rate (g/ min); on total flavonoid yield using SC-ET.

The perturbation plot (Figure 3.4a, b) demonstrates the influence of individual variables on the response, maintaining all other parameters at their optimal levels within the experimental design space. This graphic facilitates a clear depiction of the relative impact of each component on the response variable. A more pronounced slope or increased curvature in the graph signifies a more substantial influence of that variable on the response. Figure 3.4 illustrates that the phenolic yield was most sensitive to changes in flow rate, followed by pressure and temperature. The yield of flavonoids was mostly influenced by pressure and temperature, suggesting that these parameters are crucial for optimising flavonoid extraction under the specified conditions.

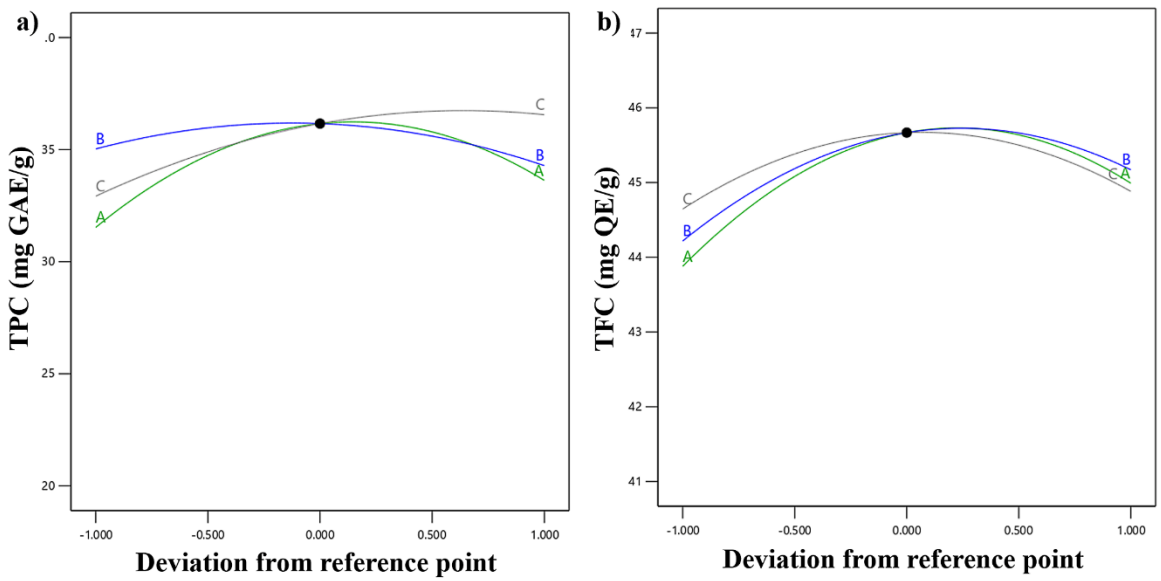

Figure 3.4 Perturbation plot for a) phenolic and b) flavonoid yield using SC-ET method

3.2.3. Optimisation of process variables for both UAE and SC-ET methods:

The optimum extraction conditions for both UAE and SC-ET were established using the desirability function of Design-Expert software to optimise the yield of phenolics and flavonoids listed in Table 3.5. The optimal yield for the UAE was predicted at 54.4 °C, with an ethanol concentration of 64.9%, an extraction period of 29.5 min, and a feed ratio of 24.7 mL/g, resulting in a desirability value of 0.96. Under these conditions, the expected phenolic and flavonoid concentrations were 42.15 mg GAE/g and 34.80 mg QE/g, respectively, whereas the experimental validation produced 41.48 ± 0.38 mg GAE/g and 34.41 ± 2.72 mg QE/g, thereby affirming the model's precision, where percentage error range within 1.13-1.62%. For SC-ET, the optimal parameters were determined to be a pressure of 284.6 bar, a temperature of 55.9 °C, and a flow rate of carbon dioxide of 16.5 g/min, yielding a desirability value of 0.914. The predicted yields were 36.66 mg GAE/g for phenolics and 45.75 mg QE/g for flavonoids. Experiments conducted under these conditions resulted in phenolic and flavonoid yields of 36.04 ± 2.15 mg GAE/g and 45.59 ± 1.79 mg QE/g, respectively, exhibiting a strong correlation with the model's expected values, with a percentage error of 1.72% and 0.35%, respectively. The agreement between predicted and experimental results for both approaches validates the reliability of the quadratic model in improving the extraction process within the specified parameter range.

Table 3.5. Optimisation table for phenolic and flavonoid extraction using UAE and SC-ET

Ultrasound-assisted Extraction		Supercritical fluid extraction with 10% ethanol	
Temperature (°C)	54.4	Pressure (bar)	284.6
Ethanol: water Concentration (%)	64.9	Temperature (°C)	55.9
Extraction Time (min)	29.5	Flow rate of carbon dioxide (g/min)	16.5
Feed Ratio (mL/g)	24.7	-	-
TPC (mg GAE/g)	42.15	TPC (mg GAE/g)	36.66
TFC (mg QE/g)	34.80	TFC (mg QE/g)	45.75
Desirability	0.959	Desirability	0.914

The results of the present study are consistent with previous research on the extraction of polyphenolic compounds from passion fruit and other agro-industrial wastes using various extraction methods (Table 3.6). Vo et al. [220] confirmed the extraction of 26.02 mg RE/g dry basis (db) of flavonoids and 38.27 mg GAE/g db of phenolics from passion fruit peel using ethanol, water, and acetone as solvents in combination with ultrasound-assisted extraction. Similarly, Wang et al. [221] utilised ultrasonic-assisted polyphenol extraction, optimised via response surface methodology, resulting in 21.03 mg GAE/g of total polyphenols. In another study, Pereira et al. [222] employed ultrasound-assisted pressured liquid extraction with 70% ethanol, yielding a total phenolic content of 2.07 ± 0.05 mg GAE/g extract.

Conversely, Huo et al. [69] employed deep eutectic solvents (DESs) to extract polyphenols from passion fruit rind, achieving a yield of 9.68 mg GAE/g dry weight, whereas an extraction utilising methanol/water and acetone/water mixtures from *P. edulis* f. *flavicarpa* peel flour resulted in phenolic content of 5.54 ± 2.47 mg GAE/100 g [223]. These differences highlight the significance of solvent polarity and process factors in ascertaining extraction efficiency.

Green extraction methods, including supercritical fluid extraction and ultrasound-assisted extraction, have demonstrated potential. Oliveira et al. [224] isolated phenolics from passion fruit seed cake by supercritical fluid extraction with 5% ethanol as a co-solvent, yielding 17.9 mg GAE/g extract. Liu et al. [225] utilised ultrasound-assisted

supercritical CO_2 extraction on *Iberis amara* seeds, yielding 2.34 g RE/100 g dry mass of flavonoids, demonstrating the efficacy of hybrid methodologies. Pereira et al. [226] demonstrated that pressurised liquid extraction (at 10 MPa and 90°C) produced 3.2 mg GAE/g dry residue of phenolics from passion fruit rind.

Traditional techniques, such as Soxhlet extraction and maceration, typically produce reduced yield. Lee et al. [227] employed 40% ethanol in a standard extraction, yielding merely 15.84 μg GAE/g from passion fruit peel powder. These findings highlight the constraints of conventional extraction methods, which frequently entail prolonged extraction durations, increased solvent usage, and diminished selectivity [222].

Conversely, advanced extraction technologies like UE and SFE have numerous benefits, including reduced solvent consumption, expedited extraction duration, enhanced selectivity, and improved preservation of thermolabile bioactive chemicals. This work validates the effectiveness and sustainability of innovative technologies, particularly ultrasound-assisted extraction, as a viable strategy for valorising agro-industrial leftovers like passion fruit rind.

Table 3.6. Comparison of phenolic and flavonoid content extracted using different extraction methods from plant-based feed sources

Feed Sources	Solvent and technique used	Extracted Bioactive compounds	Reference
Chaenomelis Fructus peel	60% ethanol, UAE	216.27 mg/g (TPC)	[228]
Passiflora edulis sp. rind	70% ethanol; UAPLE	119 mg GAE/L extract (TPC)	[222]
Opuntia ficus-indica flower	36% ethanol, UAE	24.4 mg GAE/g (TPC)	[229]
Purple passion fruit pulp	80% methanol; UAE	351.9 mg/100g solids GAE (TPC)	[230]
Passion Fruit Peel	70% ethanol; UE	382.86–428.71 µg GAE/g DM (TPC)	[231]
Wheat bran	70% ethanol, UAE	1.95-2.15 mg GAE/g (TPC)	[232]
Passiflora edulis Sims[a] and *Passiflora cincinnata* Mast[b]	ethyl acetate; liquid-liquid extraction	476.1 mg kg^{-1} GAE[a] and 365 mg kg^{-1} GAE[b] (TPC)	[233]
Passiflora edulis f. *edulis* Sims. seed	acidified ethanol (96%), ultrasonic-assisted maceration	0.32 g GA/g extract (TPC)	[97]
Passiflora edulis var. *flavicarpa seed*	Methanol extraction; Soxhlet extraction	74.9 mgGAE/g (TPC)	[110]
Olive pomace	50% ethanol, UAE	14.70 mg/g (phenols), 2.48 mg/g (Flavonoids)	[234]
Jujube By-Product	50.16% ethanol, UAE	23.83 mg GAE/g (TPC), 4.86 mg QE/g (TFC)	[235]
Mango peels	ethanol–acetone (6:4), UAE	14.93 mg GAE/g (TPC)	[236]
Passion fruit seed cake	CO_2; SFE	17.9 mgGAE/g extract (TPC)	[237]

3.3. Conclusion

This study successfully demonstrated the valorisation of yellow passion fruit rind (YPFR), an agro-industrial byproduct, by optimising two eco-friendly extraction methods, ultrasound-assisted extraction (UAE) and supercritical fluid extraction (SFE), to recover high-value polyphenolic compounds. The UAE process was optimised using response surface methodology (RSM) to assess the effects of temperature, ethanol–water concentration, extraction time, and feed ratio. Analysis of variance (ANOVA) indicated that all process factors had a significant influence on the extraction yield. Under the optimal conditions of 54.44 °C, 64.95% ethanol–water concentration, a feed ratio of 24.69 mL/g, and an extraction time of 29.52 min, the predicted UAE yields were 42.15 mg GAE/g for total phenolics and 34.80 mg QE/g for total flavonoids, with a high desirability value of 0.959. The SFE method employed supercritical CO_2 combined with 10% ethanol as a co-solvent, with temperature, pressure, and solvent flow rate as the independent variables. The model identified solvent flow rate as the most influential parameter, followed by pressure and temperature. The optimal SFE parameters—278.48 bar, 53.84 °C, and a flow rate of 18.3 g/min—produced phenolic and flavonoid yields of 36.87 mg GAE/g and 45.75 mg QE/g, respectively, achieving a desirability value of 0.984. These findings highlight the effectiveness of both UAE and SFE as sustainable extraction techniques for obtaining antioxidant-rich bioactive compounds from passion fruit rind. The polyphenol-rich extracts derived from these green processes can be employed in functional foods, nutraceuticals, and cosmeceuticals, thereby enhancing the circular bioeconomy, promoting sustainable waste management, and facilitating the creation of value-added goods from agro-industrial byproducts.

4. CHAPTER 4

Comparative analysis of ultrasound-assisted and supercritical fluid extraction of bioactive compounds from passion fruit rinds: phytochemical, functional, and analytical insights

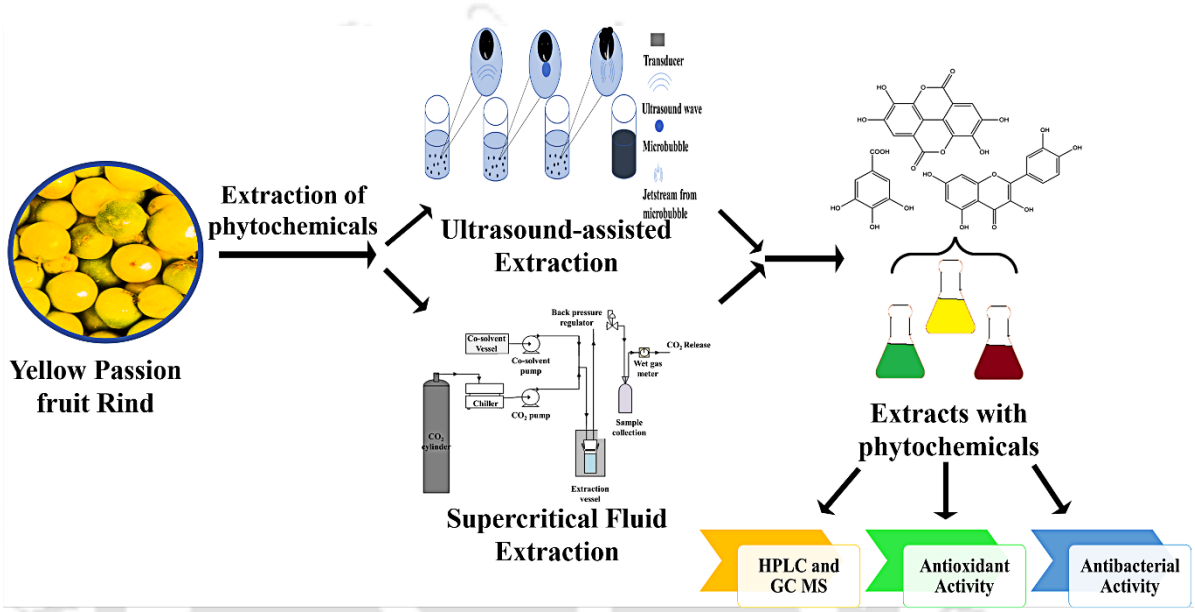

Kakali Borah, Rupesh Kumar, Sukumar Purohit, Vaibhav V Goud, 2025. Comparative study on phytochemical extraction from Passion fruit wastes using ultrasound and supercritical fluid extraction, Journal of Food Measurement and Characterisation, 1-13. DOI: 10.1007/s11694-025-03150-8

CHAPTER 4

Comparative analysis of ultrasound-assisted and supercritical fluid extraction of bioactive compounds from passion fruit rinds: phytochemical, functional, and analytical insights

This study presents a systematic analysis of bioactive compounds extracted from yellow passion fruit rind (YPFR), as detailed in Chapter 3, highlighting their therapeutic properties, including antibacterial and antioxidant activities. The extracts obtained at optimised conditions from supercritical fluid extraction with CO_2 and 10% ethanol as co-solvent (SC-ET), and ultrasound-assisted extraction (UAE) with 65% ethanol were compared for extraction yield, phytocomponents, antioxidant, and antibacterial activity. Phytochemical analysis showed significant phenolic, flavonoid, and carotenoid contents in the extracts, contributing to their increased antioxidant activities. SC-ET exhibited higher flavonoid and carotenoid concentrations; however, UAE yielded higher phenolics. These support higher antioxidant capacity in SC-ET compared to the UAE during the Global Antioxidant Score (GAS). GC-MS identified 75 compounds in UAE extracts and 47 in SC-ET extracts, whilst HPLC profiling indicated higher phenolic and flavonoid contents in SC-ET extracts, demonstrating SFE's selectivity, and GC-MS findings showed UAE's broader compound extraction range. Both extracts showed significant antibacterial activity, with SC-ET being more potent. These findings revealed the potential of using passion fruit rind to extract bioactive compounds for the food, pharmaceutical, and cosmetic industries, promoting sustainable waste management and resource recovery.

4.1. Bioactive compound analysis of the extracts

Ultrasound-assisted extraction (UAE) and supercritical fluid extraction (SFE) techniques were used to extract the phytochemicals from the yellow passion fruit rind (YPFR). Both extraction procedures have been systematically optimised for their chosen parameters using CCD-based Response Surface Methodology (RSM) to maximise yields of phenolic and flavonoid compounds. The parameters for UAE were temperature, time, feed ratio, and solvent concentration, whereas for SFE were

pressure, temperature, and flow rate. RSM, a statistical tool widely used for process optimisation, facilitated the identification of optimal parameter combinations for each method. The extracts in this study were procured under optimised conditions, ensuring they represent the maximum potential yields attainable using SFE [238] and UAE for passion fruit rind. The solvents used for supercritical fluid extraction were CO2 with 10% ethanol as a co-solvent (SC-ET) and for UAE, 65% ethanol. This approach enhanced the recovery of bioactive compounds and established a robust foundation for ensuring the reproducibility and scalability of extraction protocols.

The results showed that UAE yields higher extracts (51.39%) than SFE (2.67%). This higher yield might be attributed to the ultrasonic waves, which effectively disrupt the plant cell walls, improving solvent penetration and extraction effectiveness. However, the selectivity and specificity of SFE might limit its extraction yield [239]. Further, the phenolic (TPC), flavonoid (TFC), and carotenoid (TCC) content of the extracts were evaluated using the spectrophotometry method and expressed in mg GAE/g, mg QE/g, and μg β-carotene/g, respectively (Figure 4.1), with their corresponding standard curves are shown in Figure A1. For comparison analysis, the data from this study were compared with a prior investigation conducted by the same group, which confirmed phenolic (66.53 ± 4.36 mg GAE/g) and flavonoid (73.39 ± 2.04 mg QE/g) concentrations in the methanolic extract using the Soxhlet method, as illustrated in Table 4.1. Although the UAE showed higher TPC in the extracts, it was discovered that the extracts produced by SC-ET had the highest TFC and TCC. The supercritical carbon dioxide (SC) extract without co-solvent exhibited a low TPC and TFC; nevertheless, it had a considerably high carotenoid content. For flavonoid content, the SC-ET extract exhibited a maximum concentration of 45.59 ± 1.79 mg QE/g. This was followed by UAE (34.41 ± 2.70 mg QE/g) and SC extracts (23.24 ± 2.29 mg QE/g). A similar pattern was seen in the carotenoid content, with SC-ET demonstrating the most significant amount, followed by SC extract and UAE extract. The low polarity of supercritical carbon dioxide makes it an ideal solvent for carotenoids, thereby enabling efficient extraction [239]. However, as ethanol is polar, more polar molecules, like flavonoids and phenolics, dissolve more readily in supercritical carbon dioxide. Consequently, the SC-ET extracts exhibited higher flavonoid and phenolic contents than the SC extracts, owing to the addition of ethanol as a co-solvent. This result is consistent with a study by Setyopratomo [240], which showed that ethanol had a high extraction efficiency for

phenolics. Therefore, supercritical carbon dioxide and ethanol in SC-ET can extract both polar and non-polar bioactive compounds, whereas UAE with ethanol is successful for phenolic extraction. These findings corroborate a study by dos Santos et al. [44], which reported that the hydroethanolic (20:80) extract of yellow passion fruit seed waste with UAE methods contained 548.70 mg.GAE/100 g seeds phenolic content and 80.78 mg RUE/100 g seed of flavonoid content. Similarly, de Souza et al. [87] extracted phytochemicals from the yellow passion fruit peel using ethanol and water as solvents with the maceration technique. They obtained 39.94 mg GAE/g and 11.91 mg GAE/g of phenolics in ethanol and water extracts, respectively. Furthermore, Vigano et al. [241], demonstrated that the carotenoid content in passion fruit bagasse produced by Soxhlet extraction with n-hexane as the solvent (56.19 μg/g) was comparable to that obtained by supercritical carbon dioxide extraction (53.39 μg/g). dos Santos et al. [242], found that supercritical carbon dioxide extracts produced a higher carotenoid yield (38.64 mg β-carotene equivalent/kg) than Soxhlet extracts using petroleum ether as the solvent. These polyphenolic secondary metabolites serve a crucial role in oxidative stress defense and antioxidant activity due to their reactive hydroxyl molecules [243].

Table 4.1. Yield of total phenolic, flavonoid, and carotenoid from different extracts of YPFR and their In vitro antioxidant activities

Samples	TPC[a]	TFC[b]	TCC[c]	IC_{50} value	
				DPPH[d]	ABTS[d]
UAE	41.48 ± 0.38	34.41 ± 2.70	2.57 ± 0.61	56.03 ± 1.32	75.60 ± 0.55
SC-ET	36.04 ± 2.15	45.59 ± 1.76	20.44 ± 0.77	48.74 ± 0.67	67.57 ± 0.82
SC	9.88 ± 1.54	23.21 ± 2.29	15.28 ± 0.80	61.80 ± 1.22	76.49 ± 0.66
ME	66.53 ± 4.36[α]	73.39 ± 2.04[α]	2.58 ± 0.52	44.05 ± 1.41[α]	62.11 ± 3.89[α]

a is *mg GAE/g extract*
b is *mg QE/g extract*
c is *mg β-carotene/g extract*
d is *μg/mL*
YPFR: yellow passion fruit rind, *TPC*: total phenolic content, *TFC*: total flavonoid content, *TCC*: total carotenoid content. *UAE*: ultrasound-assisted extract, *SC-ET*: supercritical carbon dioxide with 10% ethanol extract, *SC*: supercritical carbon dioxide extract, *ME*: methanolic extract. [α]Purohit et al. [73]. Antioxidant activity (DPPH and ABTS) of different YPFR extracts were expressed in terms of IC_{50} values (μg/mL). All results were mean + standard deviation of experiments in triplicate.

4.2. Antioxidant Activity and global antioxidant score (GAS) of the extracts

Numerous bioactive substances in passion fruits contribute to antioxidant properties, challenging the assessment of each molecule. In this study, the antioxidant efficacy of the extracts was assessed by comparing the IC_{50} (concentration needed to scavenge 50% of the free radical) of the extracts in DPPH and ABTS assays. Each extract showed considerable antioxidant activity, which was then compared to ascorbic acid values (IC_{50} 2.84 ± 0.48 µg/mL DPPH, 26.67 ± 0.51 µg/mL ABTS). The results in Table 4.1 show a significant impact ($p < 0.05$) of DPPH and ABTS IC_{50} values for both extracts and standards. The UAE extract exhibited a higher IC_{50} value (56.03 ± 2.73 µg/mL), indicating lower antioxidant activity in the DPPH assay compared to SC-ET extracts (48.74 ± 1.22 µg/mL). A similar outcome was observed in ABTS; the IC_{50} value of SC-ET extracts was 67.57 ± 1.42 µg/mL, whereas 75.60 ± 0.95 µg/mL in the UAE extract. Hence, SC-ET exhibits maximum antioxidant activity, possibly due to higher TCC levels and a considerably higher flavonoid content than UAE extracts. The enhanced antioxidant activity of these extracts corresponds to the presence of carotenoids and polyphenolics, which may efficiently scavenge DPPH free radicals and donate hydrogen atoms [244,245]. Similar antioxidant activity was demonstrated by the methanolic rind extracts of yellow passion fruit reported by Purohit et al. [246], with IC_{50} values of 44.05 ± 1.41 µg/mL in the DPPH assay and 62.11 ± 3.89 µg/mL in the ABTS assay. Conversely, the DPPH IC_{50} value of the SC extracts was 61.80 ± 2.11 µg/mL.

While 40% ethanolic extract of passion fruit peel revealed the TPC content of 15.84 mg GAE/g with moderate antioxidant activity for DPPH and ABTS with a value >500 µg/mL of extract concentration to scavenge 50% of DPPH [227]. Cao et al. [247], investigated the antioxidant activity of 70% ethanolic extracts of purple hybrid passion fruit (*P. edulis x.* "Tai-Nung No. 1") peel. They measured the extract concentration required to scavenge 50% of the DPPH radicals as 29.6 ± 1.7 mg/g, whereas for ABTS as 10.3 ± 1.4 mg/g. Other studies reported similar findings, showing a strong correlation between the extract's phenolic content and its antioxidant capacity as measured by various assays. The study also indicates that the phenolic and flavonoid content of the extracts is likely the primary contributor to their antioxidant activity. Polyphenols are abundant in passion fruit by-products and act synergistically to inhibit the generation of free radicals and the development of oxyradical-mediated degenerative diseases in

humans [248]. According to Ohikhena et al. [249], the hydroxyl groups in the aromatic ring of polyphenols serve as hydrogen donors, favouring lower IC_{50} percent in DPPH and ABTS assays. Hence, due to their redox characteristic, phenolic and flavonoid compounds serve as reducing agents and radical scavengers.

The GAS was computed to rank the antioxidant ability of the extracts when correlating the outcomes of antioxidant activity tests with their phytochemical concentration. It assists in resolving the challenge of selecting the extract based on antioxidant capacity. The best extract between SC-ET and UAE samples was calculated using the global antioxidant score (GAS). The GAS value in the present analysis was calculated by adding the two T-scores for each variable (Table A1). The calculated scores implied that the SC-ET extract (GAS=3.91) has a higher total antioxidant capacity than the UAE (GAS=1.61). Although the UAE showed a higher phenolic content, the carotenoid content was limited compared to the SC-ET extract. Additionally, the flavonoid content of the SC-ET extract was higher than that of the UAE extract. These phytochemicals are good natural antioxidant agents. Analysing several antioxidant assays using a statistical model has become a novel technique to offer new possibilities for expressing the antioxidant capacity of foods and beverages. The GAS score serves as a ranking tool that could benefit both consumers and professionals in science and business.

4.4. Quantification of phenolic and flavonoid compounds using HPLC

HPLC quantification of phenolic and flavonoid compounds of YPFR extracts is detailed in Table 4.2, and the corresponding chromatograms are shown in Figure A2. In addition to flavonoids like kaempferol, myricetin, isorhamnetin, catechin, isoorientin, isovitexin, and quercetin, this study quantitatively examined phenolic acids, including gallic acid, p-coumaric acid, cinnamic acid, and ferulic acid. Purohit et al. [246] reported the notable presence of the aforementioned polyphenols in methanol and acetone extracts of the yellow passion fruit rind of Northeast India. In this work, three major phenolic compounds, namely ferulic acid, gallic acid, and p-coumaric acid in both SC-ET and UAE extracts, were identified at nearly identical retention time as the standards. Table 4.2 revealed a gallic acid concentration ~47 times higher in the SC-ET compared to UAE extracts. Isovitexin was present in the highest concentration in SC-ET extracts (90.78 mg/g), followed by ferulic acid (31.08 mg/g) and p-coumaric acid (24.74 mg/g). Similarly, in the UAE extracts, isovitexin was the predominant

compound, whereas caffeic acid was absent in both extracts. A previous study by Francischini et al. [250] showed the extraction of flavonoids from passion fruit waste using UAE employing an ethanol-water solvent, resulting in isoorientin (0.68 mg/g) and isovitexin (0.17 mg/g). However, ultrasonic extraction using 80% ethanol from banana passion fruit pulp (*Passiflora tripartita* var. *mollissima*) identified hydroxycinnamic acid derivatives, including dicaffeoylquinic acid (1.45 mg/g), and flavonoids such as myricetin derivative (0.05 mg/g), kaempferol-methoxy-methyl ether (0.67 mg/100 g), isoquercitrin (0.98 mg/100 g), isorhamnetin-O-dihexoside (0.01 mg/g), catechin (0.10 mg/g), and caffeic acid (0.01 mg/g) [251]. Aqueous extracts of passion fruit using UAE contained caffeic acid (12.2 µg/g), rutin (1.4 µg/g), and chlorogenic acid (164.7 µg/g) [221]. The HPLC profiling of SFE and UAE extracts in this study showed that the former had more significant quantities of specific phenolic and flavonoid components. This implies that SFE is more efficient at selectively extracting these bioactive chemicals, even though its yield is lower.

In passion fruit and its by-products, isovitexin and isorhamnetin are the most notable flavonoids, whereas phenolic compounds (such as gallic acid) have potent antioxidant and free radical scavenging capabilities due to their high degree of hydroxylation. The flavonoids and phenolics have synergistically worked to inhibit microbial growth. Moreover, flavonoids (like quercetin) dramatically reduced bacterial motility [252]. Therefore, these synergisms between naturally occurring polyphenolic compounds may account for remarkable antioxidant, anticancer, antimicrobial, antiinflammatory, and cardioprotective activities.

Table 4.2. Quantification of phenolics and flavonoids using HPLC

Phytochemicals	Standards	UAE	SC-ET
Phenolics	Gallic acid	7.42	13.99
	Ferulic acid	2.38	31.08
	p-Coumaric acid	0.86	24.74
	Cinnamic acid	ND	0.18
	Caffeic acid	ND	ND
Flavonoids	Quercetin	1.96	3.05
	Kaempherol	1.75	2.25

Isorhmnetin	0.39	7.40
Myricetin	1.21	0.40
Catechin	ND	2.40
Isovitexin	31.14	90.78
Isoorientin	3.60	1.03

Data are displayed in mg/g of DW. *UAE:* ultrasound-assisted extract, *SC-ET:* supercritical carbon dioxide with 10% ethanol extract. *ND:* not detected.

4.5. GC-MS profiling of the extracts

GC-MS analysis, recognised for accuracy and precision, was employed in the current study for profiling phytochemical components of the UAE and SC-ET extracts of YPFR. Associated chromatograms are displayed in Figure A2 and Figure A3, and the identified compounds, including their retention time, molecular weight, and peak area per cent (the amount of compound present), are listed in Tables A2 and A3. The major phytoconstituents present in UAE extract were: Myo-Inositol, 6TMS derivative (58.44%), Palmitic Acid, TMS derivative (2.83%), di-t-butyl-phenol (1.76%), Hexadecane, 2,6,10,14- tetramethyl (1.41%), and Quinoline Derivative (0.95%). In SC-ET extracts, the significant compounds were, Tris(2,4-di-tert-butylphenyl) phosphate (6.56%), di-t-butyl-phenol (4.62%), Arsenous acid, tris(trimethylsilyl) ester (2.64%), Hexadecane, 2,6,10,14- tetramethyl (2.12%), 1,2,4-Triazine, 2-oxide (1.85%), and Iron, tricarbonyl [N- (phenyl-2- pyridinylmethylene) benzenamine-N,N']- (1.83%). These identified phytochemicals shows various physiological properties such as Piperidine hydrochloride (anticancer, antimicrobial, antifungal, antihypertension, anti-inflammatory, anti-Alzheimer, anticoagulant agents [253]); Chizo-Inositol 6TMS derivative (anti-depression, liver problems, panic disorders and diabetes [254]); di-t-butyl-phenol (Antioxidant [255]); Quinoline Derivative (antioxidant, antimicrobial, anti-inflammatory, anticancer, cardiovascular, anticonvulsant, anthelmintic, CNS effects, analgesic, and miscellaneous activities [256]); Butylated hydroxytoluene (Antioxidant, food additive [257]); and Iron, tricarbonyl[N- (phenyl-2-pyridinylmethylene)benzenamine-N,N']- (antifungicidal acitivity [258]), etc. The finding proved that the extracts have substantial nutritional and therapeutic potential.

Previous investigations have revealed various beneficial components in varieties of passion fruit. The ultrasonic extraction of banana passion fruit (*Passiflora tripartita*

var. *mollissima*) pulp using 80% ethanol identified 82 components, comprising phenolic acids, flavan-3-ols, and flavones [251]. The methanolic extraction of banana passion fruit peel identified 31 phenolic compounds [259]. The UHPLC-QqQ-MS/MS analysis of the extract obtained from *Passiflora leschenaultii* DC observed 24 phenolic components, such as daidzein, epicatechin, and artepillin C. HS-SPME/GC-MS aroma profiling revealed 67 volatiles, including terpenes, alcohols, esters, ketones, and phenolic acids [260]. In this study, the GC-MS analysis identified a wide variety of chemical components: 47 compounds in the SC-ET extract and 75 in the UAE extract. Alkaloids, steroids, glycosides, carbohydrates, and flavonoids were among the many chemicals found in the UAE extract, demonstrating the process's efficacy and capacity to potentially extract a wide range of advantageous compounds.

4.6. Antibacterial Activity study

Both the UAE and SC-ET extracts were selected to perform the bactericidal activity test using minimum inhibitory concentration (MIC) (Figure A2) and zone of inhibition assay (ZoI) (Table A2) against various gram-positive and gram-negative bacterial strains. The results of the MIC study (Table 4.3) reveal that both the extracts showed effective inhibitory activity against all four Gram-positive bacteria, ranging from 40 mg/mL to 2.5 mg/mL. Both the extracts demonstrated antibacterial efficacy against *E. coli* and *K. pneumonia* at 40 mg/mL; and against *P. aeruginosa* at 80 mg/mL. Similarly, aqueous extracts of yellow passion fruit reported no antimicrobial activity; however, 100% ethanolic extracts showed moderate activity with a MIC of 128 µg/mL for *E. coli* and *P. aeruginosa*; whereas 256 µg/mL for *S. aureus* [87]. The extract's efficacy against all bacterial species was further assessed qualitatively using an inhibition zone study. Both extracts showed moderate antibacterial activity against *Staphylococcus epidermidis* (UAE: 12.67 mm, SC-ET: 12 mm) at 50 mg/mL; however, against *Staphylococcus aureus*, the activity was limited (5 mm).

The finding of MIC and ZOI revealed that YPFR extracts are more effective against gram-positive bacteria than gram-negative bacteria due to the presence of a complex permeability barrier in gram-negative bacteria that hinders the entry of antibacterial compounds [261]. Additionally, Oliveira et al. [224] reported that the SFE extracts of passion fruit seed and seed cake were more effective against gram-positive bacteria. Mehmood et al. [243] reported that flavonoids demonstrate potent antibacterial

properties by hindering nucleic acid production and metabolic functions in microbes, compromising membrane permeability. Furthermore, phenolic compounds inhibit bacterial development via their C3 side chain, limiting oxidation levels, while their partial hydrophobicity enhances microbial lethality by blocking protease activity and interacting with proteins and carbohydrates. Thus, the presence of polyphenolics and carotenoids in YPRF extract contributes to its potent antibacterial activity. This study aimed to address the knowledge gap on the use of passion fruit waste products as antimicrobial agents by examining raw material type, preparation, and extraction methods for assessing antibacterial activity. However, further research involving diverse microbes and practical applications, such as in food systems, is still needed.

Table 4.3. Minimum inhibitory concentration (MIC) of the extracts at optimised conditions

	Gram-negative bacteria				Gram-positive bacteria			
	EA	PA	EC	KP	SA	BS	SE	ML
UAE	80	80	40	40	20	40	5	5
SC-ET	40	40	40	80	10	20	2.5	5

All the values are displayed as extract concentration in mg/mL. *UAE:* Ultrasound-assisted extract, *SC-ET:* Supercritical carbon dioxide with 10% ethanol extract. *EA: E. aerogenes*, *PA: P. aeruginosa*, *EC: E. coli*, *KP: K. pneumoniae*, *SA: S. aureus*, *BS: B. subtilis*, *SE: S. epidermidis*, and *ML: M. luteus*.

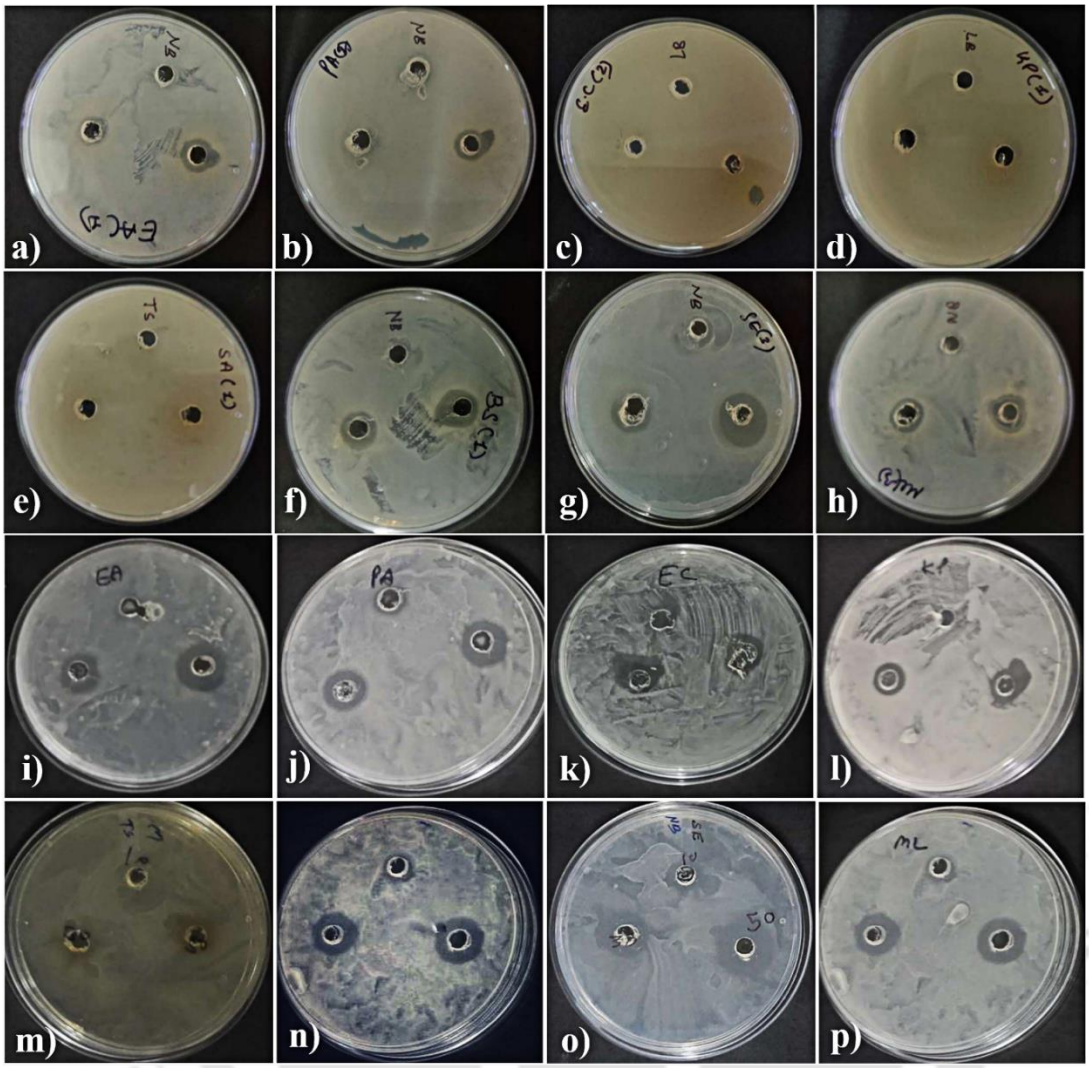

Figure 4.1. Agar well diffusion method for the zone of inhibition. Antibacterial effect of ultrasound-assisted *P. edulis* f. *flavicarpa* rind extract against gram-negative bacteria- *E. aerogenes* (EA), and *P. aeruginosa* (PA), *E. coli* (EC), *K. pneumoniae* (KP) is represented by (a-d); whereas (e-h) represents against gram-positive bacteria- *S. aureus* (SA), *B. subtilis* (BS), *S. epidermidis* (SE), and *M. luteus* (ML). Similarly, (i-p) represents the antibacterial effect of Supercritical carbon dioxide with 10% ethanol extract against the same bacterial strains respectively.

4.7. Comparison of UAE and SFE extractions in terms of environmental and economic aspects:

The food sector is promoting a circular, sustainable economy by minimising waste and producing valuable by-products. Recycling agro-industrial waste into valuable compounds needs a comprehensive evaluation of economics and sustainability in the selection of extraction technology [262]. Environmental and economic considerations are essential for large-scale phytochemical extraction. Table A5 presents a comparative analysis of the environmental and economic impacts of UAE and SFE, and their limitations are explained in section A6. UAE is energy-efficient and economical,

characterised by lower temperatures, reduced solvent consumption, and shorter extraction times, aligning with sustainable processing principles. Conversely, SFE offers enhanced selectivity and product quality but involves higher initial capital costs for equipment and increased operating expenses due to the use of pressurised CO_2 and 10% ethanol as a co-solvent. Nevertheless, SFE mitigates environmental consequences by reducing the use of substantial quantities of organic solvents and generating high-purity extracts with low post-processing requirements. Considering these aspects, the UAE is beneficial for large-scale, cost-sensitive applications, whereas SFE is preferred for high-value products where purity and quality are critical. When optimised, these technologies provide sustainable phytochemical extraction from agro-industrial waste, minimising environmental impacts and improving economic viability. In a case study, a 0.5 m^3 industrial SFE facility with CO_2/ethanol could produce extracts with a phenolic content of about 23 g/kg from grape bagasse at the production cost of $133.16/kg was found to be feasible based on economic analysis [263]. Lopeda-Correa et al. [264] performed phenolic extraction from *A. floribunda* stems using ultrasonic treatment and estimated the manufacturing cost for a 300 L unit, finding it to be $3.86 per flask—54.9% lower than the cost of Soxhlet extraction. According to Carlqvist et al. [264], ethanol poses notable sustainability challenges because it largely remains in the residual byproduct after extraction, necessitating new production. However, if recovery can be achieved with low energy input, its use could be advantageous.

4.8. Conclusions

This study evaluated the potential of supercritical fluid extraction (SFE) and ultrasound-assisted extraction (UAE) for recovering beneficial bioactive compounds from passion fruit rind, an agro-industrial waste. Owing to ultrasonic vibrations and cell wall disruption, UAE achieved a higher extraction efficiency (51.39%) than SFE (2.67%). Although less productive in yield, SFE demonstrated high selectivity, effectively isolating specific flavonoids and carotenoids, as confirmed by HPLC analysis. The strong antioxidant activity of UAE extracts was linked to their higher total phenolic content, including gallic acid (7.42 mg/g DW), ferulic acid (2.38 mg/g DW), and p-coumaric acid (0.86 mg/g DW). In contrast, SFE extracts contained greater amounts of carotenoids and flavonoids such as isovitexin (90.78 mg/g DW), isoorientin (1.03 mg/g DW), kaempferol (2.25 mg/g DW), and quercetin (3.05 mg/g DW), known for their potent anti-inflammatory and antioxidant properties. Both UAE and SFE

extracts exhibited substantial antibacterial activity against gram-positive and gram-negative bacteria, effectively inhibiting growth at low concentrations in MIC and ZOI tests. While SFE extracts showed limited activity against *Staphylococcus aureus*, UAE extracts displayed broad-spectrum antibacterial effects, likely due to their strong phenolic-driven antioxidant and antimicrobial properties. By addressing a research gap in the characterisation of passion fruit rind extracts in India, this work supports resource efficiency and sustainable waste management. However, challenges remain regarding scalability, cost-effectiveness, and environmental impact. Future improvements could be achieved through process optimisation, life-cycle assessment, and advanced compound characterisation to enhance sustainability and industrial viability.

5. CHAPTER 5

Application of natural antioxidants from yellow passion fruit rind on vegetable oil to improve the quality

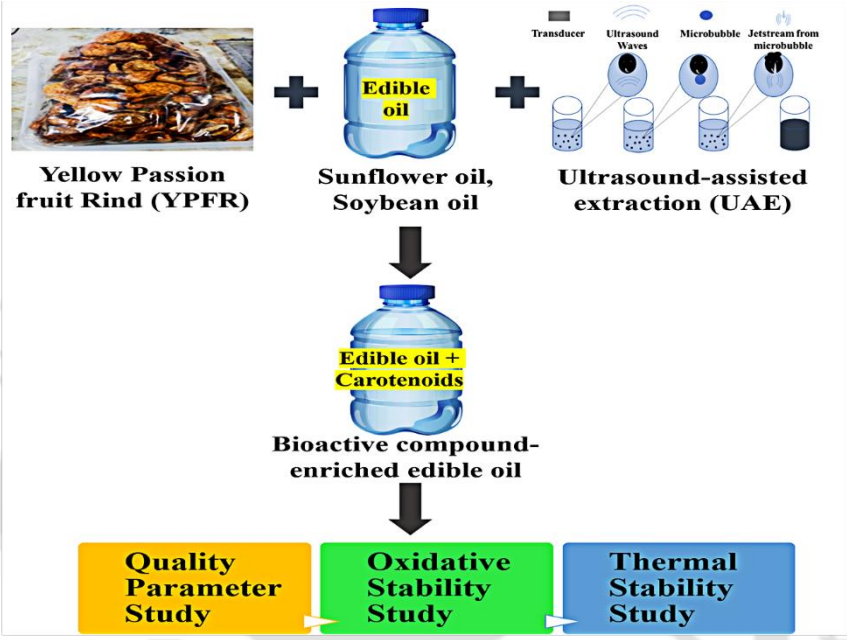

Kakali Borah, Vaibhav V Goud, 2025. One-pot method to extract natural antioxidizing agents from passion fruit rind to increase the oxidative stability of sunflower seed and soybean oils. Food Chem. 144668. https://doi.org/10.1016/j.foodchem.2025.144668

CHAPTER 5

Application of natural antioxidants from yellow passion fruit rind on vegetable oil to improve the quality

With growing concerns over oxidative degradation of edible oils and the need for sustainable alternatives to synthetic antioxidants, this study aimed to enhance oil stability through the incorporation of natural antioxidants. The previous chapter demonstrated the efficacy of ultrasound-assisted extraction (UAE) for extracting a broad spectrum of bioactive chemicals with significant yield. This study utilises the UAE with edible oil as a green solvent to extract bioactive components, intending to improve extraction efficiency and the functional quality of the oil. In the present study, carotenoid extraction from passion fruit rind using sunflower seed oil (SFO) and soybean oil (SBO) as solvents through UAE was optimised statistically. The resulting carotenoid-rich oil exhibited significantly enhanced phenolic and flavonoid content ($p < 0.05$), thus improving antioxidant capabilities. Oxidative stability studies revealed a 29.53 - 46.44% increase in induction time at 140 °C, demonstrating improved resistance to degradation in treated oils. Differential scanning calorimetry (DSC) and thermogravimetric analysis confirmed thermal stability with treated-SFO (-12.34 °C) showing a lower DSC onset temperature than treated-SBO (-9.59 °C), likely due to its increased saturated fatty acid composition. Additionally, the structural integrity of the oil remained unaffected by the extract. This study highlights the potential of natural antioxidants for stabilising edible oils.

5.1. Fatty Acid Profile of Oil:

Edible oils are prone to lipid peroxidation due to their unsaturated fatty acid composition, negatively affecting their nutritional quality and shelf stability. Fatty acids containing two double bonds oxidise 10-40 times more rapidly than those with a single double bond [265], resulting in adverse sensory attributes, nutritional deterioration, and alterations in texture and colour, which pose significant challenges for the food sector. Oxidised oils produce harmful chemicals, such as free radicals and aldehydes, leading to oxidative stress and significant health hazards. Antioxidants, including polyphenols,

tocopherols, and carotenoids; neutralise free radicals and limit oxidation chain reactions to reduce these effects [265].

SFO and SBO fatty acid profiles (Table A6) showed that SFO has a higher saturated fatty acid (SFA) content (65.88%) compared to SBO (53.08%). In contrast, SBO has slightly higher concentrations of monounsaturated (MUFA) and polyunsaturated fatty acids (PUFA), with respective levels of 33.04% and 13.87%, in comparison to SFO's 22.60% and 11.52%, supporting the findings of Kozlowska and Gruczynska [266]. According to Gilmore et al. [267], SFAs can increase levels of low-density lipoprotein and plasma cholesterol, additionally improving the oxidative stability of edible oils. Table A6 further highlights that the predominant SFA in both oils is palmitic acid, with SFO exhibiting a slightly higher concentration (14.86%) than SBO (14.33%). Oleic acid is the predominant monounsaturated fatty acid, whereas linoleic and linolenic acids are the primary polyunsaturated fatty acids in both oils. SFO is more prone to oxidation due to its high unsaturated fatty acid content, particularly linoleic acid. This sensitivity emphasises the importance of including antioxidants in these oils as a precautionary strategy against oxidation. The variation in fatty acid composition between SFO and SBO is mostly due to variations in plant varieties and ecological variables, including temperature, water availability, and overall agricultural circumstances [266].

5.2. Optimisation of Carotenoid Extraction

The dried YPFR samples were soaked in solvent-edible oils (SFO and SBO) prior to the conduction of ultrasonic extraction (UAE) of carotenoids. To maximise carotenoid output from YPFR, the UAE process was optimised using a central composite design using RSM. This study primarily focuses on optimising extraction parameters to maximise carotenoid yield (section A1.1), as edible oils are primarily non-polar, facilitating the effective solubility of lipophilic compounds such as carotenoids [268]. Temperature, treatment time, and S/L ratio were chosen as the independent parameters in this study. Their effects were assessed, showing a significant impact on the carotenoid concentration in the resulting oil, with a p-value of <0.05.

An ANOVA F-test was performed to evaluate the influence of chosen parameters on carotenoid yield using UAE with SFO and SBO. The findings demonstrated a strong correlation between experimental and predicted carotenoid outputs. The model's relevance and its variables were assessed using the F-value and p-value; the greater the

F-value, the lower the "Prob > F" value. ANOVA analysis (Table 5.1) indicated that the quadratic models for both oils were very significant ($p < 0.0001$), with F-values of 205 for SFO and 332.04 for SBO. The most significant factor for SFO was the S/L ratio (F-value 252.00), which was followed by temperature and time. In SBO, temperature emerged as the most significant factor (F-value 83.1), followed by S/L ratio and time. Lack-of-fit tests indicated no evidence of inadequate model fit for both SFO and SBO with $p > 0.05$. High regression coefficients ($r^2 = 0.995$ for SFO; 0.997 for SBO) and adjusted coefficients ($r^2_{adj} = 0.99$) validated the model's suitability. Minimal coefficients of variation (CV = 1.48% for SFO; 1.34% for SBO) underscored experimental precision. The quadratic model produced polynomial equations (5.1, 5.2) for both oils, exhibiting strong prediction performance.

$$\text{Total carotenoid content (SFO)} = 561.95 - 17.60A - 5.17B - 30.22C - 22.89AB - 1.75AC + 5.93BC - 46.00A^2 - 51.43B^2 - 31.05C^2 \quad 5.1$$

$$\text{Total carotenoid content (SBO)} = 653.24 - 17.50A - 6.60B + 10.74C + 2.88AB - 6.73AC - 10.57BC - 42.81A^2 - 64.55B^2 - 75.42C^2 \quad 5.2$$

Where A-temperature (°C), B-time (min), and C-S/L ratio (g/100 mL) were the parameters of coded terms.

Table 5.1. ANOVA table for quadratic model for optimisation of carotenoid yield using SFO and SBO

	SFO						**SBO**					
Source	**Sum of Squares**	**DF**	**Mean Square**	**F Value**	**P-value Prob > F**		**Sum of Squares**	**DF**	**Mean Square**	**F Value**	**P-value Prob > F**	
Model	91294.96	9	10143.88	205	< 0.0001	significant	1.50×10^5	9	16708.25	332.04	< 0.0001	significant
A-Temperature	4232.62	1	4232.62	85.54	< 0.0001		4181.74	1	4181.74	83.1	< 0.0001	
B-Time	365.25	1	365.25	7.38	0.0217		594.95	1	594.95	11.82	0.0063	
C-S/L ratio	12469.64	1	12469.64	252	< 0.0001		1576.67	1	1576.67	31.33	0.0002	
AB	4191.99	1	4191.99	84.72	< 0.0001		66.47	1	66.47	1.32	0.2772	
AC	24.6	1	24.6	0.4971	0.4969		361.87	1	361.87	7.19	0.023	
BC	281.6	1	281.6	5.69	0.0382		893.6	1	893.6	17.76	0.0018	
A^2	30493.38	1	30493.38	616.24	< 0.0001		26405.46	1	26405.46	524.74	< 0.0001	
B^2	38125.07	1	38125.07	770.47	< 0.0001		60039.18	1	60039.18	1193.13	< 0.0001	
C^2	13896.45	1	13896.45	280.83	< 0.0001		81964.63	1	81964.63	1628.84	< 0.0001	
Residual	494.83	10	49.48				503.21	10	50.32			

Lack of Fit	30.32	5	6.06	0.0653	0.9953	not significant	385.05	5	77.01	3.26	0.1104	not significant
R^2	0.995						0.997					

5.2.1. Interaction Effects of the Independent Variable on the Carotenoid Yield

The study shows that the chosen independent variables, viz., temperature, time, and S/L ratio, significantly affect the rate of extraction of carotenoids with $p < 0.05$. The concentration of carotenoids increases initially up to 40 °C and 45 °C during the extraction with SBO (Figure 5.1d, e) and SFO (Figure 5.1a, b), respectively. This increase is attributed to lower oil viscosity at high temperatures, which enhances substrate penetration and improves extraction efficacy [269]. However, at high temperatures, thermolabile compounds could degrade, leading to a decrease in their concentrations [191]. At high temperatures, ultrasound attenuation also occurs due to decreased bubble surface tension and increased vapour pressure [269], which reduces extraction efficiency. Carotenoid recovery from YPFR is significantly impacted by the treatment time. Ultrasonication initially enhances carotenoid output; however, extended exposure decreases it for SFO (Figure 5.1a, c) and SBO (Figure 5.1d, f). This emerges due to the time required for equilibrium between intracellular and extracellular carotenoid concentrations, and prolonged ultrasound exposure could deteriorate carotenoids [269]. A comparable trend was observed in the extraction from pomegranate peel by Goula et al. [136]. The effect of the S/L ratio on carotenoid yield in SFO and SBO is depicted in the 3D response graphic (Figure 5.1b, e). In SFO, yields increased to 15 g/100 mL, whereas SBO yields surged to 20 g/100 mL. Increased solvent viscosity at high solid-to-liquid ratios reduces cavitation efficiency; nonetheless, it enhances solvent-solute interaction and improves extraction until an appropriate threshold is reached [217]. An analogous effect observed by Ordonez-Santos et al. [270], on the extraction of carotenoids from peach peel, UAE yield rose with an S/L ratio up to a certain threshold before decreasing.

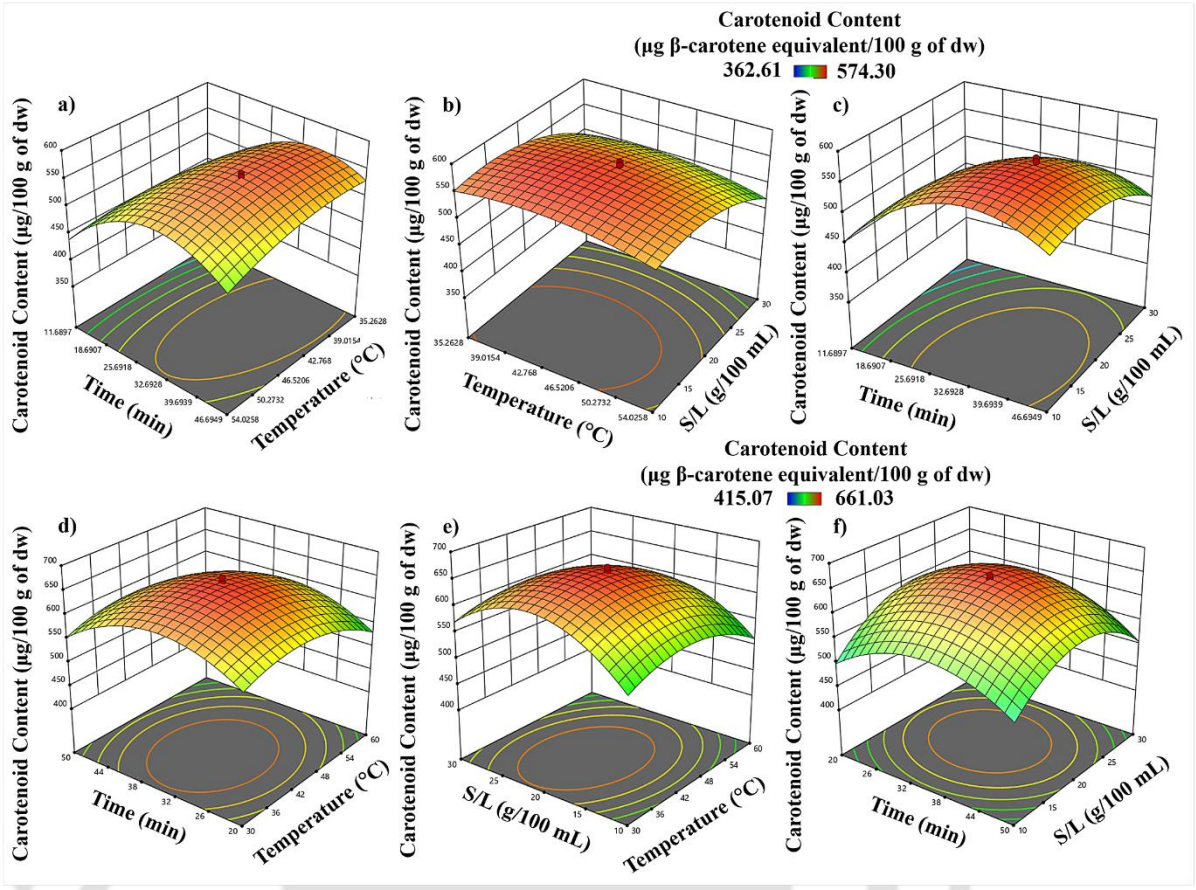

Figure 5.1. Response surface plot of effects of (a, d) Temperature (°C) and time (min); (b, e) Temperature (°C) and S/L ratio (g/100 mL); (c, f) S/L ratio (g/100 mL) and time (min) for SFO and SBO.

5.2.2. Optimisation of Process Variables and Validation

The optimal conditions for maximising carotenoid yield were predicted using the desirability function tool in the Design-Expert software. Table 5.2. displays the predicted optimal parameters, indicating that SFO extracts an expected 570.90 µg β-carotene equivalent/100 g, whilst SBO yields 655.77 µg β-carotene equivalent/100 g. Experimental outcomes closely aligned with predictions (percentage error within 0.20-0.66%), resulting in 574.69 ± 9.01 µg/100 g (SFO) and 657.11 ± 26.16 µg/100 g (SBO). Chutia and Mahanta [137] reported analogous results, extracting 1185.45 µg/100 g of dry peel carotenoid from purple passion fruit with SFO. However, Goula et al. [136] recovered 0.67 and 0.61 mg carotenoids/100 g of dry pomegranate peel using soy and sunflower seed oils, respectively. The results supported the application of edible oil as an eco-friendly solvent for carotenoid extraction in the UAE. SBO exhibited higher extraction efficacy compared to SFO, attributed to its lower viscosity, which facilitates solvent fluidity and penetration, thereby improving carotenoid extraction [269,271].

The utilisation of vegetable oils as solvents is beneficial for food, cosmetic, and pharmaceutical applications, as it eliminates the necessity for carotenoid-solvent separation [272].

Table 5.2. Optimisation table for carotenoid extraction using UAE with edible as a solvent

Solvent	Temperature	Time	S/L ratio	Total carotenoid content	Desirability
SFO	42.42	34.41	15.14	570.90	0.98
SBO	41.80	34.07	20.85	655.77	0.98

Temperature expressed as °C,
Time expressed as min,
S/L ratio expressed as g/100 mL,
Total carotenoid content expressed as μg β-carotene equivalent/100g dry weight.

5.3. Characterisation of the Oil

Ultrasonic treatment of edible oils might result in oxidation and composition alterations [273]. To assess these effects, the quality indicators of oils treated with extracts were compared to those of untreated oils, as listed in Table 5.3. The peroxide value (PV), a measure of oxidation in oils, increased for both SFOE (SFO + Extract) and SBOE (SBO + Extract). Correspondingly, the acid value (AV), indicative of hydrolytic reactions, varied from 0.3 to 0.41 mg KOH/g oil. The Codex Alimentarius Commission and the Food and Agriculture Organisation of the United Nations(FAO) stipulate that acceptable limits for edible oils include an AV of less than 6.0 mg KOH/g oil and a PV of less than 10 meq O_2/kg oil [274]. Despite the observed rise in PV and AV post-treatment, the values remained within the permissible limits. Goula et al. [136] observed a similar trend of an increase in PV after ultrasonic therapy. This is probably attributed to lipid oxidation and degradation mediated by ultrasound cavitation. Additionally, naturally available metals such as copper, in conjunction with cavitation, might facilitate the production of oxyradical molecules [275].

A comparison analysis of pure and ultrasound-treated oil under optimal conditions was performed to investigate the significant variations in their fatty acid composition due to ultrasound treatment. The saturated fatty acid composition (Table A6) of SFO and SBO remained predominantly unaltered during ultrasound-assisted extraction, presumably

due to the low-frequency condition (40 kHz). A minor decrease in PUFA content was noted, likely due to hydrolytic rancidity, wherein triglycerides and free fatty acids oxidise, resulting in the production of volatile chemicals that contribute to odour and non-volatile molecules that affect flavour [276].

Prior investigation indicated that YPFR possesses significant quantities of carotenoids, phenolics, and flavonoids [277]. Extraction using UAE with ethanol yielded a phenolic content of 41.48 ± 0.20 mg GAE/g, a flavonoid content of 34.41 ± 2.70 mg QE/g, and a carotenoid content of 2.57 ± 1.50 µg β-carotene/g of extract. The present study revealed that ultrasound extraction with edible oil as solvent exhibited significant phytochemical integration ($p < 0.05$) to the oil samples. Carotenoid concentrations in SFO and SBO attained 98.1 ± 3.93 µg β-carotene/100 g of oil and 149.08 ± 12.36 µg β-carotene/100 g of oil, respectively (Table 5.2), signifying a 1.22- and 1.27-fold enhancement following UAE treatment. The UAE additionally enhanced the TPC and TFC in oils, resulting in a threefold increase in TPC for both oils. TFC increased by 2.67 times in SFO and 2.0 times in SBO, indicating efficient extraction of carotenoids, phenolics, and flavonoids from YPFR without significant degradation of the oils. Additionally, the antioxidant activity was enhanced, as demonstrated by the IC_{50} values of DPPH for SBOE (94.08 ± 1.25 µg/mL) and SFOE (115.93 ± 1.69 µg/mL). Correspondingly, the ABTS IC_{50} values were 114.88 ±1.18 µg/mL for SBOE and 147.16 ± 1.29 µg/mL for SFOE. The IC_{50} values were calculated from the percentage scavenging plot for each sample (Figure A7). The results validate the effective phytochemical extraction from YPFR using UAE. The potential correlations among these biochemical parameters (carotenoids, phenolics and flavonoids) associated with antioxidant activity in the oil samples (before and after treatment) were analysed with Pearson correlation analysis (Table A7). The findings indicated that TPC values had significant positive relationships with TFC ($r = 0.999$) and TCC ($r = 0.891$), whereas demonstrating negative correlations with DPPH ($r = -0.995$) and ABTS assays ($r = -0.891$). A comparable negative correlation was discovered between TFC and TCC with DPPH and ABTS. The findings indicate that phenolic and flavonoid components in the oils have a more pronounced influence on enhancing antioxidant activity than carotenoids. The negative correlations between TPC, TFC, and TCC with DPPH and ABTS experiments demonstrated that samples with higher levels of bioactive chemicals had a lower IC_{50} value, indicating enhanced antioxidant activity. Additionally, a strong

correlation between TFC and TPC is observed due to flavonoids constituting a subgroup of phenolic compounds [278]. Ku et al. [279] reported a similar positive correlation between TFC and TPC.

The colour analysis of pure and treated oil samples (SFO and SBO) displayed high a* and b* values and a slight reduction in L* value (Table 5.3), indicating a darker colour with more redness and a minor inclination towards yellow relative to pure oil. Likewise, Barragan-Martinez et al. [280] observed that increased β-carotene levels result in intense colour, resulting in greater redness in canola oil/beeswax oleogel.

Table 5.3. Different quality parameters of oil samples before and after treatment.

	SFO	SFOE	SBO	SBOE	P values (Paired t-test*)
Peroxide Value (meq O_2/kg)	2.00 ± 0.09	2.71 ± 0.09	2.40 ± 0.03	3.09 ± 0.08	< 0.001
Acid Value (mg KOH/g)	0.08 ± 0.01	0.12 ± 0.01	0.39 ± 0.01	0.47 ± 0.02	0.004
Phenolic Content (mg GAE/ 100 g of oil)	2.45 ± 0.03	9.83 ± 0.18	2.81 ± 0.20	10.63 ± 0.22	< 0.001
Flavonoid Content (mg QE/ 100 g of oil)	3.33 ± 0.02	11.44 ± 0.28	4.21 ± 0.05	12.25 ± 0.24	< 0.001
Carotenoid Content (µg β-carotene/ 100 g of oil)	44.27 ± 0.99	98.10 ± 3.93	65.55 ± 2.57	149.08 ± 12.36	< 0.001
IC_{50} value DPPH (µg/mL)	334.09 ± 3.29	115.93 ± 1.69	313.41 ± 7.15	94.08 ± 1.25	< 0.001
IC_{50} value ABTS (µg/mL)	348.57 ± 8.60	147.16 ± 1.29	357.77 ± 8.32	114.88 ±1.18	< 0.001
L*	32.51 ± 0.15	28.43 ± 3.08	32.17 ± 0.51	30.44 ± 1.10	0.030
a*	-0.06 ± 0.02	0.16 ± 0.06	-0.04 ± 0.01	0.47 ± 0.02	< 0.001
b*	1.17 ± 0.12	2.91 ± 0.73	2.61 ± 0.38	4.07 ± 0.14	0.005

SFO: Sunflower oil, SFOE: Sunflower oil with YPFR extract SBO: Soybean oil, SBOE: Soybean oil with YPFR extract, Values are means ± standard deviation of three determinations.
*Paired t-test are comparison between oil samples before and after treatment.

5.4. Effect of Antioxidants on Oxidative Stability of Oil:

The oxidative stability of oils is essential in evaluating their shelf life and resistance to deterioration. However, assessing the oxidative stability of oils at ambient temperature is tedious, requiring accelerated trials at high temperatures for expedited outcomes. These experiments accelerate lipid oxidation by subjecting oils to high temperatures in the presence of excess air or oxygen. In this study, the PetroOxy test was employed to assess the oxidation stability of oil samples over an isothermal temperature range of 100-140 °C, quantifying the induction period (IP) to the stability endpoint. The Rancimat test is an established procedure that is accepted globally to determine oxidative stability. Therefore, the IP data from the PetroOxy test were transformed into Rancimat values using equation A1 [281]. The evaluation examined the stability of sunflower seed oil (SFO) and soybean oil (SBO) before and after incorporating YPFR extracts and compared the data with oil with synthetic antioxidants BHA and BHT. Figure 5.2. demonstrates the oxidative stability data of the assessed oil samples, indicated as induction periods, determined by the Rancimat techniques at five distinct isothermal temperatures (100, 110, 120, 130, and 140 °C). Additionally, the induction period at 25 °C was calculated by interpolating the data derived from the PetroOxy test, included in Figure 5.2. However, the PetroOxy IP values were reported in Table A8. The results demonstrated that oils fortified with YPFR extracts displayed significantly extended induction durations ($p < 0.05$), indicating improved oxidative resistance. SFOE oil exhibited a 46.44% increase in induction time, whilst SBOE demonstrated a 29.53% increase at 140 °C. The increased resistance in SFO might be ascribed to its reduced linoleate content, high oleate levels, and reduced maximum unsaturation (UFA 34.12%), which minimises vulnerability to oxidation. Oils with high polyunsaturated fatty acid (PUFA) levels exhibited reduced IP, aligning with evidence that PUFA oxidises up to 50 times more rapidly than monounsaturated fatty acids (MUFA) [282]. Both natural (YPFR extract) and synthetic antioxidants (BHA, BHT at 200 mg/1000 mL) enhanced the oxidative stability of the oils, with synthetic antioxidants (at 200 mg/1000 mL) having marginally lower IP values compared to the YPFR extract-added oil. However, SFO with BHT showed a higher IP value than the others. Increasing YPFR extract concentrations might further improve resistance to oxidative degradation. The YPFR extract, abundant in phenolic, flavonoid, and carotenoid components [246], has the potential as a natural antioxidant substitute for synthetic alternatives, thereby

avoiding associated negative effects. Shahidi and Zhong [128] reported that phenolic compounds (such as flavonoids, phenolic acids, and polyphenols), due to their hydrogen-donating nature, demonstrate potent antioxidant properties, such as free radical scavengers, metal chelators, and reducing agents. Whereas carotenoids reduce oil oxidation by filtering light, quenching singlet oxygen, inactivating photosensitisers, and scavenging free radicals. Research on β-carotene, lycopene, and astaxanthin highlights their effectiveness in improving oxidative stability [283]. Mishra et al. [131] reported that 20 ppm β-carotene significantly enhances stability in the absence of pro-oxidants. Moreover, myricetin (100 ppm) showed greater antioxidant efficacy than BHT (200 ppm) in refined sunflower oil [284]. Koketsu & Satoh [285] discovered that tea polyphenols exhibited superior antioxidative properties in soybean oil compared to α-tocopherol. Extracts from leafy vegetables markedly improved the oxidative stability of refined sunflower and groundnut oil during heating and storage [286]. Abdelazim et al. [287] similarly showed that sesame cake extract had higher antioxidant activity than BHT and BHA. Furthermore, section A3.2. elaborates on the specific process by which the addition of antioxidants improves the oxidative stability of oil. The antioxidant and phytochemical analyses suggest that the YPFR extract possesses the potential to enhance the stability of edible oils. However, since the fatty acid composition varies among different oils, the extent of this stability enhancement may differ accordingly [288].

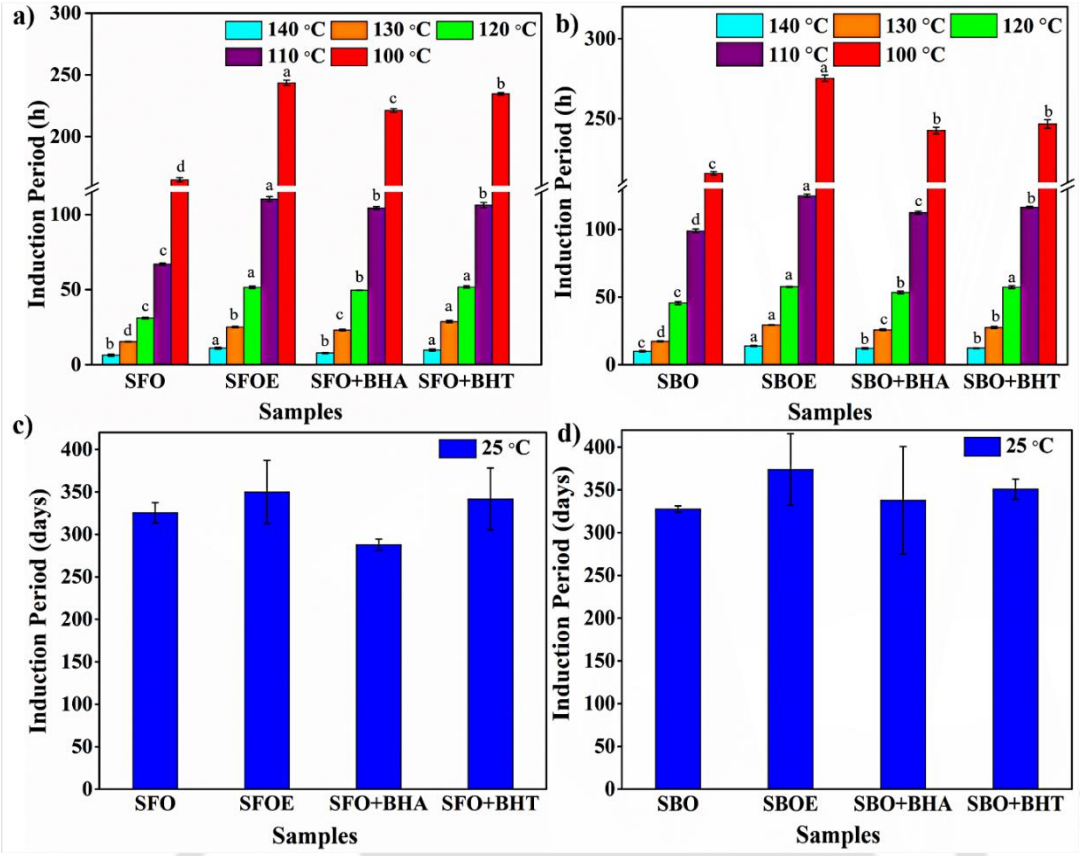

Figure 5.2. Induction periods (IPs) of oil samples by Rancimat method at (a) different isothermal temperatures (100-140 °C), and (b) 25 °C. SFO: Sunflower oil, SFOE: Sunflower oil with YPFR extract, SFO+BHA: Sunflower oil with BHA, SFO+BHT: Sunflower oil with BHT, SBO: Soybean oil, SBOE: Soybean oil with YPFR extract, SBO+BHA: Soybean oil with BHA, SBO+BHT: Soybean oil with BHT. The IPs for Rancimat method were calculated utilising PetroOxy IPs in equation A1. The IPs at 25 °C were interpolated from the PetroOxy data. Values are means ± standard deviation of three determinations. The distinct letters represent significant differences ($p < 0.05$) among individual antioxidants with each oil, as assessed by Tukey's HSD test.

5.5. Thermal Analysis of Oil:

During heating, fats and oils experience thermal oxidation, resulting in the formation of peroxides that decompose into aldehydes, ketones, epoxides, dimers, and polymers, hence deteriorating food quality. The food sector employs antioxidants to minimise these effects. Antioxidants have the capability to prevent oxidative damage and maintain food quality by avoiding flavour degradation, rancidity, and discolouration [289]. Assessing the thermal stability of oil infused with antioxidants is essential for food preservation. In the present study, thermogravimetric analysis (TGA) and differential scanning calorimetry (DSC) are performed to evaluate the effect of antioxidants on the shelf life, thermal stability, and quality of edible oil samples (pure

and antioxidant-infused) as a function of temperature. TGA technique evaluates mass and thermal variations; however, DSC determines phase transitions or chemical reactions while heat absorption or release with variation in temperature on oils [289].

5.5.1. Thermo-Gravimetric Analysis (TGA):

Figure 5.3 shows the thermal degradation patterns of pure and antioxidant-blended oil in a nitrogen environment. It shows that there was a single mass loss event, and thermal decomposition occurs between 300 and 600 °C. The oxidation of both saturated and unsaturated fatty acids explains this phenomenon [290]. The onset temperature of thermal degradation (t_{ON}) was employed to assess and compare the stability of several samples precisely. Table A10 lists the t_{ON} values derived from the extrapolation of the TGA curves for both treated and untreated oil samples, where a higher t_{ON} value indicates enhanced thermal oxidation resistance [291]. SBO and SFO subjected to YPFR extracts showed enhanced thermal stability (SBOE 383.90 °C, SFOE 374.61 °C) in contrast to untreated oils (SBO 366.79 °C, SFO 362.14 °C) and oils treated with synthetic antioxidants (Table A10). The fluctuations in stability are mostly related to the chemical makeup of oils and the existence of bioactive substances in the extracts. All three oil systems (pure oil, oil with YPFR extracts, and oil with synthetic antioxidants) showed comparable thermal behaviour (Figure 5.3 a-b), with only slight variations in their thermogravimetric profiles due to the presence of the extracts. This indicates that YPFR extracts may interact with the oils, affecting their thermodynamic stability. The findings indicate that YPFR extracts enhance the oxidative stability of oils, thereby improving their thermal properties and making them suitable for a wide range of processing and cooking applications. These extracts seem to assimilate effectively within the oil matrix, enhancing thermal stability and mitigating as well as preventing unwanted alterations.

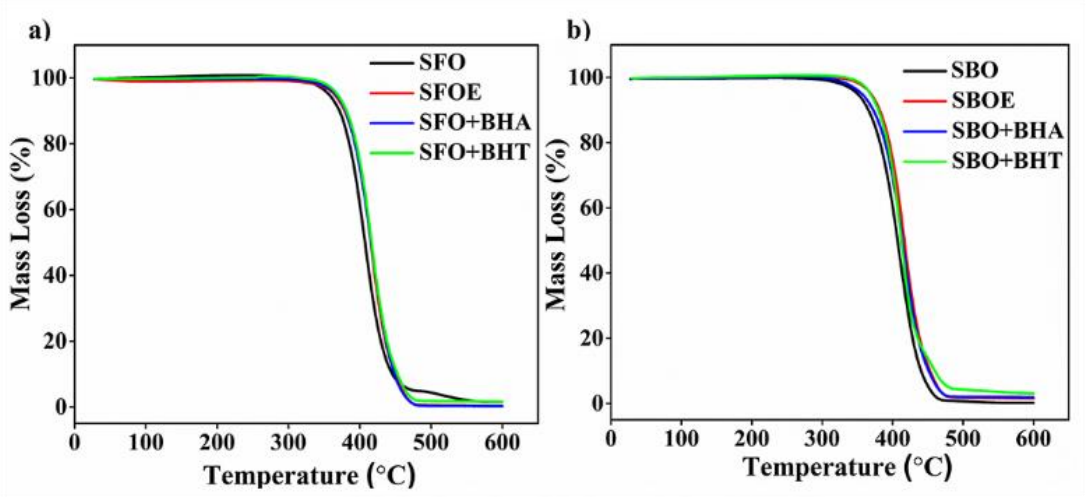

Figure 5.3. Thermogravimetric analytical curves of treated and untreated oil samples in nitrogen atmosphere. a) TGA curves of treated and untreated soybean oil, b) TGA curves of treated and untreated sunflower oil. SFO: Sunflower oil, SFOE: Sunflower oil with YPFR extract, SFO+BHA: Sunflower oil with BHA, SFO+BHT: Sunflower oil with BHT, SBO: Soybean oil, SBOE: Soybean oil with YPFR extract, SBO+BHA: Soybean oil with BHA, SBO+BHT: Soybean oil with BHT.

5.5.2. Differential Scanning Calorimetry (DSC):

The non-isothermal oxidation of SBO and SFO samples, both with and without YPFR extracts, was evaluated using DSC exotherms at 2 °C/min heating rate, as illustrated in Figure 5.4. Although all oxidation profiles exhibited the same pattern, the presence of YPFR extracts displaced the curves to low temperatures, signifying improved low-temperature stability. The appearance of peaks in the DSC exotherms indicates the commencement of oxidation in the samples. According to Litwinienko and Guttman [292], both the onset and peak temperatures correlate with the formation of initial oxidation byproducts and the decomposition of subsequent oxidation products. The onset temperature (t_{ON}) is considered as a crucial parameter for non-isothermal lipid oxidation, as it directly indicates the generation of peroxides [293]. For every sample, Table A9 shows the extrapolated onset temperature (t_{ON}), which signifies the start of the exothermic reaction. A lower pour point is generally associated with higher oxidative stability [294]. Despite the presence of YPFR extracts, the comparison study showed that SFO samples had lower t_{ON} values than SBO samples. This tendency indicates that SBO may be more susceptible to oxidation, probably because of a reduced concentration of saturated fatty acids. The incorporation of YPFR extracts reduced the t_{ON} values for both oils, thereby diminishing oxidation. Both the SBOE (-9.59 °C) and SFOE (-12.34 °C) samples showed significantly lower t_{ON} values than synthetic

antioxidant-treated or extract-free oils at a heating rate of 2 °C/min. According to the findings, YPFR extracts, which are rich in phenolic compounds and carotenoids, considerably increase the oxidative stability of SBO and SFO oils [266]. This improvement suggests that YPFR extracts could offer important protection against lipid oxidation, extending the edible oils' shelf life and thermal stability.

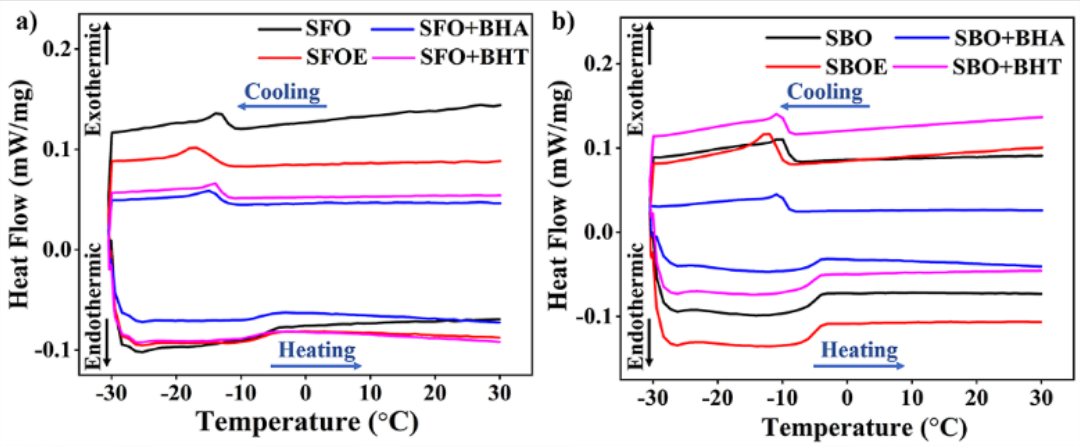

Figure 5.4. DSC heating thermogram of oil samples. a) DSC curves of treated and untreated sunflower oil, b) DSC curves of treated and untreated soybean oil. SFO: Sunflower oil, SFOE: Sunflower oil with YPFR extract, SFO+BHA: Sunflower oil with BHA, SFO+BHT: Sunflower oil with BHT, SBO: Soybean oil, SBOE: Soybean oil with YPFR extract, SBO+BHA: Soybean oil with BHA, SBO+BHT: Soybean oil with BHT.

5.6. Structural Analysis:

Fourier Transform Infrared Spectroscopy (FTIR) analysis is an effective technique for analysing oil oxidation, facilitating both qualitative and quantitative evaluations of quality indices via absorbance variations [295]. Shang et al., (2018) effectively employed FTIR to measure PV by analysing the absorbance of -OH bonds in hydroperoxides. In the present study, the structural analysis of oil samples using FTIR in the 4000-400 cm^{-1} range at room temperature, both before and after the addition of YPFR extracts, is shown in Figure 5.5. The obtained spectra demonstrated significant similarities, with distinctive absorption peaks of typical triglycerides, the key components of edible lipids and oils. A significant peak at 3009 cm^{-1} is associated with the stretching vibration of =C-H. Prominent absorption bands, attributed to C-H stretching vibrations, were seen in the 3000-2800 cm^{-1} region. Methylene ($-CH_2-$) and methyl ($-CH_3$) groups exhibited stretching vibrations at frequencies of 2923 and 2854 cm^{-1}, respectively. These groups also demonstrated bending vibrations at 1464 cm^{-1} and 1378 cm^{-1}. The prominent peak at 1740 cm^{-1} corresponds to the C=O stretching

vibration of the triglyceride ester moiety. Peaks in the 1500–650 cm^{-1} range originate from the stretching vibrations of C-O bonds and the bending of C-H bonds. Rohman & Che Man, (2012) noted that the variations among the oil samples were minimal and confined to specific spectral regions, especially regarding peak intensities in the fingerprint regions (1500-650 cm^{-1}) and at 3008-3009 cm^{-1}. The C-O stretching vibration is shown by the peak at 1159 cm^{-1} [133]. The peak at 720 cm^{-1} signifies the rocking vibrations of fatty acids, particularly $(CH_2)_n$ [298]. Sahin et al. [133] reported that due to the low concentrations, such as 200 ppm, being below the detection threshold of FTIR spectroscopy, the enriched and pure oils exhibited similar spectral patterns. As a result, even after the addition of molecules containing -OH functional groups, no peaks were detected at 3500 cm^{-1}, which is associated with the -OH stretching area. Although triglycerides with specific fatty acids dominate the composition of oils, the FTIR spectra of SBO and SFO exhibited notable similarities [299].

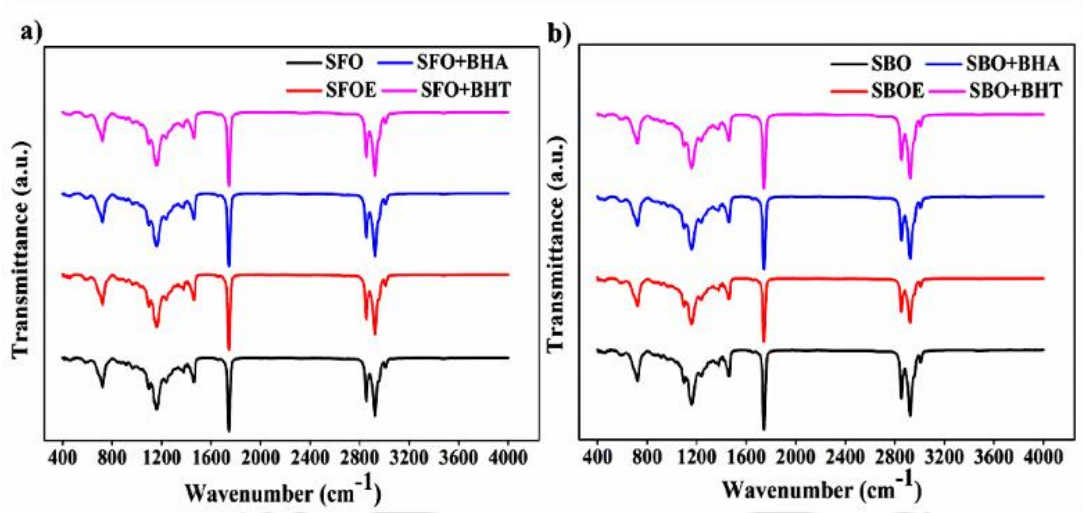

Figure 5.5. Comparative results of Fourier transform spectroscopy for a) treated and untreated Soybean oil, and b) treated and untreated soybean oil. SFO: Sunflower oil, SFOE: Sunflower oil with YPFR extract, SFO+BHA: Sunflower oil with BHA, SFO+BHT: Sunflower oil with BHT, SBO: Soybean oil, SBOE: Soybean oil with YPFR extract, SBO+BHA: Soybean oil with BHA, SBO+BHT: Soybean oil with BHT.

5.7. Conclusion:

The oxidative stability of edible oils, due to their unsaturated fatty acids, is challenged by degradation, resulting in rancidity and nutrient loss. Natural bioactive molecules emerged as healthy alternatives to synthetic antioxidants to improve oil stability. The bioactive compounds from passion fruit rinds were extracted using sunflower seed and soybean oil, and directly added to improve their stability. The ultrasound extraction

method significantly improved carotenoid, phenolic, and flavonoid content in sunflower seed oil (SFO) and soybean oil (SBO), resulting in an increase in antioxidant activities ($p<0.05$) in extract-enriched oils compared to pure oils. Although the extract-infused oil showed a darker colour with more redness due to the presence of high β-carotene, the structural analysis demonstrated no alteration in the essential structure of the oils. The oil enriched with extracts showed improved oxidative and thermal stability. The induction periods of SFO and SBO increased by 46.44% and 29.53% at 140 °C, respectively. The differential scanning spectroscopy showed a lower onset temperature in SFO samples than in SBO samples, which could be due to the lower saturated fatty acid concentration in SBO, making it more susceptible to oxidation. This approach facilitates the valorisation of agro-industrial waste, thus promoting a circular economy. Further studies might focus on enhancing the scalability of these extraction techniques, in vitro cytotoxicity effects, and flavour and sensory attributes of oil enriched with extracts.

6. CHAPTER 6

Valorisation of hemicellulosic residue from spent passion fruit rind: process optimisation and fermentation using *Pichia stipites*

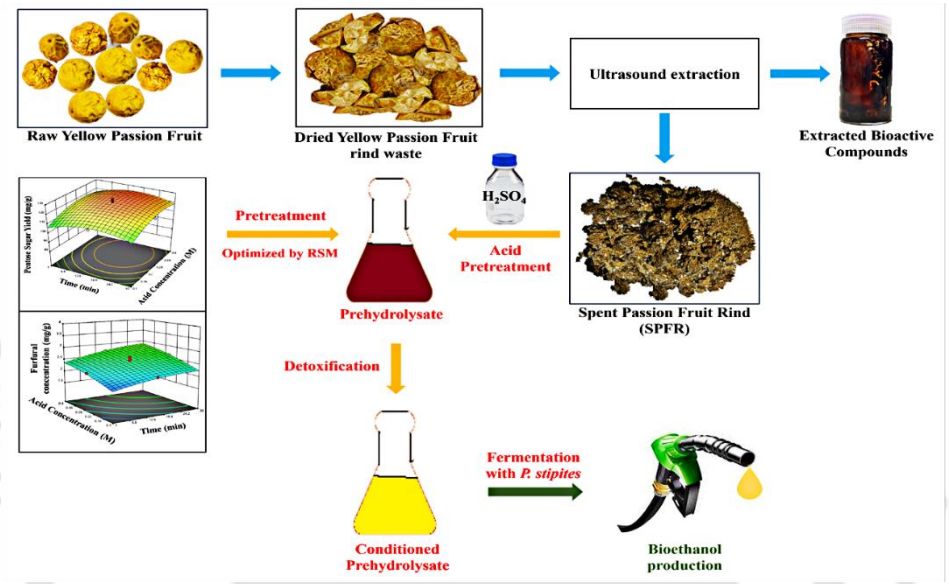

This work has been communicated as Kakali Borah, Vaibhav V Goud, 2025. Bioconversion of spent passion fruit rind to ethanol: Integrating hemi-cellulose hydrolysis and detoxification. Bioresour. Technol. Reports 31, 102193. DOI: 10.1016/j.biteb.2025.102193

CHAPTER 6

Valorisation of hemicellulosic residue from spent passion fruit rind: process optimisation and fermentation using *Pichia stipites*

Effective fermentation of the hemicellulosic fraction, which constitutes approximately one-third of lignocellulosic biomass, is essential for the advancement of second-generation bioethanol production. The residue derived from the extraction of bioactive compounds in the previous chapter retained a significant amount of structural polysaccharides, such as cellulose and hemicellulose, as well as lignin, suggesting its potential for further valorisation via bioconversion processes. This study optimises the dilute sulfuric acid pretreatment by response surface methodology (RSM) to increase xylose release and minimise fermentation inhibitors from spent passion fruit rind (SPFR) residue. The optimised parameters (114 °C, 9.8 min, and 0.2 M H_2SO_4) yielded a xylose concentration of 121.8 mg/g db, accompanied by 2.3 mg/g db furfural production. Detoxification with overliming ($Ca(OH)_2$, pH 11) further reduced inhibitory chemicals by 12–23%, improving fermentative compatibility. Subsequent fermentation of detoxified hydrolysate using Pichia (Scheffersomyces) stipitis produced an ethanol concentration of 9.7 g/L, achieving a yield of 0.42 g/g. The batch fermentation of SPFR-derived xylose-rich hydrolysate demonstrates effective bioethanol production from the hemicellulosic fraction, supporting its potential use in second-generation bioethanol.

6.1. Composition analysis of the spent passion fruit rind

The comparative assessment of raw and spent passion fruit rind (RPFR and SPFR) demonstrates slight variations in their proximate, ultimate, and chemical contents, as mentioned in Table 6.1. Both RPFR and SPFR demonstrate similar volatile matter concentration (76.9-77.2%) and carbon contents (~44.5-45.2%), signifying their appropriateness for thermochemical and biochemical conversion processes. The SPFR shows a slightly elevated carbon and hydrogen content, likely due to the extraction process that removes polar molecules, which in turn causes a slight reduction in hemicellulose, cellulose, and lignin levels. In comparison to other fruit residues such as

jackfruit, orange, pineapple, and sugar apple peels [300–302], RPFR and SPFR exhibit moderate lignocellulosic content, with RPFR including 23.4% hemicellulose and 22.5% cellulose. Although SPFR has a lower lignin percentage of 4.12% compared to RPFR (5.16%), RPFR has a slightly greater carbohydrate content than the spent substrate. This suggests that the UAE procedure during bioactive compound extraction degrades the lignin and carbohydrates in the biomass due to its cavitation effect [303]. Food waste exhibits a significant nitrogen concentration of 3.9%, potentially complicating combustion processes [304]. In contrast, citrus peels, including those from oranges and pineapples, include high volatile matter and less ash, thus enhancing the prospects for bio-oil or biochemical recovery. RPFR and SPFR exhibit a balanced composition appropriate for integrated biorefinery applications, merging the extraction of high-value chemicals with biofuel production from residual lignocellulosic materials.

Table 6.1. Comparison of chemical composition of Passion fruit rind

	RPFR	SPFR
Proximate analysis (wt%)		
Moisture	10.9	10.0
Volatile matter	76.9	77.2
Ash content	7.5	7.4
Fixed Carbon	15.6	15.4
Ultimate analysis (wt%)		
C	44.5	45.2
H	5.5	5.9
O	48	47.4
N	1.8	1.2
S	0.1	0.2
O/C ratio	1.1	1.0
H/C ratio	0.1	0.1
Calorific value (MJ/kg)	15.1	15.0
Chemical analysis (wt %)		
Extractives (%)	41.4	46.7

Total Carbohydrate	45.8	41.3
Glucan (%)	22.5	19.9
Xylan (%)	23.4	21.4
Arabinan (%)	ND	ND
Acid-insoluble lignin (%)	4.8	3.2
Acid-soluble lignin (%)	0.4	0.9

ND: Not detected. RPFR: raw passion fruit rind, SPFR: spent passion fruit rind.

6.2. Optimisation of acid hydrolysis

The acid pretreatment of SPFR with diluted H_2SO_4 was optimised using Response Surface Methodology (RSM). This study aimed to optimise the yield of xylose whilst reducing the synthesis of chemicals that inhibit it, including furfural, using the Central Composite Design (CCD) based RSM model. The impact of pretreatment temperature, duration, and acid concentration on pentose sugar and furfural production during the acid pretreatments was examined in this work. This acid pretreatment method is efficient for converting lignocellulosic biomass into fermentable sugars. This approach is valuable for converting lignocellulosic biomass into fermentable sugars and optimising their process parameters and the formation of value-added products. The experimental results of the acid pretreatments are listed in Table 6.2.

6.2.1. ANOVA results for optimisation

An Analysis of Variance (ANOVA) was performed primarily to confirm the validity of the model developed by RSM and the configurations that were found optimal. Table 6.3 summarises the ANOVA results for both the pentose sugar and furfural produced. A quadratic model was designed to assess the correlation between the pre-treatment parameters (acid concentration, temperature, and duration) and response yield in RSM. The models were fitted to the experimental data, and ANOVA was performed to evaluate their significance. The quadratic regression models for both pentose sugar and furfural yield were statistically significant ($p < 0.0001$), as per the ANOVA findings, and the high F-values suggest that the model terms considerably influence the variation in xylose production. The most significant variables were determined to be temperature and acid concentration, followed by time in the case of xylose yield. Additionally, the xylose and furfural yields are substantially influenced by the quadratic terms, emphasising the significance of non-linear influences in the optimisation process. The

regression coefficients (r^2) 0.97 and 0.96 for xylose and furfural yield, respectively, indicate the reliability of the RSM technique and the validation of the quadratic model in optimising pre-treatment configurations is validated by this thorough investigation. The subsequent equations (6.1 and 6.2) represent the regression models, derived from the ANOVA test in terms of coded components for output factors:

$$\text{Xylose yield} = 125.89 + 8.05\alpha + 1.53\beta + 4.71\gamma - 0.89\alpha\beta + 1.23\alpha\gamma - 0.44\beta\gamma - 13.47\alpha^2 - 7.06\beta^2 - 6.06\gamma^2 \quad 6.1$$

$$Furfural\ concentration = 2.51 + 0.57\alpha + 0.23\beta + 0.29\gamma - 0.01\alpha\beta + 0.17\alpha\gamma + 0.04\beta\gamma + 0.15\alpha^2 - 0.09\beta^2 - 0.08\gamma^2 \quad 6.2$$

The parameters employed for the dilute acid pretreatment process were α - temperature (°C), β - duration (min), and γ - acid concentration (M), all expressed in coded terms.

Table 6.2. The experimental design matrix for xylose and furfural content (mg/g db) derived in acid prehydrolysate from the CCD model

Temperature (°C)	Time (min)	Acid Concentration (M)	Xylose yield (mg/g db)		Furfural concentration (mg/g db)	
			Experimental	Predicted	Experimental	Predicted
80	1	0.1	86.8 ± 1.8	84.93	1.7 ± 0.2	1.6
160	1	0.1	99.1 ± 1.8	100.35	2.3 ± 0.2	2.42
80	30	0.1	89.4 ± 0.9	90.62	2.0 ± 0.0	2
160	30	0.1	104.8 ± 1.6	102.5	2.8 ± 0.2	2.78
80	1	0.4	91.4 ± 2.3	92.76	1.8 ± 0.1	1.75
160	1	0.4	115.3 ± 2.7	113.09	3.2 ± 0.3	3.27
80	30	0.4	98.9 ± 2.2	96.71	2.4 ± 0.2	2.31
160	30	0.4	112.6 ± 0.7	113.5	3.7 ± 0.2	3.79
80	15.5	0.25	102.9 ± 2.9	104.37	1.9 ± 0.0	2.08
160	15.5	0.25	117.8 ± 2.6	120.48	3.4 ± 0.3	3.23
120	1	0.25	115.8 ± 3.2	117.31	2.2 ± 0.3	2.19
120	30	0.25	118.1 ± 1.0	120.36	2.6 ± 0.3	2.65
120	15.5	0.1	113.5 ± 1.9	115.13	2.2 ± 0.3	2.14
120	15.5	0.4	122.4 ± 1.3	124.54	2.7 ± 0.1	2.72
120	15.5	0.25	126.6 ± 1.6	125.89	2.6 ± 0.4	2.51
120	15.5	0.25	128.5 ± 1.4	125.89	2.3 ± 0.1	2.51

120	15.5	0.25	129.8 ± 0.9	125.89	2.5 ± 0.1	2.51
120	15.5	0.25	122.8 ± 1.2	125.89	2.7 ± 0.1	2.51
120	15.5	0.25	129.9 ± 1.1	125.89	2.6 ± 0.1	2.51
120	15.5	0.25	125.3 ± 1.8	125.89	2.3 ± 0.2	2.51

Xylose and Furfural content expressed as mg/g db *(db: dry biomass)*

Table 6.3. The quadratic model's ANOVA analysis for optimisation of Pentose sugar and Furfural concentration during dilute sulfuric acid pretreatment on spent passion fruit rind

Response 1: Xylose yield							**Response 2: Furfural concentration**					
Source	**Sum of Squares**	**df**	**Mean Square**	**F-value**	**p-value**		**Sum of Squares**	**df**	**Mean Square**	**F-value**	**p-value**	
Model	3570.0	9	396.7	41.4	$< 1.0 \times 10^{-4}$	significant	5.0	9	0.6	28.4	$< 1 \times 10^{-4}$	significant
A-Temperature	648.4	1	648.3	67.6	$< 1.0 \times 10^{-4}$		3.3	1	3.3	168.5	$< 1 \times 10^{-4}$	
B-Time	23.3	1	23.3	2.4	0.2		0.5	1	0.5	27.3	4×10^{-4}	
C-Acid concentration	221.6	1	221.6	23.1	7.0×10^{-4}		0.8	1	0.8	42.7	$< 1 \times 10^{-4}$	
AB	6.3	1	6.3	0.7	0.4		8.0×10^{-4}	1	8.0×10^{-4}	4.1×10^{-2}	0.8	
AC	12.1	1	12.0	1.3	0.9		0.2	1	0.2	12.3	5.6×10^{-3}	
BC	1.5	1	1.5	0.2	0.7		1.3×10^{-2}	1	1.3×10^{-2}	0.7	0.4	
A^2	499.1	1	499.0	52.1	$< 1.0 \times 10^{-4}$		6.1×10^{-2}	1	6.1×10^{-2}	3.1	0.1	
B^2	136.9	1	136.9	14.3	3.6×10^{-3}		2.3×10^{-2}	1	2.3×10^{-2}	1.2	0.3	

C^2	101.0	1	101.0	10.5	8.8×10^{-3}		2.0×10^{-2}	1	1.6×10^{-2}	0.8	0.4	
Residual	95.9	10	9.6				0.2	10	2.0×10^{-2}			
Lack of Fit	57.0	5	11.4	1.5	0.3	not significant	0.1	5	1.8×10^{-2}	0.9	0.6	not significant
Pure Error	39.0	5	7.8				0.1	5	2.1×10^{-2}			
Cor Total	3665.9	19					5.2	19				
R^2	0.97						0.96					
Adjusted R^2	0.95						0.93					
C.V. %	2.8						5.6					

6.2.2. Interaction effects of the pretreatment parameters on the response

Response Surface Methodology (RSM) was employed to evaluate the interaction effects of acid concentration, temperature, and time on pentose sugar and furfural yields, with the aim of optimising the pre-treatment parameters for passion fruit rind. Thus, to maximise xylose extraction and reduce the production of by-products, it is essential to analyse these correlations, which are illustrated in Figure 6.1, a 3D plot. The following graphs demonstrate the significant impact of the process parameters on the outcomes by changing two of the parameters while maintaining the other at a fixed value.

6.2.2.1. Effect of parameters on xylose yield: The temperature and acid concentration had a significant effect on xylose yield, with $p<0.001$ as compared to the exposure time (Table 6.3). The outcomes of xylose release throughout the pretreatment procedure are displayed in Figure 6.1. Xylose release peaked at approximately 140 °C and declined with further increases in temperature and heating duration. This decrease could possibly be the result of xylose degrading into furfural at high temperatures and long residence period (Figure 6.1a). These results are consistent with the available report in the literature on microwave pretreatment of sugarcane bagasse using sulfuric acid [305]. Xylose release increased with rising temperature and acid concentration, reaching a maximum at 140 °C and 0.3 M, respectively (Figure 6.1b). Beyond these limits, the yield of xylose decreased with additional increases of inhibitory compounds. This trend is most likely the result of a hydrolysis reaction during the acid pretreatment procedure, which breaks down the carbohydrate component into inhibitory compounds under rigid conditions [306]. This result is corroborated by the release of sugars and byproducts, which accumulate in the liquid fraction [307]. The sugar content was greatly increased by raising the sulfuric acid concentration and increasing the reaction time; at 0.3 M sulfuric acid concentration and 15 min of reaction time, the highest sugar concentration was 129.97 mg/g (Figure 6.1c). Elevated sulfuric acid concentrations and extended reaction times during acid pretreatment enhance biomass digestion and increase the total sugar content of the hydrolysate. Nevertheless, the amount of total sugar decreased as sulfuric acid content and reaction time increased further. The quantities of sugars in the hydrolysate can be decreased by secondary sugar breakdown into by-products, including formic acid, levulinic acid, and hydroxymethyl furfural, which can be brought

on by extended microwave exposure and high acid concentrations [308]. Dilute acid pretreatment, usually utilising low acid concentrations at high temperatures, efficiently hydrolyses glycosidic linkages between cellulose and hemicellulose. Among frequently utilised acids, sulfuric acid is predominantly preferred for its economical nature and superior efficacy [309]. Park et al. [310] investigated the influence of different temperatures (120–180 °C), solid-to-liquid ratios (5–15% w/v), and sulfuric acid concentrations (0.5–1.5% w/w) on the hydrolysis of *Gelidium amansii*, concluding that 0.5% H_2SO_4 at 121 °C is ideal for operational efficiency. In spite of its efficacy, acid pretreatment frequently results in the generation of inhibitory by-products, including furans (0.03–8.23 g/L), acetic acid (2.61–7.70 g/L), and 5-HMF (0.09–1.59 g/L), which can substantially impede microbial metabolism and subsequent fermentation by disrupting multiple cellular pathways [311,312]. Therefore, in this study, the pretreatment conditions have been optimised for obtaining the maximum sugar with minimal release of furfural. As xylose degradation at high temperature produces furfural.

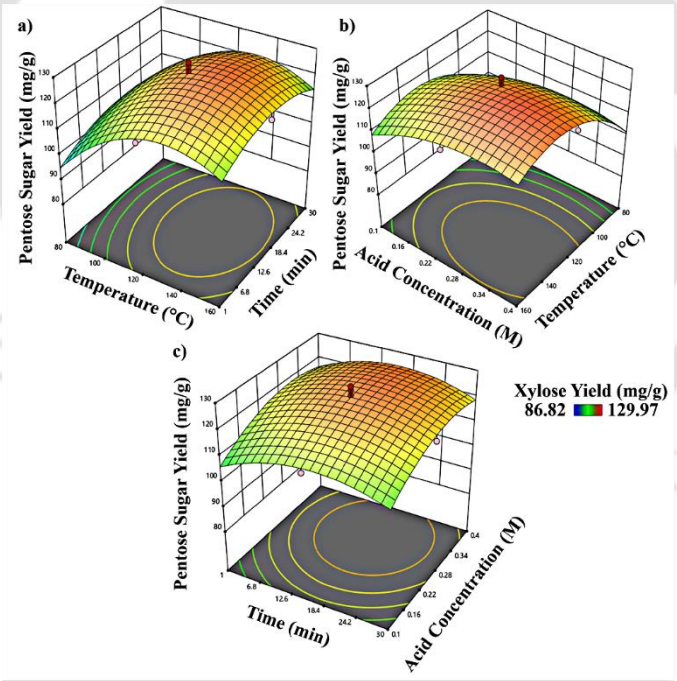

Figure 6.1. 3D contour plots of interaction effects of the different independent variables on pentose sugar yield (a) time and temperature; (b) acid concentration and temperature; and (c) acid concentration and time.

6.2.2.2. Effect of parameters on furfural release: While pretreatment increases the concentration of reducing sugars, it also results in the formation of inhibitors, as

noted in previous studies [313]. Acetic acid, furfural, and 5-HMF as the primary inhibitors present in the acid-treated SPFR prehydrolysate [314]. In this study, the process was optimised to obtain the minimal concentration of furfural, which is a by-product produced from xylose degradation, using RSM. The ANOVA finding revealed that all the parameters (temperature, time, and acid concentration) show a significant effect on the furfural yield with $p<0.001$, as depicted in Figure 6.2. Furfural, which inhibits ethanologenic organisms essential for effective fermentation, is generated at higher temperatures and with prolonged heat exposure during dilute-acid pretreatment [305]. A high acid concentration and prolonged residence time can lead to a slight reduction in furfural content (Figure 6.2c). Furfural is prone to degradation when exposed to strong acidic conditions; therefore, this reduction might be caused by further degradation of furfural into formic acid throughout the prolonged reaction period [199]. Initially, the C5 hemicelluloses are first depolymerised into xylose, which is then transformed into furfural. The decomposition of furfural yields formic acid and succinic acid [315].

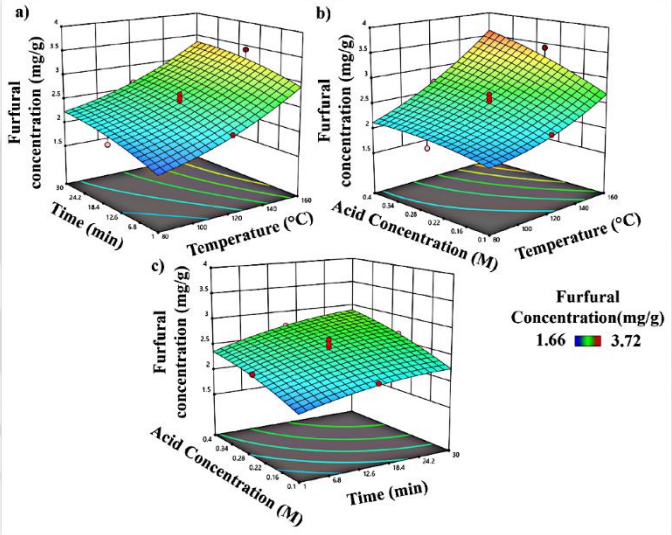

Figure 6.2. 3D contour plots of interaction effects of the different independent variables on furfural concentration (a) time and temperature; (b) acid concentration and temperature; and (c) acid concentration and time.

6.2.3. Optimisation and validation of pre-treatment conditions

The Design-Expert software predicted that the optimum temperature, time, and concentration of acids were 113.95 °C, 9.84 min, and 0.227 M, respectively, to maximise the pentose sugar production meanwhile limiting the furfural level. The expected results at the conditions mentioned above were 2.28 mg/g for furfural and

121.78 mg/g for xylose. These hypotheses were validated experimentally (at 110 °C, 10 min, 0.2 M H_2SO_4), with measured amounts of 2.11 mg/g for furfural and 122.02 mg/g for pentose sugars. The close agreement between the experimental data and the model (with a percentage error of 0.20% for xylose) demonstrates its precision and feasibility for maximising hemicellulose hydrolysis in SPFR, yielding significant pentose sugars while minimising furfural formation. A high hemicellulose content, especially xylose, and low levels of fermentative inhibitory compounds can improve the effectiveness of fermentation, which is beneficial for the formation of biofuels and value-added chemicals. This investigation offers significant perspectives in developing cost-efficient and productive processes for processing lignocellulosic biomass into fermentable sugars in the context of biorefineries. This study focused on xylose yield, the predominant pentose released during the dilute acid pretreatment of SPFR. HPLC analysis identified xylose as the primary sugar, with arabinose undetected, indicating its negligible presence, consistent with reported compositional profiles in Table 6.1. Oligomers were evaluated by quantifying xylobiose under optimal conditions, yielding low levels (1.2–1.6 g/L), indicating effective hemicellulose depolymerisation into monomeric xylose, the desired sugar for further fermentation with *Pichia stipitis*. Additionally, another experiment was conducted employing acid pre-treatment on raw passion fruit rind under the same conditions to analyse the effectiveness of processes and validate the optimised pre-treatment parameters. The findings demonstrated that the pre-treatment produced a xylose concentration of 127.81 mg/g from the RPFR. The relative efficacy of the pretreatment technique was demonstrated by comparing this yield to that of SPFR obtained under optimal conditions. Consequently, the results showed that xylose from the lignocellulosic biomass could be efficiently extracted through diluted sulfuric acid, and this might be employed to produce bioethanol.

6.3. Detoxification of the prehydrolysate

The detoxification of the prehydrolysate is a crucial stage in the synthesis of bioethanol to mitigate the adverse consequences of fermentative inhibitors and other toxic compounds that form during the feedstock pretreatment process. Furfural, formic acid, and various other by-products are examples of inhibitors that severely hinder the fermentation process, decreasing the effectiveness of ethanol generation. As a result, high fermentation efficiency and yield depend on efficient detoxification. Promta et al. [316] proved that the overliming method was a cost-effective procedure that has shown

great efficacy in eliminating inhibitors, especially furan compounds, by precipitating harmful chemicals at high pH levels. In this study, the acidity of the hydrolysate obtained at the optimised pretreatment condition was neutralised to pH 6 with calcium hydroxide [$Ca(OH)_2$]. However, a fraction of the prehydrolysate was treated with $Ca(OH)_2$ to a pH of 11, which makes it easier to neutralise acids like phenolic acid. The outcomes revealed that after detoxification, there was a substantial drop in the amounts of phenolic acid, formic acid, and furfural. In SPFR, conditioning led to a 22% and 17.39% reduction in phenolic acid content and furfural concentration, respectively. Additionally, there was a considerable 15.42% loss in xylose content following the conditioning of the hydrolysate. Similar to this, the RPFR-over limed hydrolysate showed a notable decrease in inhibitors simultaneously with a commensurate loss of carbohydrates. Figure 6.3 shows the percentage of sugar and other inhibitory substances lost in the SPFR and RPFR-over limed hydrolysate. The paired sample t-test performed on both SPFR and RPFR hydrolysate (as shown in Table A10) revealed that overliming significantly reduced (two-sided p-value <0.05) the concentration of furfural and phenolic acid, which enhances the fermentation process. However, there was additionally a noticeable decrease in sugar content as a result of this treatment. The decreases in HMF, formic acid, and acetic acid, on the contrary, were not statistically significant, indicating that the conditioning procedure had minimal impact on these substances. This may suggest that to maximise the decrease of these inhibitors and maintain sugars for the generation of bioethanol, additional optimisation or different detoxification techniques may be required.

Promta et al. [316] reported that optimum conditions, overliming effectively removed 38.37% of total furans and 50.02% of total phenolics; additionally, it resulted in a 37.81% sugar loss in the sugarcane bagasse acid hydrolysate. This sugar loss corresponds to the hydroxide degradation from $Ca(OH)_2$ that occurs during detoxification and can transform carbohydrates into nonfermentable substances such as formic, acetic acids. It was observed that the overliming process removed 16.6% of furfural, 13% of 5-HMF, 7.3% of acetic acid, and 6.3% of formic acid, in addition to an average total sugar loss of 10% in the Sorghum brown midrib hydrolysate [199]. Liu et al. [317] reported that despite offering a cost-effective detoxification procedure, excessive liming with $Ca(OH)_2$ resulted in a substantial sugar loss of 29.74% relative

to the undetoxified control. This decrease is related to hydroxide-catalysed sugar breakdown and the generation of unfermentable chemicals in alkaline conditions.

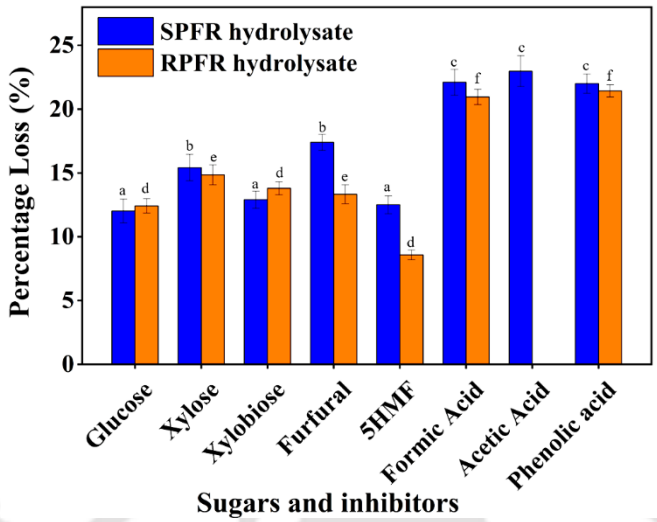

Figure 6.3. Percentage of sugars and fermentative inhibitors after conditioning

6.4. Fermentation of the hydrolysate

In this study, the hydrolysate obtained from spent and raw passion fruit rind was neutralised and fermented using *Pichia* (*Scheffersomyces*) *stipites* NCIM 3497. The sugar concentration, ethanol output, and fermentation efficiency were analysed during the fermentation process, and the findings are presented in Table 6.4. After 24 h of fermentation in SPFR after detoxification, 7.5 ± 0.3 g/L glucose and 23.1 ± 1.0 g/L xylose yielded a maximum bioethanol concentration of 9.7 g/L. However, the amounts of xylobiose in the hydrolysate were minimal (1.2–1.6 g/L), indicating a negligible impact on overall ethanol production. Additionally, Table 6.4 stated that the overlimed hydrolysate outperformed the hydrolysate without overliming, with higher ethanol yield and conversion efficiency. The hydrolysates that were not detoxified demonstrated reduced ethanol productivity compared to detoxified hydrolysates. Additionally, they needed to ferment for an extended period of 30 hours to achieve the highest amount of ethanol production. Conversely, the maximum ethanol production for detoxified hydrolysates was achieved within 24 hours, with enhanced productivity of 0.40 ± 0.01 g/L/h (for both SPFR and RPFR). Despite an average 13% sugar loss, this improvement is probably the result of the elimination of fermentative inhibitors during detoxification, as evidenced by the elimination of ~15% organic acids (furfural, 5-HMF), 22.97% acetic acid, and 22.11% formic acid. As per the result, detoxification

increased the fermentation efficiency, but non-detoxified hydrolysates with higher inhibitor concentrations hindered microbial metabolism, reducing bioethanol production [318]. Additionally, the result showed that the SPFR could effectively produce ethanol with very close ethanol productivity to RPFR.

Table 6.4. Fermentation profile of overlimed and without overlimed passion fruit rind hydrolysates

	SPFR hydrolysate		RPFR hydrolysate	
	Overlimed	Without Overlimed	Overlimed	Without Overlimed
Glucose (g/L)	7.5 ± 0.3	8.1 ± 0.6	6.8 ± 0.1	7.7 ± 1.0
Xylose (g/L)	23.1 ± 1.0	26.9 ± 1.3	22.1 ± 1.1	26.0 ± 1.6
Xylobiose (g/L)	2.9 ± 0.4	2.6 ± 0.2	3.0 ± 0.5	2.5 ± 0.1
Ethanol (g/L)	9.6	10.7	9.7	10.6
Ethanol yield (g_P/g_S)	0.42 ± 0.01	0.40 ± 0.01	0.44 ± 0.01	0.41 ± 0.01
Fermentation efficiency (%)	81.9	77.9	85.9	79.6

Figures 6.4(a-d) illustrate bioethanol production gradually increasing initially, attributable to the yeast's lag phase, a common feature of newly inoculated cultures. However, hereafter, substrate utilisation and product synthesis proceed fast, signifying rapid yeast acclimatisation. The increased sugar concentration and minimal inhibitor levels in the fermentation medium promote cellular proliferation and effective substrate utilisation [169]. It was observed that following the full consumption of glucose during the first 6 h of fermentation, the utilisation of xylose started as *P. stipitis* prefers glucose, which results in the inhibition of xylose uptake caused by glucose [209]. The findings correspond with prior investigations (Table 6.5) about bioethanol synthesis from different biomasses after detoxification. Thus, the result showed that the SPFR could effectively be used to produce ethanol. Additionally, following acid pretreatment under optimal conditions, 33.19 g of residual biomass was derived from 100 g of SPFR, consisting of 40.53% cellulose and 28.46% acid-insoluble residue. This cellulose-rich residue possesses potential for further ethanol production by enzymatic saccharification.

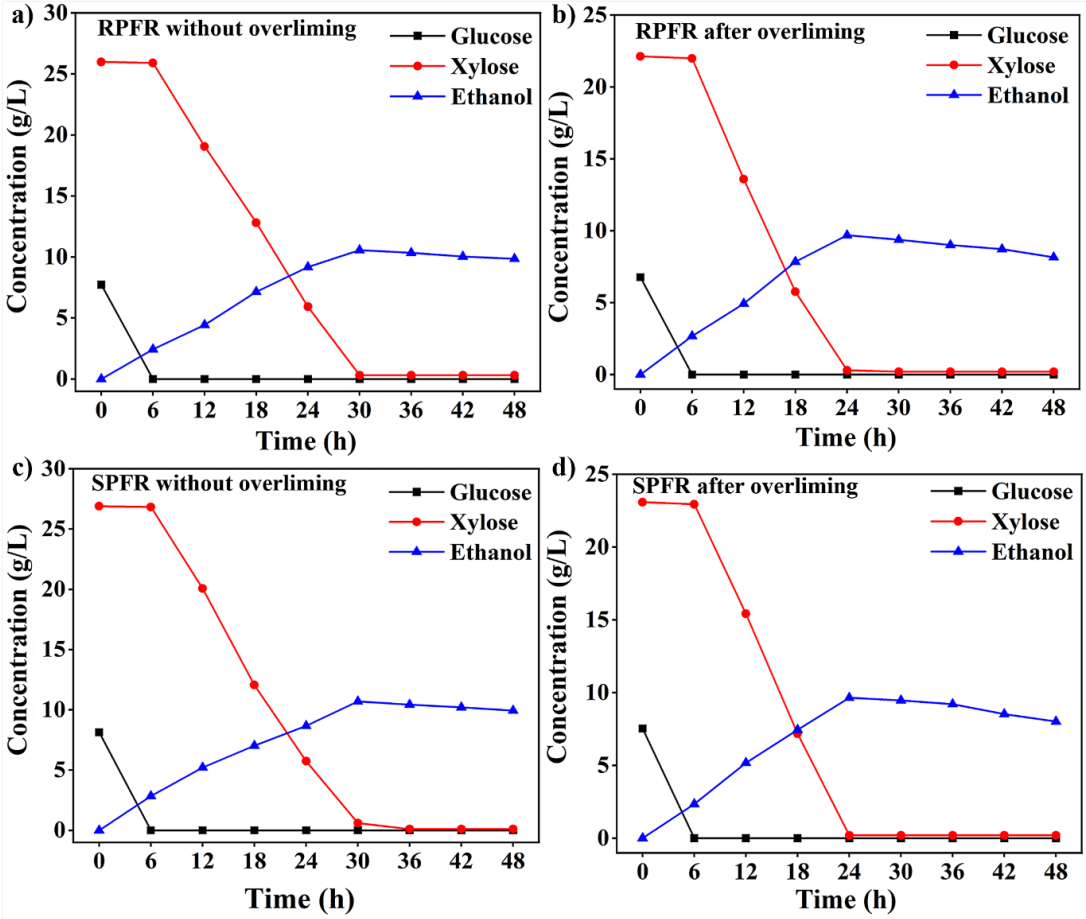

Figure 6.4. Sugar and ethanol profile of a) RPFR without conditioning, b) RPFR after conditioning, c) SPFR without conditioning, d) SPFR after conditioning.

Our results align with previous studies demonstrating improved ethanol production following detoxification. Nouri et al. [319] found that overliming detoxification of sugarcane bagasse hydrolysate improved the fermentability of concentrated hydrolysate by wild *Barnettozyma californica*, increasing ethanol output from 1.23 g/L to 3.80 g/L. A study investigated the effects of overliming on improving sugar retention and decreasing inhibitors in dilute-acid hydrolysate derived from olive stones. Detoxification at pH 10, 25 °C for 30 min considerably enhanced yeast viability while reducing furans and polyphenols, whereas pH 12 resulted in sugar depletion and the generation of new toxic chemicals [320]. The detoxification of waste potato peel hydrolysates with Fe_3O_4 nanoparticles demonstrated significant removal rates of furfural (40%), HMF (24%), acetic acid (69%), phenol (49%), and formaldehyde (35%), while retaining sugar content. This technique significantly enhanced saccharification efficiency (88.95%) and bioethanol yield (0.504 g/g) [321].

Table 6.5. Ethanol yield and productivity of different biomasses after detoxification

Biomass	Species	Detoxification method	Ethanol titre (g/L)	Ethanol yield (g_p/g_s)	Productivity	Time (h)	Reference
Raw passion fruit rind	*P. stipites* NCIM 3497	Overliming	9.7	0.44 ± 0.01	0.40 ± 0.01 g/L/h	24	This study
Raw passion fruit rind	*P. stipites* NCIM 3497	Without overliming	10.6	0.41 ± 0.01	0.35 ± 0.01 g/L/h	30	This study
Spent passion fruit rind	*P. stipites* NCIM 3497	Overliming	9.6	0.42 ± 0.01	0.40 ± 0.01 g/L/h	24	This study
Spent passion fruit rind	*P. stipites* NCIM 3497	Without overliming	10.7	0.40 ± 0.01	0.36 ± 0.01 g/L/h	30	This study
Sugarcane bagasse	*Pichia stipites* (TISTR 5806)	Overliming	11.6	0.30	0.19 g/L/h	84	[316]
Sorghum Stalks	*P. stipites* NCIM 3498	Overliming	11.6	0.46	0.47 g/L/h	24	[209]
Sugar beet pulp	*P. stipites* NRRL Y-7124	Commercial activated charcoal with overliming, activated charcoal obtained from sugar beet pulp with overliming and fly ash treatment	10.8-12.2	0.13-0.44	0.12–0.29 g/L/h	50-121	[322]
Saccharum spontaneum	*P. stipites* NCIM3498	Overliming	13.1	0.44	0.18 g/L/h	72	[323]
Sugarcane Bagasse	*P. stipitis* DSM 3651	Active charcoal	6.1	0.30	0.13 g/L/h	48	[318]

Sugarcane Bagasse	*S. cerevisiae* ATCC 96581	Overliming	11.5	0.35	0.26 g/g/h	24	[324]

6.5. Conclusion

This work supports the valorisation of spent passion fruit rind (SPFR), obtained post-bioactive compound extraction, as a viable feedstock for bioethanol production. Composition analysis confirmed the presence of significant fermentable carbohydrates, consisting of approximately 22% hemicellulose and 19% cellulose. The hemicellulosic fraction showed significant potential for hydrolysis under optimal dilute acid pretreatment conditions, producing 122.02 mg/g db of xylose with negligible furfural production of 2.11 mg/g db. The software predicted that the optimum temperature, time, and concentration of acids were 113.95 °C, 9.84 min, and 0.227 M, respectively, to obtain maximum pentose sugar while limiting furfural level. The subsequent detoxification with calcium hydroxide significantly reduced phenolic and furfural concentration by 22 % and 17.39 %, respectively. Despite a 13% reduction in sugar, the fermentation efficiency (81.97%) improved in SPFR hydrolysate after detoxification (81.97%) compared to without detoxification (77.90%). The fermentation of the detoxified hydrolysate using *Pichia* (*Scheffersomyces*) *stipitis* yielded 9.7 g/L of bioethanol, indicating the viability of SPFR as an alternative lignocellulosic substrate for ethanol production. Despite the relatively low ethanol titers observed in this study, findings highlight the underexploited potential of the hemicellulosic (xylose-rich) component of SPFR. Future studies should investigate the use of the residual cellulose-rich fraction after acid pretreatment to improve overall process efficiency.

7. CHAPTER 7

Delignification and enzymatic hydrolysis of cellulose fraction from passion fruit rind residue

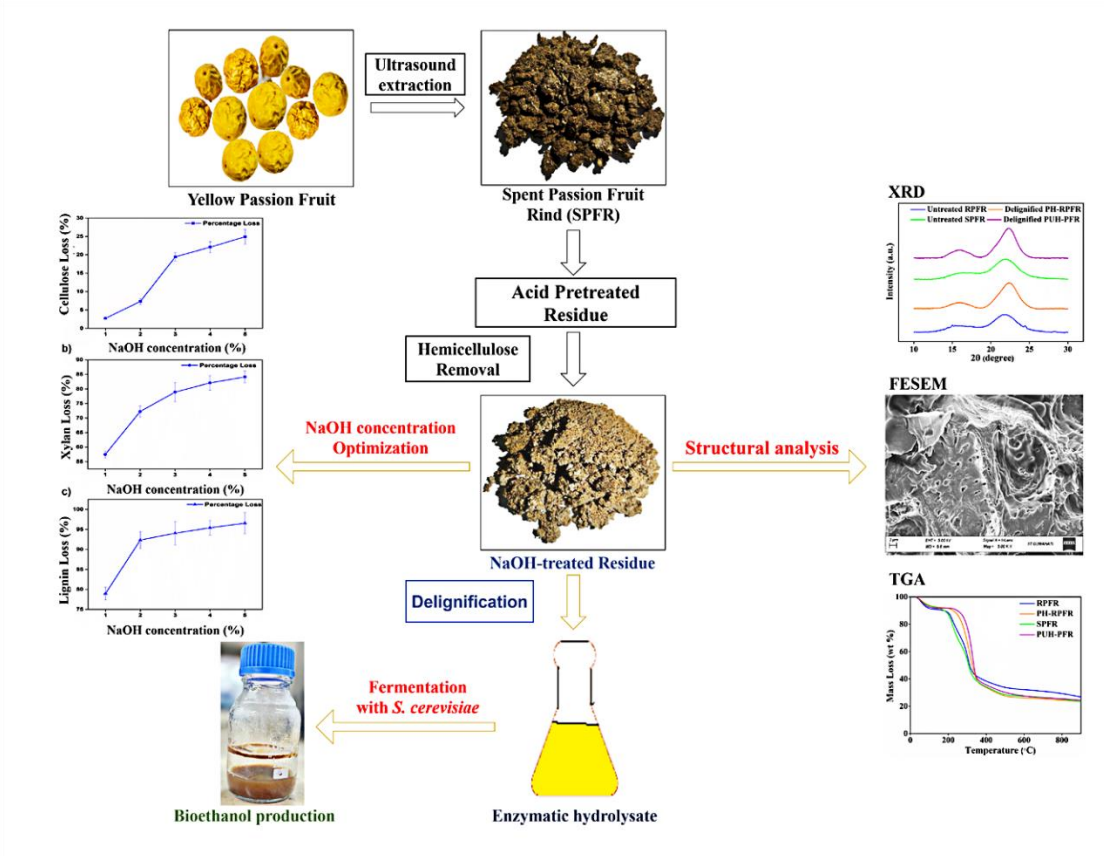

This work has been communicated as Kakali Borah, Vaibhav V Goud, 2025.Alkali Delignification and Fermentation of Spent Passion Fruit Rind to Bioethanol Production. (Submitted)

CHAPTER 7

Delignification and enzymatic hydrolysis of cellulose fraction from passion fruit rind residue

Spent passion fruit rind (SPFR), an agro-industrial byproduct, was investigated as a potential lignocellulosic feedstock for sustainable bioethanol production. The residual biomass obtained following dilute acid pretreatment (PUH-PFR) in Chapter 6 comprised a significant cellulose content of 40.53%, in addition to 28.46% lignin. To improve cellulose accessibility for enzymatic hydrolysis, alkali delignification was performed with varying concentrations of sodium hydroxide (1-5%). The 2% NaOH treatment resulted in a maximum 92.35% lignin removal with negligible cellulose loss (7.33%). The effectiveness of delignification was confirmed by an increase in the crystallinity index compared to SPFR, as determined by X-ray diffraction. The formation of a porous surface with an increased specific surface area, as evidenced by morphological analysis, indicated the removal of lignin and hemicellulose. Following enzymatic saccharification with commercial cellulase, a yield of 67.19 g/L of glucose was achieved, resulting in a saccharification efficiency of 87.42%. The hydrolysate was fermented using S. cerevisiae, yielding 30.12 g/L of ethanol.

7.1. Composition analysis of PUH-PFR

The spent passion fruit rind (SPFR), obtained post-extraction of bioactive compounds via ultrasonic extraction with vegetable oil as the solvent (chapter 5), was subjected to a dilute sulphuric acid pretreatment to eliminate the xylan component of the biomass (chapter 6). Nonetheless, a significant quantity of cellulose and lignin persists in the residual biomass (331.04 g). NREL/TP-510-42618 structural carbohydrate and lignin estimation method indicated that the passion fruit rind residue obtained from post-ultrasound-assisted extraction and sulphuric acid treatment (PUH-PFR) comprises 134.17 g of cellulose (40.53% w/w) and 94.22 g of lignin (28.46% w/w), as mentioned in Table 7.1. Furthermore, the raw passion fruit rind (RPFR) residue (residual biomass 388.47 g) after H_2SO_4 hydrolysis (PH-RPFR) contains 169.38 g of cellulose (43.60% w/w) and 113.69 g of lignin (29.27% w/w). Similarly, Chen et al. [325] obtained a

maximum holocellulose yield of 56.95% from the passion fruit peel. Passion fruit stalks were found to comprise 36.7% cellulose, 29.1% xylan, and 13.7% lignin [119], signifying a substantial carbohydrate content and moderate lignin concentration, thus presenting a viable option for saccharification procedures with appropriate pretreatment. Conversely, the analysis of passion fruit peels by Silva et al. [104] revealed a low cellulose (25.4%) and xylan (11.8%), with a significantly low lignin content of 4.9%, thereby diminishing the intensity of pretreatment necessary but possibly constraining overall sugar recovery. In contrast, Wijaya et al. [326] reported peel samples containing 28.58% cellulose, 23.01% xylan, and a substantially high lignin concentration of 36.18%, emphasising the heterogeneity in lignocellulosic composition based on geographical origin, cultivar, and harvest maturity. The increased lignin in this sample highlights the necessity of an efficient delignification approach before enzymatic saccharification.

Table 7.1. Composition of the Passion fruit by-products

	Cellulose (% w/w)	Xylan (% w/w)	Lignin (% w/w)
RPFR	22.45	23.37	11.65[a]
PH-RPFR[*]	43.60	25.08	29.27[a]
SPFR	19.93	21.39	10.65[a]
PUH-PFR[#]	40.53	26.46	28.46 [a]

[*]Calculation based on residual biomass 388.47 g, [#]Calculation based on residual biomass 331.94 g. [a]Acid insoluble residue. RPFR: raw passion fruit rind, PH-RPFR: raw passion fruit rind residue after H_2SO_4 hydrolysis, SPFR: spent passion fruit rind (SPFR), PUH-PFR: passion fruit rind residue obtained from post-ultrasound-assisted extraction and sulphuric acid treatment.

7.2. Delignification PFR residue

Increasing NaOH concentration (1–5%, w/v) improved the delignification of pretreated PUH-PFR from 78.95-96.57%, accompanied by cellulose loss ranging from 2.72-24.93% (Figure 7.1). During delignification, lignin solubility attained 78.95% and 92.35% at NaOH concentrations of 1% and 2%, respectively, reflecting a 16.97% enhancement between these levels. Subsequent increases in NaOH concentration to 3%, 4%, and 5% yielded lignin removal of 94.06%, 95.41%, and 96.57%, respectively. At high NaOH concentrations (3–5%), an increase in lignin solubility was minimal, indicating enhancements of ≤ 2% per increment. This pattern demonstrates that the

majority of lignin, predominantly surrounding cellulose, is efficiently solubilised at reduced NaOH concentrations; however, the remaining lignin integrated inside the cellulose polymer necessitates a gradual solubilisation of cellulose for its extraction [327]. Data from Figure 7.1 suggests that 19.60% to 11.55% of xylan persisted in the delignified biomass, presumably protected by cellulose. In general, lignin and hemicellulose exhibited greater solubility compared to cellulose. The results of Zhang et al. [328] showed that low NaOH concentrations are unable to infiltrate the tightly packed crystalline domains of cellulose (~10 Å intersheet distance, ~10 nm crystalline diameter). Incremental cellulose loss (20%) at NaOH concentrations of 10–30% contrasts with a mere 5% rise in lignin solubility, emphasising the trade-off. Optimal delignification (91%) with little cellulose loss (8%) was attained using 10% NaOH. Thus, the residual xylan and lignin post-delignification might be shielded by the cellulose polymer. Figure 7.1 indicates that an increase in NaOH concentration from 2% to 5% resulted in an 18% rise in cellulose loss, whereas lignin solubility improved by only 4%. Consequently, the experimental findings indicated that the highest lignin removal (92.35%) was attained with negligible cellulose loss (7.33%) at 2% NaOH. The PH-RPFR was delignified using a 2% NaOH treatment, which resulted in 79.34% lignin removal with a 10.72% loss of cellulose.

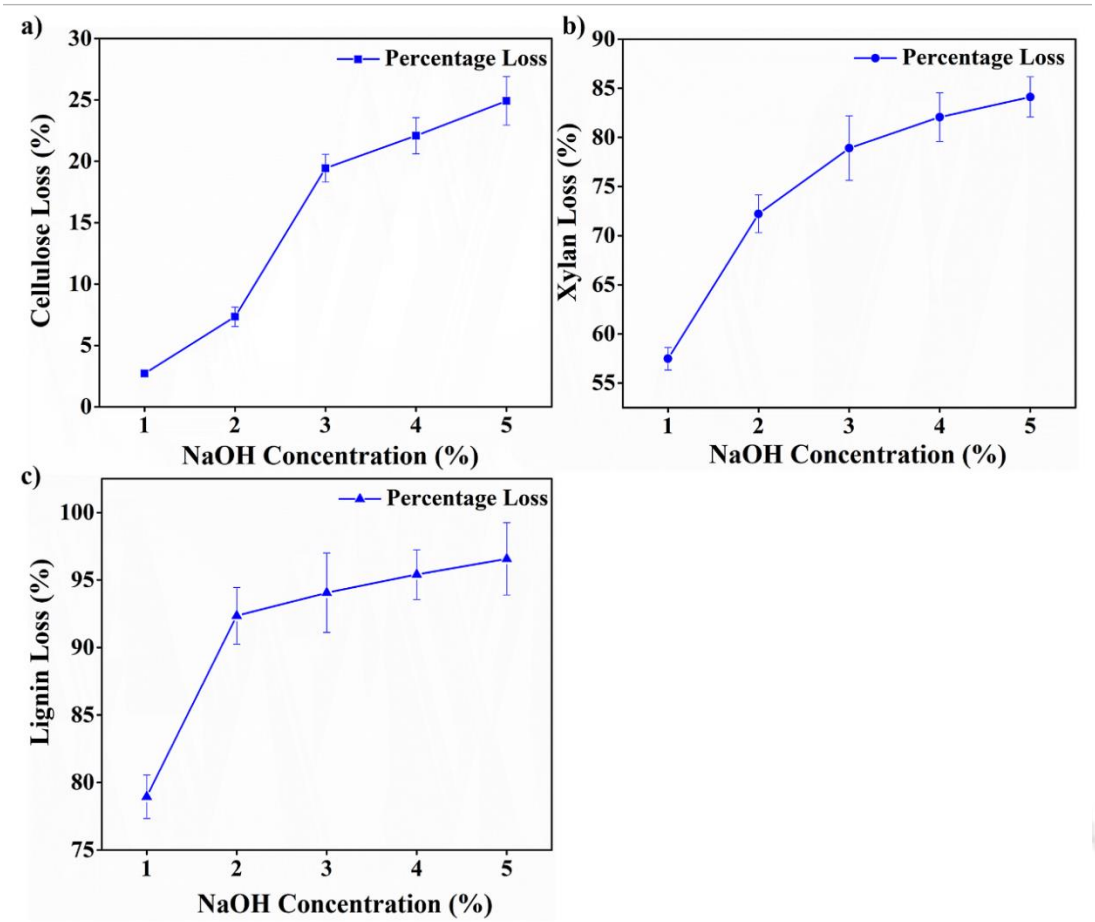

Figure 7.1. Percentage loss of (a) glucose, (b) hemicellulose, (c) lignin concentration during delignification of PUH-PFR process at varying NaOH concentration (1-5%). PUH-PFR: passion fruit rind residue obtained from post-ultrasound-assisted extraction and sulphuric acid treatment.

7.3. Characterisation of Delignified PFR residue

7.3.1. Morphology analysis of Delignified PFR residue using Field Emission Scanning Electron Microscopy (FESEM):

Morphological properties of untreated and delignified biomass were examined via FESEM to investigate structural alterations resulting from the delignification step. Figures 7.3 (a-d) represent the FESEM images of untreated and delignified raw and spent passion fruit rind biomass at 5000 magnification. Figures 7.2 (a, c) illustrate untreated RPFR and SPFR biomasses, exhibiting a smooth and compact surface structure characterised by tightly aggregated fibre bundles surrounded by lignin. However, Figures 7.2 (b, d) show that NaOH delignified biomasses and developed pores in the matrix due to biomass disintegration and fractionation; and efficient elimination of lignin and other contaminants [329,330]. By increasing the surface area, these morphological alterations promote saccharification and make it more accessible

for the cellulase enzyme to penetrate. Tharunkumar et al. [331] reported comparable results, noting structural alterations in 2% NaOH-treated paddy straw and sugarcane bagasse, which suggested lignin removal and cellulose liberation resulting from the interaction of NaOH with ester bonds in the biomass. Gao et al. [332] further showed that increasing alkali concentration enhances surface roughness in wheat straw, due to the removal of hemicellulose and lignin.

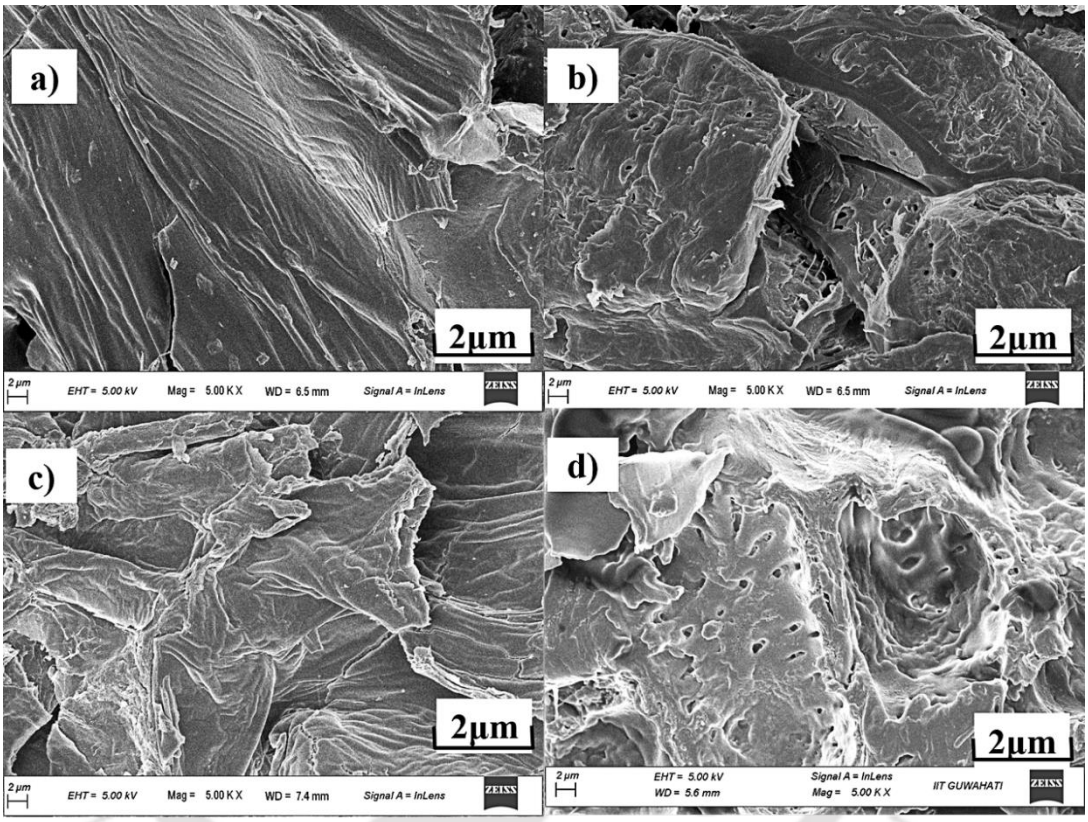

Figure 7.2. FESEM images of 1a) Untreated RPFR, 1b) NaOH-treated PH-RPFR, 2a) Untreated SPFR, 1b) NaOH-treated PUH-PFR. RPFR: raw passion fruit Rind, PH-RPFR: raw passion fruit Rind residue after H_2SO_4 hydrolysis, SPFR: spent passion fruit rind, PUH-PFR: post ultrasound-assisted extraction and sulphuric acid treatment.

7.3.2. Brunauer-Emmett-Teller analysis and elemental composition

The BET analysis revealed significant changes in the specific surface area and pore volume of both untreated (RPFR, SPFR) and treated (PH-RPFR, PUH-PFR) biomass (Table A11). The specific surface area for both PH-RPFR, PUH-PFR was increased ~5-fold compared to untreated biomasses. However, pore volume increased from 0.013-0.065 m^3/g for the NaOH-treated SPFR, indicating a significant improvement in surface area and pore volume post-treatment. A similar enhancement in pore volume was noted for RPFR and PH-RPFR samples, as shown in Table A11. The enhancement of surface area results from delignification and the extraction of the hemicellulosic component

from the raw material during NaOH treatment, thus enhancing enzymatic saccharification efficiency, as previously reported by Maibam and Goyal [333]. Additionally, CHNS elemental composition analysis indicated the following for SPFR: C: 45.2%, H: 5.9%, N: 1.2%, S: 0.2%, and O: 47.4%, whereas the CHNS composition for PUH-PFR exhibited C: 43.16%, H: 5.27%, and O: 54.77% (Table A11). A comparable trend was observed for RPFR and PH-RPFR samples, as displayed in Table A11. The absence of sulphur and nitrogen in the NaOH-treated biomass confirmed the elimination of protein content and lignin cross-linkages, as reported by Khaire et al. [334].

7.3.3. XRD analysis of Delignified PFR residue

X-ray diffraction (XRD) analysis was conducted to examine the crystalline structure of cellulose in NaOH-untreated and treated RPFR and SPFR biomass. The crystallinity of cellulose significantly influences its enzymatic hydrolysis, with crystalline parts exhibiting greater resistance to enzymatic degradation compared to amorphous regions. The crystallinity index (CI) for raw and treated biomass samples was determined using Equation 2.9, with intensity data collected between the 2θ ranges of 21.91°–22.04° and 15.91°–16.04° with Origin 9.0 software. The findings (Figure.7.3) revealed that the mild alkali treatment modifies the crystallinity of passion fruit rind, as indicated by an increase in CI from 64.33% (SPFR) to 72.80% (PUH-PFR) and from 61.91% (RPFR) to 76.14% (PH-RPFR). This increase correlates with the elimination of lignin and hemicellulose, possibly resulting from the positioning of cellulose along a specific axis. Comparable trends in CI increase have been described for other lignocellulosic biomass, including rice straw [335], bamboo [336], sugarcane tops [334], etc. The rise in CI post-delignification indicates a decrease in amorphous lignin and hemicellulose, and a corresponding enhancement in crystalline cellulose [337].

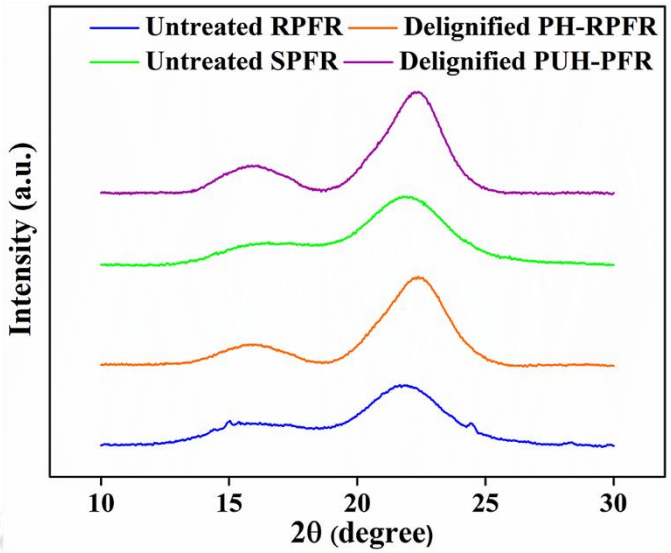

Figure 7.3. X-Ray Diffractogram of NaOH untreated and treated biomasses.

7.3.4. Functional group analysis of Delignified PFR residue

FTIR spectroscopy analysis was carried out on both untreated (RPFR, SPFR) and delignified (PH-RPFR, PUH-PFR) biomass, and the results are illustrated in Figure 7.4. The spectra of untreated biomass (RPFR, SPFR) exhibited distinct peaks at 1232-1238 cm^{-1} and 1710-1726 cm^{-1}, corresponding to the lignin and hemicellulose components, respectively. Comparable peaks at 1265 cm^{-1} and 1749 cm^{-1} for lignin and hemicellulose were reported in sugarcane bagasse biomass by Nath et al. [338]. However, the delignified biomass (PH-RPFR, PUH-PFR) displayed reduced intensities at these wavenumbers, signifying the effective elimination of lignin and hemicellulose subsequent to NaOH treatment of the passion fruit rind. The wavenumber range of 3350-2900 cm^{-1}, linked to C–H and/or O–H bond stretching vibrations, was detected in NaOH-treated biomass, supporting prior research [339]. The stretching vibration at 2865 cm^{-1}, associated with C–H bonds, indicates the total hydrocarbon content in both raw and treated passion fruit rind biomass [208]. The peak at 1320 cm^{-1} was detected in the PH-RPFR and PUH-PFR spectra, ascribed to CH_2 bond vibrations in cellulose, which was not present in the untreated biomass (RPFR, SPFR). A comparable observation was noted in alkali-treated sugarcane tops by Khaire et al. [334]. The peak at 1421 cm^{-1} in the untreated passion fruit rind, indicative of C = C bond stretching in lignin's phenolic ring, was reduced in the treated samples, confirming lignin elimination [340]. A prominent peak at 1028-1024 cm^{-1} in PH-RPFR and PUH-PFR was seen, associated with C-O vibrations, signifying enhanced cellulose exposure following

NaOH treatment relative to untreated biomass [334]. The band at 1633 cm^{-1}, linked to C = C and C = O conjugated carbonyl stretching in lignin aromatic subunit side chains [334], was reduced in the treated PFR, hence further correlated to lignin removal. The wavenumber range of 1315–1941 cm−1, indicative of lignin and related to the C–H bond of syringyl linkages among lignin, cellulose, and hemicellulose [341], demonstrated a pronounced decrease in peak intensity post-treatment, signifying the disruption of lignin's aromatic ring. The results indicate that NaOH treatment efficiently reveals the cellulosic fibres by eliminating lignin and hemicellulose.

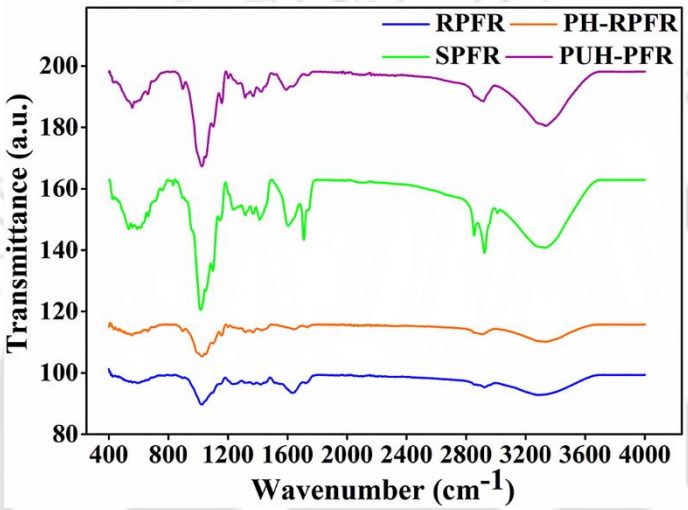

Figure 7.4. FTIR spectra of untreated and delignified passion fruit rinds. RPFR: raw passion fruit Rind, PH-RPFR: raw passion fruit Rind residue after H_2SO_4 hydrolysis, SPFR: spent passion fruit rind, PUH-PFR: post ultrasound-assisted extraction and sulphuric acid treatment.

7.3.5. TGA analysis of Delignified PFR residue

The primary structural components of lignocellulosic biomass, viz., cellulose, hemicellulose, and lignin, determine its thermal behaviour. The change in the thermal characteristics of NaOH-treated versus untreated biomasses emphasises the impact of NaOH treatment on biomass. Figure 7.5 illustrates the TGA analysis of untreated and delignified passion fruit rinds. The early phase (upto 150 °C) mass loss (~10%) depicted in Figure 7.5 corresponds to the evaporation of moisture, demonstrating comparable behaviour across all samples, indicating a uniform initial moisture content [342]. The second stage (200–400 °C) involves significant weight loss due to the decomposition of hemicellulose (200–300 °C) and cellulose (300–400 °C). Delignified biomass (PUH-PFR and PH-RPFR) exhibited a more prominent weight loss in this range, signifying increased cellulose content and reduced hemicellulose and lignin levels compared to

the untreated passion fruit rind. The thermal cellulose decomposition occurred due to decarboxylation, depolymerisation, and glycosidic bond degradation that led to char production [343]. Furthermore, the DTG peaks of cellulose degradation of NaOH-treated samples (Figure 7.5b) shift to higher temperatures relative to their unprocessed samples. The presence of hemicellulose, which degrades at lower temperatures and consequently decreases cellulose stability, might cause the reduced thermal stability of samples. The presence of hemicellulose impedes hydrolysis efficiency, restricting the removal of amorphous cellulose, which is more susceptible to destruction [343]. The final step (above 450 °C) signifies the gradual degradation of lignin across a broad temperature range due to its complex thermostable nature. Lignin degradation (150–360 °C) might take place due to carbohydrate contaminants, as observed in both untreated and processed biomass [344].

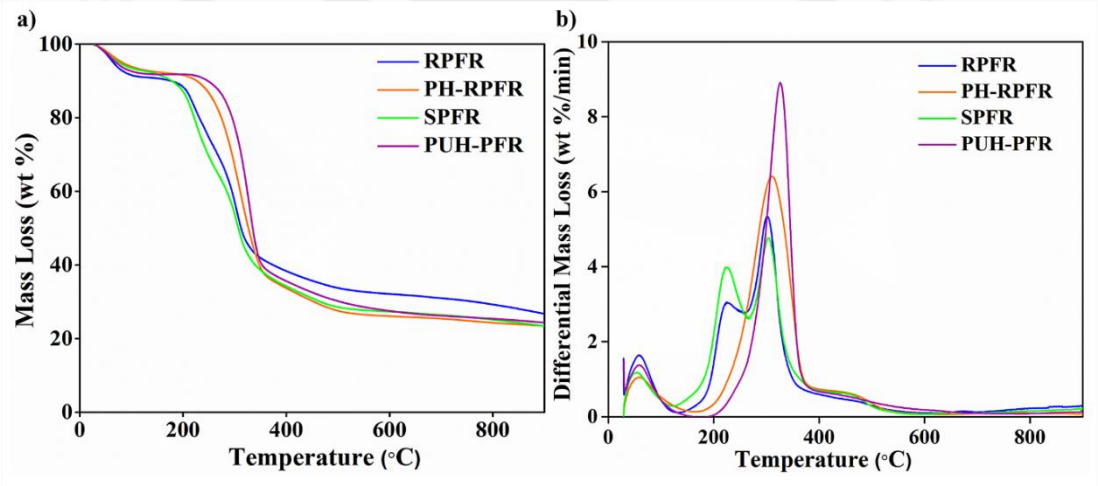

Figure 7.5. a) TGA and b) DTG Thermograms of NaOH-treated and untreated passion fruit rind samples. RPFR: raw passion fruit Rind, PH-RPFR: raw passion fruit rind residue after H_2SO_4 hydrolysis, SPFR: spent passion fruit rind, PUH-PFR: post ultrasound-assisted extraction and sulphuric acid treatment.

7.4. Enzymatic Hydrolysis

The efficiency of cellulose conversion on enzymatic saccharification determines the significance of delignification. The delignified substrate (PUH-PFR and PH-RPFR) obtained with 2% NaOH was used for the saccharification process, utilising 30 mg of cellulase protein per gram of cellulose (Figure A9). With 10% solid loading, the PUH-PFR exhibited 87.42% cellulose hydrolysis after 72 h. Conversely, the PH-RPFR exhibited a cellulose conversion rate of 79.61%, which was influenced by the presence of residual lignin (~8.59%) in the NaOH-treated substrate, which hinders cellulose

degradation. Furthermore, delignification and biomass crystallinity are two critical parameters affecting hydrolysis efficiency. Delignification of approximately 92.81% was achieved with 2% NaOH treatment in PUH-PFR, while the crystallinity index was 72.80%, in contrast to 76.14% for PH-RPFR (Figure 7.2). As a result, PUH-PFR demonstrated approximately a 15.31% enhancement in hydrolysis compared to PH-RPFR. Insufficient hydrolysis at 30 mg/g enzyme loading in PH-RPFR shows the requirement for increased enzyme concentrations to attain total cellulose conversion. A study conducted by NREL (NREL/TP-5100–61563) indicated a hydrolysis rate of 80–86.5% with enzyme loading of 19–33 mg/g. A prior investigation on sorghum stalks treated with 2% NaOH revealed a cellulose reduction of 13.5% and a hydrolysis efficiency of 99.4%. Although 1% NaOH-treated sorghum biomass led to reduced cellulose degradation, 35% of cellulose remained unconverted post-hydrolysis [205].

In the present investigation, 10% (w/v) substrate was used for enzymatic hydrolysis to avoid the development of a highly viscous slurry, which impedes mixing, enzyme distribution, and the effectiveness of cellulose hydrolysis due to mass transfer constraints. Additionally, increased solid loadings could lead to end-product inhibition due to high glucose and cellobiose concentrations. The enzymatic reaction, performed in an orbital shaker at 140 rpm, exhibited stable cellulose conversion efficiency. Reactors equipped with Rushton or helical impellers promote vigorous mixing for elevated solid concentrations (15–30% w/v), yet they frequently result in moderate cellulose conversion due to enzyme affinity for non-cellulosic constituents and end-product inhibition. Zhang et al. [328] reported a glucose yield of approximately ~77 g/L under these conditions. The current investigation found that the hydrolysate from 10% (w/v) PUH-PFR loading included 67.19 g/L glucose, 1.94 g/L cellobiose, and 0.94 g/L xylose (Figure A9), which were below the established inhibitory thresholds of 76 g/L glucose and 10 g/L cellobiose [345]. The PH-RPFR enzymatic hydrolysate contains 55.80 g/L glucose, 2.01 g/L cellobiose, and 1.07 g/L xylose (Figure A9).

7.5. Fermentation

Typically, lignocellulosic biomass comprises organic acids integrated within its polymers, including acetyl groups in hemicellulose and acids such as cinnamic acids, p-coumaric, vanillic, and ferulic in methoxylated lignin [346]. These acids can decrease the pH of the enzymatic hydrolysis medium (optimal at 4.8–5.5), thereby impacting

enzyme activity. To address this issue, hydrolysis is frequently performed using a 50 mM citrate buffer; however, this concentration suppresses glucose-fermenting bacteria, thus reducing ethanol output and productivity, rendering it commercially impractical at scale [347]. In this work, the spent biomass obtained after the extraction of a significant amount of such organic acids was utilised. Moreover, the dilute acid treatment and alkali delignification effectively eliminated substantial amounts of acetic acid and lignin, facilitating hydrolysis at a reduced citrate buffer concentration of 0.5 mM, which is 100 times lower than conventional techniques.

The enzymatic hydrolysate was fermented with *Saccharomyces cerevisiae* NCIM 3090, and the ethanol production and fermentation efficiency were measured (Table 7.2). The PUH-PFR hydrolysate demonstrated enhanced performance relative to PH-RPFR, attaining an ethanol yield of 0.45 ± 0.02 g/g and a conversion efficiency of 87.88%. The peak ethanol generation from PUH-PFR was seen at 18 h, yielding a reduced productivity of 1.67 ± 0.01 g/L/h. Conversely, PH-RPFR hydrolysate attained peak ethanol production in 18 hours, exhibiting a reduced productivity of 1 g/L/h. The findings highlight the essential importance of hydrolysate quality in influencing fermentation efficacy. PUH-PFR hydrolysate exhibited a higher fermentable sugar concentration, resulting in enhanced ethanol output, productivity, and efficiency compared to the PH-RPFR. The results highlight the necessity of enhancing the NaOH concentration in the delignification process and the enzyme concentration during saccharification to achieve maximal sugar yield in PH-RPFR. The findings indicate that non-food waste materials may be a feasible substitute for edible feedstocks in bioethanol production.

Table 7.2. A comparison of Ethanol yield and productivity of different biomasses fermented with *Saccharomyces cerevisiae*

Feed stock	Sugars	Ethanol	EY	EP	Time	Reference
PUH-PFR	67.19 ± 1.14	30.12 ± 2.74	0.45 ± 0.01	0.63 ± 0.01	48	This study
PH-RPFR	55.80 ± 1.39	22.80 ± 3.61	0.41± 0.01	0.47± 0.01	48	This study
Oil palm sap	80	40.14	0.50	1.67	24	[348]
Spent mushroom substrate	19.56	6.28	0.32	0.13	48	[349]
Sorghum stalks	162.90	74.70	0.46	2.50	30	[205]
Spent mushroom substrate	4.10	1.57	0.38	0.07	24	[350]
Spent tea waste	28.90	12.72	0.44	0.64	20	[351]

Sugars and ethanol were expressed as g/L.
EY: Ethanol yield was expressed as g_p/ g_s.
EP: Ethanol productivity, was expressed as g/ L/h.
Time was expressed as h.
PUH-PFR: post ultrasound-assisted extraction and sulphuric acid treatment, PH-RPFR: raw passion fruit rind residue after H_2SO_4 hydrolysis.

7.6. Mass balance analysis

The mass balance analysis of bioethanol production from 100 g of spent passion fruit rind (SPFR) was systematically conducted by a sequential bioconversion process comprising dilute acid pretreatment, detoxification, alkali delignification, enzymatic saccharification, and fermentation (Figure 7.6). Initially, acid pretreatment at optimised conditions yielded 26.89 g/L of xylose and 8.14 g/L of glucose in the hydrolysate (discussed in chapter 6). Following detoxification with calcium hydroxide, the hydrolysate contained 23.08 g/L of xylose and 7.54 g/L of glucose, indicating sugar loss due to breakdown or precipitation. The detoxified hydrolysate was fermented using *Pichia stipitis*, producing 12.06 g of ethanol per 100 g of SPFR, which corresponds to 152.82 L per tonne. The solid residue (33.19 g) from acid pretreatment comprised 13.42 g of cellulose, 8.76 g of hemicellulose, and 9.42 g of lignin. After NaOH-based alkali delignification, the lignin content decreased to 0.72 g, whereas 12.43 g of cellulose remained intact. The enzymatic saccharification of the cellulose-rich fraction with Celluclast 1.5L® yielded a hydrolysate containing 67.19 g/L glucose, which was further fermented with *Saccharomyces cerevisiae*, producing 4.74 g of ethanol per 100 g of SPFR, equivalent to around 6.00 L/tonne of SPFR. This approach of both fermentation streams resulted in a total ethanol yield of 158.82 litres per tonne of SPFR, i.e., 1 kg of bioethanol could be obtained from 5.95 kg of SPFR. This detailed mass balance highlights the successful valorisation of SPFR using integrated pretreatment and bioconversion methods, resulting in substantial ethanol recovery and promoting a zero-waste biorefinery strategy.

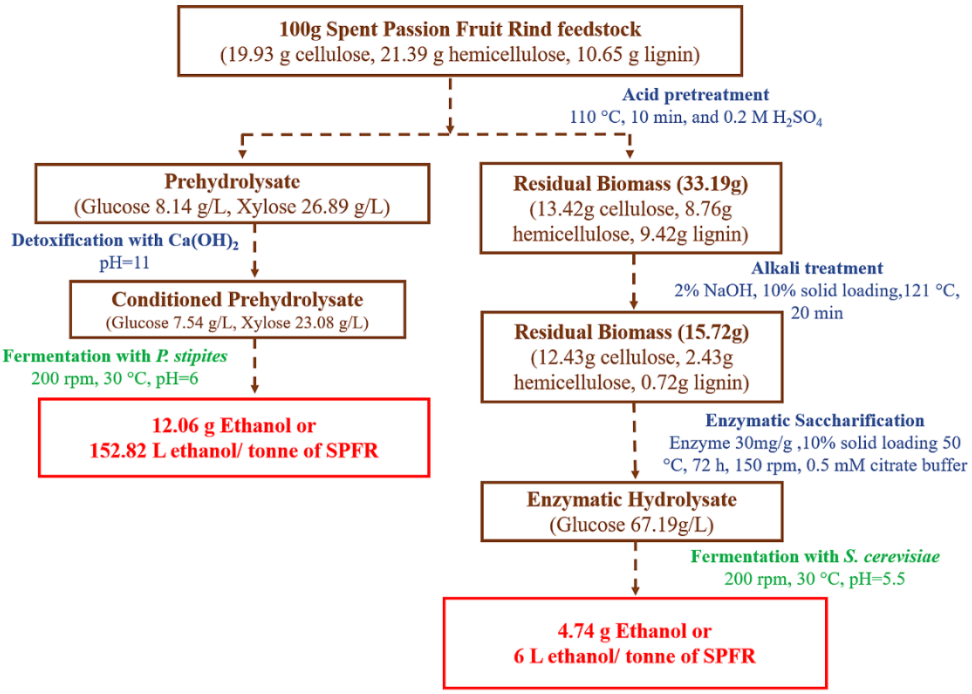

Figure 7.6. Mass balance analysis of bioethanol production from SPFR. SPFR: spent passion fruit rind

7.7. Conclusions

This study revealed the potential of spent biomass obtained after bioactive compound extraction for bioethanol production. The concentration of sodium hydroxide (NaOH) was determined to be the most significant factor affecting the solubilisation of lignin and hemicellulose, while maintaining cellulose integrity during the treatment. A 2% NaOH treatment resulted in the maximum lignin removal (92.35%) from PUH-PFR biomass, accompanied by negligible cellulose loss (7.33%). The NaOH-treated PUH-PFR developed pores in the matrix with a specific surface area increased by ~5-fold compared to raw biomass, showing the elimination of lignin and other contaminants. The increased crystallinity index (72.80%) correlates with the lignin and hemicellulose removal during delignification. The removal of hemicellulose could be evidenced by the thermogravimetric curve, as the thermogram shifted towards higher temperatures. Further, the enzymatic saccharification of delignified PUH-PFR biomass produced 67.19 ± 1.14 g/L of glucose, which yielded bioethanol of 30.12 ± 2.74 g/L by fermentation with *S. cerevisiae*. The mass balance analysis revealed that the separate fermentation of the hemicellulosic and cellulosic fractions of SPFR exhibited considerable potential for bioethanol production, resulting in a total yield of around 158.82 litres per tonne of dry biomass. The findings demonstrate the potential of SPFR

for large-scale bioethanol production. Further study might focus on techno-economic feasibility, valorisation of lignin byproducts, and co-fermentation of C5-C6 to improve yields, thereby promoting sustainable commercialisation within a circular bioeconomy approach.

8. CHAPTER 8

Overall conclusions and future scope

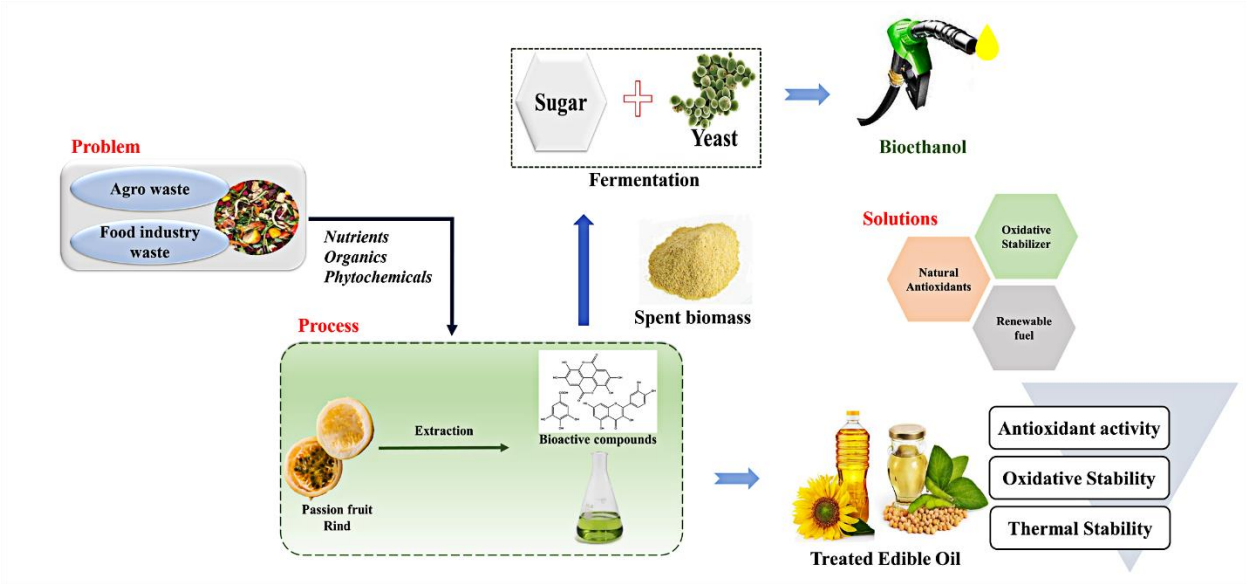

CHAPTER 8

Overall conclusions and future scope

This study focuses on valorising organic biowaste, passion fruit rind collected from Assam, India, to achieve zero-waste production. Bioactive substances were isolated and exploited as natural antioxidants to enhance the stability of edible oils (sunflower and soybean oil). The residual biomass was subsequently employed for bioethanol production via fermentation. The significant findings of this research are presented below, based on the thorough studies conducted:

8.1. Conclusions

- This study successfully revealed the valorisation of yellow passion fruit rind (YPFR), an agro-industrial byproduct, by optimising two eco-friendly extraction methods: ultrasound extraction (UE) and supercritical fluid extraction (SFE), to recover bioactive compounds rich in phenols and flavonoids. The effect of critical process factors on the extraction efficiency of phenolics and flavonoids was statistically assessed. The UE was optimised by response surface methodology (RSM), considering variables such as temperature, ethanol-water ratio, extraction duration, and solid-to-solvent ratio. The ANOVA findings indicated that all variables significantly influenced extraction performance. Under optimal conditions (54.44 °C, 64.95% ethanol, 24.69 mL/g feed ratio, and 29.52 min duration) in the UE, 42.15 mg GAE/g of total phenolics and 34.80 mg QE/g of flavonoids were achieved, yielding a high desirability value of 0.96. Supercritical CO_2 with 10% ethanol as a co-solvent (SC-ET) was employed for SFE, and parameters such as temperature, pressure, and solvent flow rate were optimised. Flow rate proved to be the predominant component, followed by pressure and temperature. The optimised SFE procedure (278.48 bar, 53.84 °C, 18.3 g/min) produced 36.87 mg GAE/g and 45.75 mg QE/g, respectively, achieving a desirability index of 0.984. The results validate the effectiveness and sustainability of both UE and SFE in extracting antioxidant-rich phytochemicals from passion fruit rind, thus supporting

circular bioeconomy objectives through the creation of value-added products for food, nutraceutical, and cosmetic uses.

- The current study investigated the feasibility of employing passion fruit rind, an agro-industrial byproduct, as a source of natural value-added compounds via two green extraction methods: supercritical fluid extraction (SFE) and ultrasound-assisted extraction (UAE). Due to the mechanical impacts of ultrasonic waves and the breakdown of cell walls, ultrasonic-assisted extraction (UAE) attained a much higher extraction efficiency of 51.39% in contrast to supercritical fluid extraction (SFE), which yielded 2.67%. Despite SFE producing a reduced total extract yield, it exhibited significant selectivity, efficiently isolating particular flavonoids and carotenoids confirmed by HPLC findings. The increased antioxidant activity reported in UAE extracts was attributed to their increased total phenolic content, particularly abundant in gallic acid, ferulic acid, and p-coumaric acid. In contrast, SFE extracts exhibited higher amounts of carotenoids and flavonoids, including isovitexin, isoorientin, kaempferol, and quercetin; compounds recognised for their potent antioxidant and anti-inflammatory effects. Both extracts demonstrated significant antibacterial activity against gram-positive and gram-negative bacteria, with MIC and ZOI assays validating their inhibitory effects at low doses. Although SFE extracts demonstrated restricted activity against *Staphylococcus aureus*, UAE extracts exhibited broad-spectrum antibacterial efficacy, likely attributable to their enhanced phenolic content and related bioactivity. This study fills a significant research gap by analysing bioactive compounds from passion fruit rind in India, thereby promoting sustainable waste valorisation and resource efficiency. Nonetheless, challenges associated with scalability, economic viability, and environmental consequences persist. Future initiatives could prioritise process improvement, chemical characterisation, and thorough life-cycle assessments to improve the sustainability and industrial profitability of these extraction techniques.
- The oxidative stability of edible oils, frequently compromised by their increased levels of unsaturated fatty acids, results in rancidity and nutritional deterioration. In this context, natural bioactive substances have emerged as safer substitutes for synthetic antioxidants in improving oil stability. This work extracted bioactive compounds from yellow passion fruit rind (YPFR) utilising

sunflower oil (SFO) and soybean oil (SBO) as solvents, which were directly integrated into the oils to enhance their stability. Ultrasound-assisted extraction (UAE) markedly enhanced both oils with carotenoids, phenolics, and flavonoids, leading to a statistically significant increase ($p < 0.05$) in antioxidant activity relative to untreated oils. Structural studies verified that the addition of YPFR extracts did not alter the intrinsic molecular structure of the oils. The extract-enriched oils demonstrated improved oxidative and thermal stability. At 140 °C, the induction durations of SFO and SBO were increased by 46.44% and 29.53%, respectively. The results of differential scanning calorimetry (DSC) indicated a shift in exothermic peaks to lower temperatures, signifying enhanced low-temperature oxidative resistance in the oil with extracts. Notwithstanding the enrichment with YPFR extracts, SFO samples exhibited lower onset temperatures (t_{ON}) compared to SBO, indicating that SBO is more susceptible to oxidation, perhaps attributable to its reduced saturated fatty acid concentration. Thermogravimetric analysis (TGA) indicated a single mass loss phase, associated with the thermal degradation of both saturated and unsaturated fatty acids within the temperature range of 300 to 600 °C. Nevertheless, the incorporation of YPFR extracts enhanced the thermal stability of both oils, with SBOE (SBO+Extract) and SFOE (SFO+Extract) demonstrating increased t_{ON} values (383.90 °C and 374.61 °C, respectively) in contrast to their untreated equivalents (366.79 °C for SBO and 362.14 °C for SFO) and those subjected to synthetic antioxidants. This method emphasises the potential of valorising agro-industrial waste by developing oils enhanced with natural antioxidants, thereby contributing to a circular economy. Subsequent investigations should explore the scalability of this extraction technique and the in vitro health advantages of the enriched oils.

- This work emphasises the viability of spent passion fruit rind (SPFR), the residual biomass after bioactive component extraction, as a feasible feedstock for bioethanol production. The compositional study of SPFR indicated a significant residual carbohydrate content, consisting of approximately 21% hemicellulose and 19% cellulose. However, efficient hemicellulose extraction is challenging due to the formation of inhibitors like furfural and hydroxymethylfurfural (HMF), which impede fermentation. At response surface methodology (RSM) optimised acid pretreatment conditions, a

substantial xylose yield of 122.02 mg/g was achieved, accompanied by a relatively low furfural concentration of 2.11 mg/g. Acid hydrolysis effectively depolymerised xylan; nevertheless, it concurrently generated other inhibitory compounds, including furans, organic acids, and phenolic acids. The detoxification with calcium hydroxide (to pH 11), the concentrations of phenolic acid and furfural were significantly ($p < 0.05$) reduced by 22% and 17.39%, respectively. In addition, this treatment reduces 15.42% xylose content. The fermentation of the detoxified hydrolysate with *Pichia stipites* yielded 9.65 g/L of ethanol. Although a 13% reduction in sugar during detoxification, fermentation efficiency increased from 77.91% in untreated hydrolysate to 81.97% in detoxified SPFR hydrolysate. The results demonstrate that SPFR is a suitable lignocellulosic substrate for bioethanol production and highlight its potential integration into biorefinery systems, thus promoting sustainable bioenergy technology.

- This study proposes a zero-waste approach by simultaneously utilising spent passion fruit rind (SPFR) for the extraction of bioactive compounds and the production of bioethanol. The residual SPFR biomass (331.04 g) acquired after acid pretreatment (PUH-PFR) comprised 40.53% (w/w) cellulose and 28.46% (w/w) lignin. Efficient delignification was essential to improve the enzymatic accessibility of cellulose. The alkaline pretreatment using sodium hydroxide (NaOH) markedly enhanced ethanol yields, highlighting its efficacy in delignification of lignocellulosic biomasses. The concentration of sodium hydroxide (NaOH) was the primary parameter affecting the removal of lignin and hemicellulose while maintaining the integrity of cellulose structure. The optimum condition among those examined was 2% NaOH treatment, which resulted in 92.35% lignin removal with merely 7.33% cellulose loss in PUH-PFR biomass. The X-ray diffraction study demonstrated that moderate alkali treatment increased the crystallinity index of the biomass from 64.33% (SPFR) to 72.80% (PUH-PFR), signifying more cellulose exposure resulting from the elimination of amorphous constituents such as lignin and hemicellulose. Morphological study and Brunauer-Emmett-Teller (BET) surface area analyses validated pore formation and enhanced surface area in delignified biomass, corroborating efficient lignin removal. Additionally, thermogravimetric analysis and derivative thermogravimetry (DTG) confirmed improved thermal stability

and increased cellulose content in alkali-treated samples, as seen by the DTG peaks shifting to higher temperatures due to reduced hemicellulose and lignin components. Following enzymatic saccharification with commercial cellulase, 67.19 g/L of glucose was obtained from delignified PUH-PFR, which was subsequently fermented by *Saccharomyces cerevisiae* to produce bioethanol at a yield of 0.45 g/g, resulting in a fermentation efficiency of 87.88%. Mass balance research revealed the capacity to produce roughly 158.82 L of bioethanol per tonne of SPFR biomass. This integrated approach highlights the viability of SPFR as a sustainable feedstock for bioethanol production and industrial scalability, subject to a comprehensive techno-economic assessment. Moreover, the lignin-rich black liquor generated during delignification possesses potential for the creation of supplementary value-added goods, thereby improving economic feasibility and environmental sustainability.

8.2. Future Scope

The findings of this study offer important insights into the efficacy of ultrasound-assisted extraction and supercritical fluid extraction for isolating bioactive molecules with notable antioxidative characteristics. These chemicals enhance the shelf life of edible oils and promote bioethanol synthesis from passion fruit rind. To enhance the industrial viability of this research, the subsequent studies are recommended:

- Analysis of the flavour and sensory attributes of edible oils infused with passion fruit extract.
- In-vitro cytotoxicity analysis of extract-enriched oils to assess their safety for ingestion.
- Lignin-rich by-product (black liquor) produced during the delignification process can be utilised for the formation of supplementary value-added goods.
- Co-fermentation of both pentose and hexose sugars is possible to enhance ethanol yield.
- Scalability potential and a techno-economic analysis to assess its industrial feasibility.

References

[1] M.S. Wagh, S. S, P.C. Nath, A. Chakraborty, R. Amrit, B. Mishra, A.K. Mishra, Y.K. Mohanta, Valorisation of agro-industrial wastes: Circular bioeconomy and biorefinery process – A sustainable symphony, Process Saf. Environ. Prot. 183 (2024) 708–725. https://doi.org/10.1016/j.psep.2024.01.055.

[2] W.J. Martinez-Burgos, E. Bittencourt Sydney, A. Bianchi Pedroni Medeiros, A.I. Magalhaes, J.C. de Carvalho, S.G. Karp, L. Porto de Souza Vandenberghe, L.A. Junior Letti, V. Thomaz Soccol, G.V. de Melo Pereira, C. Rodrigues, A. Lorenci Woiciechowski, C.R. Soccol, Agro-industrial wastewater in a circular economy: Characteristics, impacts and applications for bioenergy and biochemicals, Bioresour. Technol. 341 (2021) 125795. https://doi.org/10.1016/j.biortech.2021.125795.

[3] R. Sharma, Agro-industrial waste to energy - Sustainable management, Sustain. Mater. Technol. 41 (2024) e01117. https://doi.org/10.1016/j.susmat.2024.e01117.

[4] P.R. Yaashikaa, P. Senthil Kumar, S. Varjani, Valorization of agro-industrial wastes for biorefinery process and circular bioeconomy: A critical review, Bioresour. Technol. 343 (2022) 126126. https://doi.org/10.1016/j.biortech.2021.126126.

[5] G. Weyya, A. Belay, E. Tadesse, Passion fruit (Passiflora edulis Sims) by-products as a source of bioactive compounds for non-communicable disease prevention: extraction methods and mechanisms of action: a systematic review, Front. Nutr. 11 (2024) 1340511. https://doi.org/10.3389/fnut.2024.1340511.

[6] S. Ramaiya, J. Bujang, M. Zakaria, N. Shahbani, Floral Behaviour, Flowering Phenology and Fruit Production of Passion Fruit (Passiflora Species) in East Malaysia, J. Agric. Food Dev. 6 (2019) 1–9. https://doi.org/10.30635/2415-0142.2020.06.01.

[7] H. Chutia, M. Sharma, M.J. Das, C.L. Mahanta, Properties of Dietary Fibre From Passion Fruit Seed Obtained Through Individual and Combined Alkaline and Ultrasonication Extraction Techniques, Waste and Biomass Valorization 15 (2024) 2345–2359. https://doi.org/10.1007/s12649-023-02288-0.

[8] H.A.R. Suleria, C.J. Barrow, F.R. Dunshea, Screening and characterization of phenolic compounds and their antioxidant capacity in different fruit peels, Foods 9 (2020) 1206. https://doi.org/10.3390/foods9091206.

[9] K. Krambeck, V. Silva, R. Silva, C. Fernandes, F. Cagide, F. Borges, D. Santos, F. Otero-Espinar, J.M.S. Lobo, M.H. Amaral, Design and characterization of Nanostructured lipid carriers (NLC) and Nanostructured lipid carrier-based hydrogels containing Passiflora edulis seeds oil, Int. J. Pharm. 600 (2021) 120444. https://doi.org/10.1016/j.ijpharm.2021.120444.

[10] C. Guzman, M.A. Rojas, M. Aragon, Optimization of ultrasound-assisted emulsification of emollient nanoemulsions of seed oil of passiflora edulis var. Edulis, Cosmetics 8 (2021) 1–22. https://doi.org/10.3390/COSMETICS8010001.

[11] E.T. Stafne, T. Blare, B. Posadas, L. Downey, J. Anderson, J. Crane, R. Gazis, B. Faber, D.G. Stockton, D. Carrillo, J.P. Morales-Payan, M. Dutt, A. Chambers, D. Chavez, Survey of US Passionfruit Growers' Production Practices and Support Needs, Horttechnology 33 (2023) 357–366. https://doi.org/10.21273/HORTTECH05240-23.

[12] B.I. Martinez-Mendoza, A. Peredo-Lovillo, H.E. Romero-Luna, M. Jimenez-Fernandez, Antioxidant and anti-inflammatory properties of yeasts fermented passion fruit and soursop pulps: A focus on bioactive volatile compounds profile, Food Biosci. 56 (2023) 103112. https://doi.org/10.1016/j.fbio.2023.103112.

[13] R.S. Soumya, K.B. Raj, A. Abraham, Passiflora edulis (var. Flavicarpa) Juice Supplementation Mitigates Isoproterenol-induced Myocardial Infarction in Rats, Plant Foods Hum. Nutr. 76 (2021) 189–195. https://doi.org/10.1007/s11130-021-00891-x.

[14] X. Ye, C. Wang, T.B. Ng, W. Zhang, Study on the biocontrol potential of antifungal peptides produced by bacillus velezensis against fusarium solani that infects the passion fruit passiflora edulis, J. Agric. Food Chem. 69 (2021) 2051–2061. https://doi.org/10.1021/acs.jafc.0c06106.

[15] R.P. Lee, B. Meyer, Q. Huang, R. Voss, Sustainable waste management for zero waste cities in China: Potential, challenges and opportunities, Clean Energy 4 (2020) 169–201. https://doi.org/10.1093/ce/zkaa013.

[16] T. Barbosa Santos, F.P. de Araujo, A.F. Neto, S.T. de Freitas, J. de Souza Araujo, S.B. de Oliveira Vilar, A.J. Brito Araujo, M.S. Lima, Phytochemical Compounds and Antioxidant Activity of the Pulp of Two Brazilian Passion Fruit Species: Passiflora Cincinnata Mast. And Passiflora Edulis Sims, Int. J. Fruit Sci. 21 (2021) 255–269. https://doi.org/10.1080/15538362.2021.1872050.

[17] N.R. Castillo, D. Ambachew, L.M. Melgarejo, M.W. Blair, Morphological and agronomic variability among cultivars, landraces, and genebank accessions of purple passion fruit, passiflora edulis f. edulis, HortScience 55 (2020) 768–777. https://doi.org/10.21273/HORTSCI14553-19.

[18] G. Fischer, H.E. Balaguera-Lopez, S. Magnitskiy, Review on the ecophysiology of important Andean fruits: Solanaceae, Rev. U.D.C.A Actual. Divulg. Cient. 24 (2021) 9471–9481. https://doi.org/10.31910/rudca.v24.n1.2021.1701.

[19] N.C. Rodriguez, L.M. Melgarejo, M.W. Blair, Purple Passion Fruit, Passiflora edulis Sims f. Edulis, Variability for Photosynthetic and Physiological Adaptation in Contrasting Environments, Agronomy 9 (2019) 231. https://doi.org/10.3390/agronomy9050231.

[20] G. Sharma, Systematics of Fruit Crops (Fully Illustrated), New India Publishing, 2009. https://doi.org/10.59317/9789389571639.

[21] R. Tripathi, Prakash; Karunakaran, G; Sakthivel, T; Sankar, V; Senthilkumar, Passion fruit cultivation in India, Purple Passion Fruit (2013).

[22] G. Mandal, R. Thokchom, Production Preference and Importance of Passion Fruit (Passiflora Edulis): A Review, J. Agric. Eng. Food Technol. 4 (2020) 27–30. http://www.krishisanskriti.org/Publication.html.

[23] T.T. Jamir, H.K. Sharma, A.K. Dolui, Folklore medicinal plants of Nagaland, India, Fitoterapia 70 (1999) 395–401. https://doi.org/10.1016/S0367-326X(99)00063-5.

[24] K. Dhawan, A. Sharma, Antitussive activity of the methanol extract of Passiflora incarnata leaves, Fitoterapia 73 (2002) 397–399. https://doi.org/10.1016/S0367-326X(02)00116-8.

[25] K. Dhawan, S. Kumar, A. Sharma, Anxiolytic activity of aerial and underground parts of Passiflora incarnata, Fitoterapia 72 (2001) 922–926. https://doi.org/10.1016/S0367-326X(01)00322-7.

[26] K. Dhawan, S. Kumar, A. Sharma, Aphrodisiac activity of methanol extract of leaves of Passiflora incarnata Linn. in mice, Phyther. Res. 17 (2003) 401–403. https://doi.org/10.1002/ptr.1124.

[27] K. Dhawan, S. Kumar, A. Sharma, Comparative biological activity study on Passiflora incarnata and P. edulis, Fitoterapia 72 (2001) 698–702. https://doi.org/10.1016/S0367-326X(01)00306-9.

[28] K. Dhawan, S. Kumar, A. Sharma, Antiasthmatic activity of the methanol extract of leaves of Passifiora incarnata, Phyther. Res. 17 (2003) 821–822. https://doi.org/10.1002/ptr.1151.

[29] K. Dhawan, S. Dhawan, S. Chhabra, Attenuation of benzodiazepine dependence in mice by a tri-substituted benzoflavone moiety of Passiflora incarnata Linneaus: A non-habit

forming anxiolytic, J. Pharm. Pharm. Sci. 6 (2003) 215–222.

[30] K.R. Singh, C. Basudha, A. Ningonbam, T.B. Singh, P. Punitha, I.M. Singh, N. Prakash, Overview of Production and Processing of High Value Crops of NEH Region with Reference to Entrepreneurship Development, Train. Man. Entrep. Ski. Dev. Mark. Driven Prod. Process. High Value Crop. NEH Reg. (2017) 1.

[31] J.L. Santos-Jimenez, C. de Barros Montebianco, A.H. Vidal, S. G. Ribeiro, E. Barreto-Bergter, M.F.S. Vaslin, A fungal glycoprotein mitigates passion fruit woodiness disease caused by Cowpea aphid-borne mosaic virus (CABMV) in Passiflora edulis, BioControl 67 (2022) 75–87. https://doi.org/10.1007/s10526-021-10114-6.

[32] A.D.M. Bezerra, A.J.S. Pacheco Filho, I.G.A. Bomfim, G. Smagghe, B.M. Freitas, Data relating to threats to passion fruit production in the Neotropics due to agricultural area loss and pollinator mismatch as consequence of climate changes, Data Br. 23 (2019) 49–57. https://doi.org/10.1016/j.dib.2019.103802.

[33] C.Y. Cheok, N. Mohd Adzahan, R. Abdul Rahman, N.H. Zainal Abedin, N. Hussain, R. Sulaiman, G.H. Chong, Current trends of tropical fruit waste utilization, Crit. Rev. Food Sci. Nutr. 58 (2018) 335–361. https://doi.org/10.1080/10408398.2016.1176009.

[34] A.M.A. Fonseca, M. V. Geraldi, M.R.M. Junior, A.J.D. Silvestre, S.M. Rocha, Purple passion fruit (Passiflora edulis f. edulis): A comprehensive review on the nutritional value, phytochemical profile and associated health effects, Food Res. Int. 160 (2022) 111665. https://doi.org/10.1016/j.foodres.2022.111665.

[35] A.M.A. Fonseca, M. V. Geraldi, M.R.M. Junior, A.J.D. Silvestre, S.M. Rocha, Purple passion fruit (Passiflora edulis f. edulis): A comprehensive review on the nutritional value, phytochemical profile and associated health effects, Food Res. Int. 160 (2022) 111665. https://doi.org/10.1016/j.foodres.2022.111665.

[36] J. Zhang, S. Tao, G. Hou, F. Zhao, Q. Meng, S. Tan, Phytochemistry, nutritional composition, health benefits and future prospects of Passiflora: A review, Food Chem. 428 (2023) 136825. https://doi.org/10.1016/j.foodchem.2023.136825.

[37] B.H. Belmonte-Herrera, J.A. Domínguez-Avila, A. Wall-Medrano, J.F. Ayala-Zavala, A.M. Preciado-Saldaña, N.J. Salazar-López, L.X. López-Martínez, E.M. Yahia, R.M. Robles-Sánchez, G.A. González-Aguilar, Lesser-Consumed Tropical Fruits and Their by-Products: Phytochemical Content and Their Antioxidant and Anti-Inflammatory Potential, Nutrients 14 (2022) 3663. https://doi.org/10.3390/nu14173663.

[38] S.D. Ramaiya, J.B. Bujang, M.H. Zakaria, N. Saupi, Nutritional, mineral and organic acid composition of passion fruit (Passiflora species), Food Res. 3 (2018) 231–240. https://doi.org/10.26656/fr.2017.3(3).233.

[39] Y. Song, X.-Q. Wei, M.-Y. Li, X.-W. Duan, Y.-M. Sun, R.-L. Yang, X.-D. Su, R.-M. Huang, H. Wang, Nutritional Composition and Antioxidant Properties of the Fruits of a Chinese Wild Passiflora foetida, Molecules 23 (2018) 459. https://doi.org/10.3390/molecules23020459.

[40] S. Liu, F. Yang, J. Li, C. Zhang, H. Ji, P. Hong, Physical and chemical analysis of Passiflora seeds and seed oil from China, Int. J. Food Sci. Nutr. 59 (2008) 706–715. https://doi.org/10.1080/09637480801931128.

[41] Y. Song, X.Q. Wei, M.Y. Li, X.W. Duan, Y.M. Sun, R.L. Yang, X.D. Su, R.M. Huang, H. Wang, Nutritional composition and antioxidant properties of the fruits of a Chinese wild passiflora foetida, Molecules 23 (2018) 459. https://doi.org/10.3390/molecules23020459.

[42] Y. Hu, Q. Lin, H. Zhao, X. Li, S. Sang, D.J. McClements, J. Long, Z. Jin, J. Wang, C. Qiu, Bioaccessibility and bioavailability of phytochemicals: Influencing factors, improvements, and evaluations, Food Hydrocoll. 135 (2023) 108165. https://doi.org/10.1016/j.foodhyd.2022.108165.

[43] W. Sukketsiri, S. Daodee, S. Parhira, W. Malakul, S. Tunsophon, N. Sutthiwong, S. Tanasawet, P. Chonpathompikunlert, Chemical characterization of Passiflora edulis extracts and their in vitro antioxidant, anti-inflammatory, anti-lipid activities, and ex-vivo vasodilation effect, J. King Saud Univ. - Sci. 35 (2023) 102431. https://doi.org/10.1016/j.jksus.2022.102431.

[44] G.J. dos Santos, R.O. Defendi, E. Dusman, M.T. Biffi, G.H. Berton, A.P.P. Tonin, E.C. Meurer, R.M. Suzuki, C.C. Sipoli, L.T.D. Tonin, Valorization of Wastes from the Juice Passion Fruit Production Industry: Extraction of Bioactive Compounds from Seeds, Antioxidant, Photoprotective and Antiproliferative Activities, Waste and Biomass Valorization 14 (2023) 1233–1250. https://doi.org/10.1007/s12649-022-01937-0.

[45] G. de Souza Silva, G. da Silva Campelo Borges, C.D. Pinho da Costa Castro, S. de Tarso Aidar, A. Telles Biasoto Marques, S. Tonetto de Freitas, A.C. Poloni Rybka, H.R. Cardarelli, Physicochemical quality, bioactive compounds and in vitro antioxidant activity of a new variety of passion fruit cv. BRS Sertão Forte (Passiflora cincinnata Mast.) from Brazilian Semiarid region, Sci. Hortic. (Amsterdam). 272 (2020) 109595. https://doi.org/10.1016/j.scienta.2020.109595.

[46] L.C. Dos Santos, J.A. Mendiola, A.D.P. Sanchez-camargo, G. Alvarez-rivera, J. Vigano, A. Cifuentes, E. Ibanez, J. Martinez, Selective extraction of piceatannol from passiflora edulis by-products: Application of hsps strategy and inhibition of neurodegenerative enzymes, Int. J. Mol. Sci. 22 (2021) 6248. https://doi.org/10.3390/ijms22126248.

[47] C.C. Reis, A.M.G.N. Mamede, A. Soares, S.P. Freitas, Production of lipids and natural antioxidants from passion fruit seeds, Grasas y Aceites 71 (2020) 385. https://doi.org/10.3989/gya.0803192.

[48] Y. Song, P. Wen, H. Hao, M. Zhu, Y. Sun, Y. Zou, T. Requena, R. Huang, H. Wang, Structural features of three hetero-galacturonans from passiflora foetida fruits and their in vitro immunomodulatory effects, Polymers (Basel). 12 (2020) 615. https://doi.org/10.3390/polym12030615.

[49] R.C. Rial, T.C. Merlo, P.H. Michalski Santos, L.F. Dias Melo, R.A. Barbosa, O.N. de Freitas, C.E. Domingues Nazário, L.H. Viana, Evaluation of oxidative stability of soybean methyl biodiesel using extract of cagaite leaves (Eugenia dysenterica DC.) as additive, Renew. Energy 152 (2020) 1079–1085. https://doi.org/10.1016/j.renene.2020.01.121.

[50] P.T. Vo, H.M.N. Chieng, Q.D. Nguyen, Ultrasonic-assisted Processes to Recover Phenolics and Flavonoids from Passion Fruit Peels, Chem. Eng. Trans. 108 (2024) 13–18. https://doi.org/10.3303/CET24108003.

[51] C.A.R. da Costa, G.G.L. Machado, L.J. Rodrigues, H.E.A. de Barros, C.V.L. Natarelli, E.V. de B.V. Boas, Phenolic compounds profile and antioxidant activity of purple passion fruit's pulp, peel and seed at different maturation stages, Sci. Hortic. (Amsterdam). 321 (2023) 112244. https://doi.org/10.1016/j.scienta.2023.112244.

[52] S. Shanmugam, R.D.D. Sandes, M. Rajan, M.T.S.L. Neta, B. dos Santos Lima, M.J.M. de Jesus, M. Denadai, N. Narain, P. Thangaraj, M.R. Serafini, L.J. Quintans-Junior, A.A. de Souza Araujo, Volatile profiling and UHPLC-QqQ-MS/MS polyphenol analysis of Passiflora leschenaultii DC. fruits and its anti-radical and anti-diabetic properties, Food Res. Int. 133 (2020) 109202. https://doi.org/10.1016/j.foodres.2020.109202.

[53] E.D.L. Putra, N. Nazliniwaty, F.R. Harun, N. Nerdy, Quantification of isoorientin in three varieties of passion fruit peel ethanolic extract by high performance liquid chromatography mass spectrometry, Rasayan J. Chem. 13 (2020) 968–672. https://doi.org/10.31788/RJC.2020.1325645.

[54] M. Hu, J. Du, L. Du, Q. Luo, J. Xiong, Anti-fatigue activity of purified anthocyanins

prepared from purple passion fruit (P. edulis Sim) epicarp in mice, J. Funct. Foods 65 (2020) 103725. https://doi.org/10.1016/j.jff.2019.103725.

[55] Z.H. Pan, D.S. Ning, Y.X. Fu, D.P. Li, Z.Q. Zou, Y.C. Xie, L.L. Yu, L.C. Li, Preparative Isolation of Piceatannol Derivatives from Passion Fruit (Passiflora edulis) Seeds by High-Speed Countercurrent Chromatography Combined with High-Performance Liquid Chromatography and Screening for α-Glucosidase Inhibitory Activities, J. Agric. Food Chem. 68 (2020) 1555–1562. https://doi.org/10.1021/acs.jafc.9b04871.

[56] S. Purohit, S. Girisa, Y. Ochiai, A.B. Kunnumakkara, L. Sahoo, E. Yanase, V. V. Goud, Scirpusin B isolated from Passiflora edulis Var. flavicarpa attenuates carbohydrate digestive enzymes, pathogenic bacteria and oral squamous cell carcinoma, 3 Biotech 14 (2024) 28. https://doi.org/10.1007/s13205-023-03876-6.

[57] L.C. dos Santos, J.C.F. Johner, E. Scopel, P.V.A. Pontes, A.P.B. Ribeiro, G.L. Zabot, E.A.C. Batista, M.A.A. Meireles, J. Martinez, Integrated supercritical CO2 extraction and fractionation of passion fruit (Passiflora edulis Sims) by-products, J. Supercrit. Fluids 168 (2021) 105093. https://doi.org/10.1016/j.supflu.2020.105093.

[58] L.C.R. dos Reis, E.M.P. Facco, M. Salvador, S.H. Flôres, A. de Oliveira Rios, Antioxidant potential and physicochemical characterization of yellow, purple and orange passion fruit, J. Food Sci. Technol. 55 (2018) 2679–2691. https://doi.org/10.1007/s13197-018-3190-2.

[59] D. Arturo-Perdomo, J.P.J. Mora, E. Ibáñez, A. Cifuentes, A. Hurtado-Benavides, L. Montero, Extraction and Characterization of the Polar Lipid Fraction of Blackberry and Passion Fruit Seeds Oils Using Supercritical Fluid Extraction, Food Anal. Methods 14 (2021) 2026–2037. https://doi.org/10.1007/s12161-021-02020-5.

[60] I.M. Savic, I.M. Savic Gajic, Development of the Sustainable Extraction Procedures of Bioactive Compounds from Industrial Food Wastes and Their Application in the Products for Human Uses, Sustain. 15 (2023) 2102. https://doi.org/10.3390/su15032102.

[61] L. Grunovaite, M. Pukalskiene, A. Pukalskas, P.R. Venskutonis, Fractionation of black chokeberry pomace into functional ingredients using high pressure extraction methods and evaluation of their antioxidant capacity and chemical composition, J. Funct. Foods 24 (2016) 85–96. https://doi.org/10.1016/j.jff.2016.03.018.

[62] L. Wang, Z. Li, J. Huang, D. Liu, C. Lefebvre, J. Fan, Effect of Ultrasound-Assisted Extraction of Polyphenols from Apple Peels in Water CO2 Systems, Food Bioprocess Technol. 15 (2022) 1157–1167. https://doi.org/10.1007/s11947-022-02809-0.

[63] C. Medina-Jaramillo, E. Gomez-Delgado, A. Lopez-Cordoba, Improvement of the Ultrasound-Assisted Extraction of Polyphenols from Welsh Onion (Allium fistulosum) Leaves Using Response Surface Methodology, Foods 11 (2022) 2425. https://doi.org/10.3390/foods11162425.

[64] S.O. Essien, B. Young, S. Baroutian, Recent advances in subcritical water and supercritical carbon dioxide extraction of bioactive compounds from plant materials, Trends Food Sci. Technol. 97 (2020) 156–169. https://doi.org/10.1016/j.tifs.2020.01.014.

[65] D.N. Rizkiyah, N.R. Putra, Z. Idham, A.H.A. Aziz, M.A. Che Yunus, I. Veza, Irianto, S. Chinedu Mamah, L. Qomariyah, Recovery of Anthocyanins from Hibiscus sabdariffa L. Using a Combination of Supercritical Carbon Dioxide Extraction and Subcritical Water Extraction, Processes 11 (2023) 751. https://doi.org/10.3390/pr11030751.

[66] L. Campone, R. Celano, A.L. Piccinelli, I. Pagano, S. Carabetta, R. Di Sanzo, M. Russo, E. Ibanez, A. Cifuentes, L. Rastrelli, Response surface methodology to optimize supercritical carbon dioxide/co-solvent extraction of brown onion skin by-product as source of nutraceutical compounds, Food Chem. 269 (2018) 495–502. https://doi.org/10.1016/j.foodchem.2018.07.042.

[67] T.P. Vo, N.T.U. Nguyen, V.H. Le, T.H. Phan, T.H.Y. Nguyen, D.Q. Nguyen, Optimizing Ultrasonic-Assisted and Microwave-Assisted Extraction Processes to Recover Phenolics and Flavonoids from Passion Fruit Peels, ACS Omega 8 (2023) 33870–33882. https://doi.org/10.1021/acsomega.3c04550.

[68] L. da C. Rodrigues, P.I.N. de Carvalho, G.C. Dacanal, A.L. de Oliveira, Pressurized liquid extraction (PLE) in an intermittent process as a new alternative for production of tincture from medicinal plants: The scale up and economic evaluation for production of passion fruit (Passiflora edulis Sims) leaf hydroalcoholic extract, Food Bioprod. Process. 149 (2025) 272–283. https://doi.org/10.1016/j.fbp.2024.11.022.

[69] D. Huo, J. Dai, S. Yuan, X. Cheng, Y. Pan, L. Wang, R. Wang, Eco-friendly simultaneous extraction of pectins and phenolics from passion fruit (Passiflora edulis Sims) peel: Process optimization, physicochemical properties, and antioxidant activity, Int. J. Biol. Macromol. 243 (2023) 125229. https://doi.org/10.1016/j.ijbiomac.2023.125229.

[70] R. Vardanega, F.S. Fuentes, J. Palma, W. Bugueno-Munoz, P. Cerezal-Mezquita, M.C. Ruiz-Dominguez, Extraction of valuable compounds from granadilla (Passiflora ligularis Juss) peel using pressurized fluids technologies, Sustain. Chem. Pharm. 34 (2023) 101135. https://doi.org/10.1016/j.scp.2023.101135.

[71] D.T. Vitor Pereira, F.M. Barrales, E. Pereira, J. Vigano, A.H. Iglesias, F.G. Reyes Reyes, J. Martinez, Phenolic compounds from passion fruit rinds using ultrasound-assisted pressurized liquid extraction and nanofiltration, J. Food Eng. 325 (2022) 110977. https://doi.org/10.1016/j.jfoodeng.2022.110977.

[72] M.I. Zakwan Samudin, M.Y. Abdul Aziz, Y. Nurhayati, Total Phenolic Content and Antioxidant Activity of Passiflora edulis Extract, J. Agrobiotechnology 13 (2022) 1–9. https://doi.org/10.37231/jab.2022.13.2.291.

[73] S. Purohit, C.R. Barik, D. Kalita, L. Sahoo, V. V. Goud, Exploration of nutritional, antioxidant and antibacterial properties of unutilized rind and seed of passion fruit from Northeast India, J. Food Meas. Charact. 15 (2021) 3153–3167. https://doi.org/10.1007/s11694-021-00899-6.

[74] A. Chiavaroli, S.C. Di Simone, K.I. Sinan, M.C. Ciferri, G. Angeles Flores, G. Zengin, O.K. Etienne, G. Ak, M. Fawzi Mahomoodally, S. Jugreet, Z. Cziáky, J. Jekő, L. Recinella, L. Brunetti, S. Leone, P. Angelini, R. Venanzoni, L. Menghini, C. Ferrante, G. Orlando, Pharmacological Properties and Chemical Profiles of Passiflora foetida L. Extracts: Novel Insights for Pharmaceuticals and Nutraceuticals, Processes 8 (2020) 1034. https://doi.org/10.3390/pr8091034.

[75] N.E.H. Lezoul, M. Belkadi, F. Habibi, F. Guillen, Extraction Processes with Several Solvents on Total Bioactive Compounds in Different Organs of Three Medicinal Plants, Molecules 25 (2020) 4672. https://doi.org/10.3390/molecules25204672.

[76] C. Hidalgo Viquez, C. Cortes Herrera, M. Cerdas Nunez, Generation of analytical food composition data for traditionally consumed fruits and vegetables in Costa Rica, J. Food Compos. Anal. 123 (2023) 105546. https://doi.org/10.1016/j.jfca.2023.105546.

[77] R.M.L. Mendes, R.H.C. de Andrade, M. de F.F. Marques, E.R. de Andrade, Potential use of the passion fruit from caatinga in kefir, Food Biosci. 39 (2021) 100809. https://doi.org/10.1016/j.fbio.2020.100809.

[78] T.F. Borgonovi, J.I.I. Fugaban, J.E.V. Bucheli, S.N. Casarotti, W.H. Holzapfel, S.D. Todorov, A.L.B. Penna, Dual Role of Probiotic Lactic Acid Bacteria Cultures for Fermentation and Control Pathogenic Bacteria in Fruit-Enriched Fermented Milk, Probiotics Antimicrob. Proteins (2023) 1–16. https://doi.org/10.1007/s12602-023-10135-w.

[79] E. Santos, R. Andrade, E. Gouveia, Utilization of the pectin and pulp of the passion fruit

from Caatinga as probiotic food carriers, Food Biosci. 20 (2017) 56–61. https://doi.org/10.1016/j.fbio.2017.08.005.

[80] D. Arias-Lamos, J.B. Molina-Hernandez, M.M. Andrade-Mahecha, Evaluation of the potential use of passion fruit dehydrated epicarp (Passiflora edulis f. flavicarpa O. Deg.) in the formulation of yogurt, Rev. U.D.C.A Actual. Divulg. Cient. 22 (2019). https://doi.org/10.31910/rudca.v22.n1.2019.1145.

[81] N.M.V. de Toledo, A.C. de Camargo, P.B.M. Ramos, D.C. Button, D. Granato, S.G. Canniatti-Brazaca, Potentials and pitfalls on the use of passion fruit by-products in drinkable yogurt: Physicochemical, technological, microbiological, and sensory aspects, Beverages 4 (2018) 47. https://doi.org/10.3390/beverages4030047.

[82] M.A.C. Albuquerque, R. Bedani, J.G. LeBlanc, S.M.I. Saad, Passion fruit by-product and fructooligosaccharides stimulate the growth and folate production by starter and probiotic cultures in fermented soymilk, Int. J. Food Microbiol. 261 (2017) 35–41. https://doi.org/10.1016/j.ijfoodmicro.2017.09.001.

[83] R.F. Sampaio, V. da Cruz Lima, G.A.M. Bungart, L.D.B. Correia, T.M. Tobal, Flour of Winged-stem Passion Fruit Peel: Nutritional Composition, Incorporation in Cookies, and Sensory Acceptability, Brazilian Arch. Biol. Technol. 65 (2022) e22200776. https://doi.org/10.1590/1678-4324-2022200776.

[84] K.L. Santos, C.A.N. Alves, F. Moisés de Sousa, T.A. Souza Gusmão, E.G. Alves Filho, L. Barros de Vasconcelos, Chemometrics applied to physical, physicochemical and sensorial attributes of chicken hamburgers blended with green banana and passion fruit epicarp biomasses, Int. J. Gastron. Food Sci. 24 (2021) 100337. https://doi.org/10.1016/j.ijgfs.2021.100337.

[85] E.M. Coelho, R.G. Gomes, B.A.S. Machado, R.S. Oliveira, M. dos S. Lima, L.C. de Azêvedo, M.A.U. Guez, Passion fruit peel flour – Technological properties and application in food products, Food Hydrocoll. 62 (2017) 158–164. https://doi.org/10.1016/j.foodhyd.2016.07.027.

[86] C.F. Costa, A. Fusieger, M. Andretta, A.C. Camargo, A.F. Carvalho, D.R. Menezes, L.A. Nero, Short communication: Potential use of passion fruit (Passiflora cincinnata) as a biopreservative in the production of coalho cheese, a traditional Brazilian cheese, J. Dairy Sci. 103 (2020) 3082–3087. https://doi.org/10.3168/jds.2019-17791.

[87] M.P. de Souza, F.D. de Amorim, M.R.A. Ferreira, L.A.L. Soares, M.A. de Melo, Oxidative and storage stability in beef burgers from the use of bioactive compounds from the agro-industrial residues of passion fruit (Passiflora edulis), Food Biosci. 48 (2022) 101823. https://doi.org/10.1016/j.fbio.2022.101823.

[88] K.P. Patel, R.A. Maheshwari, *Passiflora edulis*: A Bioactive Bounty – A Comprehensive Review, J. Nat. Remedies (2024) 1203–1210. https://doi.org/10.18311/jnr/2024/36235.

[89] A. Rodriguez-Usaquen, J.J. Sutachan, W. Villarreal, G.M. Costa, E.J. Acero Mondragon, R. Ballesteros-Ramirez, S.L. Albarracin, Sub-acute toxicity evaluation of aqueous leaf extract from Passiflora edulis Sims f. edulis (Gulupa) in Wistar rats, Toxicol. Reports 11 (2023) 396–404. https://doi.org/10.1016/j.toxrep.2023.10.013.

[90] D.K.R. Holanda, N.J. Wurlitzer, A.P. Dionisio, A.R. Campos, R.A. Moreira, P.H.M. de Sousa, E.S. de Brito, P.R.V. Ribeiro, M.F. Iunes, A.M. Costa, Garlic passion fruit (Passiflora tenuifila Killip): Assessment of eventual acute toxicity, anxiolytic, sedative, and anticonvulsant effects using in vivo assays, Food Res. Int. 128 (2020) 108813. https://doi.org/10.1016/j.foodres.2019.108813.

[91] S. Purohit, S. Girisa, Y. Ochiai, A.B. Kunnumakkara, L. Sahoo, E. Yanase, V. V. Goud, Scirpusin B isolated from Passiflora edulis Var. flavicarpa attenuates carbohydrate digestive enzymes, pathogenic bacteria and oral squamous cell carcinoma, 3 Biotech 14 (2024) 1–14. https://doi.org/10.1007/s13205-023-03876-6.

[92] J.A. Villada Ramos, J. Aguillón Osma, B. Restrepo Cortes, N. Loango Chamarro, M.E. Maldonado Celis, Identification of potential bioactive compounds of Passiflora edulis leaf extract against colon adenocarcinoma cells, Biochem. Biophys. Reports 34 (2023) 101453. https://doi.org/10.1016/j.bbrep.2023.101453.

[93] K.S. da Silva, K.Y. Abboud, C.S. Schiebel, N.M.T. de Oliveira, L.R. Bueno, L.L.V. de Mello Braga, B.C. da Silveira, I.W.F. dos Santos, E. dos S. Gomes, M.B. Gois, L.M.C. Cordeiro, D. Maria Ferreira, Polysaccharides from Passion Fruit Peels: From an Agroindustrial By-Product to a Viable Option for 5-FU-Induced Intestinal Damage, Pharmaceuticals 16 (2023) 912. https://doi.org/10.3390/ph16070912.

[94] V. Venkatachalamoorthi, P.G. Shivashankarappa, S. Adimoulame, K. Gurusamy, K. Muthukrishnan, E. Govindan, Effect of Passion Fruit Juice in Removal of Smear Layer in Root Canal of Ex Vivo Human Teeth: A Scanning Electron Microscopic Study, Int. J. Clin. Pediatr. Dent. 16 (2023) S190–S194. https://doi.org/10.5005/jp-journals-10005-2631.

[95] N.K. Dewi, I.B. Putra, N.K. Jusuf, Passion fruit purple variant (Passiflora edulis Sims var. edulis) seeds extract 10% cream in acne vulgaris treatment: an open-label pilot study, Int. J. Dermatol. 59 (2020) 1506–1512. https://doi.org/10.1111/ijd.15178.

[96] J. Khongrum, P. Yingthongchai, K. Boonyapranai, W. Wongtanasarasin, N. Donrung, W. Sukketsiri, A. Prachansuwan, P. Chonpathompikunlert, Antidyslipidemic, Antioxidant, and Anti-inflammatory Effects of Jelly Drink Containing Polyphenol-Rich Roselle Calyces Extract and Passion Fruit Juice with Pulp in Adults with Dyslipidemia: A Randomized, Double-Blind, Placebo-Controlled Trial, Oxid. Med. Cell. Longev. 2022 (2022). https://doi.org/10.1155/2022/4631983.

[97] A. Yepes, D. Ochoa-Bautista, W. Murillo-Arango, J. Quintero-Saumeth, K. Bravo, E. Osorio, Purple passion fruit seeds (Passiflora edulis f. edulis Sims) as a promising source of skin anti-aging agents: Enzymatic, antioxidant and multi-level computational studies, Arab. J. Chem. 14 (2021) 102905. https://doi.org/10.1016/j.arabjc.2020.11.011.

[98] N. Nazliniwaty, F.R. Harun, E.D.L. Putra, N. Nerdy, Antiaging activity of gel preparation containing three varieties of passion fruit peel ethanolic extract, Open Access Maced. J. Med. Sci. 8 (2020) 170–174. https://doi.org/10.3889/OAMJMS.2020.3462.

[99] S. Hartanto, I.N.E. Lister, E. Fachrial, A Comparative Study of Peel and Seed Extract of Passion Fruit (Passiflora edulis) as Anti Collagenase, Am. Sci. Res. J. Eng. Technol. Sci. 54 (2019) 42–48. https://asrjetsjournal.org/index.php/American_Scientific_Journal/article/view/4722.

[100] N. Lourith, M. Kanlayavattanakul, J. Chingunpitak, Development of sunscreen products containing passion fruit seed extract, Brazilian J. Pharm. Sci. 53 (2017). https://doi.org/10.1590/s2175-97902017000116116.

[101] H. Maruki-Uchida, I. Kurita, K. Sugiyama, M. Sai, K. Maeda, T. Ito, The protective effects of piceatannol from passion fruit (Passiflora edulis) seeds in UVB-irradiated keratinocytes, Biol. Pharm. Bull. 36 (2013) 845–849. https://doi.org/10.1248/bpb.b12-00708.

[102] N.K. Jusuf, I.B. Putra, N.K. Dewi, Antibacterial activity of passion fruit purple variant (Passiflora edulis sims var. edulis) seeds extract against propionibacterium acnes, Clin. Cosmet. Investig. Dermatol. 13 (2020) 99–104. https://doi.org/10.2147/CCID.S229743.

[103] M. Lobo de Souza, D. Dourado, I. Pinheiro Lobo, V. Couto Pires, S. Nunes de Oliveira Araujo, J. de Souza Reboucas, A.M. Costa, C. Pinho Fernandes, N. Machado Tavares, N. de Paula Pereira, F. Rocha Formiga, Wild Passiflora (Passiflora spp.) seed oils and their nanoemulsions induce proliferation in HaCaT keratinocytes cells, J. Drug Deliv. Sci. Technol. 67 (2022) 102803. https://doi.org/10.1016/j.jddst.2021.102803.

[104] A.F.V. Silva, L.A. Santos, R.B. Valenca, T.S. Porto, M.A. Da Motta Sobrinho, G.J.C. Gomes, J.F.T. Juca, A.F.M.S. Santos, Cellulase production to obtain biogas from passion fruit (Passiflora edulis) peel waste hydrolysate, J. Environ. Chem. Eng. 7 (2019) 103510. https://doi.org/10.1016/j.jece.2019.103510.

[105] C. Zhao, H. Yan, Y. Liu, Y. Huang, R. Zhang, C. Chen, G. Liu, Bio-energy conversion performance, biodegradability, and kinetic analysis of different fruit residues during discontinuous anaerobic digestion, Waste Manag. 52 (2016) 295–301. https://doi.org/10.1016/j.wasman.2016.03.028.

[106] L.A. dos Santos, R.B. Valenca, L.C.S. da Silva, S.H. de B. Holanda, A.F.V. da Silva, J.F.T. Juca, A.F.M.S. Santos, Methane generation potential through anaerobic digestion of fruit waste, J. Clean. Prod. 256 (2020) 120389. https://doi.org/10.1016/j.jclepro.2020.120389.

[107] M. Megawati, A. Damayanti, R. Putri, A. Pratama, T. Muftidar, Kinetics of Enzymatic Hydrolysis of Passion Fruit Peel using Cellulase in Bio-ethanol Production, Reaktor 20 (2020) 10–17. https://doi.org/10.14710/reaktor.20.1.10-17.

[108] S.S. Pantoja, L.R. V. Da Conceição, C.E.F. Da Costa, J.R. Zamian, G.N. Da Rocha Filho, Oxidative stability of biodiesels produced from vegetable oils having different degrees of unsaturation, Energy Convers. Manag. 74 (2013) 293–298. https://doi.org/10.1016/j.enconman.2013.05.025.

[109] N. Tippayawong, P. Chumjai, Characterization and performance of biofuel from passion fruit processing residues, in: Lect. Notes Eng. Comput. Sci., 2012: pp. 733–736.

[110] S. Jain, S. Purohit, D. Kumar, V. V. Goud, Passion fruit seed extract as an antioxidant additive for biodiesel; shelf life and consumption kinetics, Fuel 289 (2021) 119906. https://doi.org/10.1016/j.fuel.2020.119906.

[111] J. Montalvo Andia, A. Larrea, J. Salcedo, J. Reyes, L. Lopez, L. Yokoyama, Synthesis and characterization of chemically activated carbon from Passiflora ligularis, Inga feuilleei and native plants of South America, J. Environ. Chem. Eng. 8 (2020) 103892. https://doi.org/10.1016/j.jece.2020.103892.

[112] M. Fu, Z. Zhu, Z. Zhang, Q. Zhuang, F. Gao, W. Chen, H. Yu, Q. Liu, Microwave assisted growth of MnO2 on biomass carbon for advanced supercapacitor electrode materials, J. Mater. Sci. 56 (2021) 6987–6996. https://doi.org/10.1007/s10853-020-05723-y.

[113] Y.L. Lin, N.Y. Zheng, Torrefaction of fruit waste seed and shells for biofuel production with reduced CO2 emission, Energy 225 (2021) 120226. https://doi.org/10.1016/j.energy.2021.120226.

[114] T. My-Thao Nguyen, T. Anh-Thu Nguyen, N. Tuong-Van Pham, Q.V. Ly, T. Thuy-Quynh Tran, T.D. Thach, C.L. Nguyen, K.S. Banh, V.D. Le, L.P. Nguyen, D.T. Nguyen, C.H. Dang, T.D. Nguyen, Biosynthesis of metallic nanoparticles from waste Passiflora edulis peels for their antibacterial effect and catalytic activity, Arab. J. Chem. 14 (2021) 103096. https://doi.org/10.1016/j.arabjc.2021.103096.

[115] M. Khan, P. Ware, N. Shimpi, Synthesis of ZnO nanoparticles using peels of Passiflora foetida and study of its activity as an efficient catalyst for the degradation of hazardous organic dye, SN Appl. Sci. 3 (2021) 1–17. https://doi.org/10.1007/s42452-021-04436-4.

[116] J. Santhoshkumar, B. Sowmya, S. Venkat Kumar, S. Rajeshkumar, Toxicology evaluation and antidermatophytic activity of silver nanoparticles synthesized using leaf extract of Passiflora caerulea, South African J. Chem. Eng. 29 (2019) 17–23. https://doi.org/10.1016/j.sajce.2019.04.001.

[117] J.C. Rivas, L.M.C. Cabral, M.H. Rocha-Leao, Stability of Bioactive Compounds of Microencapsulated Mango and Passion Fruit Mixed Pulp, Int. J. Fruit Sci. 20 (2020)

S94–S110. https://doi.org/10.1080/15538362.2019.1707746.

[118] J. Vigano, B.F. de P. Assis, G. Nathia-Neves, P. dos Santos, M.A.A. Meireles, P.C. Veggi, J. Martinez, Extraction of bioactive compounds from defatted passion fruit bagasse (Passiflora edulis sp.) applying pressurized liquids assisted by ultrasound, Ultrason. Sonochem. 64 (2020) 104999. https://doi.org/10.1016/j.ultsonch.2020.104999.

[119] Y.A. Rodriguez-Restrepo, C.M.R. Rocha, J.A. Teixeira, C.E. Orrego, Valorization of Passion Fruit Stalk by the Preparation of Cellulose Nanofibers and Immobilization of Trypsin, Fibers Polym. 21 (2020) 2807–2816. https://doi.org/10.1007/s12221-020-1342-2.

[120] J.L. Gan, Y. Cheok, Progress in Energy and Environment Enhanced removal efficiency of Methylene blue and water hardness using NaOH-modified Durian and Passion fruit peel adsorbents, Prog. Energy Environ. 16 (2021) 36–44.

[121] N.T.H. Nhung, B.T.P. Quynh, P.T.T. Thao, H.N. Bich, B.L. Giang, Pretreated Fruit Peels as Adsorbents for Removal of Dyes from Water, in: IOP Conf. Ser. Earth Environ. Sci., 2018: p. 12015. https://doi.org/10.1088/1755-1315/159/1/012015.

[122] H.P. Chao, C.C. Chang, Adsorption of copper(II), cadmium(II), nickel(II) and lead(II) from aqueous solution using biosorbents, Adsorption 18 (2012) 395–401. https://doi.org/10.1007/s10450-012-9418-y.

[123] P.R. Souza, G.L. Dotto, N.P.G. Salau, Artificial neural network (ANN) and adaptive neuro-fuzzy interference system (ANFIS) modelling for nickel adsorption onto agro-wastes and commercial activated carbon, J. Environ. Chem. Eng. 6 (2018) 7152–7160. https://doi.org/10.1016/j.jece.2018.11.013.

[124] X. Zhao, J. Zheng, S. You, C. Liu, L. Du, K. Chen, Y. Liu, L. Ma, Selective adsorption of cr (Vi) onto amine-modified passion fruit peel biosorbent, Processes 9 (2021) 790. https://doi.org/10.3390/pr9050790.

[125] LamrotYohannes, H. Feleke, M.S. Melaku, D.E. Amare, Analysis of heavy metals and minerals in edible vegetable oils produced and marketed in Gondar City, Northwest Ethiopia, BMC Public Health 24 (2024) 1–14. https://doi.org/10.1186/s12889-024-19695-0.

[126] R. Yang, L. Zhang, P. Li, L. Yu, J. Mao, X. Wang, Q. Zhang, A review of chemical composition and nutritional properties of minor vegetable oils in China, Trends Food Sci. Technol. 74 (2018) 26–32. https://doi.org/10.1016/j.tifs.2018.01.013.

[127] M. Viana da Silva, M.R.C. Santos, I.R. Alves Silva, E.B. Macedo Viana, D.A. Dos Anjos, I.A. Santos, N.G. Barbosa de Lima, C. Wobeto, N. Jorge, S.C.D.S. Lannes, Synthetic and Natural Antioxidants Used in the Oxidative Stability of Edible Oils: An Overview, Food Rev. Int. 38 (2022) 349–372. https://doi.org/10.1080/87559129.2020.1869775.

[128] S. Fereidoon, Z. Ying, Lipid oxidation and improving the oxidative stability, Chem. Soc. Rev. 39 (2010) 4067–4079. https://doi.org/10.1039/b922183m.

[129] S. Sharma, S.F. Cheng, B. Bhattacharya, S. Chakkaravarthi, Efficacy of free and encapsulated natural antioxidants in oxidative stability of edible oil: Special emphasis on nanoemulsion-based encapsulation, Trends Food Sci. Technol. 91 (2019) 305–318. https://doi.org/10.1016/j.tifs.2019.07.030.

[130] M. Taghvaei, S.M. Jafari, Application and stability of natural antioxidants in edible oils in order to substitute synthetic additives, J. Food Sci. Technol. 52 (2015) 1272–1282. https://doi.org/10.1007/s13197-013-1080-1.

[131] S.K. Mishra, P.D. Belur, R. Iyyaswami, Use of antioxidants for enhancing oxidative stability of bulk edible oils: a review, Int. J. Food Sci. Technol. 56 (2021) 1–12. https://doi.org/10.1111/ijfs.14716.

[132] A. Fadda, D. Sanna, E.H. Sakar, S. Gharby, M. Mulas, S. Medda, N.S. Yesilcubuk, A.C. Karaca, C.K. Gozukirmizi, M. Lucarini, G. Lombardi-Boccia, Z. Diaconeasa, A. Durazzo, Innovative and Sustainable Technologies to Enhance the Oxidative Stability of Vegetable Oils, Sustainability 14 (2022) 849. https://doi.org/10.3390/su14020849.

[133] S. Sahin, E. Elhussein, O. Gulmez, E. Kurtulbas, S. Yazar, Improving the quality of vegetable oils treated with phytochemicals: a comparative study, J. Food Sci. Technol. 57 (2020) 3980–3987. https://doi.org/10.1007/s13197-020-04428-z.

[134] A.R. Corbu, A. Rotaru, V. Nour, Edible vegetable oils enriched with carotenoids extracted from by-products of sea buckthorn (Hippophae rhamnoides ssp. sinensis): the investigation of some characteristic properties, oxidative stability and the effect on thermal behaviour, J. Therm. Anal. Calorim. 142 (2020) 735–747. https://doi.org/10.1007/s10973-019-08875-5.

[135] A.M.T.M. Cordeiro, M.L. Medeiros, N.A. Santos, L.E.B. Soledade, L.F.B.L. Pontes, A.L. Souza, N. Queiroz, A.G. Souza, Rosemary (Rosmarinus officinalis L.) extract: Thermal study and evaluation of the antioxidant effect on vegetable oils, J. Therm. Anal. Calorim. 113 (2013) 889–895. https://doi.org/10.1007/s10973-012-2778-4.

[136] A.M. Goula, M. Ververi, A. Adamopoulou, K. Kaderides, Green ultrasound-assisted extraction of carotenoids from pomegranate wastes using vegetable oils, Ultrason. Sonochem. 34 (2017) 821–830. https://doi.org/10.1016/j.ultsonch.2016.07.022.

[137] H. Chutia, C.L. Mahanta, Green ultrasound and microwave extraction of carotenoids from passion fruit peel using vegetable oils as a solvent: Optimization, comparison, kinetics, and thermodynamic studies, Innov. Food Sci. Emerg. Technol. 67 (2021) 102547. https://doi.org/10.1016/j.ifset.2020.102547.

[138] S.A. Byadgi, P.B. Kalburgi, Production of Bioethanol from Waste Newspaper, Procedia Environ. Sci. 35 (2016) 555–562. https://doi.org/10.1016/j.proenv.2016.07.040.

[139] N.F. Ruslan, N. Ahmad, A. Abas, A. Sanfilippo, K. Mahmoud, M.S.A. Munaim, A.H. Nour, Sustainable bioethanol production by solid-state fermentation: a systematic review, Environ. Sci. Pollut. Res. (2024). https://doi.org/10.1007/s11356-024-35406-z.

[140] N.A. Yazid, R. Barrena, D. Komilis, A. Sánchez, Solid-state fermentation as a novel paradigm for organic waste valorization: A review, Sustain. 9 (2017) 224. https://doi.org/10.3390/su9020224.

[141] A. Singh, R.R. Singhania, S. Soam, C.W. Chen, D. Haldar, S. Varjani, J.S. Chang, C. Di Dong, A.K. Patel, Production of bioethanol from food waste: Status and perspectives, Bioresour. Technol. 360 (2022) 127651. https://doi.org/10.1016/j.biortech.2022.127651.

[142] S. Hegde, T.A. Trabold, Sustainable waste-to-energy technologies: Fermentation, in: Sustain. Food Waste-to-Energy Syst., Elsevier, 2018: pp. 69–88. https://doi.org/10.1016/B978-0-12-811157-4.00005-X.

[143] S. Behera, R. Arora, N. Nandhagopal, S. Kumar, Importance of chemical pretreatment for bioconversion of lignocellulosic biomass, Renew. Sustain. Energy Rev. 36 (2014) 91–106. https://doi.org/10.1016/j.rser.2014.04.047.

[144] I.B. Holcberg, P. Margalith, Alcoholic fermentation by immobilized yeast at high sugar concentrations, Eur. J. Appl. Microbiol. Biotechnol. 13 (1981) 133–140. https://doi.org/10.1007/BF00703041.

[145] K. Manikandan, T. Viruthagiri, Optimization of C/N ratio of the medium and fermentation conditions of ethanol production from tapioca starch using co - Culture of aspergillus niger and sachormyces cerevisiae, Int. J. ChemTech Res. 2 (2010) 947–955.

[146] M. Ghareib, K.A. Youssef, A.A. Khalil, Ethanol tolerance of Saccharomyces cerevisiae and its relationship to lipid content and composition, Folia Microbiol. (Praha). 33 (1988) 447–452. https://doi.org/10.1007/BF02925769.

[147] O. Deesuth, P. Laopaiboon, P. Jaisil, L. Laopaiboon, Optimization of nitrogen and metal ions supplementation for very high gravity bioethanol fermentation from sweet sorghum juice using an orthogonal array design, Energies 5 (2012) 3178–3197. https://doi.org/10.3390/en5093178.

[148] C.A. Lin, C. Cheng, L.W. Chen, C.W. Chen, K.J. Duan, Ethanol production using the whole solid-state fermented sugarcane bagasse cultivated by Trichoderma reesei RUT-C30 supplemented with commercial cellulase, Biocatal. Agric. Biotechnol. 50 (2023) 102667. https://doi.org/10.1016/j.bcab.2023.102667.

[149] R.R. da Silva, M.A. Zaiter, M. Boscolo, R. da Silva, E. Gomes, Xylose consumption and ethanol production by Pichia guilliermondii and Candida oleophila in the presence of furans, phenolic compounds, and organic acids commonly produced during the pre-treatment of plant biomass, Brazilian J. Microbiol. 54 (2023) 753–759. https://doi.org/10.1007/s42770-023-00937-z.

[150] Z.X. Shen, S.Y. Li, Increasing the atom economy of glucose fermentation for bioethanol production in Rubisco-based engineered Escherichia coli, Bioresour. Technol. Reports 21 (2023) 101370. https://doi.org/10.1016/j.biteb.2023.101370.

[151] S. Dutta, M. Suresh Kumar, Potential use of thermophilic bacteria for second-generation bioethanol production using lignocellulosic feedstocks: a review, Biofuels 14 (2023) 851–864. https://doi.org/10.1080/17597269.2023.2184935.

[152] K. Zhang, X. Lu, Y. Li, X. Jiang, L. Liu, H. Wang, New technologies provide more metabolic engineering strategies for bioethanol production in Zymomonas mobilis, Appl. Microbiol. Biotechnol. 103 (2019) 2087–2099. https://doi.org/10.1007/s00253-019-09620-6.

[153] U. Jhariya, N.A. Dafale, S. Srivastava, R.S. Bhende, A. Kapley, H.J. Purohit, Understanding Ethanol Tolerance Mechanism in Saccharomyces cerevisiae to Enhance the Bioethanol Production: Current and Future Prospects, Bioenergy Res. 14 (2021) 670–688. https://doi.org/10.1007/s12155-020-10228-2.

[154] M. Rastogi, S. Shrivastava, Recent advances in second generation bioethanol production: An insight to pretreatment, saccharification and fermentation processes, Renew. Sustain. Energy Rev. 80 (2017) 330–340. https://doi.org/10.1016/j.rser.2017.05.225.

[155] N. Das, P.K. Jena, D. Padhi, M. Kumar Mohanty, G. Sahoo, A comprehensive review of characterization, pretreatment and its applications on different lignocellulosic biomass for bioethanol production, Biomass Convers. Biorefinery 13 (2023) 1503–1527. https://doi.org/10.1007/s13399-021-01294-3.

[156] L. Canilha, A.K. Chandel, T. Suzane Dos Santos Milessi, F.A.F. Antunes, W. Luiz Da Costa Freitas, M. Das Graças Almeida Felipe, S.S. Da Silva, Bioconversion of sugarcane biomass into ethanol: An overview about composition, pretreatment methods, detoxification of hydrolysates, enzymatic saccharification, and ethanol fermentation, J. Biomed. Biotechnol. 2012 (2012). https://doi.org/10.1155/2012/989572.

[157] H. Zhang, L. Han, H. Dong, An insight to pretreatment, enzyme adsorption and enzymatic hydrolysis of lignocellulosic biomass: Experimental and modeling studies, Renew. Sustain. Energy Rev. 140 (2021) 110758. https://doi.org/10.1016/j.rser.2021.110758.

[158] A.S.A. Da Silva, R.P. Espinheira, R.S.S. Teixeira, M.F. De Souza, V. Ferreira-Leitão, E.P.S. Bon, Constraints and advances in high-solids enzymatic hydrolysis of lignocellulosic biomass: A critical review, Biotechnol. Biofuels 13 (2020) 1–28. https://doi.org/10.1186/s13068-020-01697-w.

[159] E. Olguin-Maciel, A. Singh, R. Chable-Villacis, R. Tapia-Tussell, H.A. Ruiz, Consolidated bioprocessing, an innovative strategy towards sustainability for biofuels

production from crop residues: An overview, Agronomy 10 (2020) 1834. https://doi.org/10.3390/agronomy10111834.

[160] M.M. Ishola, A. Jahandideh, B. Haidarian, T. Brandberg, M.J. Taherzadeh, Simultaneous saccharification, filtration and fermentation (SSFF): A novel method for bioethanol production from lignocellulosic biomass, Bioresour. Technol. 133 (2013) 68–73. https://doi.org/10.1016/j.biortech.2013.01.130.

[161] S.M.R. Khattab, H. Okano, C. Kimura, T. Fujita, T. Watanabe, Efficient integrated production of bioethanol and antiviral glycerolysis lignin from sugarcane trash, Biotechnol. Biofuels Bioprod. 16 (2023) 82. https://doi.org/10.1186/s13068-023-02333-z.

[162] X. Yi, D. Yang, X. Xu, Y. Wang, Y. Guo, M. Zhang, Y. Wang, Y. He, J. Zhu, Cold plasma pretreatment reinforces the lignocellulose-derived aldehyde inhibitors tolerance and bioethanol fermentability for Zymomonas mobilis, Biotechnol. Biofuels Bioprod. 16 (2023) 1–15. https://doi.org/10.1186/s13068-023-02354-8.

[163] R. Nunta, C. Techapun, S. Sommanee, C. Mahakuntha, K. Porninta, W. Punyodom, Y. Phimolsiripol, P. Rachtanapun, W. Wang, X. Zhuang, W. Qi, K. Jantanasakulwong, A. Reungsang, A. Kumar, N. Leksawasdi, Valorization of rice straw, sugarcane bagasse and sweet sorghum bagasse for the production of bioethanol and phenylacetylcarbinol, Sci. Rep. 13 (2023) 727. https://doi.org/10.1038/s41598-023-27451-4.

[164] E. Hawaz, M. Tafesse, A. Tesfaye, S. Kiros, D. Beyene, G. Kebede, T. Boekhout, M. Groenwald, B. Theelen, A. Degefe, S. Degu, A. Admasu, B. Hunde, D. Muleta, Optimization of bioethanol production from sugarcane molasses by the response surface methodology using Meyerozyma caribbica isolate MJTm3, Ann. Microbiol. 73 (2023) 2. https://doi.org/10.1186/s13213-022-01706-3.

[165] J. Zhang, Y. Fu, Y.Y. Dong, D. Wang, J. Deng, Z. Shi, J. Yang, H. Yang, Pretreatment of bamboo with choline chloride-lactic acid integrated with calcium chloride hydrates deep eutectic solvent to boost bioconversion for ethanol production, Ind. Crops Prod. 200 (2023) 116879. https://doi.org/10.1016/j.indcrop.2023.116879.

[166] I. Ntaikou, M. Alexandropoulou, M. Kamilari, S.A. Alamri, Y.S. Moustafa, M. Hashem, G. Antonopoulou, G. Lyberatos, Saccharification of starchy food waste through thermochemical and enzymatic pretreatment, towards enhanced bioethanol production via newly isolated non-conventional yeast strains, Energy 281 (2023) 128259. https://doi.org/10.1016/j.energy.2023.128259.

[167] Y. Zhang, T. Sun, T. Wu, J. Li, D. Hu, D. Liu, J. Li, C. Tian, Consolidated bioprocessing for bioethanol production by metabolically engineered cellulolytic fungus Myceliophthora thermophila, Metab. Eng. 78 (2023) 192–199. https://doi.org/10.1016/j.ymben.2023.06.009.

[168] S. Kavitha, T. Gajendran, K. Saranya, V. Manivasagan, Bioconversion of Sargassum wightii to ethanol via consolidated bioprocessing using Lachnoclostridium phytofermentans KSM 1203, Fuel 347 (2023) 128465. https://doi.org/10.1016/j.fuel.2023.128465.

[169] J. Zanivan, C. Bonatto, T. Scapini, C. Dalastra, S.F. Bazoti, S.L.A. Júnior, G. Fongaro, H. Treichel, Evaluation of Bioethanol Production from a Mixed Fruit Waste by Wickerhamomyces sp. UFFS-CE-3.1.2, Bioenergy Res. 15 (2022) 175–182. https://doi.org/10.1007/s12155-021-10273-5.

[170] J. Hou, X. Zhang, S. Zhang, K. Wang, Q. Zhang, Enhancement of bioethanol production by a waste biomass-based adsorbent from enzymatic hydrolysis, J. Clean. Prod. 291 (2021) 125933. https://doi.org/10.1016/j.jclepro.2021.125933.

[171] N. Annamalai, H. Al Battashi, S.N. Anu, A. Al Azkawi, S. Al Bahry, N. Sivakumar, Enhanced Bioethanol Production from Waste Paper Through Separate Hydrolysis and Fermentation, Waste and Biomass Valorization 11 (2020) 121–131.

https://doi.org/10.1007/s12649-018-0400-0.

[172] J.T. Casabar, Y. Unpaprom, R. Ramaraj, Fermentation of pineapple fruit peel wastes for bioethanol production, Biomass Convers. Biorefinery 9 (2019) 761–765. https://doi.org/10.1007/s13399-019-00436-y.

[173] D. Indira, B. Das, H. Bhawsar, S. Moumita, E.M. Johnson, P. Balasubramanian, R. Jayabalan, Investigation on the production of bioethanol from black tea waste biomass in the seawater-based system, Bioresour. Technol. Reports 4 (2018) 209–213. https://doi.org/10.1016/j.biteb.2018.11.003.

[174] G.D. Saratale, M.K. Oh, Improving alkaline pretreatment method for preparation of whole rice waste biomass feedstock and bioethanol production, RSC Adv. 5 (2015) 97171–97179. https://doi.org/10.1039/c5ra17797a.

[175] A.K. Dubey, P.K. Gupta, N. Garg, S. Naithani, Bioethanol production from waste paper acid pretreated hydrolyzate with xylose fermenting Pichia stipitis, Carbohydr. Polym. 88 (2012) 825–829. https://doi.org/10.1016/j.carbpol.2012.01.004.

[176] S. Patil, M. Imran, R.S.M. Jaquline, V. Aeri, Standardization of Euphorbia tithymaloides (L.) Poit. (Root) by Conventional and DNA Barcoding Methods, ACS Omega 8 (2023) 29324–29335. https://doi.org/10.1021/acsomega.3c02543.

[177] S. Sen, B. De, N. Devanna, R. Chakraborty, Total phenolic, total flavonoid content, and antioxidant capacity of the leaves of Meyna spinosa Roxb., an Indian medicinal plant, Chin. J. Nat. Med. 11 (2013) 149–157. https://doi.org/10.1016/S1875-5364(13)60042-4.

[178] S.S. Jiao, D. Li, Z.G. Huang, Z.S. Zhang, B. Bhandari, X.D. Chen, Z.H. Mao, Optimization of supercritical carbon dioxide extraction of flaxseed oil using response surface methodology, Int. J. Food Eng. 4 (2008) 1223–1231. https://doi.org/10.2202/1556-3758.1409.

[179] P.K. Patial, A. Sharma, I. Kaur, D.S. Cannoo, Correlation study among the extraction techniques, phytochemicals, and antioxidant activity of Nepeta spicata aerial part, Biocatal. Agric. Biotechnol. 20 (2019) 101275. https://doi.org/10.1016/j.bcab.2019.101275.

[180] A. Moges, C.R. Barik, S. Purohit, V. V. Goud, Dietary and bioactive properties of the berries and leaves from the underutilized Hippophae salicifolia D. Don grown in Northeast India, Food Sci. Biotechnol. 30 (2021) 1555–1569. https://doi.org/10.1007/s10068-021-00988-8.

[181] V. Todorovic, M. Milenkovic, B. Vidovic, Z. Todorovic, S. Sobajic, Correlation between Antimicrobial, Antioxidant Activity, and Polyphenols of Alkalized/Nonalkalized Cocoa Powders, J. Food Sci. 82 (2017) 1020–1027. https://doi.org/10.1111/1750-3841.13672.

[182] S.D. Sarker, L. Nahar, Y. Kumarasamy, Microtitre plate-based antibacterial assay incorporating resazurin as an indicator of cell growth, and its application in the in vitro antibacterial screening of phytochemicals, Methods 42 (2007) 321–324. https://doi.org/10.1016/j.ymeth.2007.01.006.

[183] N.D. Devi, C. Mukherjee, G. Bhatt, L. Rangan, V. V. Goud, Co-cultivation of microalgae-cyanobacterium under various nitrogen and phosphorus regimes to concurrently improve biomass, lipid accumulation and easy harvesting, Biochem. Eng. J. 188 (2022) 108706. https://doi.org/10.1016/j.bej.2022.108706.

[184] M.S. Hernandez Zarate, M. del R. Abraham Juarez, A. Ceron Garcia, C. Ozuna Lopez, A.J. Gutierrez Chavez, J. de J.N. Segoviano Garfias, F. Avila Ramos, Flavonoids, phenolic content, and antioxidant activity of propolis from various areas of Guanajuato, Mexico, Food Sci. Technol. 38 (2018) 210–215. https://doi.org/10.1590/fst.29916.

[185] X. Xu, Y. Gao, G. Liu, Q. Wang, J. Zhao, Optimization of supercritical carbon dioxide

extraction of sea buckthorn (Hippophaë thamnoides L.) oil using response surface methodology, Lwt 41 (2008) 1223–1231. https://doi.org/10.1016/j.lwt.2007.08.002.

[186] A. Floegel, D.-O. Kim, S.-J. Chung, S.I. Koo, O.K. Chun, Comparison of ABTS/DPPH assays to measure antioxidant capacity in popular antioxidant-rich US foods, J. Food Compos. Anal. 24 (2011) 1043–1048. https://doi.org/10.1016/j.jfca.2011.01.008.

[187] P. Shah, H.A. Modi, Comparative Study of DPPH, ABTS and FRAP Assays for Determination of Antioxidant Activity, Int. J. Res. Appl. Sci. Eng. Technol. 3 (2015) 636–641. https://www.researchgate.net/publication/307464470.

[188] R. Amorati, L. Valgimigli, Advantages and limitations of common testing methods for antioxidants, Free Radic. Res. 49 (2015) 633–649. https://doi.org/10.3109/10715762.2014.996146.

[189] S. Purohit, D. Kalita, C.R. Barik, L. Sahoo, V. V. Goud, Evaluation of thermophysical, biochemical and antibacterial properties of unconventional vegetable oil from Northeast India, Mater. Sci. Energy Technol. 4 (2021) 81–91. https://doi.org/10.1016/j.mset.2021.01.004.

[190] J.R. Sarkis, A.P.F. Côrrea, I. Michel, A. Brandeli, I.C. Tessaro, L.D.F. Marczak, Evaluation of the phenolic content and antioxidant activity of different seed and nut cakes from the edible oil industry, JAOCS, J. Am. Oil Chem. Soc. 91 (2014) 1773–1782. https://doi.org/10.1007/s11746-014-2514-2.

[191] H. Chutia, C.L. Mahanta, Green ultrasound and microwave extraction of carotenoids from passion fruit peel using vegetable oils as a solvent: Optimization, comparison, kinetics, and thermodynamic studies, Innov. Food Sci. Emerg. Technol. 67 (2021) 102547. https://doi.org/10.1016/j.ifset.2020.102547.

[192] M. Goswami, K. Mondal, V. Prasannavenkadesan, V. Bodana, V. Katiyar, Effect of guar gum-chitosan composites edible coating functionalized with essential oils on the postharvest shelf life of Khasi mandarin at ambient condition, Int. J. Biol. Macromol. 254 (2024) 127489. https://doi.org/10.1016/j.ijbiomac.2023.127489.

[193] A.M. Duarte, J.S. Aquino, N. Queiroz, D.L.L. Dantas, G.S. Maciel, A.L. Souza, A comparative study of the thermal and oxidative stability of moringa oil with olive and canola oils, J. Therm. Anal. Calorim. 134 (2018) 1943–1952. https://doi.org/10.1007/s10973-018-7651-7.

[194] V.B. Borugadda, V. V. Goud, Thermal, oxidative and low temperature properties of methyl esters prepared from oils of different fatty acids composition: A comparative study, Thermochim. Acta 577 (2014) 33–40. https://doi.org/10.1016/j.tca.2013.12.008.

[195] G. Cakmak-Arslan, K. Gulsen, Evaluating the thermal stability of hazelnut oil in comparison with common edible oils in Turkey using ATR infrared spectroscopy, Vib. Spectrosc. 135 (2024) 103743. https://doi.org/10.1016/j.vibspec.2024.103743.

[196] Y. Lv, H. Yue, C. Tan, H. Liao, Characterization of a novel biodegradable active film with rose polyphenol extract and its application in edible oil packaging, Food Biosci. 63 (2025) 105784. https://doi.org/10.1016/j.fbio.2024.105784.

[197] F. Siano, S. Moccia, G. Picariello, G.L. Russo, G. Sorrentino, M. Di Stasio, F. La Cara, M.G. Volpe, Comparative study of chemical, biochemical characteristic and ATR-FTIR analysis of seeds, oil and flour of the edible Fedora cultivar hemp (Cannabis sativa L.), Molecules 24 (2019) 83. https://doi.org/10.3390/molecules24010083.

[198] P.S. Patil, C.G. Fernandes, S.C. Sawant, A.M. Lali, A.A. Odaneth, High-throughput system for carbohydrate analysis of lignocellulosic biomass, Biomass Convers. Biorefinery 13 (2023) 12889–12901. https://doi.org/10.1007/s13399-022-02304-8.

[199] N.N. Deshavath, M. Mohan, V.D. Veeranki, V. V. Goud, S.R. Pinnamaneni, T. Benarjee, Dilute acid pretreatment of sorghum biomass to maximize the hemicellulose hydrolysis with minimized levels of fermentative inhibitors for bioethanol production,

3 Biotech 7 (2017) 1–12. https://doi.org/10.1007/s13205-017-0752-3.

[200] S. Das, V. V. Goud, RSM-optimised slow pyrolysis of rice husk for bio-oil production and its upgradation, Energy 225 (2021) 120161. https://doi.org/10.1016/j.energy.2021.120161.

[201] P. Binod, K. Satyanagalakshmi, R. Sindhu, K.U. Janu, R.K. Sukumaran, A. Pandey, Short duration microwave assisted pretreatment enhances the enzymatic saccharification and fermentable sugar yield from sugarcane bagasse, Renew. Energy 37 (2012) 109–116. https://doi.org/10.1016/j.renene.2011.06.007.

[202] S. Shangdiar, Y.C. Lin, V.K. Ponnusamy, T.Y. Wu, Pretreatment of lignocellulosic biomass from sugar bagasse under microwave assisted dilute acid hydrolysis for biobutanol production, Bioresour. Technol. 361 (2022) 127724. https://doi.org/10.1016/j.biortech.2022.127724.

[203] N. Kordala, M. Lewandowska, W. Bednarski, Effect of the method for the elimination of inhibitors present in Miscanthus giganteus hydrolysates on ethanol production effectiveness, Biomass Convers. Biorefinery 13 (2023) 2089–2097. https://doi.org/10.1007/s13399-020-01255-2.

[204] G. Chaudhary, L.K. Singh, S. Ghosh, Alkaline pretreatment methods followed by acid hydrolysis of Saccharum spontaneum for bioethanol production, Bioresour. Technol. 124 (2012) 111–118. https://doi.org/10.1016/j.biortech.2012.08.067.

[205] N.N. Deshavath, V. V. Goud, V.D. Veeranki, Liquefaction of lignocellulosic biomass through biochemical conversion pathway: A strategic approach to achieve an industrial titer of bioethanol, Fuel 287 (2021) 119545. https://doi.org/10.1016/j.fuel.2020.119545.

[206] B. Sunkar, B. Bhukya, An Approach to Correlate Chemical Pretreatment to Digestibility Through Biomass Characterization by SEM, FTIR and XRD, Front. Energy Res. 10 (2022). https://doi.org/10.3389/fenrg.2022.802522.

[207] K. Sharma, S. Morla, K.C. Khaire, A. Thakur, V.S. Moholkar, S. Kumar, A. Goyal, Extraction, characterization of xylan from Azadirachta indica (neem) sawdust and production of antiproliferative xylooligosaccharides, Int. J. Biol. Macromol. 163 (2020) 1897–1907. https://doi.org/10.1016/j.ijbiomac.2020.09.086.

[208] K.C. Khaire, V.S. Moholkar, A. Goyal, Separation and characterization of cellulose from sugarcane tops and its saccharification by recombinant cellulolytic enzymes, Prep. Biochem. Biotechnol. 51 (2021) 811–820. https://doi.org/10.1080/10826068.2020.1861011.

[209] N.N. Deshavath, V.V. Dasu, V. V. Goud, P.S. Rao, Development of dilute sulfuric acid pretreatment method for the enhancement of xylose fermentability, Biocatal. Agric. Biotechnol. 11 (2017) 224–230. https://doi.org/10.1016/j.bcab.2017.07.012.

[210] R. Canadas, R. Martin-Sampedro, M. Gonzalez-Miquel, E.J. Gonzalez, I. Ballesteros, M.E. Eugenio, D. Ibarra, Microwave-assisted green solvents extraction as a sustainable approach to obtain antioxidants and enhance advanced bioethanol production from steam-exploded biomass, Renew. Energy 242 (2025) 122454. https://doi.org/10.1016/j.renene.2025.122454.

[211] P. Alam, O.M. Noman, R.N. Herqash, O.M. Almarfadi, A. Akhtar, A.S. Alqahtani, Response Surface Methodology (RSM)-Based Optimization of Ultrasound-Assisted Extraction of Sennoside A, Sennoside B, Aloe-Emodin, Emodin, and Chrysophanol from Senna alexandrina (Aerial Parts): HPLC-UV and Antioxidant Analysis, Molecules 27 (2022) 298. https://doi.org/10.3390/molecules27010298.

[212] M.S. Jovanovic, N. Krgovic, K. Savikin, J. Zivkovic, Ultrasound-Assisted Water Extraction of Gentiopicroside, Isogentisin, and Polyphenols from Willow Gentian "Dust" Supported by Hydroxypropyl-β-Cyclodextrin as Cage Molecules, Molecules 27 (2022) 7606. https://doi.org/10.3390/molecules27217606.

[213] S. Sahin, R. Samli, Optimization of olive leaf extract obtained by ultrasound-assisted extraction with response surface methodology, Ultrason. Sonochem. 20 (2013) 595–602. https://doi.org/10.1016/j.ultsonch.2012.07.029.

[214] X. Wang, X. Liu, N. Shi, Z. Zhang, Y. Chen, M. Yan, Y. Li, Erratum to "Response surface methodology optimization and HPLC-ESI-QTOF-MS/MS analysis on ultrasonic-assisted extraction of phenolic compounds from okra (Abelmoschus esculentus) and their antioxidant activity" (Food Chemistry (2023) 405(PB), (S03088146220, Food Chem. 428 (2023) 134966. https://doi.org/10.1016/j.foodchem.2023.135922.

[215] M. Sarfarazi, Q. Rajabzadeh, R. Tavakoli, S.A. Ibrahim, S.M. Jafari, Ultrasound-assisted extraction of saffron bioactive compounds; separation of crocins, picrocrocin, and safranal optimized by artificial bee colony, Ultrason. Sonochem. 86 (2022) 105971. https://doi.org/10.1016/j.ultsonch.2022.105971.

[216] B.B. Ismail, M. Guo, Y. Pu, W. Wang, X. Ye, D. Liu, Valorisation of baobab (Adansonia digitata) seeds by ultrasound assisted extraction of polyphenolics. Optimisation and comparison with conventional methods, Ultrason. Sonochem. 52 (2019) 257–267. https://doi.org/10.1016/j.ultsonch.2018.11.023.

[217] K. Kumar, S. Srivastav, V.S. Sharanagat, Ultrasound assisted extraction (UAE) of bioactive compounds from fruit and vegetable processing by-products: A review, Ultrason. Sonochem. 70 (2021) 105325. https://doi.org/10.1016/j.ultsonch.2020.105325.

[218] A.T. Khanyile, J.E. Andrew, V. Paul, B.B. Sithole, A comparative study of supercritical fluid extraction and accelerated solvent extraction of lipophilic compounds from lignocellulosic biomass, Sustain. Chem. Pharm. 26 (2022) 100608. https://doi.org/10.1016/j.scp.2022.100608.

[219] M. Bimakr, R.A. Rahman, A. Ganjloo, F.S. Taip, L.M. Salleh, M.Z.I. Sarker, Optimization of Supercritical Carbon Dioxide Extraction of Bioactive Flavonoid Compounds from Spearmint (Mentha spicata L.) Leaves by Using Response Surface Methodology, Food Bioprocess Technol. 5 (2012) 912–920. https://doi.org/10.1007/s11947-010-0504-4.

[220] P.T. Vo, H.M.N. Chieng, Q.D. Nguyen, Ultrasonic-assisted Processes to Recover Phenolics and Flavonoids from Passion Fruit Peels, Chem. Eng. Trans. 108 (2024) 13–18. https://doi.org/10.3303/CET24108003.

[221] W. Wang, Y.T. Gao, J.W. Wei, Y.F. Chen, Q.L. Liu, H.M. Liu, Optimization of ultrasonic cellulase-assisted extraction and antioxidant activity of natural polyphenols from passion fruit, Molecules 26 (2021) 2494. https://doi.org/10.3390/molecules26092494.

[222] D.T. Vitor Pereira, F.M. Barrales, E. Pereira, J. Vigano, A.H. Iglesias, F.G. Reyes Reyes, J. Martinez, Phenolic compounds from passion fruit rinds using ultrasound-assisted pressurized liquid extraction and nanofiltration, J. Food Eng. 325 (2022) 110977. https://doi.org/10.1016/j.jfoodeng.2022.110977.

[223] M.C.C. Macedo, V.T. da V. Correia, V.D.M. Silva, D.T.V. Pereira, R. Augusti, J.O.F. Melo, C.V. Pires, A.C.C.F.F. de Paula, C.A. Fante, Development and Characterization of Yellow Passion Fruit Peel Flour (Passiflora edulis f. flavicarpa), Metabolites 13 (2023) 684. https://doi.org/10.3390/metabo13060684.

[224] D.A. Oliveira, M. Angonese, C. Gomes, S.R.S. Ferreira, Valorization of passion fruit (Passiflora edulis sp.) by-products: Sustainable recovery and biological activities, J. Supercrit. Fluids 111 (2016) 55–62. https://doi.org/10.1016/j.supflu.2016.01.010.

[225] X.Y. Liu, H. Ou, J. Zuo, H. Gregersen, Supercritical CO2 extraction of total flavonoids from Iberis amara assisted by ultrasound, J. Supercrit. Fluids 184 (2022) 105581. https://doi.org/10.1016/j.supflu.2022.105581.

[226] D.T.V. Pereira, G.L. Zabot, F.G.R. Reyes, A.H. Iglesias, J. Martinez, Integration of pressurized liquids and ultrasound in the extraction of bioactive compounds from passion fruit rinds: Impact on phenolic yield, extraction kinetics and technical-economic evaluation, Innov. Food Sci. Emerg. Technol. 67 (2021) 102549. https://doi.org/10.1016/j.ifset.2020.102549.

[227] W.Z. Lee, S.K. Chang, H.E. Khoo, C.M. Sia, H.S. Yim, Influence of different extraction conditions on antioxidant properties of soursop peel, Acta Sci. Pol. Technol. Aliment. 15 (2016) 419–428. https://doi.org/10.17306/J.AFS.2016.4.40.

[228] M. Hou, Y. Zhou, C. Lin, J. Shi, H. Hou, Y. Ma, L. Zhu, Z. Bian, Green valorization of Chaenomelis Fructus agro-industrial by-products as a source of phenolics: Ultrasound-assisted extraction, adsorptive enrichment and quality control, Food Chem. 472 (2025) 142908. https://doi.org/10.1016/j.foodchem.2025.142908.

[229] F. Brahmi, F. Blando, R. Sellami, S. Mehdi, L. De Bellis, C. Negro, H. Haddadi-Guemghar, K. Madani, L. Makhlouf-Boulekbache, Optimization of the conditions for ultrasound-assisted extraction of phenolic compounds from Opuntia ficus-indica [L.] Mill. flowers and comparison with conventional procedures, Ind. Crops Prod. 184 (2022) 114977. https://doi.org/10.1016/j.indcrop.2022.114977.

[230] A. Asiimwe, J.B. Kigozi, E. Baidhe, J.H. Muyonga, Optimization of refractance window drying conditions for passion fruit puree, Lwt 154 (2022) 112742. https://doi.org/10.1016/j.lwt.2021.112742.

[231] G.K. Kobo, T. Kaseke, O.A. Fawole, Valorization of passion fruit peel for potential application in food preservation: effect of carriers on quality of encapsulated powders, Acta Hortic. 1349 (2022) 611–617. https://doi.org/10.17660/ActaHortic.2022.1349.79.

[232] N. Milicevic, P. Kojic, M. Sakac, A. Misan, J. Kojic, C. Perussello, V. Banjac, M. Pojic, B. Tiwari, Kinetic modelling of ultrasound-assisted extraction of phenolics from cereal brans, Ultrason. Sonochem. 79 (2021) 105761. https://doi.org/10.1016/j.ultsonch.2021.105761.

[233] T. Barbosa Santos, F.P. de Araujo, A.F. Neto, S.T. de Freitas, J. de Souza Araújo, S.B. de Oliveira Vilar, A.J. Brito Araújo, M.S. Lima, Phytochemical Compounds and Antioxidant Activity of the Pulp of Two Brazilian Passion Fruit Species: Passiflora Cincinnata Mast. And Passiflora Edulis Sims, Int. J. Fruit Sci. 21 (2021) 255–269. https://doi.org/10.1080/15538362.2021.1872050.

[234] S.M. Niknam, M. Kashaninejad, I. Escudero, M.T. Sanz, S. Beltran, J.M. Benito, Valorization of olive mill solid residue through ultrasound-assisted extraction and phenolics recovery by adsorption process, J. Clean. Prod. 316 (2021) 128340. https://doi.org/10.1016/j.jclepro.2021.128340.

[235] F. Berkani, M.L. Serralheiro, F. Dahmoune, A. Ressaissi, N. Kadri, H. Remini, Ultrasound Assisted Extraction of Phenolic Compounds from a Jujube By-Product with Valuable Bioactivities, Processes 8 (2020) 1441. https://doi.org/10.3390/pr8111441.

[236] T. Martinez-Ramos, J. Benedito-Fort, N.J. Watson, I.I. Ruiz-Lopez, G. Che-Galicia, E. Corona-Jimenez, Effect of solvent composition and its interaction with ultrasonic energy on the ultrasound-assisted extraction of phenolic compounds from Mango peels (Mangifera indica L.), Food Bioprod. Process. 122 (2020) 41–54. https://doi.org/10.1016/j.fbp.2020.03.011.

[237] J. Vigano, G.L. Zabot, J. Martinez, Supercritical fluid and pressurized liquid extractions of phytonutrients from passion fruit by-products: Economic evaluation of sequential multi-stage and single-stage processes, J. Supercrit. Fluids 122 (2017) 88–98. https://doi.org/10.1016/j.supflu.2016.12.006.

[238] K. Borah, R. Kumar, V. V. Goud, Extraction of Phenolics from Yellow Passion Fruit Rind Using Supercritical Carbon Dioxide Extraction, in: Agro Food Process. Technol.

Proc. NERC 2022, Springer, 2023: pp. 141–156. https://doi.org/10.1007/978-981-19-9704-4_8.

[239] M.D. Macias-Sanchez, C. Mantell, M. Rodriguez, E. Martinez de la Ossa, L.M. Lubian, O. Montero, Comparison of supercritical fluid and ultrasound-assisted extraction of carotenoids and chlorophyll a from Dunaliella salina, Talanta 77 (2009) 948–952. https://doi.org/10.1016/j.talanta.2008.07.032.

[240] P. Setyopratomo, Extraction of phenolic compounds from green tea using ethanol, ARPN J. Eng. Appl. Sci. 9 (2014) 1516–1521.

[241] J. Vigano, J.P. Coutinho, D.S. Souza, N.A.F. Baroni, H.T. Godoy, J.A. Macedo, J. Martinez, Exploring the selectivity of supercritical CO2 to obtain nonpolar fractions of passion fruit bagasse extracts, J. Supercrit. Fluids 110 (2016) 1–10. https://doi.org/10.1016/j.supflu.2015.12.001.

[242] L.C. dos Santos, J.C.F. Johner, E. Scopel, P.V.A. Pontes, A.P.B. Ribeiro, G.L. Zabot, E.A.C. Batista, M.A.A. Meireles, J. Martinez, Integrated supercritical CO2 extraction and fractionation of passion fruit (Passiflora edulis Sims) by-products, J. Supercrit. Fluids 168 (2021) 105093. https://doi.org/10.1016/j.supflu.2020.105093.

[243] A. Mehmood, S. Javid, M.F. Khan, K.S. Ahmad, A. Mustafa, In vitro total phenolics, total flavonoids, antioxidant and antibacterial activities of selected medicinal plants using different solvent systems, BMC Chem. 16 (2022) 64. https://doi.org/10.1186/s13065-022-00858-2.

[244] S. Losada-Barreiro, C. Bravo-Diaz, Free radicals and polyphenols: The redox chemistry of neurodegenerative diseases, Eur. J. Med. Chem. 133 (2017) 379–402. https://doi.org/10.1016/j.ejmech.2017.03.061.

[245] R.M. Han, J.P. Zhang, L.H. Skibsted, Reaction dynamics of flavonoids and carotenoids as antioxidants, Molecules 17 (2012) 2140–2160. https://doi.org/10.3390/molecules17022140.

[246] S. Purohit, C.R. Barik, D. Kalita, L. Sahoo, V. V. Goud, Exploration of nutritional, antioxidant and antibacterial properties of unutilized rind and seed of passion fruit from Northeast India, J. Food Meas. Charact. 15 (2021) 3153–3167. https://doi.org/10.1007/s11694-021-00899-6.

[247] Q. Cao, J. Teng, B. Wei, L. Huang, N. Xia, Phenolic compounds, bioactivity, and bioaccessibility of ethanol extracts from passion fruit peel based on simulated gastrointestinal digestion, Food Chem. 356 (2021) 129682. https://doi.org/10.1016/j.foodchem.2021.129682.

[248] A.C. de Oliveira, I.B. Valentim, C.A. Silva, E.J.H. Bechara, M.P. de Barros, C.M. Mano, M.O.F. Goulart, Total phenolic content and free radical scavenging activities of methanolic extract powders of tropical fruit residues, Food Chem. 115 (2009) 469–475. https://doi.org/10.1016/j.foodchem.2008.12.045.

[249] F. Ohikhena, O. Wintola, A.J. Afolayan, Quantitative Phytochemical Constituents and Antioxidant Activities of the Mistletoe, Phragmanthera capitata (Sprengel) Balle Extracted with Different Solvents, Pharmacognosy Res. 10 (2018) 16–23. https://doi.org/10.4103/pr.pr_65_17.

[250] D. Da Silva Francischini, A.P. Lopes, M.L. Segatto, A.M. Stahl, V.G. Zuin, Development and application of green and sustainable analytical methods for flavonoid extraction from Passiflora waste, BMC Chem. 14 (2020) 56. https://doi.org/10.1186/s13065-020-00710-5.

[251] E. Giambanelli, A.M. Gomez-Caravaca, A. Ruiz-Torralba, E.J. Guerra-Hernandez, J.G. Figueroa-Hurtado, B. Garcia-Villanova, V. Verardo, New advances in the determination of free and bound phenolic compounds of banana passion fruit pulp (Passiflora tripartita, var. mollissima (kunth) l.h. bailey) and their in vitro antioxidant and hypoglycemic

capacities, Antioxidants 9 (2020) 1–17. https://doi.org/10.3390/antiox9070628.

[252] S. Saravanan, T. Parimelazhagan, In vitro antioxidant, antimicrobial and anti-diabetic properties of polyphenols of Passiflora ligularis Juss. fruit pulp, Food Sci. Hum. Wellness 3 (2014) 56–64. https://doi.org/10.1016/j.fshw.2014.05.001.

[253] M.M. Abdelshaheed, I.M. Fawzy, H.I. El-Subbagh, K.M. Youssef, Piperidine nucleus in the field of drug discovery, Futur. J. Pharm. Sci. 7 (2021) 1–11. https://doi.org/10.1186/s43094-021-00335-y.

[254] A. Kumar, M. Asthana, P. Roy, S. Amdekar, V. Singh, Phytochemistry and pharmacology of Pyrostegia venusta: A plant of family bignoniaceae, Int. J. Phytomedicine 5 (2013) 257–261.

[255] C.O. Eleazu, K.C. Eleazu, Nutrient Composition, Antioxidant Capacity and Natural Products in Livingstone Potato (Plectranthus esculentus), J. Food Process. Preserv. 39 (2015) 3050–3058. https://doi.org/10.1111/jfpp.12570.

[256] B.S. Matada, R. Pattanashettar, N.G. Yernale, Corrigendum to "A comprehensive review on the biological interest of quinoline and its derivatives" [Bioorg. Med. Chem. 32 (2021) 115973](S0968089620308038)(10.1016/j.bmc.2020.115973), Bioorganic Med. Chem. 37 (2021) 115973. https://doi.org/10.1016/j.bmc.2021.116098.

[257] S.A. Adefegha, B.M. Okeke, G. Oboh, Antioxidant properties of eugenol, butylated hydroxylanisole, and butylated hydroxyl toluene with key biomolecules relevant to Alzheimer's diseases—In vitro, J. Food Biochem. 45 (2021) e13276. https://doi.org/10.1111/jfbc.13276.

[258] S. S., K. K., D.S. M., Pharmacognostic Standardisation of Cayratia Pedata (Lam.) Gagnep. Var. Glabra Gamble–an Endemic and Endangered Medicinal Climber in Thiashola, Nilgiris, Int. J. Pharm. Pharm. Sci. 9 (2017) 57. https://doi.org/10.22159/ijpps.2017v9i12.17352.

[259] M.J. Simirgiotis, G. Schmeda-Hirschmann, J. Borquez, E.J. Kennelly, The Passiflora tripartita (banana passion) fruit: A source of bioactive flavonoid C-glycosides isolated by HSCCC and characterized by HPLC-DAD-ESI/MS/MS, Molecules 18 (2013) 1672–1692. https://doi.org/10.3390/molecules18021672.

[260] S. Shanmugam, R.D.D. Sandes, M. Rajan, M.T.S.L. Neta, B. dos Santos Lima, M.J.M. de Jesus, M. Denadai, N. Narain, P. Thangaraj, M.R. Serafini, L.J. Quintans-Junior, A.A. de Souza Araujo, Volatile profiling and UHPLC-QqQ-MS/MS polyphenol analysis of Passiflora leschenaultii DC. fruits and its anti-radical and anti-diabetic properties, Food Res. Int. 133 (2020) 109202. https://doi.org/10.1016/j.foodres.2020.109202.

[261] D.A. Oliveira, M. Angonese, S.R.S. Ferreira, C.L. Gomes, Nanoencapsulation of passion fruit by-products extracts for enhanced antimicrobial activity, Food Bioprod. Process. 104 (2017) 137–146. https://doi.org/10.1016/j.fbp.2017.05.009.

[262] V.M. Lavenburg, K.A. Rosentrater, S. Jung, Extraction methods of oils and phytochemicals from seeds and their environmental and economic impacts, Processes 9 (2021) 1839. https://doi.org/10.3390/pr9101839.

[263] A.M. Farias-Campomanes, M.A. Rostagno, M.A.A. Meireles, Production of polyphenol extracts from grape bagasse using supercritical fluids: Yield, extract composition and economic evaluation, J. Supercrit. Fluids 77 (2013) 70–78. https://doi.org/10.1016/j.supflu.2013.02.006.

[264] M. Lopeda-Correa, B.E. Valdes-Duque, J.F. Osorio-Tobon, Ultrasound-Assisted Extraction of Phenolic Compounds from Adenaria floribunda Stem: Economic Assessment, Foods 11 (2022) 2904. https://doi.org/10.3390/foods11182904.

[265] M. Viana da Silva, M.R.C. Santos, I.R. Alves Silva, E.B. Macedo Viana, D.A. Dos Anjos, I.A. Santos, N.G. Barbosa de Lima, C. Wobeto, N. Jorge, S.C.D.S. Lannes,

Synthetic and Natural Antioxidants Used in the Oxidative Stability of Edible Oils: An Overview, Food Rev. Int. 38 (2022) 349–372. https://doi.org/10.1080/87559129.2020.1869775.

[266] M. Kozlowska, E. Gruczynska, Comparison of the oxidative stability of soybean and sunflower oils enriched with herbal plant extracts, Chem. Pap. 72 (2018) 2607–2615. https://doi.org/10.1007/s11696-018-0516-5.

[267] L.A. Gilmore, S.F. Crouse, A. Carbuhn, J. Klooster, J.A.E. Calles, T. Meade, S.B. Smith, Exercise attenuates the increase in plasma monounsaturated fatty acids and high-density lipoprotein cholesterol but not high-density lipoprotein 2b cholesterol caused by high-oleic ground beef in women, Nutr. Res. 33 (2013) 1003–1011. https://doi.org/10.1016/j.nutres.2013.09.003.

[268] M. Tzanova, V. Atanasov, Z. Yaneva, D. Ivanova, T. Dinev, Selectivity of Current Extraction Techniques for Flavonoids from Plant Materials, Processes 8 (2020) 1222. https://doi.org/10.3390/pr8101222.

[269] J. Nie, D. Chen, J. Ye, Y. Lu, Z. Dai, Optimization and kinetic modeling of ultrasonic-assisted extraction of fucoxanthin from edible brown algae Sargassum fusiforme using green solvents, Ultrason. Sonochem. 77 (2021) 105671. https://doi.org/10.1016/j.ultsonch.2021.105671.

[270] L.E. Ordonez-Santos, J. Martinez-Giron, D.X. Rodriguez-Rodriguez, Extraction of total carotenoids from peach palm fruit (Bactris gasipaes) peel by means of ultrasound application and vegetable oil, DYNA 86 (2019) 91–96. https://doi.org/10.15446/dyna.v85n207.74840.

[271] O.O. Fasina, Z. Colley, Viscosity and specific heat of vegetable oils as a function of temperature: 35°C to 180°C, Int. J. Food Prop. 11 (2008) 738–746. https://doi.org/10.1080/10942910701586273.

[272] S. Lara-Abia, A. Gomez-Maqueo, J. Welti-Chanes, M.P. Cano, High Hydrostatic Pressure-Assisted Extraction of Carotenoids from Papaya (Carica papaya L. cv. Maradol) Tissues Using Soybean and Sunflower Oil as Potential Green Solvents, Food Eng. Rev. 13 (2021) 660–675. https://doi.org/10.1007/s12393-021-09289-6.

[273] D. Pingret, G. Durand, A.S. Fabiano-Tixier, A. Rockenbauer, C. Ginies, F. Chemat, Degradation of edible oil during food processing by ultrasound: Electron paramagnetic resonance, physicochemical, and sensory appreciation, J. Agric. Food Chem. 60 (2012) 7761–7768. https://doi.org/10.1021/jf301286f.

[274] A.A. De Boer, A. Ismail, K. Marshall, G. Bannenberg, K.L. Yan, W.J. Rowe, Examination of marine and vegetable oil oxidation data from a multi-year, third-party database, Food Chem. 254 (2018) 249–255. https://doi.org/10.1016/j.foodchem.2018.01.180.

[275] F. Chemat, I. Grondin, P. Costes, L. Moutoussamy, A.S.C. Sing, J. Smadja, High power ultrasound effects on lipid oxidation of refined sunflower oil, Ultrason. Sonochem. 11 (2004) 281–285. https://doi.org/10.1016/j.ultsonch.2003.07.004.

[276] B. Hernandez-Santos, J. Rodriguez-Miranda, E. Herman-Lara, J.G. Torruco-Uco, R. Carmona-Garcia, J.M. Juarez-Barrientos, R. Chavez-Zamudio, C.E. Martinez-Sanchez, Effect of oil extraction assisted by ultrasound on the physicochemical properties and fatty acid profile of pumpkin seed oil (Cucurbita pepo), Ultrason. Sonochem. 31 (2016) 429–436. https://doi.org/10.1016/j.ultsonch.2016.01.029.

[277] K. Borah, R. Kumar, S. Purohit, V. V. Goud, Comparative study on phytochemical extraction from passion fruit wastes using ultrasound and supercritical fluid extraction, J. Food Meas. Charact. (2025). https://doi.org/10.1007/s11694-025-03150-8.

[278] R.E. Mutha, A.U. Tatiya, S.J. Surana, Flavonoids as natural phenolic compounds and their role in therapeutics: an overview, Futur. J. Pharm. Sci. 7 (2021) 1–13.

https://doi.org/10.1186/s43094-020-00161-8.

[279] K.M. Ku, H.S. Kim, S.K. Kim, Y.-H. Kang, Correlation Analysis Between Antioxidant Activity and Phytochemicals in Korean Colored Corns Using Principal Component Analysis, J. Agric. Sci. 6 (2014) 1. https://doi.org/10.5539/jas.v6n4p1.

[280] L.P. Barragan-Martinez, L. Alvarez-Poblano, E.J. Vernon-Carter, J. Alvarez-Ramirez, Effects of β-carotene on the color, textural, rheological and structural properties of canola oil/beeswax oleogel, J. Food Meas. Charact. 16 (2022) 3946–3956. https://doi.org/10.1007/s11694-022-01449-4.

[281] L. Botella, F. Bimbela, L. Martín, J. Arauzo, J.L. Sánchez, Oxidation stability of biodiesel fuels and blends using the Rancimat and PetroOXY methods. Effect of 4-allyl-2,6-dimethoxyphenol and catechol as biodiesel additives on oxidation stability, Front. Chem. 2 (2014) 43. https://doi.org/10.3389/fchem.2014.00043.

[282] A. Szterk, M. Roszko, E. Sosińska, D. Derewiaka, P.P. Lewicki, Chemical composition and oxidative stability of selected plant oils, JAOCS, J. Am. Oil Chem. Soc. 87 (2010) 637–645. https://doi.org/10.1007/s11746-009-1539-4.

[283] N. Fakourelis, E.C. LEE, D.B. MIN, Effects of Chlorophyll and β-Carotene on the Oxidation Stability of Olive Oil, J. Food Sci. 52 (1987) 234–235. https://doi.org/10.1111/j.1365-2621.1987.tb14018.x.

[284] A. Roedig-Penman, M.H. Gordon, Antioxidant properties of myricetin and quercetin in oil and emulsions, J. Am. Oil Chem. Soc. 75 (1998) 169–180. https://doi.org/10.1007/s11746-998-0029-4.

[285] M. Koketsu, Y. Satoh, ANTIOXIDATIVE ACTIVITY OF GREEN TEA POLYPHENOLS IN EDIBLE OILS, J. Food Lipids 4 (1997) 1–9. https://doi.org/10.1111/j.1745-4522.1997.tb00076.x.

[286] B.N. Shyamala, S. Gupta, A. Jyothi Lakshmi, J. Prakash, Leafy vegetable extracts—antioxidant activity and effect on storage stability of heated oils, Innov. Food Sci. Emerg. Technol. 6 (2005) 239–245. https://doi.org/10.1016/j.ifset.2004.12.002.

[287] A.A. Abdelazim, A. Mahmoud, M.F. Ramadan-Hassanien, Oxidative stability of vegetable oils as affected by sesame extracts during accelerated oxidative storage, J. Food Sci. Technol. 50 (2013) 868–878. https://doi.org/10.1007/s13197-011-0419-8.

[288] A.R. Rao, R. Sarada, G.A. Ravishankar, Stabilization of astaxanthin in edible oils and its use as an antioxidant, J. Sci. Food Agric. 87 (2007) 957–965. https://doi.org/10.1002/jsfa.2766.

[289] H. Rahmania, S. Kato, K. Sawada, C. Hayashi, H. Hashimoto, S. Nakajima, Y. Otoki, J. Ito, K. Nakagawa, Revealing the thermal oxidation stability and its mechanism of rice bran oil, Sci. Rep. 10 (2020) 14091. https://doi.org/10.1038/s41598-020-71020-y.

[290] C.C. Garcia, P.I.B.M. Franco, T.O. Zuppa, N.R.A. Filho, M.I.G. Leles, Thermal stability studies of some cerrado plant oils, J. Therm. Anal. Calorim. 87 (2007) 645–648. https://doi.org/10.1007/s10973-006-7769-x.

[291] J. Li, J. Liu, X. Sun, Y. Liu, The mathematical prediction model for the oxidative stability of vegetable oils by the main fatty acids composition and thermogravimetric analysis, Lwt 96 (2018) 51–57. https://doi.org/10.1016/j.lwt.2018.05.003.

[292] G. Litwinienko, T. Kasprzycka-Guttman, The influence of some chain-breaking antioxidants on thermal-oxidative decomposition of linolenic acid, J. Therm. Anal. Calorim. 54 (1998) 203–210. https://doi.org/10.1023/A:1010189507864.

[293] B. Qi, Q. Zhang, X. Sui, Z. Wang, Y. Li, L. Jiang, Differential scanning calorimetry study - Assessing the influence of composition of vegetable oils on oxidation, Food Chem. 194 (2016) 601–607. https://doi.org/10.1016/j.foodchem.2015.07.148.

[294] J. Salimon, N. Salih, E. Yousif, Improvement of pour point and oxidative stability of

synthetic ester basestocks for biolubricant applications, Arab. J. Chem. 5 (2012) 193–200. https://doi.org/10.1016/j.arabjc.2010.09.001.

[295] M. Wang, J. Chen, B. Jing, L. Zhang, Y. Dong, X. Yu, Analysis of Reaction Kinetics of Edible Oil Oxidation at Ambient Temperature by FTIR Spectroscopy, Eur. J. Lipid Sci. Technol. 122 (2020). https://doi.org/10.1002/ejlt.201900302.

[296] J. Shang, X. Wu, K. Hu, Z. Huyan, Q. Li, X. Yu, A simple and practical method to determine peroxide values in edible oils via infrared quartz cuvette-based Fourier transform infrared spectroscopy, Anal. Methods 10 (2018) 3675–3679. https://doi.org/10.1039/C8AY00594J.

[297] A. Rohman, Y.B. Che Man, Quantification and classification of corn and sunflower oils as adulterants in olive oil using chemometrics and FTIR spectra, Sci. World J. 2012 (2012). https://doi.org/10.1100/2012/250795.

[298] R. Jamwal, Amit, S. Kumari, S. Sharma, S. Kelly, A. Cannavan, D.K. Singh, Recent trends in the use of FTIR spectroscopy integrated with chemometrics for the detection of edible oil adulteration, Vib. Spectrosc. 113 (2021) 103222. https://doi.org/10.1016/j.vibspec.2021.103222.

[299] A. Rohman, R. Ariani, Authentication of nigella sativa seed oil in binary and ternary mixtures with corn oil and soybean oil using FTIR spectroscopy coupled with partial least square, Sci. World J. 2013 (2013). https://doi.org/10.1155/2013/740142.

[300] J.L.F. Alves, J.C.G. da Silva, G.D. Mumbach, M. Di Domenico, V.F. da Silva Filho, R.F. de Sena, R.A.F. Machado, C. Marangoni, Insights into the bioenergy potential of jackfruit wastes considering their physicochemical properties, bioenergy indicators, combustion behaviors, and emission characteristics, Renew. Energy 155 (2020) 1328–1338. https://doi.org/10.1016/j.renene.2020.04.025.

[301] P.D. Pathak, S.A. Mandavgane, B.D. Kulkarni, Fruit peel waste: Characterization and its potential uses, Curr. Sci. 113 (2017) 444–454. https://doi.org/10.18520/cs/v113/i03/444-454.

[302] Y.L. Lin, N.Y. Zheng, C.H. Hsu, Torrefaction of fruit peel waste to produce environmentally friendly biofuel, J. Clean. Prod. 284 (2021) 124676. https://doi.org/10.1016/j.jclepro.2020.124676.

[303] S.J. Klausen, A.B. Falck-Ytter, K.O. Strætkvern, C. Martin, Evaluation of the Extraction of Bioactive Compounds and the Saccharification of Cellulose as a Route for the Valorization of Spent Mushroom Substrate, Molecules 28 (2023) 5140. https://doi.org/10.3390/molecules28135140.

[304] B.R. Patra, S. Nanda, A.K. Dalai, V. Meda, Slow pyrolysis of agro-food wastes and physicochemical characterization of biofuel products, Chemosphere 285 (2021) 131431. https://doi.org/10.1016/j.chemosphere.2021.131431.

[305] M. Ahi, M. Azin, S.A. Shojaosadati, E. Vasheghani-Farahani, M. Nosrati, Optimization of sugarcane bagasse hydrolysis by microwave-assisted pretreatment for bioethanol production, Chem. Eng. Technol. 36 (2013) 1997–2005. https://doi.org/10.1002/ceat.201300233.

[306] F.R. Amin, H. Khalid, H. Zhang, S. Rahman, R. Zhang, G. Liu, C. Chen, Pretreatment methods of lignocellulosic biomass for anaerobic digestion, AMB Express 7 (2017) 1–12. https://doi.org/10.1186/s13568-017-0375-4.

[307] S. Imman, T. Kreetachat, P. Khongchamnan, N. Laosiripojana, V. Champreda, K. Suwannahong, C. Sakulthaew, C. Chokejaroenrat, N. Suriyachai, Optimization of sugar recovery from pineapple leaves by acid-catalyzed liquid hot water pretreatment for bioethanol production, Energy Reports 7 (2021) 6945–6954. https://doi.org/10.1016/j.egyr.2021.10.076.

[308] S. Khamtib, P. Plangklang, A. Reungsang, Optimization of fermentative hydrogen

production from hydrolysate of microwave assisted sulfuric acid pretreated oil palm trunk by hot spring enriched culture, Int. J. Hydrogen Energy 36 (2011) 14204–14216. https://doi.org/10.1016/j.ijhydene.2011.05.117.

[309] K. fee Chong, Y. Lu, Y. Han, Y. Shen, S. Thangalazhy-Gopakumar, S. Shi, L. Han, A Review on the Over-liming Detoxification of Lignocellulosic Biomass Prehydrolysate for Bioethanol Production, Appl. Biochem. Biotechnol. (2025). https://doi.org/10.1007/s12010-025-05212-5.

[310] J.-H. Park, H.-C. Cheon, J.-J. Yoon, H.-D. Park, S.-H. Kim, Optimization of batch dilute-acid hydrolysis for biohydrogen production from red algal biomass, Int. J. Hydrogen Energy 38 (2013) 6130–6136. https://doi.org/10.1016/j.ijhydene.2013.01.050.

[311] Z.-T. Zhao, J. Ding, J.-W. Pang, M.-Y. Bao, G. Luo, B.-Y. Wang, B.-F. Liu, L.-Y. Zhang, N.-Q. Ren, S.-S. Yang, Pretreatments of lignocellulosic biomass for biohydrogen biorefinery: Recent progress, techno-economic feasibility and prospectives, Crit. Rev. Environ. Sci. Technol. (2025) 1–27. https://doi.org/10.1080/10643389.2025.2484892.

[312] Z. Tan, X. Li, C. Yang, H. Liu, J.J. Cheng, Inhibition and disinhibition of 5-hydroxymethylfurfural in anaerobic fermentation: A review, Chem. Eng. J. 424 (2021) 130560. https://doi.org/10.1016/j.cej.2021.130560.

[313] E. Jayex Panakkal, M. Sriariyanun, J. Ratanapoompinyo, P. Yasurin, K. Cheenkachorn, W. Rodiahwati, P. Tantayotai, Influence of Sulfuric Acid Pretreatment and Inhibitor of Sugarcane Bagasse on the Production of Fermentable Sugar and Ethanol, Appl. Sci. Eng. Prog. 15 (2022). https://doi.org/10.14416/j.asep.2021.07.006.

[314] Q. Lyu, R.A. Dar, F. Baganz, A. Smoliński, A.-H.M. Rasmey, R. Liu, L. Zhang, Effects of Lignocellulosic Biomass-Derived Hydrolysate Inhibitors on Cell Growth and Lipid Production During Microbial Fermentation of Oleaginous Microorganisms—A Review, Fermentation 11 (2025) 121. https://doi.org/10.3390/fermentation11030121.

[315] J. du Pasquier, G. Paes, P. Perre, Chemical degradation, yields, and interactions of lignocellulosic compounds of poplar wood during dilute acid pretreatment assessed from a comprehensive data set, Ind. Crops Prod. 215 (2024) 118643. https://doi.org/10.1016/j.indcrop.2024.118643.

[316] T. Promta, P. Thonkamdee, K. Sasujit, Optimization of overliming detoxification of sugarcane bagasse hydrolysate by using response surface methodology for bio-ethanol production, Maejo Int. J. Energy Environ. Commun. 6 (2024) 1–10. https://doi.org/https://doi.org/10.54279/mijeec.v6i1.253749.

[317] G. Liu, Z. Yi, J. Li, L. Yang, Y. Fang, A. Du, K. He, H. Zhao, Y. Jin, Detoxification with resin promotes the shift from acidogenesis to solventogenesis and prevents acid crash during butanol fermentation from wheat straw, Biomass Convers. Biorefinery 14 (2024) 16857–16866. https://doi.org/10.1007/s13399-023-04023-0.

[318] L. Canilha, W. Carvalho, M.D.G. De Almeida Felipe, J.B. De Almeida E Silva, M. Giulietti, Ethanol production from sugarcane bagasse hydrolysate using Pichia stipitis, Appl. Biochem. Biotechnol. 161 (2010) 84–92. https://doi.org/10.1007/s12010-009-8792-8.

[319] H. Nouri, M. Ahi, M. Azin, S.L. Mousavi Gargari, Detoxification vs. adaptation to inhibitory substances in the production of bioethanol from sugarcane bagasse hydrolysate: A case study, Biomass and Bioenergy 139 (2020) 105629. https://doi.org/10.1016/j.biombioe.2020.105629.

[320] J. Andary, N. Ouaini, R. Abou-Khalil, Diluted Acid Hydrolysate of Olive Stones: Overliming and Biomass Fermentation, Fermentation 11 (2025) 100. https://doi.org/10.3390/fermentation11020100.

[321] A.P. Adebule, I.A. Sanusi, E.B.G. Kana, Nano-based surface adsorption detoxification of process inhibitors for improved bioethanol productivity, Bioresour. Technol. Reports 25 (2024) 101783. https://doi.org/10.1016/j.biteb.2024.101783.

[322] H. Gunan Yucel, Z. Aksu, Ethanol fermentation characteristics of Pichia stipitis yeast from sugar beet pulp hydrolysate: Use of new detoxification methods, Fuel 158 (2015) 793–799. https://doi.org/10.1016/j.fuel.2015.06.016.

[323] A.K. Chandel, O. V. Singh, M.L. Narasu, L.V. Rao, Bioconversion of Saccharum spontaneum (wild sugarcane) hemicellulosic hydrolysate into ethanol by mono and co-cultures of Pichia stipitis NCIM3498 and thermotolerant Saccharomyces cerevisiae-VS 3, N. Biotechnol. 28 (2011) 593–599. https://doi.org/10.1016/j.nbt.2010.12.002.

[324] C. Martin, M. Galbe, C.F. Wahlbom, B. Hahn-Hagerdal, L.J. Jonsson, Ethanol production from enzymatic hydrolysates of sugarcane bagasse using recombinant xylose-utilising Saccharomyces cerevisiae, Enzyme Microb. Technol. 31 (2002) 274–282. https://doi.org/10.1016/S0141-0229(02)00112-6.

[325] Q. Chen, G. Ke, Y. Hu, P. Fei, J. Wu, Preparation and application of holocellulose, cellulose nanofibers, and silver-loaded cellulose nanofibers from passion fruit peel, Cellulose 30 (2023) 1437–1448. https://doi.org/10.1007/s10570-022-05025-3.

[326] C.J. Wijaya, S.N. Saputra, F.E. Soetaredjo, J.N. Putro, C.X. Lin, A. Kurniawan, Y.H. Ju, S. Ismadji, Cellulose nanocrystals from passion fruit peels waste as antibiotic drug carrier, Carbohydr. Polym. 175 (2017) 370–376. https://doi.org/10.1016/j.carbpol.2017.08.004.

[327] P. Kumar, D.M. Barrett, M.J. Delwiche, P. Stroeve, Methods for pretreatment of lignocellulosic biomass for efficient hydrolysis and biofuel production, Ind. Eng. Chem. Res. 48 (2009) 3713–3729. https://doi.org/10.1021/ie801542g.

[328] J. Zhang, D. Chu, J. Huang, Z. Yu, G. Dai, J. Bao, Simultaneous saccharification and ethanol fermentation at high corn stover solids loading in a helical stirring bioreactor, Biotechnol. Bioeng. 105 (2010) 718–728. https://doi.org/10.1002/bit.22593.

[329] A.J. David, T. Krishnamurthi, Sustainable process for fractionation of lignin by the microwave-assisted chemical additive approach: Towards sugarcane leaf biorefinery and characterization, Int. J. Biol. Macromol. 258 (2024) 128888. https://doi.org/10.1016/j.ijbiomac.2023.128888.

[330] U. Asghar, M. Irfan, M. Iram, Z. Huma, R. Nelofer, M. Nadeem, Q. Syed, Effect of alkaline pretreatment on delignification of wheat straw, Nat. Prod. Res. 29 (2015) 125–131. https://doi.org/10.1080/14786419.2014.964712.

[331] J. Tharunkumar, V.K. Arosha, A.K. Bajhaiya, S. Rakesh, Optimizing alkaline pretreatment for delignification of paddy straw and sugarcane bagasse to enhance bioethanol production, Biomass Convers. Biorefinery (2024) 1–11. https://doi.org/10.1007/s13399-024-05458-9.

[332] C. Gao, J. Yang, L. Han, Systematic comparison for effects of different scale mechanical-NaOH coupling treatments on lignocellulosic components, micromorphology and cellulose crystal structure of wheat straw, Bioresour. Technol. 326 (2021) 124786. https://doi.org/10.1016/j.biortech.2021.124786.

[333] P.D. Maibam, A. Goyal, Approach to an efficient pretreatment method for rice straw by deep eutectic solvent for high saccharification efficiency, Bioresour. Technol. 351 (2022) 127057. https://doi.org/10.1016/j.biortech.2022.127057.

[334] K. Chandrakant Khaire, V. Suryakant Moholkar, A. Goyal, Alkaline pretreatment and response surface methodology based recombinant enzymatic saccharification and fermentation of sugarcane tops, Bioresour. Technol. 341 (2021) 125837. https://doi.org/10.1016/j.biortech.2021.125837.

[335] B.R. Prasad, P. Suman, R.K. Padhi, Physicochemical Characterization and

Delignification Enhancement of Lignocellulosic Biomass for Sustainable Bioenergy, Iran. J. Sci. 48 (2024) 843–853. https://doi.org/10.1007/s40995-024-01651-7.

[336] H. Yu, C. Gui, Y. Ji, X. Li, F. Rao, W. Huan, L. Li, Changes in Chemical and Thermal Properties of Bamboo after Delignification Treatment, Polymers (Basel). 14 (2022) 2573. https://doi.org/10.3390/polym14132573.

[337] M.M. Kininge, P.R. Gogate, Intensification of alkaline delignification of sugarcane bagasse using ultrasound assisted approach, Ultrason. Sonochem. 82 (2022) 105870. https://doi.org/10.1016/j.ultsonch.2021.105870.

[338] P. Nath, P.D. Maibam, S. Singh, V. Rajulapati, A. Goyal, Sequential pretreatment of sugarcane bagasse by alkali and organosolv for improved delignification and cellulose saccharification by chimera and cellobiohydrolase for bioethanol production, 3 Biotech 11 (2021) 59. https://doi.org/10.1007/s13205-020-02600-y.

[339] S.L. Sunar, R.K. Oruganti, D. Bhattacharyya, D. Shee, T.K. Panda, Pretreatment of sugarcane bagasse using ionic liquid for enhanced enzymatic saccharification and lignin recovery: process optimization by response surface methodology, Cellulose 31 (2024) 2151–2173. https://doi.org/10.1007/s10570-024-05768-1.

[340] E.M. Podgorbunskikh, A.L. Bychkov, E.I. Ryabchikova, O.I. Lomovsky, The Effect of Thermomechanical Pretreatment on the Structure and Properties of Lignin-Rich Plant Biomass, Molecules 25 (2020) 995. https://doi.org/10.3390/molecules25040995.

[341] A. Aishwarya, P.D. Maibam, A. Goyal, Statistical optimization of thermo-chemical pretreatment of elephant grass for efficient delignification and enzymatic saccharification, Biomass Convers. Biorefinery 15 (2025) 7483–7494. https://doi.org/10.1007/s13399-024-05650-x.

[342] A.N. Tabish, M. Kazmi, M.A. Hussain, I. Farhat, M. Irfan, H. Zeb, U. Rafique, H. Ali, M.H. Saddiqi, M.S. Akram, Biomass Waste Valorization by Acidic and Basic Leaching Process for Thermochemical Applications, Waste and Biomass Valorization 12 (2021) 6219–6229. https://doi.org/10.1007/s12649-021-01420-2.

[343] M. Beroual, D. Trache, O. Mehelli, L. Boumaza, A.F. Tarchoun, M. Derradji, K. Khimeche, Effect of the Delignification Process on the Physicochemical Properties and Thermal Stability of Microcrystalline Cellulose Extracted from Date Palm Fronds, Waste and Biomass Valorization 12 (2021) 2779–2793. https://doi.org/10.1007/s12649-020-01198-9.

[344] D. Haldar, M.K. Purkait, Thermochemical pretreatment enhanced bioconversion of elephant grass (Pennisetum purpureum): insight on the production of sugars and lignin, Biomass Convers. Biorefinery 12 (2022) 1125–1138. https://doi.org/10.1007/s13399-020-00689-y.

[345] S.I. Mussatto, G. Dragone, M. Fernandes, A.M.F. Milagres, I.C. Roberto, The effect of agitation speed, enzyme loading and substrate concentration on enzymatic hydrolysis of cellulose from brewer's spent grain, Cellulose 15 (2008) 711–721. https://doi.org/10.1007/s10570-008-9215-7.

[346] F.M. Girio, C. Fonseca, F. Carvalheiro, L.C. Duarte, S. Marques, R. Bogel-Lukasik, Hemicelluloses for fuel ethanol: A review, Bioresour. Technol. 101 (2010) 4775–4800. https://doi.org/10.1016/j.biortech.2010.01.088.

[347] A. Arora, D.J. Carrier, Understanding the pine dilute acid pretreatment system for enhanced enzymatic hydrolysis, ACS Sustain. Chem. Eng. 3 (2015) 2423–2428. https://doi.org/10.1021/acssuschemeng.5b00417.

[348] A. Billateh, B. Cheirsilp, Efficient Biovalorization of Oil Palm Trunk Waste as a Low-Cost Nutrient Source for Bioethanol Production, Energies 17 (2024) 3217. https://doi.org/10.3390/en17133217.

[349] R. Devi, S. Kapoor, R. Thakur, E. Sharma, R.K. Tiwari, S.J. Joshi, Lignocellulolytic

enzymes and bioethanol production from spent biomass of edible mushrooms using Saccharomyces cerevisiae and Pachysolen tannophilus, Biomass Convers. Biorefinery (2022) 1–15. https://doi.org/10.1007/s13399-022-02406-3.

[350] M.P. Sudhakar, M. Ravel, K. Perumal, Pretreatment and process optimization of bioethanol production from spent biomass of Ganoderma lucidum using Saccharomyces cerevisiae, Fuel 306 (2021) 121680. https://doi.org/10.1016/j.fuel.2021.121680.

[351] Y. Yucel, S. Goycıncık, Optimization of ethanol production from spent tea waste by Saccharomyces cerevisiae using statistical experimental designs, Biomass Convers. Biorefinery 5 (2015) 247–255. https://doi.org/10.1007/s13399-014-0138-2.

[352] A.M. Goula, M. Ververi, A. Adamopoulou, K. Kaderides, Green ultrasound-assisted extraction of carotenoids from pomegranate wastes using vegetable oils, Ultrason. Sonochem. 34 (2017) 821–830. https://doi.org/10.1016/j.ultsonch.2016.07.022.

[353] R. Farhoosh, R. Niazmand, M. Rezaei, M. Sarabi, Kinetic parameter determination of vegetable oil oxidation under Rancimat test conditions, Eur. J. Lipid Sci. Technol. 110 (2008) 587–592. https://doi.org/10.1002/ejlt.200800004.

[354] Y.L. Machado, A.A. Dantas Neto, J.L.C. Fonseca, T.N.C. Dantas, Antioxidant stability in vegetable oils monitored by the ASTM D7545 method, JAOCS, J. Am. Oil Chem. Soc. 91 (2014) 1139–1145. https://doi.org/10.1007/s11746-014-2470-x.

[355] E. Choe, D.B. Min, Mechanisms and factors for edible oil oxidation, Compr. Rev. Food Sci. Food Saf. 5 (2006) 169–186. https://doi.org/10.1111/j.1541-4337.2006.00009.x.

APPENDIX

A1. Standard curves for Total phenolic, flavonoid and carotenoid content quantification

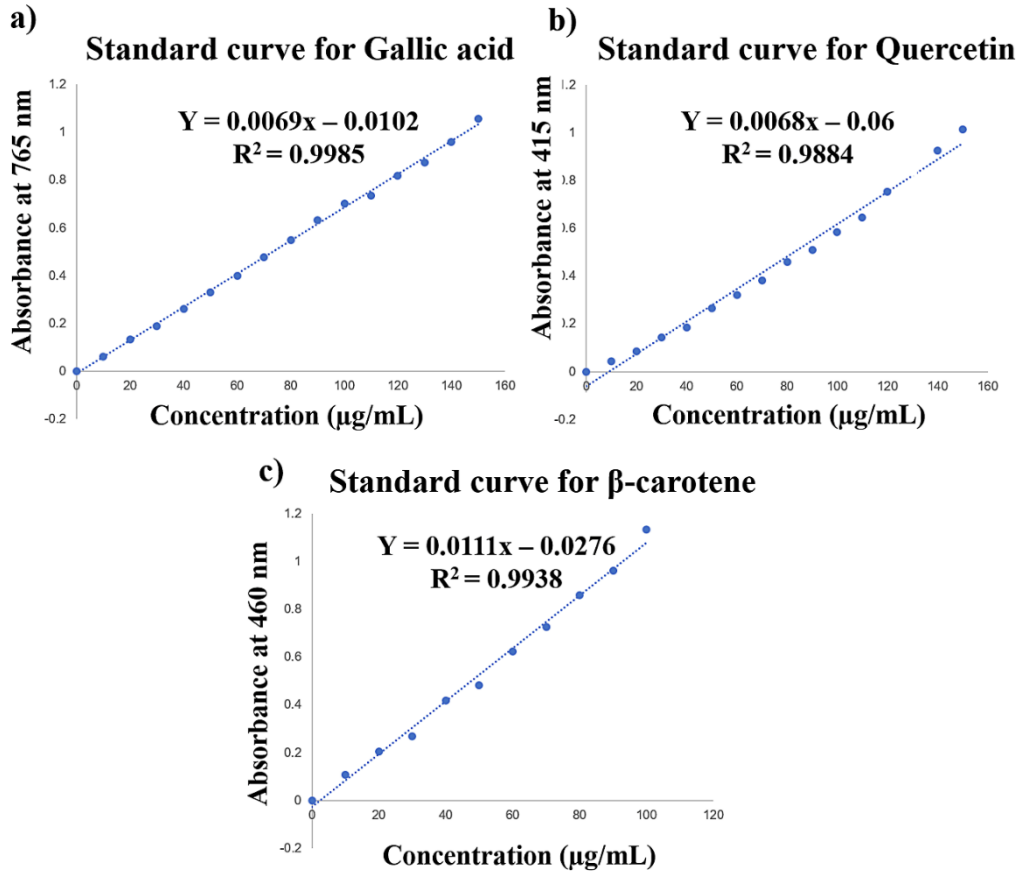

Figure A8.1. Standard curve for a) gallic acid, b) quercetin, c) β-carotene

A2. Global antioxidant score

Table A1.1. Total phenolic, Total flavonoid, Total carotenoid, Antioxidant capacity and Global antioxidant score

	TPC[a]	TFC[b]	TCC[c]	DPPH[d]	ABTS[d]	GAS
SC-ET	41.48	34.41	2.57	48.79	46.01	1.61
UAE	36.04	45.59	20.44	50.71	47.58	3.91
SC	9.88	23.21	15.28	48.647	46.14	1.07
ML extract	66.53	73.39	2.58	48.26	43.57	2.01

a is mg GAE.g^{-1} extract
b is mg QE.g^{-1} extract
c is mg β-carotene.g^{-1} extract
d is value of Percentage scavenged at 50 µg.mL^{-1} extract concentration
GAS value is determined using the formula Tscore=[(X-min)/(max-min)], where X is the variable of each unique sample and min and max are the variable's smallest and largest values of X. UAE: ultrasound-assisted extract, SC-ET: supercritical carbon dioxide with 10 per cent ethanol extract, SC: supercritical carbon dioxide extract, ML extract: methanolic extract.

A3. Phyto Profiling

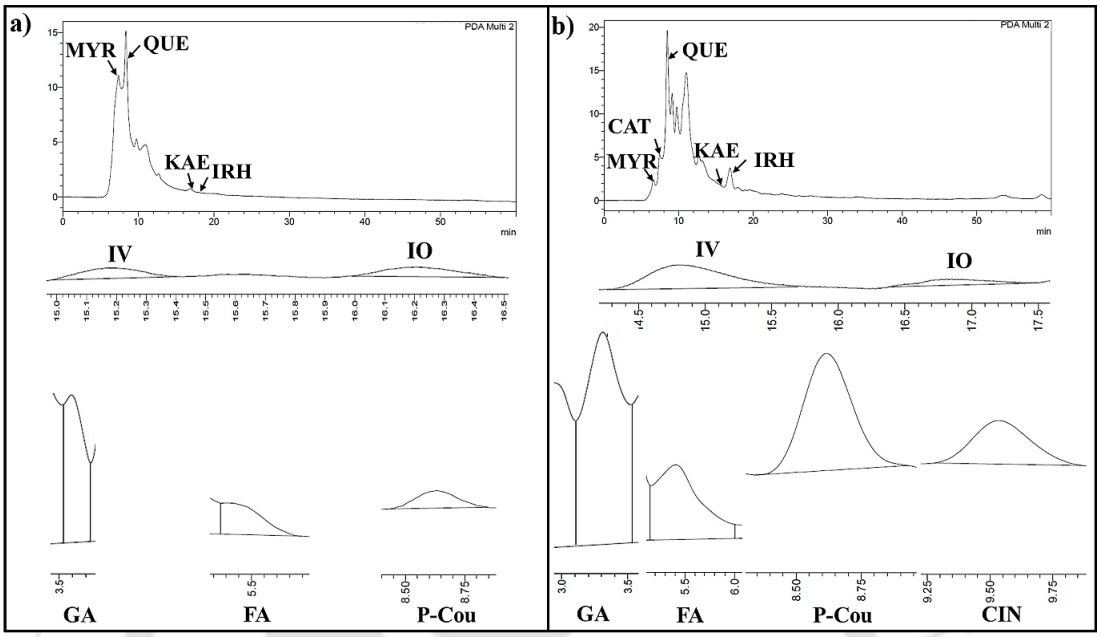

Figure A1.2. HPLC chromatograms of A) UAE extract and B) SC-ET extract for identification of phenolic and flavonoid compounds. MYR: Myricetin; CAT: Catechin; QUE: Quercetin; KAE: Kaempherol; IRH: Isorhmnetin; IV: Isovitexin; IO: Isoorientin; GA: Gallic acid; FA: Ferulic acid; p-Cou: p-Coumaric acid; CIN: Cinnamic acid.

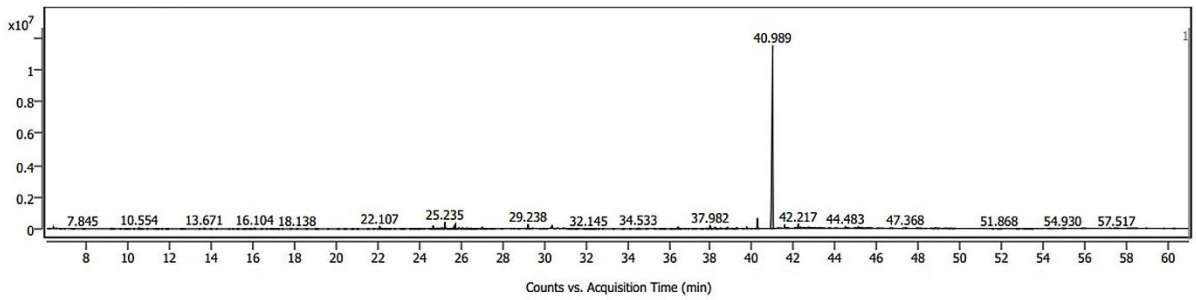

Figure A1.3. GC-MS chromatogram of UAE extract

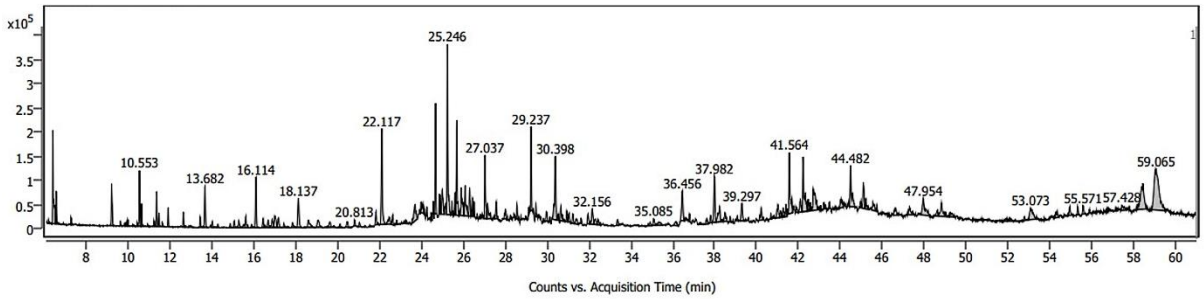

Figure A1.4. GC-MS chromatogram of SC-ET extract

Table A1.2. GC-MS analysis of UAE extracts of YPFR

RT (min)	Compound Name	Formula	Molecular weight	Peak Area Percent
6.421	Arsenous acid, tris(trimethylsilyl) ester	$C_9H_{27}AsO_3Si_3$	342.49	0.28
6.734	Methyl 2-methyl-4-(dodecylthio)-4-oxopropanoate	$C_{18}H_{34}O_3S$	330.52	0.05
6.958	(2S)-N-Tertbutoxycarbonyl-2-(1-azido-4-(2-tetrahydropyranyloxy)butyl)pyrrolidine	$C_{18}H_{32}N_4O_4$	368.47	0.03
7.376	2-[1',2',3'-tris(tButyl)]cyclopropenyl-3,3-dimethylbutan-2-one	$C_{21}H_{38}O$	306.52	0.06
7.85	Ethylsilyl ethenyl ether	$C_4H_{10}OSi$	102.21	0.12
9.23	1-[methyl(phenyl)phosphoryl]-2-naphthol	$C_{17}H_{15}O_2P$	282.27	0.2
9.642	E/Z-3-{3'-(3",3"-Dimethyl-1"-butynyl)benzothiophen-2'-yl)-2-oxiranecarbonitrile	$C_{17}H_{15}NOS$	281.37	0.05
11.862	D-glyceraldehyde 2TMS	$C_9H_{22}O_3Si_2$	234.44	0.05
11.921	triethyl-(1,1,3,3-tetraketo-4-triethylsilyl1,3-dithietan-2-yl)silane	$C_{14}H_{32}O_4S_2Si_2$	384.70	0.06
12.606	1,1,1,3,5,5,7,7,7-Nonamethyl-3-(trimethylsiloxy)tetrasiloxane	$C_{12}H_{36}O_4Si_5$	384.84	0.18
12.641	2-[(p-tolyl)methoxy]-2-methoxy-5,5-dimethyl-.delta.(3)-1,3,4-oxadiazoline	$C_{13}H_{18}N_2O_3$	250.29	0.01
13.45	2-methyl-3-(methylthio)-1,2,4-thiadiazine 1,1-dioxide	$C_5H_8N_2O_2S_2$	192.26	0.05

15.624	Piperidine hydrochloride	$C_5H_{12}ClN$	121.61	0.08
18.131	2,6-Dimethyldecane	$C_{12}H_{26}$	170.33	0.19
21.835	(3Z,6Z)-Dodeca-3,6-dien-1-ol	$C_{12}H_{22}O$	182.30	0.1
24.08	(5r*,6r*)-6-methyl-7-oxo-1-azabicyclo[3.2.1]octane	$C_7H_{13}NO$	127.18	0.2
24.859	((1S,2S)-2-azido-1-(4-methoxyphenyl)cyclohexyl)(4-methoxyphenyl)methanone	$C_{21}H_{23}N_3O_3$	365.42	0.33
24.992	3-hydroxy-4,4-dimethyldihydro(2-13C)furan-2-one	$C_6H_{10}O_3$	130.14	0.35
25.105	Butylated hydroxy toluene	$C_{15}H_{24}O$	220.35	0.44
25.241	di-t-butyl-phenol	$C_{14}H_{22}O$	206.32	1.76
25.742	Quinoline Derivative	$C_{18}H_{18}N_2O$	278.35	0.95
26.437	Borane, diethyl(decyloxy)-	$C_{14}H_{31}BO$	226.21	0.22
26.951	3.alpha.-Hydroxymethyl2,2-dimethylpenam S,Sdioxide	$C_8H_{13}NO_2$	155.19	0.09
27.557	2,3,4,4-Tetramethyl-4-(1,1-dimethylethyl)-1-hexene	$C_{14}H_{28}$	196.37	0.2
28.016	Penta-3,4-dienoic acid	$C_5H_6O_2$	98.10	0.1
28.967	[2-13C]Cyclohexane-1,3-dione	$C_6H_8O_2$	112.13	0.17
29.233	Hexadecane, 2,6,10,14-tetramethyl	$C_{20}H_{42}$	282.55	1.41
29.461	Tridecanol, 2-ethyl-2-methyl	$C_{16}H_{34}O$	242.44	0.11
29.824	3-Allyl-1,7,7- trimethylbicyclo[2.2.1]hept-2-en-2-yl Diethyl Phosphate	$C_{17}H_{29}O_4P$	328.38	0.04
30.12	1,1,1-trifluoro-2- octadecanol	$C_{18}H_{35}F_3O$	324.46	0.06

31.371	2- and 4-(Trimethoxyacetoxy)-2,5,5-trimethyl-3-hexanone	$C_{14}H_{26}O_3$	242.35	0.12
31.942	(Z)-2-nonadecene	$C_{19}H_{38}$	266.50	0.17
32.136	2,3-Dimethylthiirane 1,1-dioxide	$C_4H_8O_2S$	120.17	0.27
34.537	Lyxose,O,O,O,O-TMS MEOX1	$C_{18}H_{45}NO_5Si_4$	467.89	0.37
34.968	Propanetriol trimethylsilyl ether dev.	$C_{12}H_{32}O_3Si_3$	308.64	0.18
35.348	8,13-Dimethylicosa3,5,7,13,15,17-hexane2,19-dione	$C_{22}H_{22}O_2$	318.41	0.16
36.791	n-Cetyl thiocyanate	$C_{17}H_{33}NS$	283.51	0.14
37.171	1-Heptyl-1H-(1,2,3)-triazole-N-{[2'-(hydroxyethoxy)ethylamino]ethyl}-4-carboxamide	$C_{14}H_{27}N_5O_2$	297.40	0.15
37.57	3',3',5'-Trimethylcyclohexyl (cis)-(2-thienylglyoxyl)carboxylate	$C_{15}H_{20}O_3S$	280.38	0.17
37.85	Chizo-Inositol, 6TMS derivative	$C_{24}H_{60}O_6Si_6$	613.24	0.23
38.339	1,4-Dioxa-7-azaspiro[4.4]non-6-ene-N-oxide	$C_6H_9NO_3$	143.14	0.04
38.819	trimethyl-[2,3,4,5-tetrakis(trimethylsilyloxy)cyclohexoxy]silane	$C_{21}H_{52}O_5Si_5$	525.06	0.48
39.073	3,3-dimethyl-1-propa1,2-dienoxy-butane	$C_9H_{16}O$	140.22	0.26
39.582	2H-1,2,3,4-tetrazole-5-carboxamide	$C_2H_3N_5O$	113.08	0.07
39.745	Scyllo-Inositol, 6TMS derivative	$C_{24}H_{60}O_6Si_6$	613.24	0.52
40.253	Palmitic Acid, TMS derivative	$C_{19}H_{40}O_2Si$	328.60	2.83
40.976	Myo-Inositol, 6TMS derivative	$C_{24}H_{60}O_6Si_6$	613.24	58.44

41.162	[3-(13)CO]-2,3-thiophenedicarboxylic acid anhydride	$C_6H_2O_3S$	154.14	0.01
41.274	Methyl 16-acetylhydroxypalmitate	$C_{19}H_{36}O_4$	328.49	0.19
42.093	5,5-Dimethyl-4,5-dihydro-3H-pyrrol-3-one 1-oxide	$C_6H_9NO_2$	127.14	0.25
42.321	1,2-bis(5'-Hydrazinyl-1Htetrazol-1'-yl)-ethane	$C_4H_{10}N_{12}$	226.20	0.52
42.737	4-Allyl-1-ethoxy-3-phenylbenzo[c]-(1,2)-oxaphosphinine-1-Oxide	$C_{19}H_{19}O_3P$	326.33	0.65
43.052	.alpha.-D-threo-Hex-3-enopyranoside, methyl 6-azido-3,6-dideoxy-4-Omethyl	$C_8H_{13}N_3O_4$	215.21	0.3
43.296	1,2- Hydrazinedicarboxylic acid,1-(cyclohexylcarbonyl)-2-(2-pyridinylthio)-,diethyl ester, N-oxide	$C_{18}H_{25}N_3O_6S$	411.47	0.24
43.682	Prostaglandin F1a TMS ester tri TMS ether	$C_{32}H_{68}O_5Si_4$	645.22	0.07
43.991	7-Chloro-1-phenyl-3-hepten-1-yne	$C_{13}H_{15}Cl$	206.71	0.09
44.084	4,4'-Bi-1,3,2-dioxaborolane, 2,2'-diethyl	$C_8H_{16}B_2O_4$	197.83	0.06
44.48	Sulfurous acid, 2-ethylhexyl tridecyl ester	$C_{21}H_{44}O_3S$	376.64	0.52
44.955	Ethanone, 1-[5-(1,1-dimethylethyl)-2-ethyl-4-methyl-1,3,2-dioxaborolan-4-yl]-	$C_{11}H_{21}BO_3$	212.09	0.24
45.096	Iron, tricarbonyl[N-(phenyl-2-pyridinylmethylene)benzenamine-N,N']-	$C_{21}H_{14}FeN_2O_3$	398.19	0.69
45.329	1-(1-azidoethyl)cyclohex1-ene	$C_8H_{13}N_3$	151.21	0.18
45.625	Boron, [3-[[dimethyl(1-methyl-1-butenyl)silyl]thio]-1-propanethiolato(2-)]ethyl-,(t-4)-	$C_{12}H_{25}BS_2Si$	272.35	0.47

45.747	2-Diazo-5-methyl-3-oxohexanal	$C_7H_{10}N_2O_2$	154.17	0.19
46.276	2-Propanone, 1-diazo-3-(trimethylsilyl)-	$C_6H_{12}N_2OSi$	156.26	0.02
46.76	5-Hydroxy-2,2,4,4-tetramethyl-4-octanone	$C_{12}H_{24}O_2$	200.32	0.09
47.365	2,3,4,6-Tetra-Otrimethylsilyl-1-[1,7-dicarba-closododecaboran-(12)-1-yl]-D-glucopyranose,.alpha./.beta.	$C_{20}H_{54}B_{10}O_6Si_4$	611.09	0.37
48.347	Cyclopentylmethyl phenyl telluride	$C_{12}H_{14}Te$	285.84	0.04
48.822	(2'R,3R)-4-[2'-t-butyl-4'-oxo-4'H-1',3'-dioxin-6'-yl]-3-methylbutyrphenylaldehyde	$C_{13}H_{20}O_4$	240.29	0.37
49.335	Benzoin tetrahydropyranyl ethyl	$C_{19}H_{16}O_3$	292.33	0.2
49.547	3,3-dimethyl-1-propa1,2-dienoxy-butane	$C_9H_{16}O$	140.22	0.11
52.724	2-[2-[2-chloranyl-5-nitro3-(2-pyridin-2-ylethynyl)phenyl]ethynyl]pyridine	$C_{20}H_{10}ClN_3O_2$	359.76	0.07
54.925	Methyl ethyl 2,2,4-trichlorotridecanoate	$C_{16}H_{27}Cl_3O_4$	389.74	0.12
55.038	Dibutyl 2-Oxodecyl phosphate	$C_{18}H_{37}O_5P$	364.46	0.08
57.208	Methyl 5-methyl-4H1,2,3-triazole-4-carboxylate	$C_5H_7N_3O_2$	141.13	0.03
59.793	1,2,3-tri(tButyl)cyclopropenylium tribromide	$C_{15}H_{27}Br_3$	447.09	0.05

Table A1.3. GC-MS analysis of SC-ET extracts of YPFR

RT (Min)	Compound Name	Formula	Molecular weight	Peak Area Percent
6.422	Arsenous acid, tris(trimethylsilyl) ester	$C_9H_{27}AsO_3Si_3$	342.49	2.64
9.232	Cyclotetrasiloxane,octamethyl	$C_8H_{24}O_4Si_4$	296.62	1.12
10.655	Octyl(t-Butyl)Carbonate	$C_{12}H_{26}O_3$	218.33	0.46
11.253	1-tert-butyl-3-diazo-urea	$C_5H_{10}N_4O$	142.16	0.11
11.922	triethyl-(1,1,3,3-tetraketo-4-triethylsilyl1,3-dithietan-2-yl)silane	$C_{14}H_{32}O_4S_2Si_2$	384.70	0.40
12.647	2-[(p-tolyl) methoxy]-2-methoxy-5,5-dimethyl-.delta.(3)-1,3,4-oxadiazoline	$C_{13}H_{18}N_2O_3$	250.29	0.38
15.627	Piperidine hydrochloride	$C_5H_{12}ClN$	121.61	0.56
16.45	Nonane,4,5-dimethyl-	$C_{11}H_{24}$	156.31	0.29
17.006	2,5,8-Trimethylnonane	$C_{12}H_{26}$	170.33	0.67
18.136	Decane, 3,8-dimethyl-	$C_{12}H_{26}$	170.33	1.28
21.838	1,4-Methanocycloocta[d]pyridazine,1,4,4a,5,6,9,10,10aoctahydro-11,11-dimethyl-,(1.alpha.,4.alpha.,4a.alpha.,10a.alpha.)-	$C_{13}H_{20}N_2$	204.31	0.49
23.24	3-hydroxy-4,4- dimethyldihydro(2-13C)furan-2-one	$C_6H_{10}O_3$	130.14	0.17
23.69	1,2,3-Trimethyl-3-(1'-methylpropyl)indoleninium iodide	$C_{15}H_{22}IN$	343.25	1.14
24.267	Methaneselenoic acid,O-(1,1-diethylpropyl) ester	$C_8H_{16}OSe$	207.17	0.16
24.861	2-Azido-2,4,4,6,6- pentamethylheptane	$C_{12}H_{25}N_3$	211.35	0.36

25.247	di-t-butyl-phenol	$C_{14}H_{22}O$	206.32	4.62
26.438	Borane, diethyl(decyloxy)-	$C_{14}H_{31}BO$	226.21	0.5
26.52	2,3,4,4-Tetramethyl-4-(1,1-dimethylethyl)-1-hexene	$C_{14}H_{28}$	196.37	0.32
26.832	1-Octadecanol	$C_{18}H_{36}O$	268.48	0.18
27.583	Cyclooctasiloxane, hexadecamethyl	$C_{16}H_{48}O_8Si_8$	593.23	0.6
28.012	2-Azido-2,4,4,6,6-pentamethylheptane	$C_{12}H_{25}N_3$	211.35	0.37
29.24	Hexadecane, 2,6,10,14-tetramethyl	$C_{20}H_{42}$	282.55	2.12
29.355	2-Diazo-5-methyl-3-oxohexanal	$C_7H_{10}N_2O_2$	154.17	0.04
29.977	3-Allyl-1,7,7-trimethylbicyclo[2.2.1]hept-2-en-2-yl Diethyl Phosphate	$C_{17}H_{29}O_4P$	328.38	0.37
30.128	1,1,1-trifluoro-2-octadecanol	$C_{18}H_{35}F_3O$	324.46	0.11
31.959	(Z)-2-nonadecene	$C_{19}H_{38}$	266.50	0.39
32.161	2,3-Dimethylthiirane 1,1-dioxide	$C_4H_8O_2S$	120.17	0.76
34.921	Neopentyl 2,2-dimethylpropanoate dimer isomer	$C_{20}H_{38}O_4$	342.51	0.17
36.803	n-Cetyl thiocyanate	$C_{17}H_{33}NS$	283.51	0.24
40.688	2,3-Dimethoxy-12bphenyl-5,6-dihydroisoindolo[1,2-a]-isoquinolin-8(12bH)-one	$C_{24}H_{21}NO_3$	371.43	0.11
41.006	Oxirane,diethylboryloxymethyl	$C_7H_{15}BO_2$	142.00	0.69
41.403	3-(2-Propenoxy)-1,2-epoxyoctane	$C_{11}H_{20}O_2$	184.27	0.43
42.453	Phosphoric acid, diethyl pentyl ester	$C_9H_{21}O_4P$	224.23	0.39

42.7	1,2,4-Triazine,2-oxide	$C_3H_3N_3O$	97.08	1.85
43.217	2,4-(Trimethoxyacetoxy)-2,5,5-trimethyl-3-hexanone	$C_{14}H_{26}O_3$	242.35	0.28
43.48	(E)-1-(Dimethoxyphosphoryl)but-2-enyl dimethyl phosphate	$C_8H_{18}O_7P_2$	288.17	0.17
44.022	2-Oxopropyl 4-chlorobenzoselenoate	$C_{10}H_9ClO_2Se$	275.59	0.56
44.484	Iron, tricarbonyl[N-(phenyl-2-pyridinylmethylene)benzenamine-N,N']-	$C_{21}H_{14}FeN_2O_3$	398.19	1.83
45.098	Heptacosane	$C_{27}H_{56}$	380.73	1.15
46.61	Silicate anion tetramer	$C_{24}H_{72}O_{12}Si_{12}$	889.84	0.46
48.823	2-Methylundec-2-en-4-ol	$C_{11}H_{22}O$	170.29	1.07
52.143	6,6-Difluoro-5-hydroxy5-methyl-1-undecen-7-one	$C_{14}H_{24}F_2O_2$	262.34	0.42
53.068	2'H-Androst-16-eno[16,17-e][1,2]oxazine-3'- carbonitrile,3-(acetyloxy)-2'-cyclohexyl-3',4',16,17-tetrahydro-4'-(hydroxymethyl)-(3.beta.,5.alpha.,16.beta.,17.beta.)-	$C_{22}H_{34}O_2$	330.50	1.23
54.936	Methyl ethyl 2,2,4-trichlorotridecanoate	$C_{16}H_{27}Cl_3O_4$	389.74	0.35
55.322	1-(2-Cyclopropylcyclopentyl)but-3-en-2-one	$C_{12}H_{16}O$	176.25	0.23
57.426	1-(1-azidoethyl)cyclohex1-ene	$C_8H_{13}N_3$	151.21	0.46
59.07	Tris(2,4-di-tertbutylphenyl)phosphate	$C_{42}H_{63}O_4P$	662.92	6.56

A4. Antibacterial activity

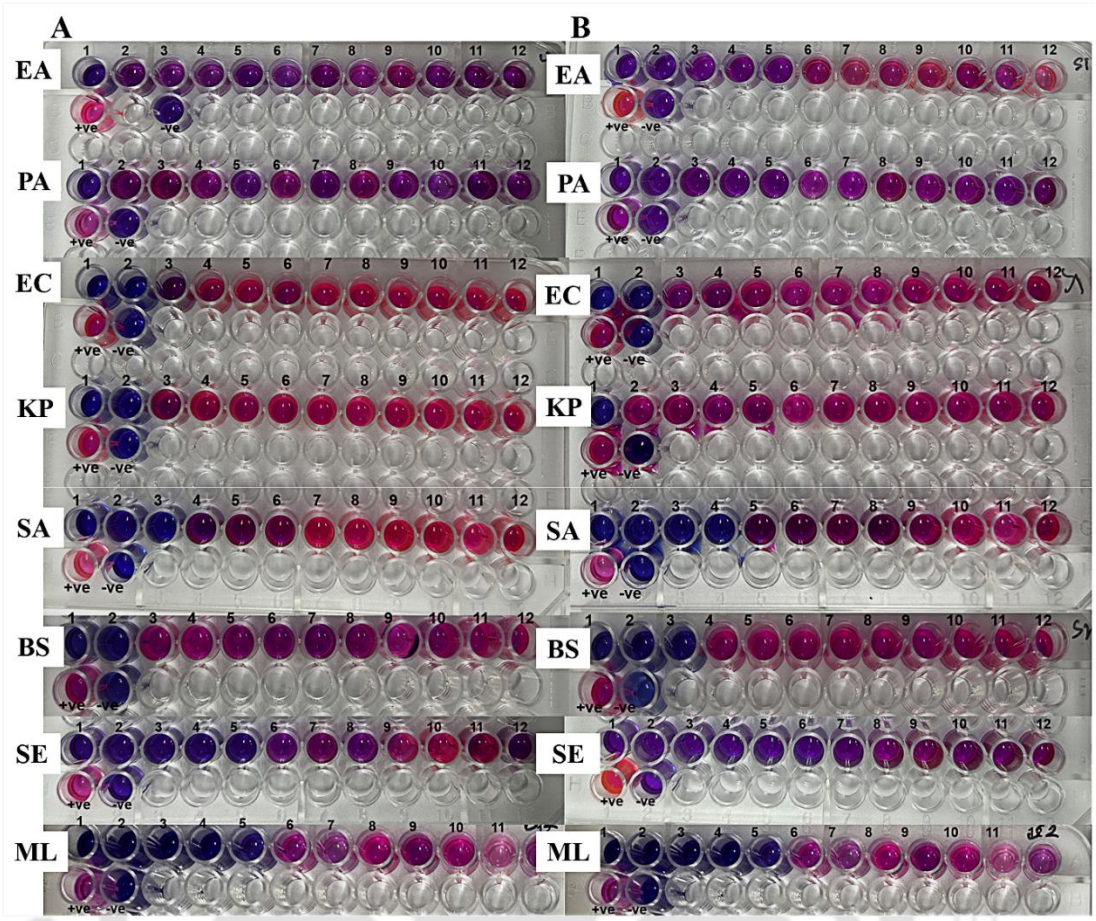

Figure A1.5. Minimum inhibitory concentration test of A) Ultrasound-assisted extract and B) Supercritical carbon dioxide with 10% ethanol yellow passion fruit rind extract with various gram-negative and gram-positive bacteria at different concentration of the extracts. EA: Enterobacter aerogenes, PA: Pseudomonas aeruginosa, EC: Escherichia coli, KP: Klebsiella pneumoniae; SA: Staphylococcus aureus, BS: Bacillus subtilis, SE: Staphylococcus epidermidis, and ML: Micrococcus luteus. The extracts concentration range varying from 80 mg/mL-9.76 µg/mL represented by 1-12, +ve and -ve represents the positive and negative control of the experiment.

Table A1.4. Zone of inhibition (ZOI) study of the extracts at optimised conditions (in mm)

Bacterial strain	Concentration	UAE	SC-ET	Control
EA	10*	ND	ND	ND
	30*	3.8 ± 0.69	8.5 ± 0.87	ND
	50*	7.1 ± 0.97	10 ± 1.00	ND
PA	10*	ND	ND	ND
	30*	3.25 ± 0.80	9 ± 1.95	ND
	50*	8.6 ± 0.46	11 ± 1.05	ND
EC	10*	ND	ND	ND
	30*	ND	5.5 ± 1.32	ND
	50*	7.5 ± 0.87	7 ± 1.32	ND
KP	10*	ND	ND	ND
	30*	ND	7.1 ± 0.85	ND
	50*	6 ± 0.85	10.9 ± 1.49	ND
SA	10*	ND	ND	ND
	30*	ND	ND	ND
	50*	7 ± 0.56	5 ± 1.00	ND
BS	10*	ND	ND	ND
	30*	5.5 ± 0.92	ND	ND
	50*	8.9 ± 2.02	7.17 ± 0.29	ND
SE	10*	ND	6 ± 1.73	ND
	30*	7 ± 1.05	9.5 ± 1.50	ND
	50*	12.67 ± 1.39	12 ± 1.00	ND
ML	10*	ND	5 ± 1.73	ND
	30*	3.8 ± 0.61	8 ± 1.00	ND
	50*	7.6 ± 0.61	11.17 ± 1.04	ND

Every data is reported as the mean SD of three independent experiments. * : The study employ extracts with varying concentrations (10 mg/ml, 30 mg/ml, and 50 mg/ml). UAE: Ultrasound-assisted extract, SC-ET: Supercritical carbon dioxide with 10% ethanol extract, ML: methanol extract, ND: not detected. EA: *Enterobacter aerogenes*, PA: *Pseudomonas aeruginosa*, EC:

Escherichia coli, KP: *Klebsiella pneumoniae*, SA: *Staphylococcus aureus*, BS: *Bacillus subtilis*, SE: *Staphylococcus epidermidis*, and ML: *Micrococcus luteus*, ND: Not detected.

A5. Assessment of Environmental and Economic Factors

Table A1.5. Comprehensive Assessment of Environmental and Economic Factors in the UAE and SFE

Parameters	UAE	SC-ET
Solvent usage	Moderate (65% ethanol)	Low (CO_2 + 10% ethanol)
Extraction duration	Short (30 min)	Longer (2 h)
Energy consumption	Low	Moderate to high
Equipment cost	Low	High
Operational cost	Low to Moderate	High
Environmental impact	Moderate (due to ethanol use)	Low (as CO_2 recyclable)
Product yield	High (51.39%)	Low (2.67%)
Production purity	Moderate	High
Scalability	High	Moderate
Suitability for high value products	Moderate	Excellent

A6. Limitations

This study highlights the promise of passion fruit rind as a source of bioactive chemicals using UAE and SFE, despite notable challenges persisting. The UAE offers scalability at minimal costs and time; nonetheless, it necessitates improvement in energy distribution, reactor design, and solvent recovery for industrial applications. SFE, despite producing high-purity extracts, encounters significant expenses associated with high-pressure equipment and low extraction yields (2.67% compared to UAE yield 51.39%). Therefore, it requires co-solvent utilisation, operational efficiency, and reactor scalability. Both systems require cost and benefits evaluations considering the economic and environmental concerns associated with the utilisation of ethanol as a solvent or co-solvent in UAE and SFE, additionally, energy-demanding CO2 pressurisation in SFE. The impact on the environment must be assessed via life-cycle analysis (LCA). Moreover, although phenolic, flavonoid, and carotenoid profiling has been performed, further characterisation of minor chemicals and antibacterial mechanisms is necessary to explore synergistic bioactivities and applications in pharmaceuticals, food, and cosmetics. reducing these constraints can enhance the sustainability and economic viability of specific extraction systems.

A7. Extraction of Bioactive Compounds from Yellow Passion Fruit Rind (YPFR) using Sunflower seed oil and Soybean oil

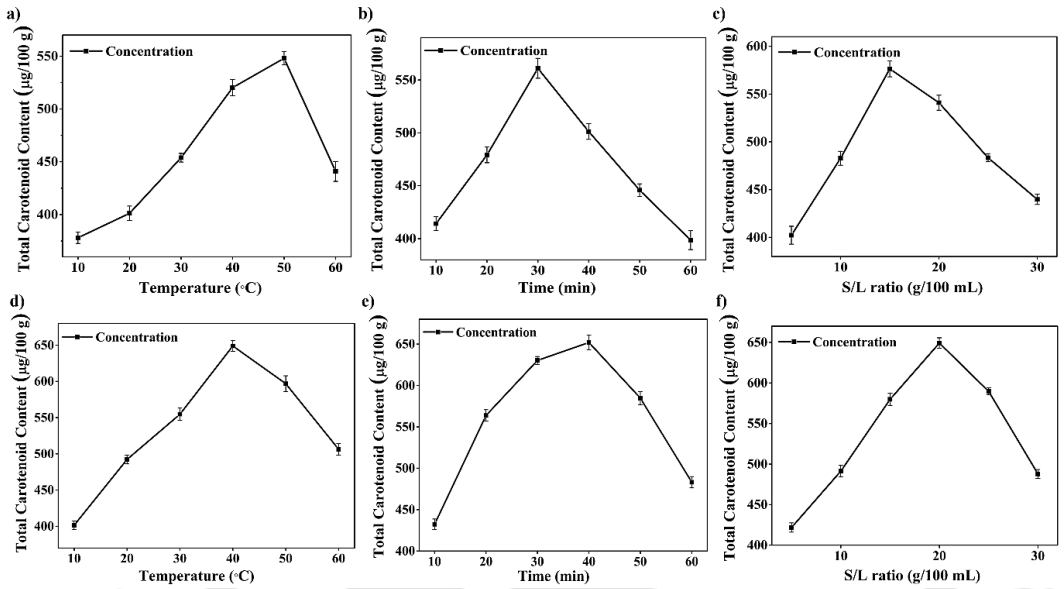

Figure A1.6. Preliminary screening of the impact of the independent variable on the total carotenoid yield for (a-c) SFO and (d-f) SBO by varying one factor at a time. (a, d) Variation of temperature at 30min and 20 g/100mL, (b, e) Variation of time at 45 °C and 20 g/100mL, and (c, f) Variation of S/L ratio at 45 °C and 30min.

The temperature range was selected based on the preliminary investigation using a single variable at a time (Figure A1). Sunflower oil exhibited an increased carotenoid yield up to 50 °C due to improved solubility and diffusion, followed by a decrease beyond that temperature, perhaps attributable to carotenoid degradation or reduced cavitation. Consequently, a temperature range of 30–60 °C was chosen for RSM optimisation to achieve maximum efficiency while reducing thermal degradation. Furthermore, in ultrasound-assisted extraction, temperature significantly affects cavitation, viscosity, and solute solubility, particularly in viscous solvents such as edible oils. Previous literature further supports the utilisation of this temperature range for carotenoid extraction. For instance, analogous investigations utilising UAE with oils as solvents have demonstrated effective extraction at temperatures above 60 °C without considerable degradation, thus validating our chosen range [137,352].”

A8. Characterisation of the vegetable oils

Table A1.6. Fatty acid composition of the soybean and sunflower oil

FFA composition	SFO	SFOE	SBO	SBOE
C14:0 (Myristic)	9.29	7.75	10.26	10.08
C16:0 (Palmitic)	32.32	33.68	29.24	29.14
C16:1 (Palmitoleic)	4.86	3.98	12.76	9.90
C18:0 (Stearic)	5.65	7.06	4.05	4.55
C18:1n9c (Oleic)	17.73	21.57	20.29	23.93
C18:2n6c (Linoleic)	5.64	5.33	5.22	5.17
C18:3n3 (α-Linolenic)	5.87	4.98	8.66	7.82
C20:0 (Arachidic)	10.08	8.50	ND*	ND*
C22:0 (Behenic)	8.55	7.15	9.54	9.41
SFA (%)	65.88	64.14	53.08	53.18
MUFA (%)	22.60	25.55	33.04	33.83
PUFA (%)	11.52	10.31	13.87	12.99

*ND: Not Detected, SBO: Soybean oil, SFO: Sunflower oil, SFA: Saturated Fatty Acids, MUFA: Monounsaturated Fatty Acids PUFA: Polyunsaturated Fatty Acids.

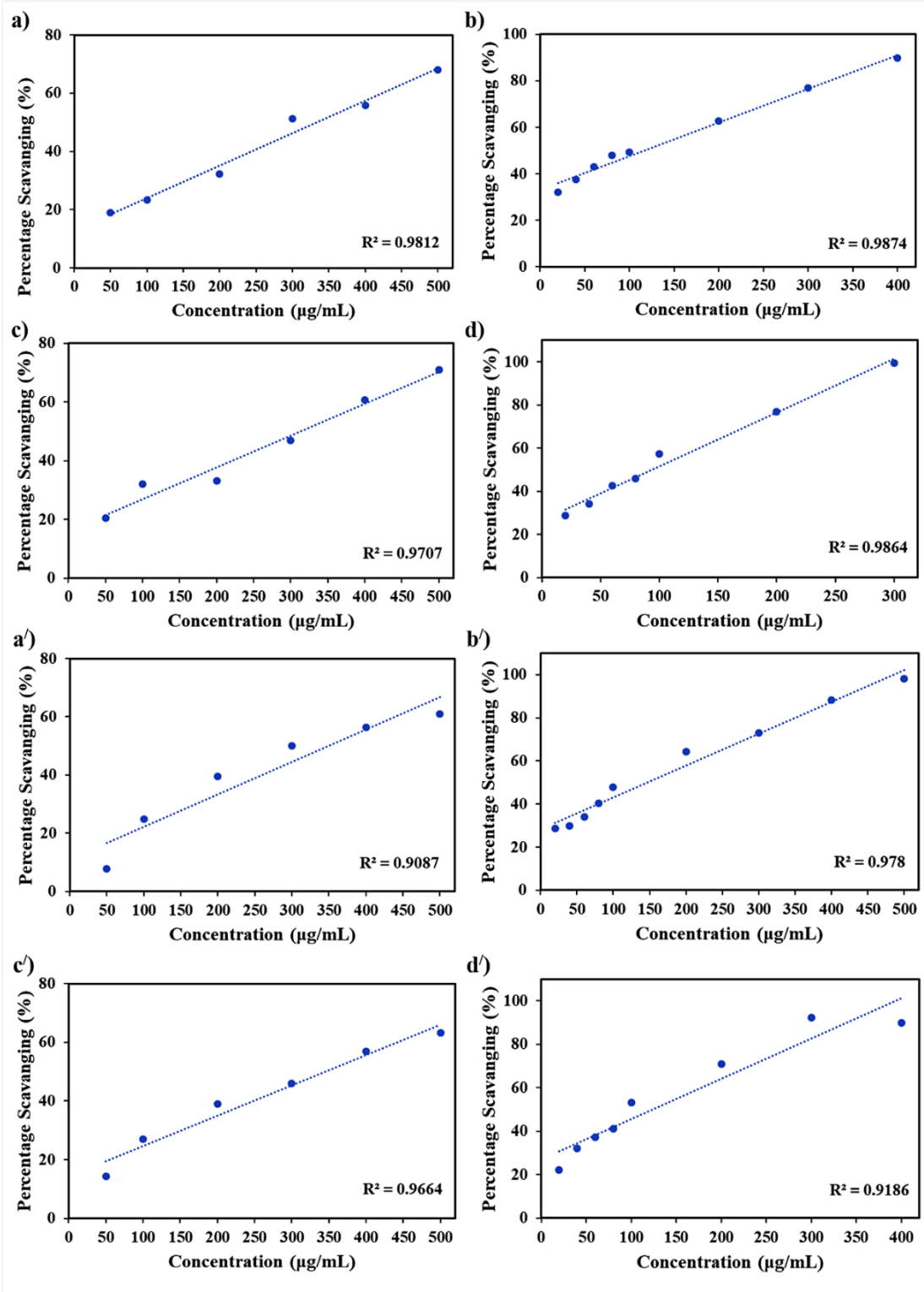

Figure A1.7. Concentration vs percentage scavenge plots for a) SFO, b) SFOE, c) SBO, d) SBOE for DPPH assay. (a/-d/) represents the same for ABTS assay.

Table A1.7. Pearson correlation coefficient between TPC, TFC, TCC, DPPH and ABTS

	TPC	TFC	TCC	DPPH	ABTS
TPC	1	0.999**	0.891	-0.995**	-0.995**
TFC	0.999**	1	0.895	-0.989*	-0.998**
TCC	0.891	0.895	1	-0.864	-0.917
DPPH	-0.995**	-0.989*	-0.864	1	0.980*
ABTS	-0.995**	-0.998**	-0.917	0.980*	1

Soybean and sunflower oil with and without Yellow Passion Fruit Rind extract. Total Phenolic content (TPC), Total Flavonoid content (TFC), Total Carotenoid Content (TCC), 2,2-diphenyl-1-picrylhydrazyl (DPPH), 2,2'-azino-bis(3-ethylbenzothiazoline-6-sulfonic acid (ABTS). ** Correlation is significant at the 0.01 level (2-tailed), * Correlation is significant at the 0.05 level (2-tailed).

A9. Oxidative Stability of oil

A9.1. Conversion of PetroOxy induction period (IP) values to Rancimat

Several expedited techniques have been devised to evaluate edible oils' ability to withstand oxidation. As the rate of reaction is proportional to temperature, all of these accelerated procedures require the use of elevated temperatures. The Rancimat test is widely utilised among them because of its repeatability and convenience of use. This test makes it possible to calculate the oxidative stability index (OSI) or induction period (IP), which is the amount of time before the oil begins to rapidly deteriorate. Because the OSI may be calculated at different temperatures, it is possible to assess the relative oxidative stability of edible oils across a temperature range while maintaining a constant air pumping pressure [353]. Nevertheless, the Rancimat test only identifies the extremely volatile oxidation products; non-volatile compounds, such as gum, stay in the sample unnoticed. Consequently, the Rancimat test only offers a partial examination of oxidation products. However, the PetroOxy method uses high pressure to control sample volatility. It calculates the induction duration as the time required for the O_2 pressure levels to drop by 10% from the highest pressure attained during the analysis. Consequently, it provides a comprehensive analysis of the sample's oxidation stability and includes all oxidation products [110].The oxidative stability of the oil was determined using the PetroOXY method (ASTM D7545). This method is believed to be faster than the ones outlined in EN 14112 and ASTM D2274 [354]. The PetroOxy test results could be converted to Rancimat IP utilising Equation (S1) [281].

$$\text{Rancimat (min)} = 31.89 \times \text{PetroOxy (min)} - 214.65, r^2 = 0.915 \qquad \text{(A1.1)}$$

Table A1.8. Induction periods (IPs) of oil samples by PetroOxy method at different isothermal temperatures

Samples	Induction Periods (IPs) in min					
	140 °C	130 °C	120 °C	110 °C	100 °C	25 °C
SFO	18.8 ± 1.25^{b}	35.69 ± 0.52^{d}	65.17 ± 1.06^{c}	132.74 ± 1.48^{c}	317.09 ± 3.25^{b}	14706.00 ± 543.15
SFOE	27.53 ± 1.16^{a}	54.02 ± 0.85^{b}	103.64 ± 1.56^{a}	214.30 ± 2.96^{a}	464.96 ± 3.85^{a}	15811.60 ± 1681.07
SFO+BHA	21.51 ± 0.58^{b}	50.19 ± 0.92^{c}	100.08 ± 0.25^{b}	203.09 ± 1.85^{b}	422.82 ± 2.69^{b}	13011.34 ± 297.27
SFO+BHT	25.24 ± 1.25^{a}	60.83 ± 1.54^{a}	104.15 ± 1.47^{a}	206.70 ± 3.40^{b}	448.14 ± 2.11^{a}	15438.28 ± 1641.96
SBO	25.36 ± 0.86^{c}	39.27 ± 0.85^{d}	92.44 ± 2.15^{c}	192.78 ± 2.46^{d}	412.62 ± 2.05^{c}	14793.57 ± 169.54
SBOE	32.85 ± 0.91^{a}	62.08 ± 0.37^{a}	115.05 ± 0.55^{a}	241.5 ± 2.18^{a}	524.67 ± 3.84^{a}	16891.72 ± 1891.14
SBO+BHA	29.55 ± 1.09^{b}	55.39 ± 1.21^{c}	107.33 ± 1.89^{b}	218.08 ± 2.25^{c}	317.09 ± 3.25^{b}	15265.03 ± 2838.48
SBO+BHT	29.76 ± 0.43^{b}	58.68 ± 1.49^{b}	114.68 ± 2.07^{a}	225.73 ± 1.41^{b}	464.96 ± 3.85^{b}	15848.34 ± 532.08

All data were expressed as min.
Values are means ± standard deviation of three determinations.
SFO: Sunflower oil, SFOE: Sunflower oil with YPFR extract, SFO+BHA: Sunflower oil with BHA, SFO+BHT: Sunflower oil with BHT, SBO: Soybean oil, SBOE: Soybean oil with YPFR extract, SBO+BHA: Soybean oil with BHA, SBO+BHT: Soybean oil with BHT.
The IPs at 25 °C were interpolated from the PetroOxy data.
The distinct letters represent significant differences ($p < 0.05$) among individual antioxidants with each oil, as assessed by Tukey's HSD test.

A9.2. Mechanism of improving oxidation stability of oil by antioxidant addition:

Among several methods to prevent lipid oxidation, antioxidants are the most beneficial, cost-effective, and commonly employed by food manufacturers to avoid quality degradation. Antioxidants in minimal quantity limit oxidation via mechanisms including free radical scavenging, singlet oxygen quenching, peroxide inactivation, metal ion chelation, and inhibition of pro-oxidative enzymes. Mishra et al., (2021) classified them as primary antioxidants and secondary based on their mode of action.

The primary antioxidants (such as phenolic compounds) disrupt oxidation by neutralising free radicals via donating hydrogen as below:

$$R\bullet + AH \rightarrow RH + A\bullet$$

$$ROO\bullet + AH \rightarrow ROOH + A\bullet$$

$$RO\bullet + AH \rightarrow ROH + A\bullet$$

The resultant antioxidant radicals are stabilised via electron delocalisation within the phenolic ring, producing stable resonance hybrids. These low-reactive radicals fail to produce more radicals, thus successfully terminating the chain reaction. Furthermore, they can enhance the scavenging of free radicals, facilitating the inhibition of oxidation. Thus, the primary antioxidants neutralise two lipid radicals by donating a hydrogen atom to one and taking an electron from the other, resulting in stable, non-radical products [128].

$$ROO\bullet + A\bullet \rightarrow ROOA$$

$$RO\bullet + A\bullet \rightarrow ROA$$

$$A\bullet + A\bullet \rightarrow AA$$

Secondary antioxidants delay oxidation by neutralising promoters such as metal ions, singlet oxygen, pro-oxidative enzymes, and other oxidants. Reducing agents (oxygen scavengers) neutralise lipid peroxides by redox processes. Thioethers, for example, transform hydroperoxides into stable molecules via a non-radical mechanism. Metal ions facilitate oxidation by producing free radicals through electron transfer. However, metal chelators (such as citric acid) mitigate the pro-oxidant effects of metal ions by forming stable complexes and decreasing their redox potential. Carotenoids, including β-carotene, reduce singlet oxygen by absorbing excess energy and releasing heat by physical quenching. Chemical quenching can also occur via reactions at conjugated double bonds, resulting in the formation of hydroperoxides. The efficacy of carotenoids

in quenching singlet oxygen increases with the amount of double bonds, with a single β-carotene molecule able to quench up to 1,000 singlet oxygen molecules [128,355].

$$^{1}O_2 + \beta\text{-carotene} \rightarrow {}^{3}\beta\text{-carotene}^* + {}^{3}O_2$$

$$^{3}\beta\text{-carotene}^* \rightarrow \beta\text{-carotene} + \text{Heat}$$

A10. Thermal Analysis of oil

Table A1.9. t_{ON} of treated and untreated oil samples obtained from extrapolation of DSC curve

Samples	t_{OFF} (°C)	t_{PEAK} (°C)	t_{ON} (°C)
SFO	*-15.43*	*-12.74*	*-10.85*
SFOE	*-20.74*	*-16.89*	*-12.34*
SFO+BHA	*-18.35*	*-14.44*	*-11.42*
SFO+BHT	*-16.09*	*-13.92*	*-11.79*
SBO	*-11.87*	*-9.87*	*-8.12*
SBOE	*-15.12*	*-12.17*	*-9.59*
SBO+BHA	*-12.34*	*-10.94*	*-8.96*
SBO+BHT	*-12.01*	*-10.23*	*-9.10*

SFO: Sunflower oil, SFOE: Sunflower oil with YPFR extract, SFO+BHA: Sunflower oil with BHA, SFO+BHT: Sunflower oil with BHT, SBO: Soybean oil, SBOE: Soybean oil with YPFR extract, SBO+BHA: Soybean oil with BHA, SBO+BHT: Soybean oil with BHT.

A11. Preliminary screening

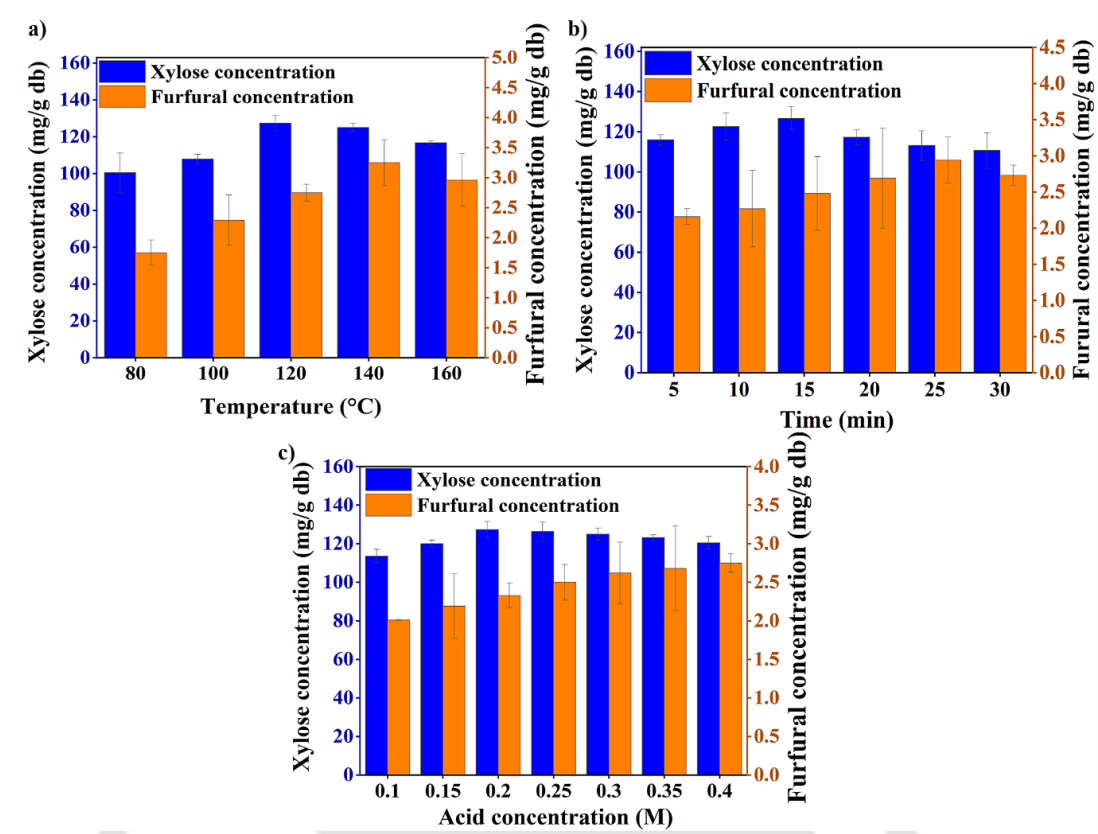

Figure A1.8. Preliminary screening (a-c) of the impact of the independent variable on the xylose and furfural concentration (mg/g db) after acid pretreatment by varying one factor at a time. (a) Variation of temperature at 15 min and 0.2 M acid concentration, (b) variation of time at 120 °C and 0.2 M acid concentration, and (c) variation of acid concentration at 120 °C and 15 min.

A12. Paired sample t-test analysis of acid prehydrolysate

Table A1.10. Paired sample t-test analysis of different sugars and inhibitors in without overlimed and overlimed hydrolysate

	Mean	SD	SE	t	Df	One-sided p	Two-sided p
Glu-WO & Glu-O	0.63	0.55	0.25	2.56	4	0.03	0.06
Xyl-WO & Xyl-O	1.97	0.77	0.31	6.25	5	<0.001	0.002
Xybi-WO & Xybi-O	0.41	0.29	0.15	2.76	3	0.03	0.07
Fur-WO & Fur-O	0.03	0.01	0.008	4.13	5	0.002	0.01
HMF-WO & HMF-O	0.06	0.03	0.02	3.08	2	0.006	0.09
ForA-WO & ForA-O	0.69	0.48	0.24	2.89	3	0.04	0.06
AceA-WO & AceA-O	0.87	0.74	0.52	1.66	1	0.07	0.35
Phe-WO & Phe-O	0.32	0.15	0.06	5.21	5	0.007	0.003

SD: Standard deviation, SE: Standard error mean, Glu-WO: Glucose without overlimed, Glu-O: Glucose overlimed, Xyl-WO: Xylose without overlimed, Xyl-O: Xylose overlimed, XyBi-WO: Xylobiose without overlimed, XyBi-O: Xylobiose overlimed, Fur-WO: Furfural without overlimed, Fur-O: Furfural overlimed, HMF-WO: 5HMF without overlimed, HMF-O: 5HMF overlimed, ForA-WO: Formic acid without overlimed, ForA-O: Formic acid overlimed, AceA-WO: Acetic acid without overlimed, AceA-O: Acetic acid overlimed, Phe-WO: Phenolic acid without overlimed, Phe-O: Phenolic acid overlimed

A13. Characterisation of delignified passion fruit rind

Table A1.11. Brunauer-Emmett-Teller analysis and elemental composition of untreated and delignified passion fruit rinds

	RPFR	PH-RPFR	SPFR	PUH-PFR
Brunauer-Emmett-Teller analysis				
BET surface area (m^2/g)	20.82	109.43	24.38	120.30
Pore volume (mm^3/g)	0.006	0.061	0.013	0.065
Elemental analysis				
Carbon	44.50	43.19	45.20	43.16
Hydrogen	5.50	4.73	5.90	5.27
Oxygen	48	47.28	47.40	54.77
Nitrogen	1.80	0.07	1.20	0
Sulfur	0.10	0	0.20	0

RPFR: raw passion fruit Rind, PH-RPFR: raw passion fruit Rind residue after H_2SO_4 hydrolysis, SPFR: spent passion fruit rind, PUH-PFR: post ultrasound-assisted extraction and sulphuric acid treatment.

A14. Composition analysis of enzymatic hydrolysate

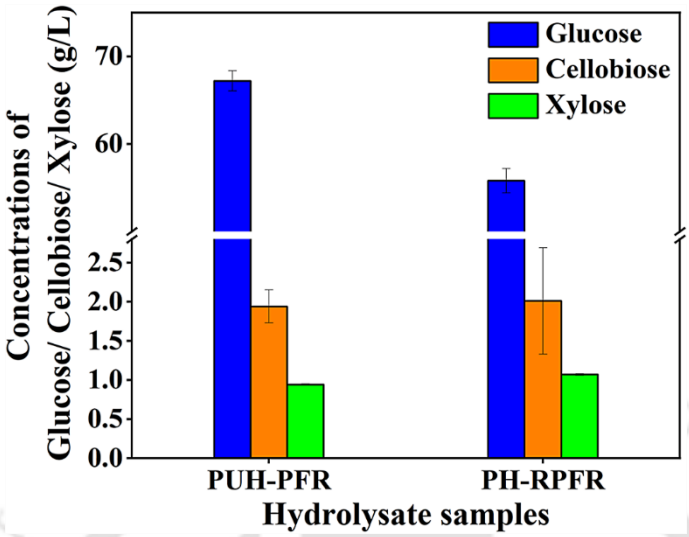

Figure A1.9. Composition of the enzymatic hydrolysate at 30 mg/g enzyme loading. PH-RPFR: raw passion fruit Rind residue after H_2SO_4 hydrolysis, PUH-PFR: post ultrasound-assisted extraction and sulphuric acid treatment.

Research Output

Journals

1. **Kakali Borah**, Vaibhav V Goud, 2025. Bioconversion of spent passion fruit rind to ethanol: Integrating hemi-cellulose hydrolysis and detoxification. Bioresour. Technol. Reports 31, 102193. DOI: 10.1016/j.biteb.2025.102193

2. **Kakali Borah**, Vaibhav V Goud, 2025. One-Pot Method to Extract Natural Antioxidizing Agents from Passion Fruit Rind to Increase the Oxidative Stability of Sunflower Seed and Soybean Oils, *Food Chemistry*. 144668. DOI: 10.1016/j.foodchem.2025.144668

3. **Kakali Borah**, Rupesh Kumar, Sukumar Purohit, Vaibhav V Goud, 2025. Comparative study on phytochemical extraction from Passion fruit wastes using ultrasound and supercritical fluid extraction, *Journal of Food Measurement and Characterization*, 1-13. DOI: 10.1007/s11694-025-03150-8

4. **Kakali Borah,** Vaibhav V Goud, 2025. Alkali Delignification and Fermentation of Spent Passion Fruit Rind to Bioethanol Production, Bioresource Technology, **(Submitted).**

5. Sukumar Purohit, **Kakali Borah**, Vaibhav V Goud, 2025. Unlocking the Potential of Passion Fruit Waste By-Products through Biorefinery and Bioresource Innovation, Bioresour. Technol. Reports. **(Submitted,** authors contributed equally**).**

Book Chapters/Proceedings

1. "Extraction of Phenolics from Yellow Passion Fruit Rind Using Supercritical Carbon Dioxide Extraction." **Kakali Borah**, Rupesh Kumar, Vaibhav V Goud, 2023. Agro and Food Processing Technologies: Proceedings of NERC 2022. Springer Nature Singapore 141-156. DOI: 10.1007/978-981-19-9704-48
2. Book Chapter titled as "Sustainable Waste to Energy Technologies: Fermentation." **Kakali Borah** and Vaibhav V. Goud, 2023. In Biodegradable Waste Processing for Sustainable Developments. Dr. Arbind Prasad and Dr. Atanu Kumar Paul (Eds). CRC Press 2023. 150-172. DOI: 10.1201/9781003502012-7.

3. "Sustainable Approach to Passion Fruit Waste Utilisation: Statistical Optimisation of Ultrasonic Extraction of Polyphenols." **Kakali Borah**, Rupesh Kumar, Vaibhav V Goud, 2025. Current Progress in Interdisciplinary Research: Selected Papers of RIC 2024. Springer Nature Singapore 3. ISBN:978-981-95-1852-4.
4. Book Chapter titled as "Biofuel Decision-Making in Asia/India: Integrating Techno-Economic and Environmental Perspectives." **Kakali Borah** and Vaibhav V. Goud, 2024. Sustainability in Biomass and Biorefinery: Processing and Opportunities. Dr. Arbind Prasad and Dr. Atanu Kumar Paul (Eds). CRC Press. 2024. **(Submitted)**
5. Book Chapter titled as "Thermochemical Conversions: Hydrothermal Carbonization, Pyrolysis, and Syngas Production." **Kakali Borah,** Sabari Nandi and Vaibhav V. Goud. Biomass Valorisation and Green Engineering: Materials Innovation, Energy Solutions, and Sustainability Trends. Dr. Kaustubh Khaire and Dr. Amlan Das (Eds). CRC Press. 2024. **(Accepted)**

Poster/Presentation on Conference

1. **Kakali Borah**, Vaibhav V. Goud, "Valorizing Agro-Industrial Waste: Bioethanol Production from Delignified Spent Passion Fruit Rind Residue" 2025 ASSET International Conference on Advances in Sustainable Solutions for Energy Transitions 2025, 02-04 January 2025 in Guwahati, India, 2025.
2. **Kakali Borah**, Vaibhav V. Goud, "Valorisation of Passion fruit Rind for the Production of Bioethanol: Statistical Optimisation of Hemicellulose and Fermentation with *Pichia stipites*" 2024 SEEP International Conference on Sustainable Energy and Environmental Protection Conference 2024, 09-12 September 2024 in Vienna, Austria, 2024.
3. **Kakali Borah**, Rupesh Kumar, Vaibhav V. Goud, "A Sustainable Approach to Passion Fruit Waste Utilization: Statistical Optimization of Ultrasonic Extraction of Polyphenols" 2024 RIC Research and Industrial Conclave - Integration 2024, 09-11 August 2024 in IIT Guwahati, India, 2024.
4. **Kakali Borah**, Rupesh Kumar, Vaibhav V. Goud, "Optimisation of the techniques used for valorization of *Passiflora* wastes using RSM" 2023 ICFTN International Conference on Food Technology and Nutrition, 12-13 December 2023 in Paris, France, 2023.

5. **Kakali Borah**, Vaibhav V. Goud, "RSM-Based Optimization of Recovery of Phenolic Compounds from Passion Fruit Rind Using Ultrasound-Assisted Extraction" 2023 ICNPU International Conference on Natural Products utilization: From Plants to Pharmacy Shelf, 30 May-02 June 2023, Sts Constantine and Helena Resort, Bulgaria, 2023.
6. **Kakali Borah**, Sukumar Purohit and Vaibhav V. Goud, "In-situ Extraction of Carotenoid from Passion Fruit Peel to Improve Quality of Vegetable Oil" 2021 BREEECH International Conference on Biotechnology for Resource Efficiency, Energy, Environment, Chemicals and Health (BREEECH 2021), 1-4 Dec 2021, CSIR-IIP, Dehradun, India.

Achievements:

1. Reviewer Certificate (2025): Awarded contribution to manuscript review - Food Analytical Methods (Springer Nature).
2. Best Oral Presenter (2024): Awarded 1st prize for Oral Presentation in RIC Research and Industrial Conclave-Integration, organised by- IIT Guwahati, India.
3. Prime Minister Research Fellow (2020): Awarded PMRF Fellowship for doctoral programme, from Ministry of Education, Government of India.
4. MHRD Fellowship (2019): Awarded Fellowship for doctoral programme, from the Ministry of Education, Government of India.

Workshops:

1. Foundation of Python in Data Science (March 2024). Organised by- Students' Academic Board, IIT Guwahati.
2. Implementation of MSME Innovation Scheme-Intellectual Property Right (IPR) (February 2024). Organised by- MSME development and Facilitation Office, Guwahati; Ministry of MSME, GoI; IIT Guwahati.
3. Applied Statistical Modeling and Data Analytics for Petroleum Engineering and Related Applications (November 2022). Organised by- Department of Chemical Engineering, IIT Guwahati and SPE IIT Guwahati Student Chapter.
4. Sustainable Energy Utilisation Technology for Green Hydrogen and Renewable Fuels (October 2022) Organised by School of Energy Science and Engineering,

IIT Guwahati and Technology Innovation Hub, IIT Guwahati Technology Innovation and Development Foundation (IITG-TI and DF).

5. Python Training for Scientific Computing and Data Science (April 2022). Organised by- Students' Academic Board, IIT Guwahati.
6. Intellectual Property Rights for Academic and Research Institutions (February 2021). Organised by TEQIP sponsored short term course Department of Mechanical Engineering, IIT Guwahati.
7. Latex Workshop (October 2021). Organised by- Research Scholar Forum (RSF) Mathematics, IIT Guwahati.